

ANNA HÄMÄLÄINEN

# Increasing Sludge Valorization by Combining Thermochemical Treatment with Anaerobic Digestion

Focus on hydrothermal carbonization and pyrolysis



ANNA HÄMÄLÄINEN

Increasing Sludge Valorization  
by Combining Thermochemical  
Treatment with Anaerobic Digestion

Focus on hydrothermal  
carbonization and pyrolysis

ACADEMIC DISSERTATION

To be presented, with the permission of  
the Faculty of Engineering and Natural sciences  
of Tampere University,

for public discussion in the auditorium K1702  
of Konetalo, Korkeakoulunkatu 6, Tampere,  
on 20<sup>th</sup> of October, at 12 o'clock.

## ACADEMIC DISSERTATION

Tampere University, Faculty of Engineering and Natural Sciences  
Finland

*Responsible  
supervisor  
and Custos*

Professor  
Jukka Rintala  
Tampere University  
Finland

*Supervisor*

Associate Professor  
Marika Kokko  
Tampere University  
Finland

*Pre-examiners*

Associate Professor  
María de los Ángeles de la Rubia  
Autonomous University of Madrid  
Spain

Associate Professor  
Sebastian Schwede  
Mälardalen University  
Sweden

*Opponent*

Associate Professor  
Luca Fiori  
University of Trento  
Italy

The originality of this thesis has been checked using the Turnitin OriginalityCheck service.

Copyright ©2023 Anna Hämäläinen

Cover design: Roihu Inc.

ISBN 978-952-03-3077-4 (print)

ISBN 978-952-03-3078-1 (pdf)

ISSN 2489-9860 (print)

ISSN 2490-0028 (pdf)

<http://urn.fi/URN:ISBN:978-952-03-3078-1>



ClimateClic CC-000025FI  
PunaMusta Printing

Carbon dioxide emissions from printing Tampere University dissertations have been compensated.

PunaMusta Oy – Yliopistopaino  
Joensuu 2023

Iskälle



# ACKNOWLEDGEMENTS

This thesis was carried out in at the Faculty of Engineering and Natural Sciences, Tampere University (formerly Department of Chemistry and Bioengineering, Tampere University of Technology). I am grateful for the financial support this thesis received from Maj and Tor Nessling Foundation, Gasum Gas Fund, and Tampere University of Technology Foundation.

Most grateful I am to my supervisor Prof. Jukka Rintala and co-supervisor Associate Prof. (tenure track) Marika Kokko, for all the guidance and support, and for giving me the possibility and resources to pursue a doctoral degree. In addition to my supervisors, I want to thank Viljami Kinnunen for kindly planning and co-authoring my publications and giving essential expertise about the practical needs of the industry. My thanks also go to co-authors Tuomo Hilli for your expertise and Pritha Chatterjee for helping and teaching me both in the laboratory and in formulating academic publications. I also want to thank Henrik Tolvanen for co-authoring, and more importantly, for being a friend and helping also with the life outside work.

I want to thank the pre-examiners of this thesis, Associate Professor María de los Ángeles de la Rubia from Autonomous University of Madrid, and Associate Professor Sebastian Schwede from Mälardalen University, for taking your time and thoroughly go through my thesis and giving your valuable feedback. I am also very grateful to Associate Professor Luca Fiori from University of Trento for kindly agreeing to act as the opponent at the public examination of my thesis.

Specifically, I want to thank Antti Nuottajärvi and Mika Karttunen for the most kind and constant problem-solving assistance with the practical laboratory matters. In addition, I want to express my gratitude to the fellow students Veera Koskue, Tiina Karppinen and Arto Hiltunen for being good and understanding friends, and giving me peer-support, which at first helped me to integrate to Tampere.

Finally, I want to thank my best friend and partner Pectu, for transforming my life into a dream and for providing support with all the issues I have encountered during my academic journey. And most of all, my mother and father. This thesis is dedicated to my dear father who passed away before my dissertation took place but who certainly would have enjoyed seeing it and reading this.

Tampere, August 2023

Anna Hämäläinen





# ABSTRACT

Wastewater sludges represent a high-volume resource for recycled nitrogen, phosphorous, carbon and renewable energy. They are typically managed through anaerobic digestion (AD) for increasing the sludge stability and decreasing pathogens, thus improving sludge applicability as soil amendment, in landscaping, and in nutrient recovery, and for producing renewable energy in the form of biogas. In practice, mere AD is insufficient in exploiting the full energy potential of wastewater sludges and in converting sludge in the most feasible form for nutrient and carbon recovery. Therefore, thermochemical treatments to complement the present wastewater sludge management could be introduced. The objective of this thesis was to assess the potential of hydrothermal carbonization (HTC) and pyrolysis in the refining of municipal sewage sludge digestate and of pulp and paper mill mixed sludge for increasing nutrient recovery, carbon sequestration potential, and energy recovery in combination with AD.

The HTC treatment produced hydrochar and HTC filtrate, the characteristics of which depended on the feedstock material and of the HTC conditions used. The dewaterability of municipal sewage sludge digestate was significantly improved as the hydrochar total solid (TS) contents increased to up to 60% from the solids content of mechanically dewatered digestate (25%). While the effect of HTC on the dewaterability of industrial pulp and paper mill mixed sludge was minor, its energy content improved from 14.9 up to 20.5 MJ/kg in the hydrochars. The phosphorous concentrations of digestate hydrochars increased from 3.2–3.7% TS up to 5.7 % TS, supporting nutrient recovery applications, while mixed sludge hydrochars were found to be more applicable in carbon sequestration due to low nutrient contents relative to digestate hydrochars and up to a 33% increase in carbon content from untreated mixed sludge. All the produced HTC filtrates had up to 12–15-fold higher biodegradable organics content and 3–5-fold higher methane production potential in AD than untreated sludge filtrates. In addition to the HTC filtrates, AD was found to be a viable disposal and treatment method also for pyrolysis liquid originating from the pyrolysis of municipal digestate, having a neutral effect on biogas production and no inhibition. The integration assessment of HTC to a centralized biogas plant showed to improve biogas (by 1%) and nitrogen product (by 33%) production, while the biogas plant energy consumption was not remarkably increased.

In conclusion, HTC represents potential refining technology for wastewater sludges for enabling more complete recovery of nutrients, carbon, and energy from wastewater sludges than sole AD. The findings of this work encourage the implementation of thermochemical treatments to the existing biogas plants and to industrial wastewater treatment plants for increasing resource efficiency.



# TIIVISTELMÄ

Jätevesilietteet edustavat korkean volyymin kierrätysravinteiden (typpi ja fosfori), hiilen ja uusiutuvan energian lähdettä. Jätevesilietteitä käsitellään tyypillisesti anaerobisella mädätyksellä, jotta sen stabiilius kasvaa ja patogeenien määrä laskee, täten kasvattaen lietteen hyödynnettävyyttä maanparannusaineena, viherrakentamisessa ja ravinteiden talteenotossa, ja jotta siitä voidaan tuottaa uusiutuvaa energiaa biokaasun muodossa. Käytännössä mädätys yksinään on riittämätön hyödyntämään jätevesilietteiden koko energiasisältöä ja muokkaamaan lietettä parhaaseen mahdolliseen käyttökelpoisuuteen ravinteiden ja hiilen talteenottoa varten. Tästä syystä, termokemiallisia käsittelyjä pitäisi ottaa käyttöön täydentämään jätevesilietteiden käsittelyä. Tämän työn tavoitteena oli arvioida märkäpyrolyysin (HTC) ja kuivapyrolyysin mahdollisuuksia mädätetyn yhdyskuntajätevesilietteen sekä teollisen paperi- ja sellutehtaan sekalietteen jalostamisessa ravinteiden talteenottoa, hiilen varastointia sekä biokaasun tuottoa varten.

HTC-käsittelyllä tuotettiin hydrohiiltä ja suodosta, joiden ominaisuudet riippuivat lietesyötteestä sekä HTC:n prosessiolosuhteista. Mädätetyn yhdyskuntajätevesilietteen vedetöintiominaisuudet parantuivat huomattavasti, sillä hydrohiilen kiintoaineen määrä kasvoi jopa 60 prosenttiin kokonaismassasta alkuperäisen, käsittelemättömän ja mekaanisesti vedetöidyn mädätteen kiintoainepitoisuuden ollessa 25%. Käsittelyjen vaikutus teollisen paperi- ja sellutehtaan sekalietteen vedetöintiominaisuuksiin oli pieni, mutta sekalietteen energiasisältö kasvoi alkuperäisestä lämpöarvosta 14.9 MJ/kg hydrohiilen 20.5 MJ/kg. Mädätteen hydrohiilen fosforipitoisuudet kasvoivat 3.2–3.7 prosentista kuiva-ainetta jopa 5.7 prosenttiin kuiva-ainetta, puoltaen ravinteiden talteenotto-ovelluuksia, kun taas sekalietteen hydrohiilen todettiin olevan soveltuvampi hiilen varastointiin, johtuen mädäte-hydrohiileen verraten matalan ravinnepitoisuuden sekä jopa 33 prosentin kasvaneen hiilipitoisuuden vuoksi. Kaikki tuotetut HTC-suodokset sisälsivät 12–15 kertaisen määrän biohajoavaa orgaanista ainetta sekä 3–5 kertaa korkeamman metaanin tuottopotentiaaloin verrattuna käsittelemättömiin lietesuodoksiin. HTC-suodosten ohella, anaerobinen mädätys soveltuvi myös mädätteen kuivapyrolyysissä tuotetun pyrolyysinesteen hävittämiseen ja käsittelyyn, sillä havaittiin, että pyrolyysinesteen vaikutus jätevesilietteen mädätysprosessiin oli neutraali eikä inhibitiota tapahtunut. Biokaasulaitoksen ja HTC:n integrointiarviointi osoitti, että biokaasun tuotantomäärä kasvoi 1% ja tyypituotteen 33%, vaikkei biokaasulaitoksen energiankulutus lisääntynyt merkittävästi.

Työn tulokset osoittivat, että jätevesilietteiden jalostus HTC:llä mahdollistaa kokonaisvaltaisemman ravinteiden, hiilen ja energian talteenoton kuin anaerobinen mädätys yksinään. Työn löydökset rohkaisevat termokemiallisten käsittelyjen käyttöönottoa biokaasulaitosten ja teollisten jätevesikäsitteilyjen yhteyteen lisäämään jätevesilietteen hyödyntämistä.



# CONTENTS

1	Introduction .....	1
2	Background .....	3
2.1	Wastewater sludge generation.....	3
2.2	Wastewater sludge treatment and utilization needs .....	4
2.2.1	Anaerobic digestion.....	7
2.2.2	Thermal treatments.....	10
2.2.2.1	Hydrothermal carbonization.....	12
2.2.2.2	Pyrolysis .....	15
2.2.3	Products utilization after thermal treatment.....	16
2.2.3.1	Char fraction.....	16
2.2.3.2	Anaerobic treatability of liquids .....	17
2.2.4	Deployment of HTC using scale-up assessments.....	20
3	Research objectives .....	21
4	Materials and methods.....	22
4.1	Experimental design.....	22
4.2	Studied materials.....	22
4.3	Experimental set-ups.....	24
4.3.1	Laboratory HTC treatments.....	24
4.3.2	BMP assays.....	25
4.3.3	Semi-continuous reactor experiments .....	25
4.4	Extrapolation to large scale.....	26
4.5	Analytical methods and calculations.....	28
5	Results and discussion.....	33
5.1	Effect of HTC on digested sewage sludge and pulp and paper mixed sludge .....	33
5.1.1	Mass distribution.....	33
5.1.2	Phosphorous and nitrogen recovery.....	36
5.1.3	Hydrochar energy recovery .....	40
5.1.4	Hydrochar in carbon sequestration.....	43
5.1.5	HTC filtrates' biogas production.....	44
5.2	Effect of pyrolysis liquid addition on methane production from sewage sludge and thermally pretreated sewage sludge .....	46
5.2.1	Characterization of pyrolysis liquid for AD .....	46
5.2.2	Pyrolysis liquid in semi-continuous AD reactors.....	47
5.3	Scale-up assessment of HTC integration in biogas plants .....	48
5.3.1	Mass, nutrient, and carbon flows and recoveries.....	48
5.3.2	Energy balance.....	49
6	Conclusions and recommendations for future research.....	52

## List of Figures

- Figure 1.** Simplified schematic representation of typical wastewater treatment process utilizing activated sludge treatment, presenting the sources of primary and secondary sludge. Tertiary treatment method varies depending on wastewater treatment plant (therefore dashed).
- Figure 2.** Wastewater sludge management *via* processing it into renewable energy and nutrient products. A: Typical sludge stabilization with anaerobic digestion (AD) and composting. B: Coupling of AD and thermochemical treatment with liquid product recycling for biogas production, also showing the possibility to use the char product in AD (De la Rubia et al., 2018; Ferrentino et al., 2020; Torri and Fabbri, 2014). C: Thermochemical treatment for mixed sludge without prior AD of sludge and showing the possibility of a thermal liquid product utilization in AD (Oliveira et al., 2013). D: Coupling of a thermochemical treatment and AD treating secondary and primary sludge separately (Medina-Martos et al., 2020).
- Figure 3.** Schematic diagram of the steps of microbiological degradation pathways in anaerobic digestion. Adapted from Appels et al. (2008) and Tchobanoglous (2014). LCFA: long chain fatty acid, VFA: volatile fatty acid.
- Figure 4.** Simplified reaction mechanism of the main sludge constituents during hydrothermal carbonization. The sludge composition and reaction conditions (residence time and solid load) determine the amount and type of reaction intermediates remaining in the liquid product. Reaction intermediates with grey background illustrate high molecular weight intermediates that are subjected to further degradation. Adapted from Ischia and Fiori, (2021), Keiller et al. (2019), Libra et al. (2011). VOC : volatile organic compound, PAH: polycyclic aromatic hydrocarbon
- Figure 5.** Simplified illustration of the original layout (A) and the HTC integrated layout (B) of the studied centralized biogas plant (Paper IV). The orange dashed arrows represent the possible locations of the CHP units. LBG: liquefied biogas, CHP: combined heat and power, HE: heat exchanger, HTC: hydrothermal carbonization, WWTP: wastewater treatment plant.
- Figure 6.** Mass distribution of concentrated digestate (25% TS) (A), diluted digestate (15% TS) (B), concentrated mixed sludge (32% TS) (C), and diluted mixed sludge (15% TS) (D) after HTC treatment at specific conditions and filtration. For the mixed sludges, the mass distribution after mere filtration is also shown, named as mixed sludge (MS) cakes (Papers I and II).
- Figure 7.** Phosphorous concentrations in the concentrated digestate (A), diluted digestate (B), concentrated mixed sludge (C), and diluted mixed sludge (D), and in their respective hydrochars and HTC filtrates. For the mixed sludges, also the filter cake and cake filtrate phosphorous concentration are shown. Notice the different scale of the liquid total phosphorous between the digestates and mixed sludges (Papers I and II).
- Figure 8.** Nitrogen distribution of concentrated digestate (25% TS) (A), diluted digestate (15% TS) (B), concentrated mixed sludge (32% TS) (C), and diluted mixed sludge (15% TS) (D) after HTC treatment at specific conditions and filtration. For the mixed sludges, the nitrogen distribution after mere filtration is also shown, named as mixed sludge (MS) cakes (Papers I and II).
- Figure 9.** Energy yields, ash contents (in % of total solids (TS)), and higher heating values (HHV) of concentrated digestate hydrochar (A), diluted digestate hydrochar (B), concentrated mixed sludge hydrochar (C), and diluted mixed sludge hydrochar (D) (Papers I and II).
- Figure 10.** The cumulative methane production curves of digestate HTC filtrates (A) and mixed sludge HTC filtrates (B) as well as their cake filtrates. The methane productions of the inocula have been subtracted from the results (Papers I and II).
- Figure 11.** Methane yields (A) and SCOD of digestates (B) in semi-CSTR experiment with pyrolysis liquid addition (Paper III).

## List of Tables

- Table 1.** Characteristics of municipal sewage sludge (Kacprzak et al., 2017; Tchobanoglous, 2014) and industrial pulp and paper mill sludge (Bayr and Rintala, 2012; Meyer and Edwards, 2014).
- Table 2.** Characteristics of municipal sewage sludge (Astals et al., 2012) and pulp and paper mill primary and secondary sludges (Bayr and Rintala, 2012) before and after anaerobic digestion.
- Table 3.** Overview of the thermal treatments used or studied for wastewater sludge treatment and/or management.
- Table 4.** Anaerobic digestion related characteristics of selected liquid products from hydrothermal carbonization and pyrolysis.
- Table 5.** Summary of the experiments used in this thesis.
- Table 6.** Characteristics of the studied materials. The THSS theoretical illustrates the effect of THP on the sludge characteristics when the effect of dilution in the THP process with steam (from 16 to 10% TS) is extracted (calculation is shown in Eq. 11).
- Table 7.** The operational parameters used in the semi-continuous reactor experiments (Paper III).
- Table 8.** Summary of the analytical methods and equipment used in this thesis.
- Table 9.** Equations used in the energy demand calculations for the biogas plant with HTC integration (Paper IV).
- Table 10.** Solids and ash contents of digestates and mixed sludge, and their respective hydrochars' solids and ash contents, and solid yields after different HTC treatments. For mixed sludge, also the characteristics of their non-HTC-treated filter cakes are shown (Papers I and II).
- Table 11.** Nitrogen, ammonium nitrogen, and phosphate concentrations of the HTC filtrates of digestates, mixed sludges, and mixed sludge cake filtrates (Papers I and II).
- Table 12.** Heating values, energy densifications, and elemental compositions (C, H, N, S, O) of digestates, mixed sludges, and their respective hydrochars (Papers I and II).
- Table 13.** The changes in the amounts of the outflowing products and in the nutrient amounts of the outflowing products following from the HTC integration to biogas plant (Paper IV).
- Table 14.** The annual energy demand of the different unit processes and their total energy demand in a biogas plant with HTC integration and without (original layout) (Paper IV).

# ABBREVIATIONS

AD	Anaerobic digestion
BMP	Biochemical methane potential
COD	Chemical oxygen demand
CSTR	Continuously stirred tank reactor
DAF	Dry ash free
HCl	Hydrogen chloride
HHV	Higher heating value
5-HMF	5-hydroxymethylfurfural
HRT	Hydraulic retention time
HTC	Hydrothermal carbonization
LCFA	Long-chain fatty acid
LHV	Lower heating value
N <sub>tot</sub>	Total nitrogen
NH <sub>4</sub> -N	Ammonium nitrogen
NO <sub>x</sub>	Nitrogen oxides
OH	Hydroxyl
OLR	Organic loading rate
PAH	Polycyclic aromatic hydrocarbon
PO <sub>4</sub> <sup>2-</sup>	Phosphate
SCOD	Soluble chemical oxygen demand
SO <sub>x</sub>	Sulphur oxides
SS	Sewage sludge
THP	Thermal pre-hydrolysis
THSS	Thermally pre-hydrolyzed sewage sludge
TKN	Total Kjeldahl nitrogen
TS	Total solids
TVFA	Total volatile fatty acids
VFA	Volatile fatty acid
VOC	Volatile organic compound
VS	Volatile solids
WWTP	Wastewater treatment plant



## ORIGINAL PUBLICATIONS

- Publication I **Hämäläinen, A.**, Kokko, M., Kinnunen, V., Hilli, T., Rintala, J., 2021. Hydrothermal carbonisation of mechanically dewatered digested sewage sludge—Energy and nutrient recovery in centralised biogas plant. *Water Research*, 201, 117284.
- Publication II **Hämäläinen, A.**, Kokko, M., Kinnunen, V., Hilli, T., Rintala, J., 2021. Hydrothermal carbonization of pulp and paper industry wastewater treatment sludges - characterization and potential use of hydrochars and filtrates. *Bioresource Technology*, 355, 127258.
- Publication III **Hämäläinen, A.**, Kokko, M., Chatterjee, P., Kinnunen, V., Rintala, J. 2022. The effects of digestate pyrolysis liquid on the thermophilic anaerobic digestion of sewage sludge—Perspective for a centralized biogas plant using thermal hydrolysis pretreatment. *Waste Management*, 147, 73–82.
- Publication IV **Hämäläinen, A.**, Kokko, M., Tolvanen, H., Kinnunen, V., Rintala, J. 2023. Towards the implementation of hydrothermal carbonization for nutrients, carbon, and energy recovery in centralized biogas plant treating sewage sludge. *Submitted to Journal of Cleaner Production*.

## AUTHOR CONTRIBUTIONS

- Publication I AH wrote the first draft of the manuscript and is the corresponding author. AH conducted most of the laboratory experiments and interpreted the results. JR and MK supervised the work and participated in the planning and writing of the manuscript by revising and editing. VK provided the study materials and participated in the planning of the experiments with TH.
- Publication II AH wrote the first draft of the manuscript and is the corresponding author. AH conducted the laboratory experiments and interpreted the results. JR and MK supervised the work and participated in the planning and writing of the manuscript by revising and editing. VK provided the study materials and participated in the planning of the experiments with TH.
- Publication III AH wrote the first draft of the manuscript and is the corresponding author. AH conducted the laboratory experiments and interpreted the results. PC helped in some of the laboratory work and participated in the writing of the first draft. JR and MK supervised the work and participated in the planning and writing of the manuscript by revising and editing. VK provided the study materials and participated in the planning of the experiments and revision of the manuscript.
- Publication IV AH wrote the first draft of the manuscript and is the corresponding author. AH planned, designed, and conducted the scale-up study calculations and interpreted the results. JR and MK supervised the work and participated in the writing of the manuscript by revising and editing. HT participated in revising the calculations and manuscript. VK participated in the planning of the layout design and revision of the manuscript.

# 1 INTRODUCTION

Wastewater treatment is currently implemented to remove organic matter and nutrients from wastewaters to prevent environmental load upon water discharge (Tchobanoglous, 2014). This treatment process produces large quantities of wastewater sludge, of which amount increases together with population increase and tightening quality criteria for discharged waters (Tchobanoglous, 2014). Traditionally, this wastewater sludge has been regarded as waste subjected for disposal although containing considerable amounts of organic matter, carbon, nutrients, and renewable energy of value. At the same time, to counteract global climate change, renewable energy sources are increasingly being introduced to replace fossil fuels, and carbon sequestration is being understood as a tool to mitigate global warming. Hence, due to their large, daily, and unavoidable production, wastewater sludges could represent a resource for renewable energy production, nutrient recycling in agriculture, and carbon storage. However, the prevailing sludge processing fails to fully exploit the potential of wastewater sludges, therefore, novel approach to sludge treatment and valorization is required, which could ultimately shift wastewater treatment plants (WWTP) from being waste treatment facilities into resource recovery facilities.

The challenge of utilizing wastewater sludges of municipal or industrial sources is the concern of a potential presence of organic and inorganic contaminants, pathogens, microplastics, and heavy metals (Alvarenga et al., 2015; Corradini et al., 2019). These contaminants and pollutants are being recognized as preventing factors of sludge utilization in soils for agriculture and for carbon storage. Moreover, wastewater sludges require stabilization due to uncontrolled putrefaction potential and nutrient leaching (Anjum et al., 2016). A traditional stabilization process for wastewater sludges has been anaerobic digestion (AD) which produces besides stabilized sludge digestate also renewable energy in the form of biogas (Appels et al., 2008). AD is however incapable of removing or destroying contaminants to a level which would satisfy the requirements for intended fertilization or land application. Therefore, digested municipal wastewater sludge, *i.e.*, sewage sludge digestate is typically used for landscaping purposes, while incineration of sewage sludge digestate has been adopted as a disposal method elsewhere in Europe (Kacprzak et al., 2017). Incineration has also frequently been used to dispose and decrease the volumes of industrial pulp and paper wastewater sludge (Bayr and Rintala, 2012) because its presence in landfill may cause leaching and greenhouse gas production, and thus is not permitted by the European Union Waste Framework Directive (2018/851/EC) (European parliament, 2018). However, due to the introduction of circular economy, also incineration is facing limitations for being energetically inefficient and failing to recover nutrients and organic carbon. Thus, the current sludge and digestate management practices require complementing technologies to ensure the efficient use of nutrients while enhancing the utilization of the energy potential of wastewater sludges.

Thermochemical conversion treatments, such as hydrothermal carbonization (HTC) and pyrolysis, represent a readily implementable technology which upgrade wastewater sludge into value-added products (Catenacci et al., 2022; Hoekman et al., 2011). These treatments convert biomass into solid char, liquid product, and gas fractions, by which they allow more complete recovery of sludge constituents into nutrient products, carbon, and renewable energy compared with mere AD. Wastewater sludge composition varies according to its origin and wastewater treatment process, but all sludges share the feature of having high moisture content and biodegradable organic constituents. Therefore, of the

thermochemical treatments, HTC appears efficient for being able to convert moist biomass into value-added products without the necessity of pre-drying of biomass (Gao et al., 2020). Drying of the high-water-content sludges can account for more than half of the wastewater treatment costs at pulp and paper mills because of the difficulty of dewatering sludge that contains extra-cellular polymeric substances (Meyer et al., 2018).

HTC treatment of high-moisture sludges improves their dewaterability by altering the structure and physicochemical properties through chemical reactions (Libra et al., 2011; Meyer et al., 2018). This improved dewaterability enables sludge separation into a solid char and liquid products which contain nutrients and energy with potentially increased exploitability. The nutrient and energy contents of char depends on the feedstock composition and HTC conditions, due to which chars from municipal and pulp and paper mill sludge differ in their potentials for either soil application purposes for nutrient and carbon recovery or for energy recovery as a renewable fuel. The characteristics of the liquid product vary similar to the char, but they commonly share high organics content, which shows potential for biogas production as also other thermochemical liquids have been extensively studied as substrates for AD (Ferrentino et al., 2020; Seyedi et al., 2020; Wirth and Mumme, 2014). Although, pyrolysis and HTC liquids have been acknowledged as potential biogas sources, they can also be inhibitory to the microorganisms that produce biogas in AD due to their chemical constituents produced during the thermochemical treatment (Hübner and Mumme, 2015). The main motivations of employing thermochemical treatments in wastewater sludge or digestate management include the destruction of pathogens, possible reduction of contaminants, sludge volume decrease, and improved applicability of the sludge thereof. The biogas production potential of the liquid product becomes advantageous when thermochemical conversion technologies are combined with sludge management systems that utilize AD.

The objective of this thesis was to evaluate the potential of HTC in municipal and industrial pulp and paper mill wastewater sludge management and processing into value-added products concerning nutrient, carbon, and energy recoverability. The prospect of combining thermochemical conversion technology with anaerobic digestion of wastewater sludge was assessed by studying pyrolytic and HTC liquid products in AD and by conducting extrapolation calculations. This thesis first provides a literature review on wastewater sludge production, AD, and thermal technologies, followed by summaries of the methods and results and discussion of this thesis. Lastly, conclusions and recommendations for future research are provided.

## 2 BACKGROUND

### 2.1 Wastewater sludge generation

At WWTP, wastewaters are treated in a series of different unit processes, aiming to produce effluent water that can be discharged to natural water bodies (Metcalf and Eddy 2014). The treatment includes physical, chemical, and biological processes (Demirbas et al., 2017). A typical wastewater treatment process scheme is presented in Fig 1, in which preliminary treatment first removes coarse solids and grit. In the following primary treatment, fine and suspended solids are allowed to settle to the bottom of the tank from where they are scraped off and collected as primary sludge. Before primary sedimentation, phosphorous precipitating chemicals, such as  $\text{FeSO}_4$ , can be added to promote phosphorous removal from water into the solid sludge (Ylivainio et al., 2021). In activated sludge process (or secondary treatment), suspended and non-settleable solids, nitrogen and phosphorous are removed by the exploitation of microorganisms which oxidize and convert solids into simple end products and new cell biomass (Tchobanoglous, 2014). In the aeration tank (Fig. 1), ammonium nitrogen is oxidized into nitrite and nitrate by specific bacteria (nitrification), while other bacteria in the oxygen-depleted regions of the tank reduce these oxidized nitrogen compounds into gaseous nitrogen that is released into the atmosphere (denitrification) (Tchobanoglous, 2014). In industrial wastewater treatment, such as in pulp and paper industry, where wastewater is poor in nutrients, nitrogen and phosphorous can be supplied before the activated sludge process to support the microorganism function and enable good biological performance (Bayr and Rintala, 2012; Meyer and Edwards, 2014). After the aeration tank, the solids and microbial biomass are allowed to settle in secondary sedimentation from where the solids are collected as secondary sludge. Part of the secondary sludge is returned to the aeration tank to recycle the active microbes-containing sludge for continuing the removal of organics from the influent wastewater (Tchobanoglous, 2014). The sedimented primary and secondary sludges (ca. 98% moisture) represent the main by-product from wastewater treatment (Appels et al., 2008).

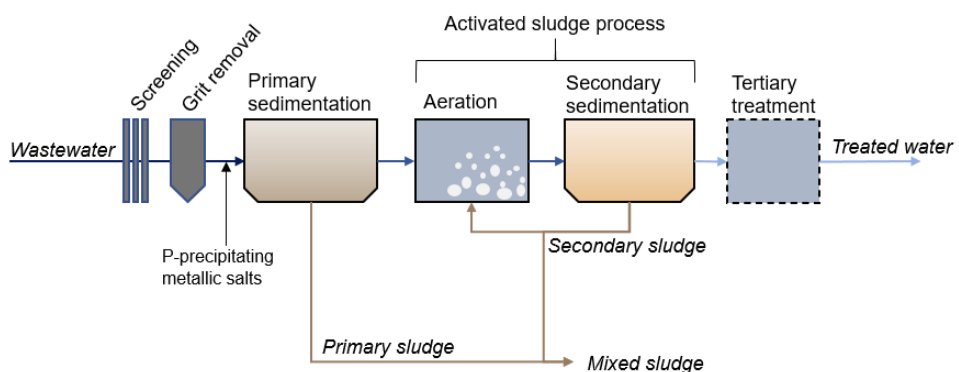


**Figure 1.** Simplified schematic representation of typical wastewater treatment process utilizing activated sludge treatment, presenting the sources of primary and secondary sludge. Tertiary treatment method varies depending on wastewater treatment plant (therefore dashed).

The generated primary and secondary sludge differ in their compositions and characteristics, which also vary considerably between municipal and industrial wastewater treatment facilities, and between mills and treatment processes (Table 1) (Meyer and Edwards, 2014; Tchobanoglous, 2014). Nevertheless, some generalizations of the distinguishing sludge characteristics can be drawn. Municipal sewage sludge is a semi-solid slurry of 50-70% of organic matter that consists of proteins, sugars, lipids, and nutrients, but also of pollutants (Demirbas et al., 2017; Kacprzak et al., 2017). Municipal primary sludge has a high content of volatile solids (VS) and minerals present in wastewater, whereas secondary sludge is mainly composed of microbial biomass generated in aeration unit and nutrients (Gherghel et al., 2019). Municipal sewage sludge has a small content of lignin compared with industrial pulp and paper mill sludges of which primary sludge consists of lignocellulosic wood fibers, papermaking fillers, pitch, lignin by-products and ash (Puhakka et al., 1992). Pulp and paper mill secondary sludge consist mostly of microbial biomass, cell-decay products, extra-cellular polymeric substances, and non-biodegradable lignin (Meyer et al., 2018). In physical means, secondary sludge is more difficult to dewater than primary sludge, thus, for the ease of processing, they are often mixed (Meyer et al., 2018). Primary sludge has higher potential for biodegradation than secondary sludge that has already experienced biodegradation in the activated sludge process and has a lower content of biodegradable cellulose (Bayr and Rintala, 2012; Demirbas et al., 2017). Depending on the possible use of phosphorous precipitating agents, the sludges contain iron or aluminum bound phosphorous. The possible nutrient supplementation before the activated sludge process in pulp and paper wastewater treatment can lead to significantly higher nutrient concentrations in the secondary sludge compared to primary sludge (Meyer and Edwards, 2014).

**Table 1.** Characteristics of municipal sewage sludge (Kacprzak et al., 2017; Tchobanoglous, 2014) and industrial pulp and paper mill sludge (Bayr and Rintala, 2012; Meyer and Edwards, 2014).

Parameter	Municipal sewage sludge		Pulp and paper mill sludge	
	Primary	Secondary	Primary	Secondary
TS (%)	2.0–8.0	0.4–1.2	1.5–6.5	1.0–2.0
VS (% TS)	60–85	60–85	51–80	65–97
pH	5.0–8.0	6.5–8.0	5.0–11.0	6.0–7.6
Total nitrogen (% TS)	1.5–4.0	2.4–5.0	0.1–0.5	3.3–7.7
Total phosphorous (% TS)	0.8–2.8	2.8–11.0	n.a.	0.5–2.8
Cellulose (% TS)	8–15	7–10	36–45	19–27
Protein (% TS)	20–30	32–41	n.a.	22–52 <sup>a</sup>
Lipids (% TS)	5–8	5–12	n.a.	2–10
Lignin (% TS)	n.a.	n.a.	20–24	36–50

n.a. not available; TS, total solids; VS, volatile solids

<sup>a</sup> in % of VS

## 2.2 Wastewater sludge treatment and utilization needs

Disposal of wastewater sludges is challenging due to their large volumes and high moisture content. Wastewater sludges are also malodorous, contain pathogens and have potential for putrefaction and for a release of greenhouse gases, restraining their disposal in landfills (Appels et al., 2008). Thus, sludge stabilization is needed to reduce the amount of favorable environment for microorganism growth, *i.e.*, the quantity of VS in the sludge where microorganisms flourish. Typically, sludges are stabilized through alkaline stabilization (addition of lime), aerobic digestion, AD, and composting (Tchobanoglous, 2014).

Currently, AD represents the dominant stabilization method and is most applicable for concentrated sludges produced in municipal or industrial wastewater treatment (Tchobanoglous, 2014).

There is also an increasing need to recover phosphorous and nitrogen for agricultural purposes to replace depleting mineral phosphorous sources and energy intensive nitrogen fertilizer production. Wastewater sludge represents a raw material, and its reuse fits into the circular economy concept where resources are re-used in the system of material use and production (Gherghel et al., 2019). Municipal sewage sludge contains large quantities of nutrients, carbon, and organic material originating from household wastewaters, which could be used to replace nutrients and energy otherwise obtained from non-renewable resources (Gherghel et al., 2019). However, in Finland, the prevailing method to dispose pulp and paper industry wastewater sludges is incineration, which fails to complete the circle of material and energy use, and due to this, are becoming restricted being inefficient in recovering energy and nutrients (Bayr and Rintala, 2012). Wastewater sludge also represents a sink for pathogenic microbes, inorganic contaminants, such as heavy metals, and organic contaminants, such as pesticides, surfactants, hormones, and pharmaceuticals (Kacprzak et al., 2017). Recently, also microplastics have raised concern (Xu and Bai, 2022). For this reason, several countries prohibit or restrict the use of sewage sludge for agricultural food production, although the pathogen and contaminant concentrations would be below the limit values set by the European Union. In Finland, less than 5% of sewage sludge digestates are used for agricultural purposes (Kacprzak et al., 2017). Therefore, sludge management and development of sludge treatment technologies are essential in improving sludge use as a resource and in regarding environmental protection because of the risk of spreading of pollutants, contaminants, nutrient leaching, and CO<sub>2</sub> emissions (Gherghel et al., 2019).

Sludge management processes that turn sludge from a waste into a resource with increased value are expected to emerge. Novel sludge management options target to improve resource recovery, sludge dewaterability, and biogas production, while wastewater treatment is being developed to reduce the volume of sludge generated (Merzari et al., 2019). Such sludge management options utilize the renewable energy production potential of wastewater sludges through AD and thermal methods together with material and nutrient recovery and recycling (Kacprzak et al., 2017; Spinosa et al., 2011). Because a single process for sludge treatment which would enable nutrient and energy recovery, would be economically feasible and socially acceptable is nonexistent, process combinations that maximize the material recycling and recovery with a low energy input are recommended (Spinosa et al., 2011). A system consisting of AD, dewatering, and thermal treatment is considered readily implementable to complete the aims of municipal and pulp and paper mill WWTPs. The following Fig. 2 illustrates examples of simplified sludge processing schemes which aim for both renewable energy and nutrient recovery.

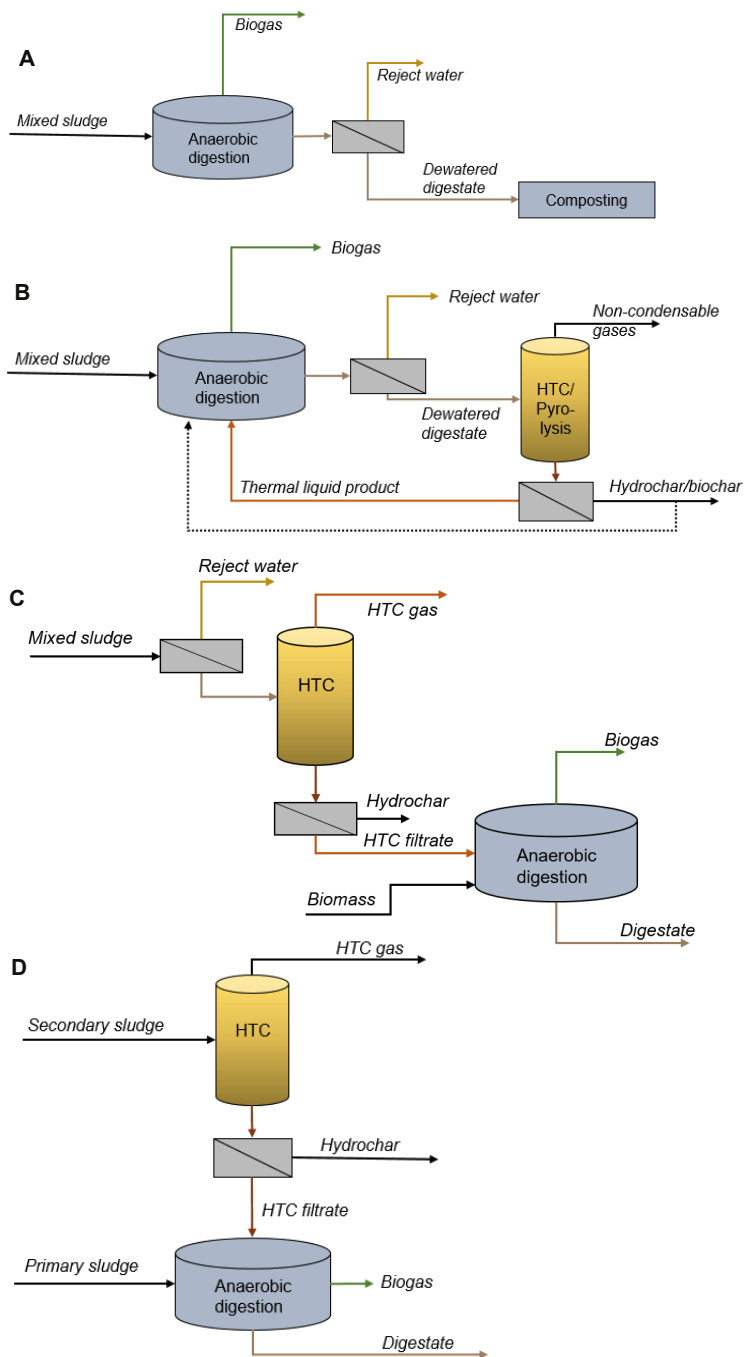


**Figure 2.** Wastewater sludge management via processing into renewable energy and nutrient products. A: Typical sludge stabilization with anaerobic digestion (AD) and composting. B: Coupling of AD and thermochemical treatment with liquid product recycling for biogas production, also showing the possibility to use the char product in AD (De la Rubia et al., 2018; Ferrentino et al., 2020; Torri and Fabbri, 2014). C: Thermochemical treatment for mixed sludge without prior AD of sludge and showing the possibility of a thermal liquid product utilization in AD (Oliveira et al., 2013). D: Coupling of a thermochemical treatment and AD treating secondary and primary sludge separately (Medina-Martos et al., 2020).



## 2.2.1 Anaerobic digestion

Wastewater sludges, either a mixture of primary and secondary sludges or separate sludge streams, are often treated in AD in connection to WWTPs or in detached centralized biogas plants. AD has been applied in sludge stabilization since the early 1900s (Mulchandani and Westerhoff, 2016), aiming to prevent spontaneous degradation and enable sludge utilization in nutrient and organic matter recovery. More recently, the global targets to replace fossil fuels with renewable energy prompts the utilization of AD that produces renewable energy in the form of biogas (65–70% CH<sub>4</sub>, 30–35% CO<sub>2</sub>) which can be purified into methane to be used as fuel similarly to natural gas (Appels et al., 2008). AD is a biological stabilization process that enables controlled stabilization of sludge, reduces sludge mass, and improves its dewaterability.

Biochemically, AD occurs in the absence of oxygen when inorganic compounds function as electron acceptors instead of oxygen, resulting in microbiological degradation of organic biomolecules, generating methane and carbon dioxide (Madigan et al., 2019). The anaerobic degradation process occurs in four stages – hydrolysis, acidogenesis, acetogenesis and methanogenesis – which symbiotically produce intermediates and reaction products for the following stage (Fig. 3) (Appels et al., 2008; Tchobanoglous, 2014).

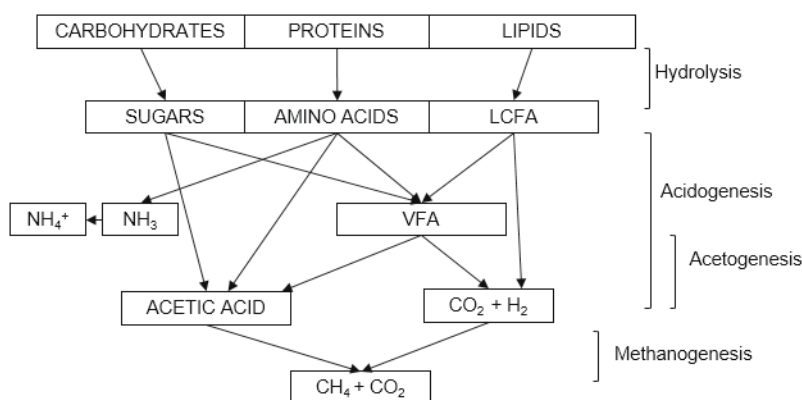


**Figure 3.** Schematic diagram of the steps of microbiological degradation pathways in anaerobic digestion. Adapted from Appels et al. (2008) and Tchobanoglous (2014). LCFA: long chain fatty acid, VFA: volatile fatty acid.

In hydrolysis, extracellular enzymes excreted by fermentative bacteria hydrolyze macromolecules (proteins, polysaccharides, and fats) into amino acids, sugars, and long chain fatty acids. In acidogenesis, these hydrolyzed constituents are fermented into new bacterial cell material but also into volatile fatty acids (VFAs), alcohols, CO<sub>2</sub>, H<sub>2</sub>, NH<sub>3</sub>, and H<sub>2</sub>S. Subsequently in acetogenesis, VFAs and other intermediates generated in acidogenesis are further converted into acetic acid, CO<sub>2</sub>, and H<sub>2</sub>. In the last stage, methanogenic microorganisms (archaea) use acetic acid and H<sub>2</sub> as substrates for methane production: acetic acid is split into CH<sub>4</sub> and CO<sub>2</sub> by aceticlastic methanogens, while CO<sub>2</sub> is reduced by hydrogenotrophic methanogens through electron transfer from H<sub>2</sub>. Typically, aceticlastic methanogens produce 70% of the methane generated, while hydrogenotrophic methanogens 30%; the shares can however shift towards hydrogenotrophic pathway due to high ammonia concentration (Chen et al., 2008).

Each microorganism in AD has optimum temperature and pH, therefore, unless a two-stage AD is applied, the AD process conditions compromise between the optimal conditions (Harirchi et al., 2022).

The predominant temperature ranges used are mesophilic (25–40°C) and thermophilic (50–60°C), although psychrophilic (<20°C) processes can also be utilized (Mao et al., 2015). Thermophilic temperatures often provide higher methane yields due to the increase of the biochemical reaction rates (brock book), which also enable the use of shorter retention times in AD operation. However, mesophiles are regarded more robust against process changes and inhibition than thermophiles due to their slower growth rate, increasing the stability of AD operation (Harirchi et al., 2022). The four stages of AD are most productive at slightly different pH: hydrolysis is optimal at pH above 6.0, acidogenesis at 5.5–8.0, acetogenesis at 6.5–8.0, and methanogenesis at 7.0–8.0 (Harirchi et al., 2022). Therefore, AD is performed at near neutral pH from 7 to 8, which is achieved using buffering substances, such as CaCO<sub>3</sub>, but the buffering capacity can also be completely inherent by the presence of ammonium nitrogen (Chen et al., 2008). Usually, low pH indicates VFA accumulation that inhibits methanogenesis, whereas too high pH can cause free ammonia (pK<sub>a</sub> 9.25) accumulation that inhibits microorganisms' growth (Harirchi et al., 2022).

Temperature determines the rate of digestion, particularly the rate of hydrolysis and methanogenesis, which together with the substrate's volatile matter content, determine the AD processing parameters, *i.e.*, hydraulic retention time (HRT), solids retention time (SRT), and organic loading rate (OLR). HRT equals to the liquid volume in the reactor divided by the volume of the liquid removed, and it usually varies for sludges from 20 to 30 d (Tchobanoglous, 2014). Too short HRT usually causes VFA accumulation, while too excessive HRT results in inefficient utilization of substrate (Mao et al., 2015). While HRT defines the time the substrate stays in digester, SRT defines the time the microorganisms stay in the digester. In completely mixed reactors, *e.g.*, in continuously stirred tank reactors (CSTR), HRT equals SRT because there is no biomass recirculation (Mao et al., 2015). OLR is the amount of organic matter (defined as VS or chemical oxygen demand (COD)) that is fed into the digester in a specific time frame. Too high OLR can lead to overloading where the faster biochemical reactions (hydrolysis/acidogenesis) produce more intermediates than the slower reactions (methanogenesis) are capable of consuming (Mao et al., 2015). When OLR is lower than could be used, optimum methane yields are not achieved (Mao et al., 2015). OLR and HRT are interconnected in a sense that as OLR is increased, HRT is decreased.

Being a biological process, AD is prone to inhibition where the growth and activity of microorganism are decreased (Chen et al., 2008). Inhibition can take place due to improper process conditions leading for example to ammonia inhibition and VFA accumulation. Ammonia inhibition often follows from the hydrolysis and acidogenesis of high protein content substrates which release extensively ammonia nitrogen (Mao et al., 2015). In the lack of sufficient buffering capacity, the non-ionizable form of ammonia (NH<sub>3</sub>) permeates cell membranes of methanogens, decreasing their intracellular pH and disrupts cell homeostasis (Chen et al., 2008). Ammonia can also inhibit specific methanogenic enzyme reactions (Rajagopal et al., 2013). Nitrogen deficiency can also cause operational issues due to low buffering, which can lead to VFA accumulation and pH decrease (Bayr and Rintala, 2012). The balance between NH<sub>3</sub> and its ionizable form, ammonium (NH<sub>4</sub><sup>+</sup>), is dependent on the prevailing temperature and pH, and therefore, thermophilic digestion has an increased risk for ammonia inhibition. Ammonia accumulation can lead to process failure, decreased methane yields, and VFA accumulation due to disturbance in the microbial relationships between H<sub>2</sub> producing and converting microorganisms (Rajagopal et al., 2013). VFA accumulation can also result from too short retention times which fail to provide sufficiently time for VFA utilizing microorganism to grow (Mao et al., 2015). This often appears as increased propionate concentrations due to the slow growth rate of propionate degrading microorganisms.

Microorganisms' activity can also be slowed down or ceased by insufficient trace element availability or their toxicity and by certain compounds present in the AD feedstock (Chen et al., 2008). For example, lack

or non-bioavailable form of necessary trace elements can limit microorganisms activity (Chen et al., 2008), but too high concentration can be inhibitory to methanogens (Zhang et al., 2015). Many trace elements are classified as heavy metals, which restricts their excessive supplementation concerning the environmental load upon the land application of digestate. There is also a wide range of organic compounds which are potentially inhibitory for microorganisms and can accumulate in the digestion process (Chen et al., 2008). Such compounds that have been identified causing inhibition include different benzenes, furfurals, phenols, alcohols, ethers, ketones, acrylates, amines, amides, and pyridine (Chen et al., 2008; do Carmo Precci Lopes et al., 2018; Seyedi et al., 2019).

The residue from AD, so called digestate, contains partially degraded organic matter, microbial biomass, and inorganic nutrients. Digestates are characterized with decreased COD, total VFA (TVFA), and VS contents and increased contents of mineralized nitrogen ( $\text{NH}_4^+$ ) and pH respective to the undigested sludge due to organics degradation (Luste and Luostarinen, 2010). However, some compounds are not degraded in AD, for example lignin, that is not biodegradable under anaerobic conditions by enzymatic hydrolysis and remains unchanged in lignocellulosic digestates, while cellulose and hemicellulose are removed by up to 70% and 27%, respectively (Bayr and Rintala, 2012). The carbon content decreases in digestates from that of sludge due to organics conversion into biogas, but the total nutrient contents are conserved. The digestate composition and characteristics, *e.g.*, carbon, nitrogen, and phosphorous contents, define its quality for end-use applications. Examples of the effect of AD on sludge characteristics are shown in Table 2.

**Table 2.** Characteristics of municipal sewage sludge (Astals et al., 2012) and pulp and paper mill primary and secondary sludges (Bayr and Rintala, 2012) before and after anaerobic digestion.

Parameter	Municipal sewage sludge			Pulp and paper mill sludge			
	Raw	Mesophilic digestate	Thermophilic digestate	Raw primary	Primary digestate	Raw secondary	Secondary digestate
TS (%)	2.9–3.3	2.0–2.3	2.1–2.4	2.7–3.8	2.2 ± 0.2	3.6–4.0	2.2 ± 0.2
VS (%)	2.1–2.5	1.3–1.5	1.4–1.6	2.2–3.2	1.6 ± 0.1	2.9–3.3	1.7 ± 0.1
pH	6.3–6.8	7.5–8.0	7.6–8.0	6.2–6.8	6.8–7.1	7.6–7.8	6.6–6.8
COD (g/L)	36.5–45.6	21.0–25.6	23.6–27.4	1.4–1.8 <sup>a</sup>	2.1 ± 0.2 <sup>a</sup>	0.4–0.7 <sup>a</sup>	2.4 ± 0.3 <sup>a</sup>
TVFA (mg/L)	471–1598	0–66	966–1558	n.a.	50 ± 20	n.a.	60 ± 40
$\text{NH}_3$ (mg N/L)	69–145	583–627	747–834	<1 <sup>b</sup>	0.8 ± 0.1 <sup>b</sup>	8–31 <sup>b</sup>	0.7 ± 0.0 <sup>b</sup>
BMP mesophilic (L $\text{CH}_4$ /kg VS)	260–420	n.a.	n.a.	210 ± 40	n.a.	50 ± 0	n.a.
BMP thermophilic (L $\text{CH}_4$ /kg VS)	240–350	n.a.	n.a.	230 ± 20	n.a.	100 ± 10	n.a.

n.a. not available/applicable; TS, total solids; VS, volatile solids; COD, chemical oxygen demand; TVFA, total volatile fatty acids; BMP, biochemical methane potential

<sup>a</sup> soluble COD

<sup>b</sup> as  $\text{NH}_4\text{-N}$

Because sewage sludge has tendency to accumulate pollutants originating from wastewater, such as heavy metals, organic pollutants, and pathogens (Mulchandani and Westerhoff, 2016), its use in land applications is strictly regulated by EU (Kacprzak et al., 2017), while agricultural and biowaste digestates are typically utilized as fertilizers and soil improvers in agriculture. Sewage sludge digestates are therefore primarily incinerated for energy recovery in Middle-Europe (Catenacci et al., 2022). Generally, the use of digestate in fertilization is applicable for short transportation distances because of the high digestate volumes and moisture contents (70–90% depending on the dewatering technology). Owing to the digestate high moisture content, the energy gain from its direct incineration is diminished due to the need of prior

thermal drying (Stoica et al., 2009). In addition, sewage sludge digestate is considered as waste, subjecting it to waste incineration regulations which require separate waste incineration plants charging gate fees (Kacprzak et al., 2017).

## 2.2.2 Thermal treatments

Thermal treatments generally indicate biomass heating to a certain temperature for a certain period. The use of increased temperatures in biomass or sludge treatment enables more rapid decrease in biomass volume and improvement in quality by diminishing contaminant contents and possibilities for further spontaneous putrefaction (Bougrier et al., 2008; Gao et al., 2020). Another advantage of thermal treatments over biochemical processes is the full exploitability of the organic fraction in biomass, which offers several utilization opportunities for the biomass being treated (Di Costanzo et al., 2021). Thermal treatments can be divided into mild thermal treatments and thermochemical conversion methods. The mild thermal treatments simply rely on heating up the biomass to temperatures of 70–180°C, benefitting pathogen inactivation and organics solubilization (Zhen et al., 2017). Such treatment technologies include hygienization and thermal pre-hydrolysis (THP), which last about 30–60 min (Astals et al., 2012; Higgins et al., 2017). Hygienization has become more common at industrial scale primarily with food and biowaste AD due to the tightened EU regulations concerning the hygienic standards of animal by-products not intended for human consumption (EC No 1774/2002), while THP has been adapted to biogas plants since a decade ago (Bougrier et al., 2008). Thermochemical conversion technologies employ increased temperatures (>180°C), and the residence times range from 0.5 h up to 8 h (Gao et al., 2020), converting the biomass feedstock into three product fractions: solid char, liquid, and gas. Traditionally, thermochemical conversion has been utilized in the biorefining of virgin biomasses, such as lignocellulose, while their employment in sludge or digestate management are still being investigated as only a few of the related studies refer to industrial-scale or pilot-scale tests (Catenacci et al., 2022). An overview of the most common thermal treatments applied or studied for sludge or digestate treatment is presented in Table 3.

The occurrence of chemical bond cleaving reactions differentiates hygienization and THP from thermochemical conversion technologies. In thermochemical conversions, bonds between carbon, hydrogen and oxygen are being broken down through dehydration, decarboxylation, and hydrolysis reactions, releasing chemical energy and altering the sludge structure (Funke and Ziegler, 2010; Ischia and Fiori, 2021). These reactions typically decrease the amount of oxygen in the biomass, either by supplying excessively or stoichiometrically oxygen for the bond-cleaving reactions (combustion) or by completely restricting the oxygen availability (pyrolysis). Combustion, however, differs from the other thermochemical processes by obtaining merely thermal energy, whereas hydrothermal carbonization (HTC), hydrothermal liquefaction (HTL), pyrolysis, and gasification, which are characterized by lower temperatures and inert atmospheres, obtain thermal energy and increase the biomass value as product materials (Sousa and Figueiredo, 2016). Furthermore, thermochemical treatments can be enhanced with the use of catalysts which increase the selectivity of the desired product, its commercial potential and process efficiency in terms of decreasing coke deposition (Gao et al., 2020).

**Table 3.** Overview of the thermal treatments used or studied for wastewater sludge treatment and/or management.

Technology	Reaction conditions	Feed	Products (yield <sup>a</sup> in %)	Features	References
Hygienization	T = 70°C t = 1 h	>1%TS	Hygienized sludge	Pre- or post-treatment for AD Pathogen inactivation	Astals et al., (2012)
Thermal pre-hydrolysis	T = 120–180°C t = 30–60 min	>1%TS	Pre-hydrolyzed sludge	Pre-treatment for AD Pathogen destruction Increases biodegradability and improves biogas production Decreases sludge viscosity	Bougnier et al. (2008) Higgins et al. (2017)
Thermal drying	T = 70–180°C t = 0.5–2 h p = 1 bar	15–40% TS	Dried sludge (60–95% TS)	Pre-treatment for thermochemical conversions Moisture removal Pathogen destruction	Flaga (2007)
Hydrothermal carbonization (HTC)	T = 180–250°C t = 0.5–8 h p = 20–40 bar	5–30% TS	Hydrochar (yield 45–70%) Liquid filtrate (5–30%) Gas (2–25%)	Targets char production Increases dewaterability Liquid with biochemical methane potential Pathogen destruction	Libra et al., 2011 Catenacci et al., 2022
Hydrothermal liquefaction (HTL)	T = 250–350°C t = 0.5–8 h p = 100–150 bar	5–30% TS	Biochar Bio-crude oil Aqueous liquid Gas (CO <sub>2</sub> )	Targets liquid production Increases dewaterability Pathogen destruction Catalysts (NaOH) and solvents (acetone/ethanol) used for HTL of sewage sludge	Mulchadani and Westerhoff 2016
Pyrolysis	T = 400–900°C t = 10–60 min p = 1 bar	80–95% TS	Biochar (12–35%) Pyrolysis oil (30–75%) Gas (13–35%)	Conducted in the absence of O <sub>2</sub> Defined according to process conditions into slow (torrefaction), intermediate and fast pyrolysis Destroys pathogens, organic compounds	Libra et al., 2011
Gasification	T = 800–900°C t = 10–20 s p = 1 bar	75–95% TS Small particle size	Syngas (H <sub>2</sub> , CO) (85%) Ash	Sub-stoichiometric amount of O <sub>2</sub> High tar production causes operational issues	Gao et al., 2020 Catenacci et al., 2022 Libra et al., 2011
Combustion/incineration	T = 700–1400°C t = seconds p = 1 bar	>40% TS	Ash Exhaust gas	Stoichiometric amount of O <sub>2</sub> Reduces sludge volume by up to 90%, concentrates metals in the ash, and destroys organic pollutants and pathogens Exhaust gas requires treatment	Liang et al. (2021)

<sup>a</sup>yield = realized amount of product/total initial amount of feedstock

The different thermochemical conversion technologies of biomass share similar reaction pathways, in which the biomass solids degrade into liquid and gaseous products and rearrange into new solid structures (Libra et al., 2011). However, depending on the type of the treatment technology and the biomass feedstock composition, the characteristics, yields and applicability of the char, liquid, and gas products vary. For example, at pyrolytic conditions, hemicelluloses decompose at temperatures of 200–400°C and cellulose at 300–400°C, while lignin has gradual decomposition between temperatures of 180°C and 600°C. In contrast, at hydrothermal conditions, the same lignocellulosic constituents start to decompose already at lower temperatures; hemicelluloses at 180–220°C, cellulose approximately at 220°C, and lignin at 180–220°C (Libra et al., 2011). This is because hydrothermal conditions enable hydrolysis reactions that have low activation energy and thereby biomass decomposition begins at lower temperatures than in pyrolysis where no oxidation of biomass takes place due to absence of oxygen. Hence, the treatment temperature largely affects the products' composition, which can though be manipulated with pH adjustments to some degree (Wang et al., 2018). Gasification and hydrothermal liquefaction (HTL) are excluded from further inspection for they are predominantly used for syngas (Gao et al., 2020) or bio-oil production (Mulchandani and Westerhoff, 2016), respectively.

To differentiate the solid products from HTC and pyrolysis, char from HTC is typically named as hydrochar for being produced as a solid-liquid mixture, while char from pyrolysis is named as biochar for resembling charcoal but having intended application elsewhere than in energy generation (Catenacci et al., 2022). Hydrochar generally has higher H/C and O/C ratios than biochar because during HTC the occurrence of decarboxylation reactions relative to dehydration reactions is higher than during pyrolysis, *i.e.*, the carbon content is more decreased relative to hydrogen or oxygen contents (Libra et al., 2011). This leads to biochar often having higher carbon content than hydrochar, which could determine their order of preference in carbon sequestration applications, for example. Hydrochar and biochar have been studied in several applications including agricultural use (Chu et al., 2020), nutrient recovery (Zhao et al., 2018), adsorption medium for heavy metals and pesticides (Nguyen et al., 2021), carbon sequestration (Breulmann et al., 2017), inhibition prevention in AD (Torri and Fabbri, 2014), and energy recovery (Danso-Boateng et al., 2015). In contrast, the liquid or oil products from HTC and pyrolysis have been suggested as sources for chemicals (Chorazy et al., 2020), nutrients (Roy et al., 2022), and biogas (Salman et al., 2017).

### 2.2.2.1 Hydrothermal carbonization

Of the thermal treatments used, HTC represents a promising technology owing to its relatively low temperature range, applicability to moist biomass, and known technology (Wang et al., 2018). It has attracted interest for its potential role in the refining of various virgin biomasses (Pecchi and Baratieri, 2019) and in the management of sludges (Ahmed et al., 2021; Lin et al., 2015). The HTC has reduced need for prior dewatering of the sludge, and enables lower treatment temperatures (180–300°C) compared with other thermochemical technologies (Table 3). In addition, the atmospheric emissions (CO<sub>2</sub> and ammonia) are reported being lower than in pyrolysis (Celletti et al., 2021). HTC transforms sludge into easily dewaterable slurry, and 5–10% of the amount of sludge is converted to gas composed mainly of CO<sub>2</sub> with traces of CH<sub>4</sub>, H<sub>2</sub> and CO (Danso-Boateng et al., 2015). The slurry is separated by filtration or centrifuge into hydrochar and a liquid filtrate, oftentimes called process water (Berge et al., 2011).

The moisture in the biomass functions as an aqueous medium and has an essential role as solvent, reactant, or catalyst in HTC (Catenacci et al., 2022), which results from the autogenously generated pressure of 20–40 bar (Fang et al., 2018). In addition of functioning as a solvent, water can be a

transportation medium of the reaction intermediates and degradation fragments (Funke and Ziegler, 2010). During HTC, sludge undergoes several reactions which produce gaseous compounds, soluble products in the liquid phase, and precipitates from the degraded sludge components back into the solid phase (hydrochar). These reactions include hydrolysis, dehydration, decarboxylation, condensation, and polymerization (Fig. 4) (Funke and Ziegler, 2010). Due to sludge complexity and reactor temperature profiles, many of these reactions occur in parallel (Libra et al., 2011). However, not all sludge undergoes these reactions, as in fact, hydrochar is produced through two distinct reaction pathways. The insoluble or non-hydrolyzed components in the sludge are converted by solid-solid pyrolysis-like reactions into *primary char* (Ischia and Fiori, 2021; Keiller et al., 2019), while the fraction of sludge which experiences hydrolysis decomposes into degradation products in the water medium, where they recondense and repolymerize (solid-liquid reactions) forming *secondary char* (Ischia and Fiori, 2021; Keiller et al., 2019). The secondary char is often composed of coke (Keiller et al., 2019) and has hydrophobic surface because of the repolymerized decomposition products that deposit on the hydrochar surface (Ischia and Fiori, 2021). The dissolved intermediates that do not repolymerize or condense, possibly because of the short residence time, remain in the liquid phase and are recovered in the liquid product after dewatering the slurry. In other words, the liquid product composition can be controlled by selecting suitable treatment temperature and residence time that result in desired concentrations of organics and degradation products. Sludge carbonization is a complex series of these reactions that are dependent on the biomass component structure and chemical properties (Ischia and Fiori 2021). Due to this complexity and the occurrence of several mass transfer phenomena, a full understanding of the reaction kinetics is still lacking.

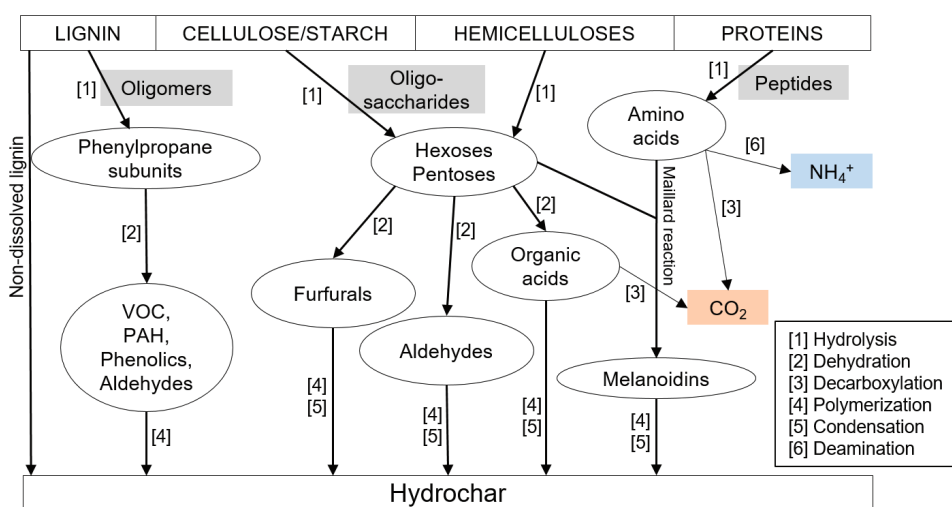


**Figure 4.** Simplified reaction mechanism of the main sludge constituents during hydrothermal carbonization. The sludge composition and reaction conditions (residence time and solid load) determine the amount and type of reaction intermediates remaining in the liquid product. Reaction intermediates with grey background illustrate high molecular weight intermediates that are subjected to further degradation. Adapted from Ischia and Fiori, (2021), Keiller et al. (2019), Libra et al. (2011). VOC: volatile organic compound, PAH: polycyclic aromatic hydrocarbon

The sludge composition and structure determine the extent of the hydrothermal reactions. Pure feedstocks composed of one component can be fully carbonized, whereas a full carbonization of sludge constituents that have chemical bonds between the individual polymer structures, and thus, increased activation energies, would require longer residence times than applicable with HTC (Wang et al., 2018).

For example, in lignocellulosic sludges, insoluble lignin prevents the degradation of cellulose and hemicelluloses by their enclosure and by deposition on cellulose surface (Li et al., 2014; Wang et al., 2018). In addition, crystalline cellulose is resistant to hydrolysis if the treatment severity is insufficient, yielding nano-sized porous structures in hydrochar, while the absence of such crystalline structures yields carbonaceous nanoparticles (Libra et al., 2011). Hence, sludges having a high degree of lignin and/or crystalline cellulose, experience more solid-solid conversion reactions, preserving more of the initial biomass structure in the hydrochar, and producing more primary char than sludges with less resistant constituents (Wang et al., 2018). As a rule, insoluble lignin converts into primary char, whereas soluble lignin, hemicelluloses, cellulose, and other non-lignocellulosic compounds (lipids, phenolics, free sugars) react through dissolved intermediates forming secondary char (Keiller et al., 2019).

Proteins that constitute plant cell walls are prone to quickly denature at elevated temperatures, making them insoluble and sticking on the cell wall, being directly incorporated into the hydrochar (Keiller et al., 2019). An indication of protein insolubility is the similar level of nitrogen in the sludge and in its respective hydrochar. Generally, however, proteins are water soluble, and at elevated temperatures and in the presence of pressurized water, they are converted into amino acids by hydrolysis of peptide (Wang et al., 2018). Peptide bonds are more stable than the glycosidic bonds in cellulose and starch, thus their hydrolysis and depolymerization is slower (Rogalinski et al., 2008). Protein hydrolysis is however enhanced by acidity of the reaction medium, which in the presence of carbohydrate degradation is increased due to the increasing sugar monomer concentrations (Rogalinski et al., 2008). The released amino acids experience decarboxylation and deamination reactions, producing for example ammonia that is present as ammonium ions in the liquid phase (He et al., 2015). Higher HTC temperatures tend to convert more protein into ammonium (He et al., 2015). With sufficient residence time, the free amino acids and sugars can start to undergo Maillard reactions producing melanoidins (aldehydes, furans, pyrroles, pyrazines, and pyridines) which give hydrochar and filtrates brown-colored appearance with characteristic odor (Danso-Boateng et al., 2015; He et al., 2013). Nitrogen containing sludge thus leads to the formation of aromatic nitrogen structures in the hydrochar (Wang et al., 2018).

The outcome of HTC depends not only on the feedstock composition but also on the applied temperature, residence time, and solid load. The treatment temperature governs properties of the water medium of which viscosity decreases as temperature increases, leading to enhanced penetration into the sludge matrix and the initiation of the decomposition reactions (Funke and Ziegler, 2010). The temperature also determines the reaction rates, providing the energy needed to exceed the activation energies of the bond-breaking reactions (Wang et al., 2018). Temperature increases from 230°C to 250°C have led to increased decreases of H/C and O/C ratios in sewage sludge (Kim et al., 2014) and pulp and paper mill sludge (Mäkelä et al., 2016), indicating increased degree of dehydration and decarboxylation reactions. In addition, the degree of solid-solid reactions of the non-dissolved fragments are mostly dependent on the temperature (Wang et al., 2018). The residence time represents a variable that determines the extent of the polymerization and condensation reactions which ultimately lead to the formation of secondary char. Hence, by prolonging residence time hydrochar yield (the share of the product recovered of the initial feedstock amount) could be increased by providing more time for the reactions of the dissolved fragments that form secondary char to occur (Funke and Ziegler, 2010). Similarly, the concentration of different fragments in the liquid product can be affected by the length of the residence time (Ferrentino et al., 2020). The effect of solid load on HTC outcome has been less extensively studied than that of temperature and time. In general, however, with increased solid loads, the fragmented monomer concentration rises faster than with lower solid loads, which could initiate their repolymerization earlier, leading to increased precipitation (Funke and Ziegler, 2010). Thus, high solid loads can be worthwhile to shorten the residence



time and thus the energy demand of HTC. Lower solid loads have been reported to release more carbon into the liquid phase, resulting in liquids of increased COD (Aragón-Briceno et al., 2020). As the liquid products contain organics, they are classified as wastewater, which subjects them for further treatment requirements.

The dehydration reactions taking place under the HTC conditions improve the sludge dewaterability, by releasing hydrophilic proteins and carbohydrates from sludge. In addition, the precipitates on hydrochar surface are hydrophobic, further increasing water repulsion (Wang et al., 2014). The dewaterability is more improved when higher treatment temperatures are used (Wang et al., 2014), but the increase becomes less apparent at temperatures above 200°C (Kim et al., 2014). Compared with the temperature applied, the influence of the residence time on dewaterability is less pronounced, but a 30 min residence time has been observed to be a turning point for a significant dewaterability improvement (Wang et al., 2014), implying HTC should last a minimum of 30 min. Studies concerning the dewatering technique of the HTC slurries have been rare. However, it has been studied that dewatering at elevated temperatures (up to 180°C) outperforms dewatering at room temperature (18°C), producing hydrochar with a moisture content of below 30%, while at 18°C the moisture content remained at approximately 40% (Wang et al., 2014). The separation technique of hydrochar and filtrate can also affect the following nutrient contents of the hydrochar and liquid product (Libra et al., 2011).

#### 2.2.2.2 Pyrolysis

Pyrolysis is typically used for low-moisture, usually pre-dried, biomasses and conducted in the absence of oxygen (Libra et al., 2011). The products from pyrolysis of biomass include biochar, pyrolysis gas ( $H_2$ ,  $CO$ ,  $CO_2$ ,  $CH_4$ ), and pyrolysis oil (Catenacci et al., 2022). The pyrolysis temperature directly affects the product distribution and yields, and, as a rule, lower pyrolysis temperatures ( $\sim 290^\circ C$ ) produce biochar, moderate temperatures ( $\sim 500^\circ C$ ) pyrolysis oil, and higher temperatures ( $\sim 750\text{--}900^\circ C$ ) mainly generate pyrolysis gas (Azua et al., 2013; Bridgwater, 2012). Pyrolysis can also be defined according to the heat transfer rates and residence times used: (1) in slow pyrolysis (long residence time and slow heat transfer) biochar is the main product, while (2) intermediate pyrolysis and (3) fast pyrolysis employ shorter residence times and faster heat transfer rates. Thus, the intermediate and fast pyrolysis target to produce pyrolysis oil, but the oil from intermediate pyrolysis is of lower viscosity and tar content than that the oil from fast pyrolysis (Hornung, 2012). The intermediate pyrolysis oil is also characterized by its tendency to separate into two phases: a tarry organic phase (bio-oil) (52–57% of the pyrolysis oil) and an aqueous phase (*i.e.*, pyrolysis liquid 43–48%) (Bridgwater, 2012; Park et al., 2008; Torri and Fabbri, 2014).

Pyrolysis has attracted interest in the refinement of digestates owing to the digestates' high amount of poorly biodegradable and/or unbiodegradable organics, which can be exploited with pyrolysis. The primary aim of pyrolysis integration into biogas plants is to produce digestate biochar which is potentially more valuable in further use than digested and composted sewage sludge as such (Sousa and Figueiredo, 2016): biochar is of smaller volume, and more suitable for carbon sequestration and for fertilizer use than digestate (Breulmann et al., 2017; Kambo and Dutta, 2015). Biochar also has higher energy value than digestate, therefore, pyrolysis integration to biogas plant could increase the overall energy efficiency of the plant if biochar is combusted for energy (Salman et al., 2017).

The bio-oil fraction from pyrolysis is considered a useful product for fuel and chemical manufacturing (Bridgwater, 2012), because it contains a variety of compounds including acids, alcohols, amines, and aldehydes originating from the sludge and the reactions taking place in the pyrolysis itself, and only 2–10

w% of water (Park et al., 2008). On the contrary, the pyrolysis liquid from sewage sludge digestate often represents a waste management issue because it is mostly comprised of water, while the other constituents depend on the pyrolysis temperature (Fonts et al., 2012), the biomass ash content and the number of OH-groups in the sewage sludge digestate (Fonts et al., 2009). The organic compounds in pyrolysis liquid (polar ketones and amines (Park et al., 2008), VFAs, ammonium-nitrogen, and phenolics (Seyedi et al., 2019)) subject it to disposal regulations and require careful management (Torri and Fabbri, 2014).

## 2.2.3 Products utilization after thermal treatment

### 2.2.3.1 Char fraction

Hydrochar and biochar can be utilized in energy production, carbon sequestration, and nutrient recovery. Energy can be recovered with direct combustion as fuel. Nutrients can be recovered *via* conventional soil application of chars on agricultural fields or leaching of nutrients from char (Zhao et al., 2018). The research on hydrochar applicability have mainly attributed the energy recovery potential of hydrochar, whereas biochar has been more often studied concerning soil application. Chars have also been studied as an absorbent medium, *e.g.*, pollutant and ammonium removal from water, because of their porous structure, surface functional groups, and surface charge that resemble activated carbon (Nguyen et al., 2021). The distribution of sludge constituents and reaction products, such as nutrients, heavy metals, and minerals between the char and liquid products define their further management and utilization alternatives (Merzari et al., 2019).

Direct energy recovery from chars is favored by the decreased H/C and O/C ratios and increased higher heating values (HHV) compared with the initial feedstock. A negative aspect concerning combustion of chars is the increased ash content, which particularly concerns sewage sludge digestates (Catenacci et al., 2022). High ash contents are problematic because ash causes slagging and fouling in combustion furnaces (Parmar and Ross, 2019). Thus, thermochemical conversion conditions that produce chars with lower ash, sulfur, and nitrogen contents than the original sludge have been investigated to further support hydrochar combustion over sludge. For example, acid leaching has been suggested for reducing the ash content prior char combustion (Marin-Batista et al., 2020). However, even though the moisture content of chars is reduced compared to sludge, it still could lead to poor thermal efficiency in combustion (Lucian and Fiori 2017).

Nutrient recovery from char has been of interest as sludge derived chars retain much of the Ca, K, and P present in the original sludge (Libra et al., 2011). Compared to digested sludge, chars have improved stability and lower volume owing to their altered solids structure and low moisture content. Thus, chars can be more easily stored for longer periods of time and transported longer distances, without emitting residual CH<sub>4</sub> and CO<sub>2</sub> from storing nor increasing CO<sub>2</sub> emissions from transportation (Catenacci et al., 2022). On the other hand, during thermochemical conversion, nitrogen is distributed between all the three products (char, liquid, and gas), which is markedly influenced by the treatment temperature and time. For example, increased temperatures convert more protein into ammonia that mainly resides in the liquid product as ammonium nitrogen (He et al., 2013). Even up to 40–60% of nitrogen in digested sludge can solubilize into liquid phase during HTC (Aragón-Briceño et al., 2020). In contrast, the quantity of dissolved phosphorous decreases with temperature increase (Huang and Tang, 2015). Phosphorous recovery and bioavailability has been of discussion because it is largely dependent on the use of phosphorous precipitation chemicals at municipal WWTP. Such chemicals, usually Al or Fe salts, bind to phosphorous,

which likely prevent its dissolution into the liquid phase and possibly also its uptake by plants (Ylivainio et al., 2021).

Comparing hydrochar and biochar, hydrochar has a less stable carbon structure than biochar (Breulmann et al., 2017), which increases the rate of decomposition of hydrochar on soil and therefore hydrochar tends to release nutrients more quickly, making it unsuitable for long-term fertilization (Jager et al. 2020). For similar reasons, the carbon sequestration potential of hydrochar compared to biochar is argued to be poorer (Breulmann et al., 2017). Both chars, however, evidently store carbon in soils better than their non-thermally treated counterparts (Adjuik et al., 2020).

One of the matters that affect the applicability of the char as nutrient source in agriculture or in carbon sequestration is the heavy metal concentration and environmental load, as thermochemical treatments can lead to heavy metal accumulation in the char fractions (Kambo and Dutta, 2015). This particularly concerns municipal sewage sludge originating chars. The heavy metal load can be decreased by considering the loading rate of the char with periodical fertilization (Libra et al., 2011). Other contaminants present in wastewater sludges, *i.e.*, microplastics and pharmaceuticals, have been reported to be removed completely and/or partially by HTC, depending on the plastic polymer and HTC temperature (vom Eyser et al., 2015; Xu and Bai, 2022). Phytotoxicity of chars is another factor to be considered regarding their soil application. For example, furan content can limit plant growth, as well as high Na content and high pH which decrease plant nutrient uptake (Celletti et al., 2021). High pH of char could though replace lime supply to fields (de Jager et al., 2020).

### 2.2.3.2 Anaerobic treatability of liquids

The liquid product fraction from thermochemical treatments is of large quantities, often dilute, and regarded as a problematic wastewater stream. However, as the liquid product contains several organic degradation products from the conversion reactions it has been proposed to be utilized in methane production in AD together with the main substrate. Other suggested utilization possibilities for the liquid fraction include circulation in the HTC process to improve fuel properties of hydrochar (Kabadayi Catalkopru et al., 2017) and as a growth medium for algae as the liquid fraction can provide readily available nutrients and trace elements (Roy et al., 2022).

Integration of the liquid management through AD in connection with HTC or pyrolysis can contribute to the energy demand of the thermal process by producing biogas (Wirth et al., 2012). HTC liquid has been proven to degrade relatively fast compared with organic wastes conventionally used in AD (Wirth and Mumme, 2014), which could be due to the presence of easily degradable acetic acid in thermal liquids (Seyedi et al., 2019). In addition, the ease to digest thermal liquids can also be due to the absence of high-molecular weight compounds, which accelerates the first hydrolysis stage of AD (Wirth et al., 2015). However, sole digestion of thermal liquids may require nutrient supplementation for the microorganisms to function properly, particularly when nonbioavailable iron-precipitated nutrients are present (Wirth et al., 2015; Wirth and Mumme, 2014). In co-digestion of thermal liquid and main substrate, nutrient and trace element supplementation may not be needed, as conventional substrates, such as sewage sludge, can provide them sufficiently (Seyedi et al., 2019; Wirth and Mumme, 2014). In contrast, the concern with co-digestion is the possible presence of inhibitory compounds in the liquids, as methanogenesis has been determined being the rate-limiting step because of compounds such as phenols, benzenes, aldehydes, and nitrogen-containing compounds (Seyedi et al., 2019; Wirth et al., 2015). Therefore, use of acclimated substrate for the co-digestion of the liquids is recommended (Seyedi et al., 2019).

Different HTC and pyrolysis conditions result in different liquid compositions due to the temperature and residence time that define which degradation reactions take place and the degree the reactions of the intermediate products proceed. HTC liquids from sewage sludge have seemed suitable for AD if the HTC temperatures are lower than 180–200°C and the residence times below 15–30 min (reviewed in Merzari et al. (2019)). Most essential characteristics of the liquids regarding AD include COD, TS, VS, TVFA, ammonia, pH, and biochemical methane potential (BMP) (Holliger et al., 2016), which are influenced besides by the treatment conditions also by the feedstock (Table 4). For example, the alkalinity of the liquid seems highly dependent on the protein and nitrogen content of the initial sludge or biomass (Aragón-Briceño et al., 2020; Berge et al., 2011). As high solid loads result in liquids of high concentrations of organic and inorganic compounds, it could be presumed that high TS content sludge could produce liquids of high methane productivity. Recent research however suggests that beyond 15% TS load in HTC, a saturation point for the contents of COD and VFA exists (Aragón-Briceño et al., 2020).

**Table 4.** Anaerobic digestion related characteristics of selected liquid products from hydrothermal carbonization and pyrolysis.

Sludge	Treatment conditions	BMP (L CH <sub>4</sub> /kg COD)	COD (g/L)	pH	Reference
Digested sewage sludge (HTC for 30 min)	180°C at 16.5% TS	325 ± 11	56.20	7.40	Marin-Batista et al. (2020)
	210°C at 16.5% TS	279 ± 9	61.50	7.90	
	240°C at 16.5% TS	<20	53.90	8.90	
Digested sewage sludge (HTC for 60 min)	160°C at 4.5% TS	260	12.60	9.15	Aragón-Briceño et al. (2017)
	220°C at 4.5% TS	277	13.00	7.14	
	250°C at 4.5% TS	226	12.20	8.08	
Pulp and paper mill primary sludge (HTC for 3 h)	180°C at 12.5% TS	n.a.	126	5.19	Merzari et al. (2021)
	200°C at 12.5% TS	n.a.	345	4.79	
	220°C at 12.5% TS	n.a.	253	4.35	
Pulp and paper mill secondary sludge (HTC for 3 h)	240°C at 12.5% TS	n.a.	331	4.07	Merzari et al. (2021)
	180°C at 12.5% TS	n.a.	24	7.17	
	200°C at 12.5% TS	n.a.	43	6.31	
Manure and maize digestate (pyrolysis for 45 min)	220°C at 12.5% TS	n.a.	67	7.40	Hübner and Mumme (2015)
	240°C at 12.5% TS	n.a.	81	6.93	
	330°C	199.1 ± 18.5	74.3	3.88	
	430°C	194.1 ± 18.8	75.6	4.31	
	530°C	129.3 ± 19.7	48.5	4.83	

n.a., not available; BMP, biochemical methane potential; COD, chemical oxygen demand; HTC, hydrothermal carbonization

The COD content determines the potential of the liquid to generate methane in AD as it reflects the extent of organic compound content in the liquid. During thermochemical treatment, hydrolysis reactions generate VFAs, soluble proteins, and benzenes, while the dehydration, condensation, polymerization, and aromatization reactions generate ammonium nitrogen, alkenes, phenolics and aromatic compounds (Danso-Boateng et al., 2015; Escala et al., 2013; Ferrentino et al., 2020). Lignocellulosic HTC liquids are characterized by containing lignin degradation products, including furfurals and phenols (Berge et al., 2011). The COD content can increase up to 10-fold respective to sewage sludge digestate before HTC treatment (Aragón-Briceño et al., 2017), and is typically constituted by VFAs to varying degree, the concentrations of which vary between 2.0–6.0 g/L (Danso-Boateng et al., 2015; Nyktari et al., 2017).

Because VFAs are also produced in acidogenesis during AD, the HTC liquids can provide more substrates for acetogenesis and methanogenesis. But high VFA contents can also inhibit methanogens if the buffering capacity of AD is not sufficient to prevent pH from declining. In addition, several organic compounds, such as glycerol and furfurals can inhibit the microorganisms, particularly if the methanogens are susceptible to phenolic compounds (Chen et al., 2008). Also too high concentrations of COD (30 g/L) could disturb the microbial balance in the digester, leading to over-acidification (Hübner and Mumme, 2015).

The degree of organic compounds (COD) in the liquid can correlate with the BMP of the liquid unless the COD is also constituted by inhibitory organics (phenols and PAHs) in addition to biodegradable constituents. Increased temperatures and residence times have been reported to decrease the BMP (Ferrentino et al., 2020), which presumably derives from further decomposition of organic acids and Maillard reaction products, such as furans and pyridines, which can be toxic to anaerobic microorganisms (Chen et al., 2008; Danso-Boateng et al., 2015). Other compounds which could be toxic to microorganisms include phenols, furfurals, and 5-hydroxymethylfurfural (5-HMF) which are produced from lignin degradation and sugar dehydration (Wirth and Mumme, 2014). Following from the inhibition of methanogens, methane content in the biogas can decrease (Danso-Boateng et al., 2015; Nyktari et al., 2017).

In addition to the presence of inhibitory compounds, pH and buffering capacity of the liquid product affect its digestion. Due to the presence of organic acids, the liquids are often acidic, but alkaline liquids are often generated from proteinaceous sludges (Aragón-Briceno et al., 2020; Berge et al., 2011). The pH is also dependent on the solid load in HTC, as the concentration of ammonium nitrogen increases with higher solids loads. Similarly, the acidity of the liquid products can increase at higher solids loads as more acidic degradation compounds are generated. Liquids having unsuitable high or low pH for digestion, can be diluted with AD effluent or used together with substrates which also need pH adjustments before AD (Nyktari et al., 2017). However, it has been shown that liquid of pH of 3.88 can be co-digested resulting in a neutral pH in the digester (Wirth and Mumme, 2014). The buffering capacity of the liquid products owes to the ammonium nitrogen or ammonia content which also support AD by being an essential nutrient for bacterial growth (Merzari et al., 2019). Clear and systematic effect of ammonia varies, as ammonia concentrations above 200–1000 mg/L but also as low as 15–30 mg/L have caused ammonia inhibition and rises in pH (reviewed in Merzari et al., 2019).

The prevention of thermal liquid inhibition on AD has also been investigated. As higher thermal treatment temperatures often result in increased inhibition of the liquid products, HTC temperatures below 180–200°C and pyrolysis temperatures of 330°C and 430°C have been recommended to be used. The inhibitory effect is particularly observed in AD batch tests (Hübner and Mumme, 2015; Yang et al., 2018), but continuous flow anaerobic reactor studies, which enable gradual increase in the feeding amount of the liquid, have proven microbial adaptation (Seyedi et al., 2020; Torri and Fabbri, 2014). For example, phenolic compounds are recalcitrant in AD, but at sufficiently low concentrations (about 2000 mg/L) and with inoculum adaptation they can be degraded (Wirth et al., 2015). Gradual increase of OLR from 1 to 5 g-COD/L d has been used to adapt the microorganisms for sole HTC liquid digestion (Wirth et al., 2015). AD has even been reported to detoxify the liquid product, degrading volatile organic compounds, such as furfural, 5-HMF, phenols, and catechol (Hübner and Mumme, 2015). Hydrochar can also be added in AD to support methane production (Ferrentino et al., 2020) and prevent inhibition by capturing the inhibitory compounds (Torri and Fabbri, 2014).

## 2.2.4 Deployment of HTC using scale-up assessments

HTC deployment for converting waste sludge into solid fuel has motivated to study its effect on the energy balance of AD plants (Wang et al., 2018). The integration concept of HTC and AD has raised interest for maximizing the biogas plant efficiency, HTC serving in the treatment of low-biodegradable and high moisture content digestates. Such integration also enables the exploitation of the liquid by-product from HTC in AD. For these reasons, HTC has attracted more interest over pyrolysis as it has higher energy recovery application potential of both the char and liquid products. HTC also avoids the pre-drying need of digestate and uses lower temperatures, theoretically resulting in more favorable energy balance than pyrolysis (Catenacci et al., 2022).

Research suggests that lower HTC temperatures and treatment times promote biogas production from the HTC liquid, whereas hydrochar properties and applicability are improved at higher HTC temperatures and times. Therefore, several scale-up assessments aim to determine the most energetically feasible HTC conditions and integration configuration (De la Rubia et al., 2018). The energy balance is affected by the TS load of the feedstock, higher solids contents (15–30%) supporting self-sufficiency of the HTC process due to increased steam recovery and the HTC liquid methane production (Aragón-Briceño et al., 2020; Danso-Boateng et al., 2015).

The advantages of HTC integration to AD plant seem to be dependent on the hydrochar use as a fuel source, as studies conclude that a positive energy balance is attained with all HTC conditions studied if hydrochar is used as a fuel (Aragón-Briceño et al., 2021b; Danso-Boateng et al., 2015). The integration has also been reported to reduce environmental impacts (from 72 to 18 kg CO<sub>2</sub>-eq/t of sludge) compared with standalone AD, if hydrochar is to replace fossil fuels (Medina-Martos et al., 2020). The capital investment required for retrofitting HTC to AD plant or WWTP have also been acknowledged to increase the overall treatment costs (Aragón-Briceño et al., 2021b; Medina-Martos et al., 2020). The deployment of HTC on industrial level necessitates the development of continuous reactor configurations, which allow flexibility in the residence times and avoid lag-times of charging and discharging. Moreover, continuous reactor requires an effective pump system which allows pumping of sludge of various TS contents against high pressures (Lucian and Fiori, 2017).

Nutrient recovery has been included in scale-up assessments primarily from the liquid product, while hydrochar is considered for energy recovery *via* combustion in the existing literature (Aragón-Briceño et al., 2021b; Salman et al., 2019). This is even though the high nutrient content of hydrochar from sewage sludge and its potential role in nutrient recovery is acknowledged (Medina-Martos et al., 2020). As stated above, hydrochar produced from waste material, such as sewage sludge digestate and pulp and paper industry sludge, faces tightening regulations regarding incineration. Meanwhile, nutrient recovery from waste materials is being increasingly encouraged and regulated in EU (EU 2019/1009, 2019). Therefore, scale-up and integration assessments should instead of hydrochar energy recovery, also include the possibility of hydrochar use in nutrient recycling, and evaluate the influence on energy balances, nutrient amounts, and economics. Furthermore, hydrochar potential in carbon sequestration can be expected to benefit the environmental and economic gain received from utilizing hydrochar in soils instead of energy production in the future.

### 3 RESEARCH OBJECTIVES

The main objective of this thesis was to evaluate the potential of HTC in wastewater sludge management and in wastewater sludge processing into value-added products concerning nutrient, carbon, and energy recovery. The aim was divided into four sub-objectives, the first focusing on the solid fraction (hydrochar) properties obtained from HTC of municipal digested and pulp and paper industry wastewater sludges, and the second on the management of liquid filtrates from the thermal treatments (HTC and pyrolysis). The third sub-objective was related on the pyrolysis liquid and its treatability in AD considering potential inhibition. Finally, the effects of HTC integration into a centralized biogas plant were theoretically estimated, the feasibility of which was assessed by the value of the end-products and energy balance of the biogas plant. The objectives were divided as follows (the related paper is given in brackets):

- 1) To evaluate the effect of HTC on the nutrient, carbon and energy recovery of digested sewage sludge and pulp and paper mixed sludge (I, II)
- 2) To assess the anaerobic digestibility of liquid filtrates from the HTC or pyrolysis of wastewater sludge (I, II, III)
- 3) To assess pyrolysis liquid treatment and its potential inhibition in AD (III)
- 4) To evaluate the changes in mass and nutrient flows and energy balance of a centralized biogas plant after HTC integration (IV)

## 4 MATERIALS AND METHODS

### 4.1 Experimental design

An overview of the objectives and the experiments conducted to the studied materials in this thesis are presented in Table 5. This thesis examined HTC treatments for digested municipal sewage sludge and pulp and paper industry's mixed sludge concerning the product fraction characteristics and applicability. The product fractions were analyzed with nutrient and elemental analyses and with calorimetry. The suitability of the HTC filtrates and pyrolysis liquid in AD were studied with BMP batch assays. The alleviation of the inhibitory effect from pyrolysis liquid on AD was studied in laboratory-scale semi-CSTRs. The effect from pyrolysis liquid addition to AD was evaluated by analyzing the digestate characteristics and biogas yields. Lastly, based on the results from the laboratory experiments, theoretical HTC integration to a full-scale biogas plant was assessed based on the effect on the mass, nutrient, and energy balances.

**Table 5.** Summary of the experiments used in this thesis.

Objective	Studied materials	Experiments	Paper
Effect of HTC on nutrient, carbon, and energy recoveries from sludge	Digested SS, mixed sludge	Laboratory HTC, chemical analysis, calorimetry	I, II
Evaluate the anaerobic digestibility of liquid fraction from thermally treated sludge	HTC filtrates, pyrolysis liquid	BMPs	I, II, III
Evaluate inhibitory effect of pyrolysis liquid on AD	SS, THSS, pyrolysis liquid	Laboratory semi-CSTRs, chemical analysis	III
Effect on mass, nutrient, and energy balances from digestate HTC integration to a centralized biogas plant	SS, digested SS, HTC filtrate, hydrochar	Theoretical calculations	IV

HTC, hydrothermal carbonization; SS, sewage sludge; BMP, biochemical methane potential; AD, anaerobic digestion; THSS, thermally pre-hydrolyzed sewage sludge; CSTR, continuously stirred tank reactor

### 4.2 Studied materials

All the materials studied in this thesis were obtained from a centralized biogas plant in Topinoja (Turku, Finland) which treated during the experiments annually 75,000 t (ca. 23% TS, 16,500 t-TS/a) of mechanically dewatered sewage sludge transported from six regional municipal wastewater treatment plants, producing 30,000 t of dewatered digestate (ca. 30% TS, 9,000 t-TS/a), and from a pulp and paper mill in Eastern Finland. The studied materials included mechanically dewatered digestate of municipal wastewater sewage sludge (Paper I), reject water (Paper I), dewatered sewage sludge, thermally pre-hydrolyzed sewage sludge (THSS) (Paper III), pyrolysis liquid (Paper III), and pulp and paper industry mixed sludge (Paper II). The reject water was obtained from the mechanical dewatering unit of digested sewage sludge with polymer addition (Paper I). The THSS was obtained from a thermal pre-hydrolysis



unit of sewage sludge performed at the biogas plant in a THP unit (Cambi®, 130–140°C, 4 bar for 20 minutes), before which the sewage sludge is diluted with process waters to 16% TS. In the THP unit the temperature is raised with steam injection, which leads to a dilution to 12% TS content of the sludge. The non-condensable gases from the THP unit are directed to the AD process through a different route than the THP-treated sludge, and, as for this study, the THSS sample was taken from the AD feeding line, the non-condensable gases are not present in the THSS sample.

The pyrolysis liquid was obtained from an intermediate pyrolysis pilot treating mechanically dewatered digested sewage sludge (TS 30%) at the Topinoja biogas plant (Paper III). The pilot pyrolysis process comprised of a screw pre-dryer and vacuum dryer that in addition to removing water (TS content increased to 70–80%) also pre-heated the sludge for the following pyrolysis unit that had two screw-type reactors operating in parallel and at normal pressure. The pilot had a capacity of 600–800 kg/h. The pyrolysis temperature was around 400°C, and the residence time was around one hour. The approximate product mass rates from the pyrolysis were 150–200 kg/h sludge biochar, 50–70 kg/h pyrolysis gas, and 50–70 kg/h pyrolysis liquid, which contained unfractionated oil and aqueous liquid.

The studied pulp and paper industry sludge was a mixture of primary and secondary sludge (referred to as a mixed sludge) (Paper II). This mixed sludge originated from an activated sludge process used in treating wastewater from pulp and paper mill integration (Finland). The mill uses wood as a raw material and has both kraft and mechanical pulping processes. The mixed sludge had been mechanically dewatered at the mill. The characteristics of the material used in this thesis are shown in Table 6.

**Table 6.** Characteristics of the studied materials. The THSS theoretical illustrates the effect of THP on the sludge characteristics when the effect of dilution in the THP process with steam (from 16 to 10% TS) is extracted (calculation is shown in Eq. 11).

Parameter	Dewatered digestate	Reject water	Mixed sludge	Sewage sludge	THSS theoretical	THSS measured	Pyrolysis liquid
pH	7.50	8.00	5.4	6.3	6.1	6.1	9.1
TS (%)	25.6 ± 0.6	n.a.	32.1 ± 0.8	15.56 ± 0.5	15.56	10.13 ± 1.0	0.12
VS (%)	14.6 ± 0.3	n.a.	28.0 ± 0.6	11.78 ± 0.5	12	7.7 ± 0.8	0.08
Ash at 550°C (% TS)	43 ± 0.1	n.a.	12.7 ± 0.4	n.d.	n.d.	n.d.	n.d.
HHV (MJ/kg TS)	11.49 ± 0.2	n.a.	14.87 ± 0.02	n.d.	n.d.	n.d.	n.d.
C (% TS)	30.30 ± 0.4	n.a.	42.4 ± 0.1	n.d.	n.d.	n.d.	n.d.
H (% TS)	4.40 ± 0.02	n.a.	5.78 ± 0.02	n.d.	n.d.	n.d.	n.d.
N (% TS)	3.5 ± 0.1	n.a.	1.24 ± 0.04	n.d.	n.d.	n.d.	n.d.
S (% TS)	2.3 ± 0.2	n.a.	0.37 ± 0.03	n.d.	n.d.	n.d.	n.d.
SCOD (g/L)	2.1 ± 0.01	10.3 ± 0.01	4.3 ± 0.02	35.88 ± 0.5	49.5	32.2 ± 1.4	3.6 ± 0.1
TVFA (g/l COD)	0.0	1.4 ± 0.1	n.d.	21.9 ± 1.7	10.0	6.5 ± 1.4	0.9 ± 0.1
Total phosphorous (g/kg TS)	37.2	2.3 <sup>a</sup>	19.5	n.d.	n.d.	n.d.	n.d.
Total N (g/l)	35.2 ± 0.1	3.9	n.d.	7.8	6.9	4.6	3.6
NH <sub>4</sub> -N (mg/L)	n.d.	2.91	98.1	932.8	1061.4	691	61.5

TS, total solids; VS, volatile solids; HHV, higher heating value; SCOD, soluble chemical oxygen demand; TVFA, total volatile fatty acids; THSS, thermally pre-hydrolyzed sewage sludge

<sup>a</sup> in g/L.

The inoculum for the BMP assays of the digestate HTC filtrates was mesophilic municipal biowaste digestate (Riihimäki, Finland) (Paper I), while for the mixed sludge HTC filtrates, the inoculum used was

granular sludge (7.4% TS, 6.8% VS) from a mesophilic upflow anaerobic sludge blanket (UASB) reactor treating industrial wastewater (Singh et al., 2019) (Paper II). The inoculum for the semi-CSTR experiments was thermophilic digestate from the anaerobic digester at the Topinoja biogas plant (Paper III). Before each CSTR was inoculated with 4 L of the thermophilic inoculum, the inoculum was warmed in a closed container to the reactor temperature in a 55°C water bath for 2 d.

## 4.3 Experimental set-ups

### 4.3.1 Laboratory HTC treatments

The HTC treatments were conducted in a two-liter Parr® 4500 pressure reactor with an external circulating cooling water system and internal rotary mixer (Papers I, II). The mixer was not used for mixed sludge samples due to their fibrous texture (Paper II). Each treatment had one replicate. For the HTC treatments, the digestate and mixed sludge was used as received (25% TS and 32% TS, referred to as concentrated digestate (Paper I) and concentrated mixed sludge (Paper II), respectively) and as diluted with reject water (digestate) or tap water (mixed sludge) (15% TS) (referred to as diluted digestate and diluted mixed sludge). The dilutions were performed right before the HTC treatments. The sample wet weight for the experiments was 1 kg for digestates (15 and 25% TS) and for diluted mixed sludge (15% TS) or 700 g for concentrated mixed sludge (32% TS), and the treatment temperatures were 210°C, 230°C or 250°C with residence times of 30 or 120 min. The heating of the reactor vessel to the target temperatures was achieved within ca. 70–95 minutes. The temperature was manually adjusted using Parr® 4848 reactor controllers. The vessel pressure started to increase after the inside temperature reached 100 °C and then increased to 20 to 40 bar depending on the applied temperature. The vessel was held at the target temperature for the pre-set residence time. The realized temperatures fluctuated but remained within  $\pm 9$  °C from the targeted temperature. The 250°C runs started when the vessel temperature had reached 245 °C because of difficulties in attaining the targeted temperature within 90 minutes. In all the runs, after the residence time, the heating was switched off, an arbitrary volume of gas was released, and cooling water circulation was initiated in the water jacket. The gas release reduced the inside pressure and temperature by 2–4 bar and 1–4°C, respectively, of which purpose was to prevent possible condensation. The water cooling lasted until the vessel temperature had decreased to 40–70 °C, which was achieved within 30–40 minutes. After the HTC treatments, the whole sample volume was weighed, recovered, and stored at 4 °C prior to solid–liquid separation by filtration.

Filtration of the HTC-treated sludges (called slurry) was conducted in a small-scale pressurized filtration unit. The temperature during filtration was ca. 60°C, which was attained by warming up the samples in a water bath before filtration. The heated sample was placed onto a filter cloth inside a cylinder. The pressure in the closed cylinder gradually increased: 5 minutes to 1 bar, 10 minutes to 4 bar and then to the final pressure of 15 bar. The total pressing time for the samples varied between 20 and 30 min. The end-products of filtration are called hydrochar (solid fraction) and filtrate (liquid fraction), while the reference products of the original sludges are referred to as the cake and cake filtrate. The hydrochar product is comprised of both moisture that was not removed by filtration and of dry solids that are obtained after evaporation. The weights of the recovered filtrate and hydrochar were recorded. In mass balance calculations, both the weight of the hydrochar as well as the TS content of the hydrochar are considered.

### 4.3.2 BMP assays

The biochemical methane potentials (BMP) were determined at mesophilic (35°C) (Papers I and II) and thermophilic (55°C) (Paper III) conditions in triplicate in 120 mL serum bottles with a liquid volume of 64 mL (Papers I and II) or 60 mL (Paper III). The BMP assays of HTC and cake filtrate contained inoculum at concentration of 2 g-VS/L and HTC or cake filtrate at concentrations of 2 g-soluble COD (SCOD)/L (Papers I and II). The BMP assays studying pyrolysis liquid (Paper III) contained inoculum (7.7 g-VS/L) and sewage sludge or THSS at 3.8 g-VS/L or pyrolysis liquid at 1.4 g-SCOD/L concentrations. Pyrolysis liquid was also added in batches containing sewage sludge or THSS in volumes of 1% or 5% of the wet weight of the substrate (v/w) in question (sewage sludge or THSS). Each batch also contained 4 g/L (Papers I and II) or 5 g/L (Paper III) of buffer (NaHCO<sub>3</sub>), and distilled water that was added to reach the liquid volumes. The initial pH was adjusted to between 7 and 8 with 1 M HCl, after which the bottles were closed with gas-tight rubber stoppers and flushed with nitrogen gas for 3 min to create anaerobic conditions inside the bottles. Assays containing only inoculum, buffer, and water functioned as a blank, and their methane production was subtracted from the methane production of the sample assays. The methane concentrations were measured one to three times a week, and prior to every measurement, the bottles were manually shaken to mix the contents. The methane concentration was analyzed with gas chromatography, and the methane volume was calculated from the methane percentage in the serum bottle headspace as described in Angelidaki et al. (2009). The methane concentrations and volumes were reported as the averages of the triplicate assays.

### 4.3.3 Semi-continuous reactor experiments

Three parallel 6 L semi-continuously fed semi-CSTRs (referred to as R1, R2, and R3) were operated for 221 d at 55°C (Paper III). The working liquid volume was 4 L, except for R3, in which it was decreased to 3.5 L on day 143 to manage sludge floating. Heating coils in an insulated frame with water recirculation provided a constant temperature for the reactors. The reactor contents were mixed with a mechanical mixer semi-continuously (11 rpm, 30 min on and 30 min off) until day 140, after which the mixing was changed to a continuous mode. The reactors were manually fed every weekday according to the desired organic loading rate (OLR) by taking the mass of sewage sludge or THSS feed that had the precise amount of daily VS. Before feeding, a measured mass of digestate (reactor content) was removed to keep the reactor liquid surface level constant. The mixing was stopped while feeding. The biogas produced was collected *via* gas-tight tubes (Masterflex Tygon) in 10 L aluminum gas bags (Supelco), from which the CH<sub>4</sub> and CO<sub>2</sub> contents were measured with gas chromatography and the gas volume with water displacement method.

The initial OLR was 3 kg-VS/m<sup>3</sup>d and HRT 19.6 d, which were used to simulate the operation parameters used in the full-scale plant where the materials originated from. The OLRs, HRTs, feedstock, and pyrolysis liquid additions during the course of the reactor operation are shown in Table 7.

**Table 7.** The operational parameters used in the semi-continuous reactor experiments (Paper III).

Days	Reactor	Feedstock	OLR (kg-VS/m <sup>3</sup> d)	HRT (d)	Pyrolysis liquid (% (w/w))	Feed TS (%)	Feed VS (%)
0 - 44	R1	THSS	3	19.6	0	10.1	7.7
	R2	THSS	3	19.6	0	10.1	7.7
	R3	THSS	3	19.6	0	10.1	7.7
45 - 76	R1	THSS	3	19.6	0	10.1	7.7
	R2	THSS	3	19.6	0	10.1	7.7
	R3	SS	3	19.6	0	10	7.8
77 - 85	R1	THSS	2.3	13	0	5.9	4.4
	R2	THSS	3	12	0.15	8.1	6.1
	R3	SS	2.4	13	0.15	6	4.3
86 - 125	R1	THSS	2.3	13	0	5.9	4.4
	R2	THSS	3	13	0.5	8.1	5.9
	R3	SS	2.4	13	0.5	6.2	4.5
130 - 152	R1	THSS	1.2	26	0	5.9	4.4
	R2	THSS	1.7	26	0.5	8.1	5.9
	R3	SS	1.3	26	0.5	6.2	4.5
153 - 221	R1	THSS	1.2	26	0	5.9	4.4
	R2	THSS	1.2	26	1	5.9	4.4
	R3	SS	1.3	26	1	5.8	4.1

OLR, organic loading rate; HRT, hydraulic retention time; TS, total solids; VS, volatile solids; THSS, thermally pre-hydrolyzed sewage sludge; SS, sewage sludge

#### 4.4 Extrapolation to large scale

The mass and nutrient flows and energy demand in a centralized biogas plant treating municipal sewage sludge were calculated to assess the feasibility of HTC integration in treating digested sewage sludge (Paper IV). The assessment compared the effect of HTC on the flows and energy demands of different unit processes with the intention to replace the currently employed hygienization of digestate. The aim was to assess the possible changes in the product volumes and nutrient concentrations as well as the net energy balance of the biogas plant comparing the original layout with the HTC integrated layout (Paper IV). Figure 5 presents the biogas plant unit processes and mass flows included in the assessment, entailing four thermophilic ADs, digestate dewatering unit (decanter centrifuge), evaporator-stripping columns, and biogas upgrading to liquefied biogas (LBG). The currently deployed hygienization, being comprised of 3 tanks, was situated between the AD and digestate dewatering units. The HTC unit, being alternative to hygienization and comprising of one tank and a filtration unit, was placed after digestate dewatering to treat the solid fraction of digestate. In addition, CHP units for biogas upgrading and for dewatered digestate or hydrochar were included as alternative energy recovery routes to LBG and nutrient recovery from the solid product, respectively.

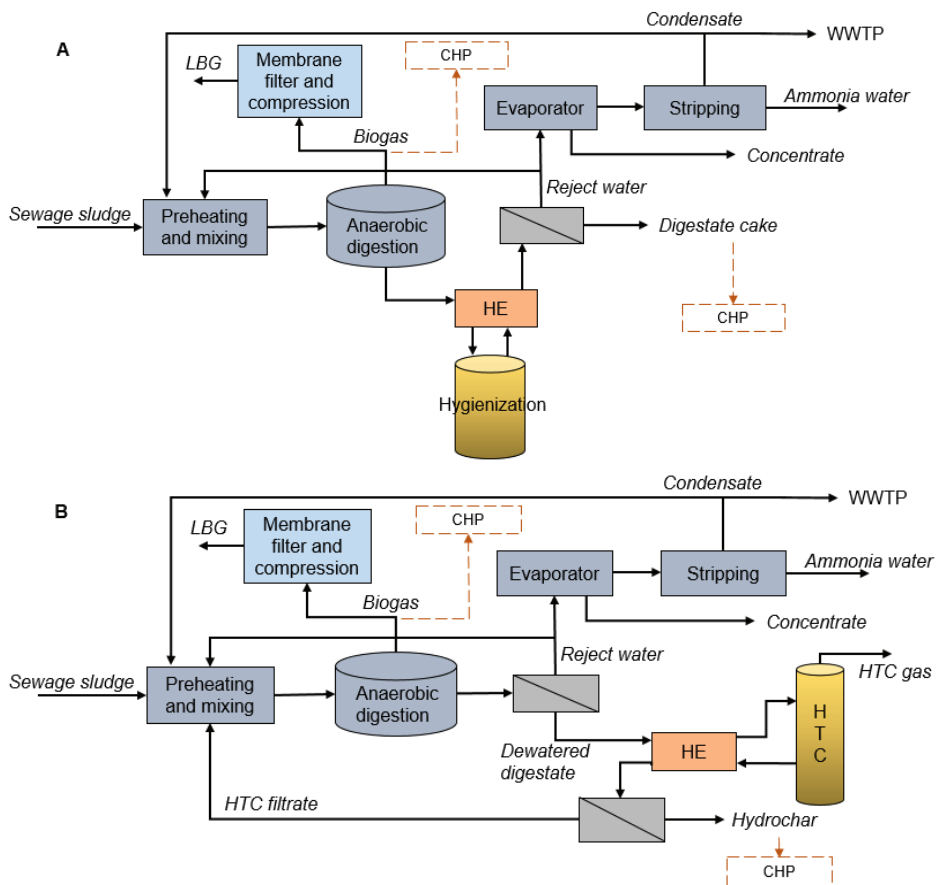


**Figure 5.** Simplified illustration of the original layout (A) and the HTC integrated layout (B) of the studied centralized biogas plant (Paper IV). The orange dashed arrows represent the possible locations of the CHP units. LBG: liquefied biogas, CHP: combined heat and power, HE: heat exchanger, HTC: hydrothermal carbonization, WWTP: wastewater treatment plant.

The HTC and the hygienization processing units were dimensioned to treat ca. 41,400 t/a of dewatered digestate (30% TS) or ca. 190,000 t (wet weight)/a of digestate (8% TS), respectively, operating 24 hours a day for 365 days a year. Both HTC and hygienization were designed to be coupled with counterflow heat exchangers which preheat the digestate feed to 175°C or 65°C before it enters the HTC (230°C, 30 min) or hygienization (70°C, 1 h) and recover heat from the outflowing HTC slurry or hygienized digestate, respectively. Both processes worked batch-wise, each batch lasting for 90 min and including preheating, feeding, and product removal and cooling. In the HTC process, the preheating in the heat exchanger and the rest of the heating need (55°C) in the HTC reactor was assumed to last for 30+30 min. In hygienization, digestate preheating is carried out within 30 min, and the hygienization treatment lasting for 60 min. In addition, the HTC process includes filtration that mechanically separates the HTC slurry after heat recovery into hydrochar and HTC filtrate. The HTC conditions, *i.e.*, temperature of 230°C, pressure of 30 bar, and a residence time of 30 min were selected based on Paper I.

For the centralized biogas plant, the incoming dewatered sewage sludge (95,000 t/a wet weight) is transported from several sewage treatment plants at TS content of 28%. The transported sewage sludge is

diluted with process waters to 12% TS, for which condensate from stripping and part of the reject water generated in the dewatering unit are used. The rest of the reject water is directed to evaporator-stripping unit for producing concentrate, liquid ammonia water, and condensate. With the HTC integration, the generated HTC filtrate is used for the dilution of the incoming sewage sludge, where it replaces part of the reject water in the diluting waters, and thus affecting the overall mass and nutrient flows by enabling more reject water to be used for ammonium recovery in the evaporator-stripping unit.

## 4.5 Analytical methods and calculations

The chemical analyses, methods and equipment used are summarized in Table 8.

**Table 8.** Summary of the analytical methods and equipment used in this thesis.

Analysis	Method and apparatus	Paper
TS/moisture content, VS, and ash (s)	APHA 2540	I-III
pH (l)	WTW ProfiLine pH 3210 with SenTix® 41 electrode	I-III
Chemical oxygen demand (COD) (l)	Samples were centrifuged and analyzed with dichromate method according to SFS 5504	I-III
Volatile fatty acids (VFAs) (l)	Acetate, propionate, iso-butyrate, butyrate, iso-valerate and valerate were determined using gas chromatography (GC-2010 Plus Capillary, Shimadzu (Japan) with FID)	I-III
TKN (s)	AOAC 1990 using Foss Kjeltach 2400 Analyzer Unit	III
N (l)	LCK 238 and LCK 338 test kits + DR 2800 spectrophotometer HACH (USA)	I-III
NH <sub>4</sub> -N (l)	LCK 303 and LCK 305 test kits + DR 2800 spectrophotometer HACH (USA)	I-III
PO <sub>4</sub> <sup>2-</sup> (l)	LCK 349 test kit + DR 2800 spectrophotometer HACH (USA) Ion chromatography according to SFS-EN ISO 10304-1 (Dionex DX-120, Thermo Fischer Scientific (USA), IonPac CS12A cation exchange column and CSRS 300 suppressor (4 mm)) with AS50 autosampler	III I-II
Elemental analysis (CHNS) (s)	Thermo Fischer Scientific (USA) FlashSmart Elemental Analyzer (CHNS/O) with TCD using BBOT as standard	I-II
P, Na, Al, Si, K, Ca, Cr, Fe, Ni, Cu, Zn, As, Cd, Pb, Hg (s and l)	Inductively coupled plasma mass spectrometry (ICP-MS) (Thermo Fischer Scientific iCAPTM RQ (USA)), sample preparation with microwave digestion (CEM Corporation MARS 6, Teflon vessels) in HNO <sub>3</sub> and H <sub>2</sub> O <sub>2</sub>	I-II
CH <sub>4</sub> and CO <sub>2</sub> (g)	Gas chromatography (Shimadzu GC-2014 with Agilent 80/100 Porapak N)	III
CH <sub>4</sub> (g)	Gas chromatography (PerkinElmer Clarus 500 with Supleco MOL Sieve 5A PLOT 30 m x 0.53 mm)	I-III
Gas volume (g)	Water replacement method	III
Calorific value (HHV, LHV) (s)	ISO 1928 using Parr® 6725 Semi-micro Oxygen Bomb Calorimeter	I-II

TS, total solids; VS, volatile solids; s, solid sample; l, liquid sample; g, gaseous sample; HHV, higher heating value; LHV, lower heating value

Samples for the VFA analysis were filtered through 0.45 µm and analyzed immediately after sampling or stored at -18°C until the analysis. For obtaining soluble concentration of COD (SCOD), samples were filtered through 0.45 µm before sample preparation.

The BMPs were calculated according to Eq. 1.1 (Papers I–II) and Eq. 1.2:

$$BMP \left( \frac{L \text{ CH}_4}{kg \text{ SCOD}} \right) = \frac{V_{CH_4}}{m_{substrate} \cdot SCOD} \quad (1.1)$$

$$BMP \left( \frac{L \text{ CH}_4}{kg \text{ VS}} \right) = \frac{V_{CH_4}}{m_{substrate} \cdot VS} \quad (1.2)$$

where  $V_{CH_4}$  is the cumulative methane production (ml),  $m_{substrate}$  is the mass of substrate (kg),  $SCOD$  is the SCOD of the substrate (g/kg), and  $VS$  is the volatile solids of the substrate (g/kg).

The parameters used for assessing the energy properties, *i.e.*, solid yield and energy densification ( $E_d$ ) of the digestates and the respective hydrochars, were calculated with Eq. 2–3 (Paper I).

$$\text{Solid yield (\%)} = \frac{m_{product}}{m_{sludge}} \cdot 100 \quad (2)$$

$$E_d = \frac{HHV_{product}}{HHV_{sludge}} \quad (3)$$

where  $m$  is the dry mass (kg) (overnight at 105°C, equals TS), *product* stands for either hydrochar or cake, and *sludge* for digestate or mixed sludge, and  $HHV$  is the higher heating value (MJ/kg-TS). Same parameters on dry ash-free basis were calculated as follows in Eq. 4–5 (Paper II).

$$\text{Solid yield (\%, daf)} = \frac{\frac{m_{product}}{1 - \frac{ash_{product}}{100}}}{\frac{m_{sludge}}{1 - \frac{ash_{sludge}}{100}}} \cdot 100\% \quad (4)$$

$$E_d(\text{daf}) = \frac{\frac{HHV_{product}}{1 - \frac{ash_{product}}{100}}}{\frac{HHV_{sludge}}{1 - \frac{ash_{sludge}}{100}}} \quad (5)$$

where *daf* signifies dry ash-free. The energy yield represents the amount of recovered energy in the hydrochar or cake from the original sludge, and is calculated with Eq. 6 (Papers I and II):

$$\text{Energy yield (\%)} = \frac{m_{product} \cdot HHV_{product}}{m_{sludge} \cdot HHV_{sludge}} \cdot 100\% \quad (6)$$

The ash-free carbon content was calculated with Eq. 7 (Paper II) as follows:

$$\text{Carbon content (\%, daf)} = \frac{C_{sample}}{1 - \frac{ash}{100}} \quad (7)$$

where  $C$  denotes sample total carbon content (%), respectively and *sample* denotes either digestate, mixed sludge, cake, or hydrochar.

The energy content ( $E_{filtrate}$  (MJ/L)) and energy recoveries ( $E_{r,filtrate}$ ) of the filtrates were calculated according to Eq. 8–9 (Paper I) as follows:

$$E_{filtrate} = \varepsilon \cdot BMP \cdot SCOD \quad (8)$$

$$E_{r,filtrate} (\%) = \frac{E_{filtrate} V_{filtrate}}{HHV m_{sludge}} \quad (9)$$

where  $\varepsilon$  represents the energy density of methane (0.0378 MJ/L), BMP is the biochemical methane potential of filtrate (L-CH<sub>4</sub>/kg-SCOD), *SCOD* is the SCOD of filtrate (kg/L), and  $V_{filtrate}$  is the volume of filtrate (L).

When comparing the SCOD and TVFA concentrations of the mixed sludge and diluted mixed sludge filtrates (Paper II), a computational factor was used to consider the addition of water used for dilution in diluted mixed sludge samples. Thus, the diluted mixed sludge filtrate SCOD and VFA concentrations were obtained with Eq. 10.

$$\text{Concentration as undiluted} = \frac{c \cdot V_{HTC \text{ filtrate}}}{V_{HTC \text{ filtrate}} + V_{cake \text{ filtrate}} - V_{water \text{ added}}} \quad (10)$$

where  $c$  denotes concentration (g/L) (SCOD, VFA) and  $V$  volume (L).

In the semi-CSTR experiments (Paper III), the specific methane yield was calculated for each week by summing the methane produced during a week (Monday to Monday) and the VS added during the week (Monday to Friday). The reactors were fed for 5 d a week, but the OLR in kg-VS/m<sup>3</sup> d is expressed as the average daily amount of VS fed to the reactors over a one-week period. The reactor results cover the average of the results from the time of the latest HRT because it was assumed that the digestive conditions were stable enough after a reasonable adaptation period to reliably describe the applied conditions, rather than the adaptation to the conditions.

In Paper III, to differentiate the effects of THP treatment from dilution by steam in the THP process on sewage sludge characteristics, a computational THSS was calculated (Eq. 11) that eliminates the effects from dilution with steam, as follows:

$$THSS_{computational} = THSS_{measured} \cdot \frac{TS_{THSS \text{ measured}} (\%)}{TS_{sewage \text{ sludge}} (\%)} \quad (11)$$

The energy demand of the centralized biogas plant was estimated both for heat and electricity for assessing HTC integration concerning the energy balance (Paper IV). The equations used in the energy demand calculations are presented in Table 9.



**Table 9.** Equations used in the energy demand calculations for the biogas plant with HTC integration (Paper IV).

Equation	Term explanations
Heat demand of AD unit ( $Q_{AD}$ )	
$Q_{AD} = \sum m_i c_p (T_{AD} - T_i) + U_{AD} A_{AD} (T_{AD} - T_o) \quad (12)$	$m_i$ : (dry) mass of sewage sludge/diluting water (kg) $c_p$ : specific heat capacity of sewage sludge/diluting water (kJ/kgK) $T_{AD}$ : digestion temperature (K) $T_i$ : temperature of the substrate (K) $U_{AD}$ : overall heat transfer coefficient (W/m <sup>2</sup> K) $A_{AD}$ : digester heat transfer area (m <sup>2</sup> ) $T_o$ : outside temperature (K)
The overall heat transfer coefficient ( $U_r$ )	
$\frac{1}{U_r} = \frac{1}{h_{c,i}} + \frac{1}{h_{c,o}} + \frac{l_s}{k_s} + \frac{l_i}{k_i} \quad (13)$	$h_{c,i}$ and $h_{c,o}$ : convective heat transfer coefficients inside and outside the reactor (W/m <sup>2</sup> K) $l_c$ : thickness of the stainless-steel wall (m) $l_i$ : thickness of the insulation layer (m) $k_s$ : thermal conductivity of the reactor steel wall (W/mK) $k_i$ : thermal conductivity of the insulation (W/mK)
Energy demand of a dewatering unit ( $E_{dewatering}$ )	
$E_{dewatering} = m_{TS} \varepsilon \quad (14)$	$m_{TS}$ : mass of TS in digestate or slurry to be dewatered (kg) $\varepsilon$ : electricity requirement for dewatering (369 kJ/kg-TS) (Lu et al., 2020)
Energy demand of a thermal treatment unit ( $Q_{h,pre}$ , $Q_h$ , and $Q_r$ )	
$Q_{h,pre} = m_d c_{p,d} (T_p - T_o) + m_w (h_w(T_p) - h_w(T_d)) \quad (15)$	$Q_{h,pre}$ : energy needed to heat the digestate (J) $m_d$ : mass of TS in the digestate (kg) $c_{p,d}$ : specific heat capacity of digestate TS (J/kgK) $T_p$ : preheating temperature (K) $T_o$ : temperature of digestate before heating (K) $m_w$ : mass of water in the digestate (kg) $h_w(T)$ is the enthalpy of water at specific temperatures (kJ/kg) $Q_h$ : energy needed to heat the digestate to the treatment temperature (J) in the reactor $T_r$ : treatment temperature (K) $\Delta H_r$ : heat of reaction of digestate carbonization (kJ/kg) $Q_r$ : heat loss from reactor (J) $t_r$ : treatment time (s) $A_r$ : reactor heat transfer area (m <sup>2</sup> ) $t_h$ : time reserved for heating in the reactor (s)
$Q_h = m_d c_{p,d} (T_r - T_p) + m_w (h_w(T_r) - h_w(T_p)) + m_d \Delta H_r \quad (16)$	
$Q_r = t_r A_r U_r (T_r - T_o) + t_h A_r U_r \left( \frac{T_r - T_p}{2} - T_o \right) \quad (17)$	
Energy transferred in an ideal counterflow heat exchanger ( $Q_{hx} = q_c = q_h$ )	
$q_{h/c} = (m_{d,h/c} c_{p,d,h/c} + m_{w,h/c} c_{p,w,h/c}) (T_{h/c,a} - T_{h/c,b}) \quad (18)$	$q_{h/c}$ : energy transferred or received by the hot (h) /cold (c) medium (J) $m_{d,h/c}$ : mass of feed TS (kg) $c_{p,d,h/c}$ : specific heat capacity of the feed TS (J/kgK) $m_{w,h/c}$ : mass of water in the feed (kg) $c_{p,w,h/c}$ : specific heat capacity of water (J/kgK) $T_{h/c,a}$ : temperature of the entering hot stream or the exiting cold stream (K) $T_{h/c,b}$ : temperature of the exiting hot stream or the entering cold stream (K) $U_{hx}$ : overall heat transfer coefficient of sludge in the heat exchanger (W/m <sup>2</sup> K) $A_{hx}$ : heat exchanger area (m <sup>2</sup> ) $\Delta T_{LM}$ : logarithmic mean temperature difference (K)
$Q_{hx} = U_{hx} A_{hx} \Delta T_{LM} \quad (19)$	

Heat losses in the pipelines were not considered since no specific layout was fixed and they would anyway be low. The AD electricity consumption (mixing and pumping) was estimated to be 3% of the energy content in the produced biogas (Erlach 2014). The energy demand of the evaporator-stripping unit was calculated from the reject water volumes for treatment, which were 25 and 23 kWh/t for electricity and heat (in the form of steam), respectively (data from Topinoja biogas plant). The thermal treatment units' (HTC and hygienization) energy demand calculations comprised of three steps: preheating of the digestate or dewatered digestate in the heat exchangers (step 1, Eq. 15), heating of the digestate or dewatered digestate to the treatment temperature in the reactors (step 2, Eq. 16), and maintaining the treatment temperature in the reactor for the required time (step 3, Eq. 17)). For the thermal treatments, one ideal counterflow heat exchanger was assumed per reactor to both cool down and heat-up the digestate. The heat exchangers were assumed not to have heat losses. The electrical energy required by HTC and hygienization was neglected in this thesis.

The CHP unit for the energy recovery from biogas or from hydrochar or hygienized digestate was assumed to have conversion efficiencies of 38% for electricity and 48% for heat, the CHP itself consuming 5% of the electricity produced (Tampio et al., 2016). The energy from the combustion of the dried digestate cake or hydrochar was calculated using their lower heating values (LHV) (10.83 MJ/kg-TS and 10.60 MJ/kg-TS, respectively (Paper I)).

## 5 RESULTS AND DISCUSSION

### 5.1 Effect of HTC on digested sewage sludge and pulp and paper mixed sludge

#### 5.1.1 Mass distribution

The HTC treatment of both studied sludges – sewage sludge digestate and pulp and paper mill mixed sludge – yielded three fractions, *i.e.*, hydrochar, HTC filtrate, and HTC gas, the relative mass yields of which were depended on the applied HTC conditions. Fig. 6 presents the mass distribution of the digestate, mixed sludge, and their diluted correspondents after HTC treatment and filtration. The mass distribution was affected by the initial sludge TS content by resulting in higher generated amounts of filtrate with the diluted sludges, and in the case of digestate, also the calculated amount of gas was increased in the treatments of the diluted digestate. The severity of the HTC treatments affected the mass distribution by increasing the amount of dissolved solids with increasing severity, which led to decreasing hydrochar masses and increasing filtrate masses. Based on the mass distribution, the calculated amount of formed gas was significantly increased only at the most severe conditions (250°C for 120 min), particularly in the treatment of mixed sludges, being 37%–40% of the initial mass, while its amount after the less severe treatments (at 210°C and 230°C) was < 2% of the initial mass.

The different conditions of the HTC treatment influenced the dewaterability of the HTC slurry, which appeared as different hydrochar compositions (dry solids and moisture) between the HTC treatments. In the case of digestate, the filtration equipment failed to separate the non-HTC-treated digestates into cake and cake filtrate, while the HTC slurries were easily separated, yielding hydrochars which had increased TS contents after the severer HTC treatment conditions: concentrated digestate hydrochar TS increased from 39% (at 210°C) to 63% (at 250°C), and diluted digestate hydrochars from 35% (at 210°C) to 54% (at 250°C). Concerning mixed sludge, also the non-HTC-treated sludges were separable with the filtration equipment similarly to the HTC slurries. The mixed sludge hydrochar TS contents were not affected by changing the HTC treatment conditions relative to the cake TS contents (Table 10). The improved efficiency of the mechanical dewatering after HTC treatment of digestate is likely because of the digestate structure altering chemical reactions that remove oxygen during carbonization (Erlach, 2014; Wang et al., 2019).

The solid yields on ash free basis of digestate hydrochars ranged from 92% to 105%, while the mixed sludge hydrochars had lower ash free solid yields, ranging from 48% to 93% (Table 10). Both the HTC temperature and residence time affected decreasingly the solid yields of mixed sludge hydrochars, while for those of digestate, the HTC conditions had no clear effect.

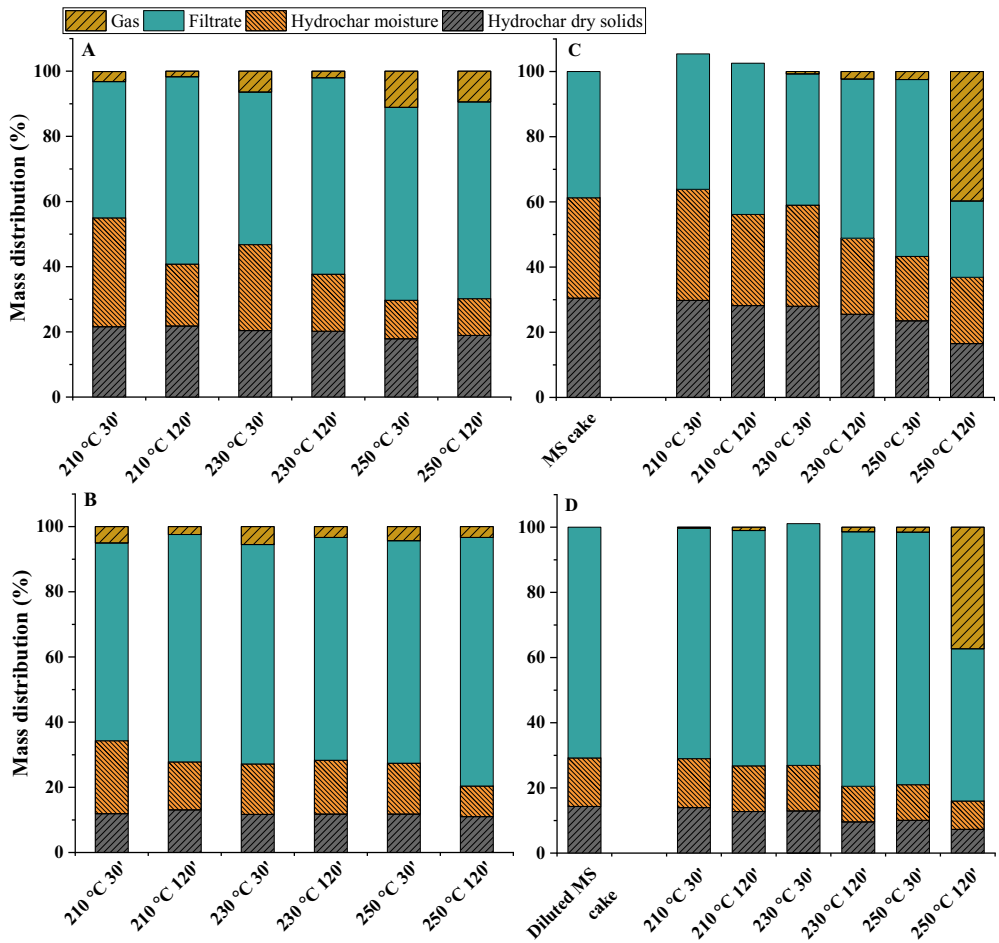


**Figure 6.** Mass distribution of concentrated digestate (25% TS) (A), diluted digestate (15% TS) (B), concentrated mixed sludge (32% TS) (C), and diluted mixed sludge (15% TS) (D) after HTC treatment at specific conditions and filtration. For the mixed sludges, the mass distribution after mere filtration is also shown, named as mixed sludge (MS) cakes (Papers I and II).

**Table 10.** Solids and ash contents of digestates and mixed sludge, and their respective hydrochars' solids and ash contents, and solid yields after different HTC treatments. For mixed sludge, also the characteristics of their non-HTC-treated filter cakes are shown (Papers I and II).

Material	TS (%)	VS (%)	Ash (%)	Solid yield (% daf)
Concentrated digestate	25.0 ± 0.3	14.0 ± 0.2	43.1 ± 0.1	n.a.
Concentrated digestate hydrochars				
210°C for 30 min	39.3 ± 0.4	19.8 ± 0.1	49.6 ± 0.5	97.6 ± 2.7
210°C for 120 min	53.4 ± 0.6	25.9 ± 0.4	51.8 ± 0.1	103.4 ± 2.2
230°C for 30 min	43.6 ± 1.4	21.1 ± 0.8	51.6 ± 0.3	96.4 ± 3.4
230°C for 120 min	53.7 ± 1.4	24.9 ± 0.9	53.7 ± 0.5	100.3 ± 2.5
250°C for 30 min	60.2 ± 0.7	26.8 ± 0.3	55.5 ± 0.1	92.4 ± 2.2
250°C for 120 min	62.7 ± 1.5	27.1 ± 0.7	56.7 ± 0.2	98.9 ± 3.3
Diluted digestate	15.0 ± 0.7	8.0 ± 0.4	43.0 ± 0.4	n.a.
Diluted digestate hydrochars				
210°C for 30 min	34.7 ± 1.5	16.7 ± 1.1	51.8 ± 1.2	93.1 ± 4.0
210°C for 120 min	47.3 ± 0.6	22.6 ± 0.3	52.2 ± 0.2	105.4 ± 5.4
230°C for 30 min	43.0 ± 0.5	20.4 ± 0.1	52.6 ± 0.2	93.2 ± 4.8
230°C for 120 min	41.6 ± 0.3	19.2 ± 0.2	53.7 ± 0.2	95.7 ± 5.2
250°C for 30 min	43.1 ± 0.2	20.0 ± 0.1	54.0 ± 0.1	96.2 ± 5.6
250°C for 120 min	54.0 ± 0.5	23.2 ± 0.4	57.0 ± 0.2	95.5 ± 4.9
Concentrated mixed sludge	32.1 ± 0.8	28.0 ± 0.6	12.7 ± 0.4	n.a.
Concentrated mixed sludge cake	49.7 ± 1.0	43.8 ± 0.8	11.9 ± 0.04	95.2 ± 4.8
Concentrated mixed sludge hydrochars				
210°C for 30 min	46.64 ± 1.1	40.7 ± 1.0	12.7 ± 0.2	93.0 ± 1.1
210°C for 120 min	50.24 ± 1.4	43.8 ± 1.2	12.8 ± 0.05	88.1 ± 1.5
230°C for 30 min	47.39 ± 0.2	40.9 ± 0.2	13.8 ± 0.02	87.4 ± 2.5
230°C for 120 min	52.16 ± 5.0	46.6 ± 0.7	15.3 ± 0.1	79.7 ± 5.0
250°C for 30 min	54.34 ± 5.7	45.9 ± 5.0	15.5 ± 0.4	73.5 ± 3.6
250°C for 120 min	49.07 ± 7.5	36.1 ± 4.3	19.7 ± 2.0	51.6 ± 3.4
Diluted mixed sludge	15.5 ± 1.2	13.5 ± 1.0	12.8 ± 0.3	n.a.
Diluted mixed sludge cake	49.0 ± 1.5	43.0 ± 1.7	12.2 ± 0.7	95.4 ± 0.8
Diluted mixed sludge hydrochars				
210°C for 30 min	48.21 ± 1.3	42.4 ± 1.1	12.0 ± 0.2	93.2 ± 3.7
210°C for 120 min	47.63 ± 0.6	41.7 ± 0.6	12.5 ± 0.2	85.0 ± 3.3
230°C for 30 min	48.08 ± 0.7	41.7 ± 0.6	13.2 ± 0.1	86.3 ± 1.4
230°C for 120 min	46.81 ± 0.8	39.6 ± 0.7	15.5 ± 0.1	64.0 ± 2.3
250°C for 30 min	47.84 ± 0.3	40.1 ± 0.3	16.1 ± 0.1	66.9 ± 2.5
250°C for 120 min	45.38 ± 0.2	36.5 ± 0.1	19.6 ± 0.2	48.4 ± 1.6

TS, total solids; VS, volatile solids; db, dry basis; daf, dry ash free; n.a. not applicable

## 5.1.2 Phosphorous and nitrogen recovery

The contents of nitrogen in the solid samples (hydrochars, digestates, mixed sludges and cakes) were as presented in Table 12 (Section 5.1.3). The liquid phase nutrient concentrations are shown in Table 11. The sewage sludge digestate nitrogen and phosphorous contents were several folds higher than those of the mixed sludge samples, which is because of their different origin and prior treatment methods. Phosphorous concentration in the hydrochars and cakes are shown in Fig. 7 and the nitrogen distributions into the HTC products are presented in Fig. 8. The total nitrogen lost in the gas phase were 3–20% (digestate) and 0–36% (mixed sludge), which, however, were calculated by difference, therefore giving some room for error.

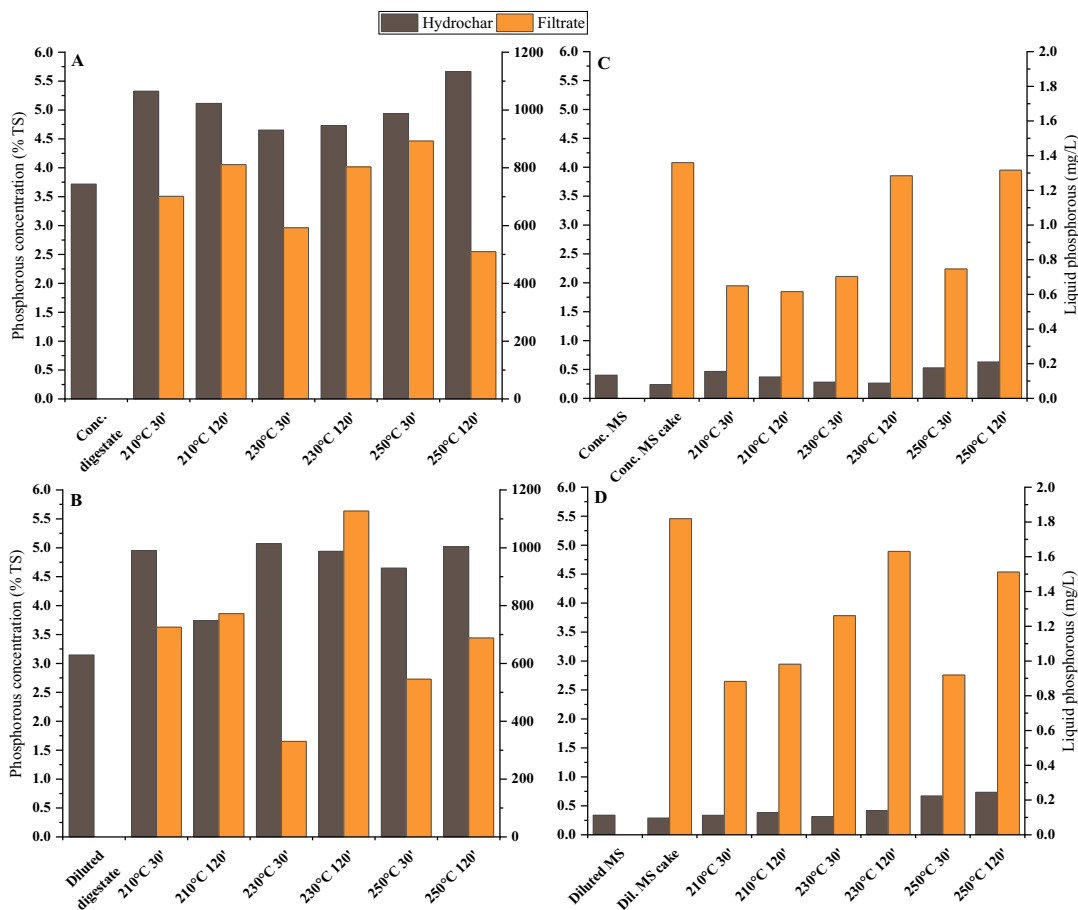


**Figure 7.** Phosphorous concentrations in the concentrated digestate (A), diluted digestate (B), concentrated mixed sludge (C), and diluted mixed sludge (D), and in their respective hydrochars and HTC filtrates. For the mixed sludges, also the filter cake and cake filtrate phosphorous concentration are shown. Notice the different scale of the liquid total phosphorous between the digestates and mixed sludges (Papers I and II).

**Table 11.** Nitrogen, ammonium nitrogen, and phosphate concentrations of the HTC filtrates of digestates, mixed sludges, and mixed sludge cake filtrates (Papers I and II).

Sample	N (g/L)	NH <sub>4</sub> -N (g/L)	NH <sub>4</sub> -N/N <sub>tot</sub> (%)	PO <sub>4</sub> <sup>2-</sup> (mg/L)
HTC filtrates of concentrated digestate				
210°C for 30min	5.4	2.62	48	39.9
210°C for 120min	6.1	3.23	53	48.5
230°C for 30min	5.3	2.85	54	48.4
230°C for 120min	5.6	3.35	60	99.1
250°C for 30min	4.9	2.71	55	67.5
250°C for 120min	5.0	2.93	59	67.5
HTC filtrates of diluted digestate				
210°C for 30min	4.6	2.33	50	128.8
210°C for 120min	4.8	2.59	54	96.9
230°C for 30min	4.3	2.50	58	86.5
230°C for 120min	4.6	2.83	61	87.9
250°C for 30min	4.3	2.83	65	119.3
250°C for 120min	4.3	2.76	64	176.2
Conc. mixed sludge cake filtrate	0.18	0.10	56	0.0
HTC filtrates of concentrated mixed sludge				
210°C for 30min	1.2	0.13	11	15.8
210°C for 120min	0.7	0.10	13	20.5
230°C for 30min	0.9	0.05	6	28.7
230°C for 120min	0.7	0.01	2	43.8
250°C for 30min	0.8	0.01	1	60.8
250°C for 120min <sup>a</sup>	0.3	0.02	6	33.1
Diluted mixed sludge cake filtrate	0.1	0.07	48	0.0
HTC filtrates of diluted mixed sludge				
210°C for 30min	0.9	0.15	17	28.2
210°C for 120min	0.9	0.13	14	31.3
230°C for 30min	0.8	0.09	10	34.8
230°C for 120min	0.6	0.02	3	35.5
250°C for 30min	0.7	0.01	2	51.7
250°C for 120min	0.5	0.01	2	65.1

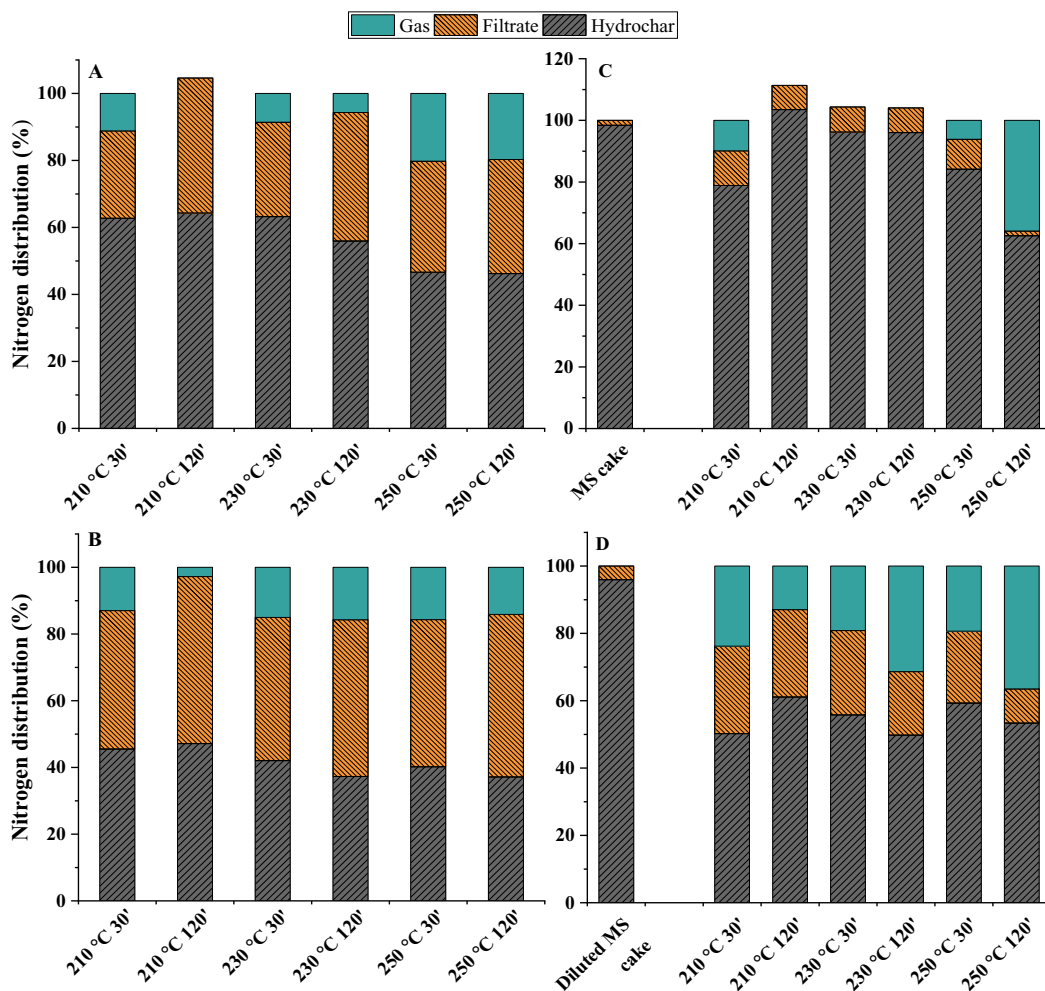


**Figure 8.** Nitrogen distribution of concentrated digestate (25% TS) (A), diluted digestate (15% TS) (B), concentrated mixed sludge (32% TS) (C), and diluted mixed sludge (15% TS) (D) after HTC treatment at specific conditions and filtration. For the mixed sludges, the nitrogen distribution after mere filtration is also shown, named as mixed sludge (MS) cakes (Papers I and II).

Phosphorous was nearly fully recovered in the hydrochar fractions, *i.e.*, >90% in the digestate and >99% in the mixed sludge. The different HTC conditions gave little variety, only the longer treatment times seemed to slightly enhance phosphorous dissolution from the digestate. The sludge TS content affected phosphorous dissolution only for digestate, the lower TS content slightly promoting the dissolution. Hence, the dissolved phosphorous in the HTC filtrates were slightly higher for the diluted digestate (4-13%) than for the concentrated digestate (2-5%). It has been reported that lower solids loading (studied TS ranged from 2.5 to 30%) of sewage sludge digestate promotes phosphorous solubility which can be attributed to the decreased precipitation of phosphorous with metal ions that are present in lesser amounts with lower solids input (Aragón-Briceño et al., 2020). In the case of sewage sludge digestate, the use of aluminium or iron salts in phosphorous precipitation at WWTPs, decreases the phosphorous dissolution in the following treatments of the digestate. The sewage sludge used in the present study, originated from a WWTP that uses iron salts for phosphorous precipitation, which resulted in iron



concentrations of 180–230 mg/g-TS in the digested sewage sludge. Similarly, the mixed sludge used in the present study contained aluminum at a content of 56 mg/kg-TS, which was a probable reason for the low phosphorous solubility. Thus, to enable the utilisation of phosphorous, it should be either leached from the hydrochar (Becker et al., 2019), or the hydrochar should be amenable as a fertilizer (Bargmann et al., 2014). If fertilizer use is being considered, the amount of plant available phosphorous should be determined, as it can be bound to the metals and mineral compounds of which size and surface properties change when HTC temperature increases from 180°C to 240°C, decreasing its usability (Huang and Tang, 2015; McIntosh et al., 2022). In addition, if hydrochar has a lowered pH the plant sorption capacity is reduced (Libra et al., 2011).

Although the amount of total phosphorous was low in all the mixed sludge HTC filtrates (0.18% of total phosphorous), and somewhat higher in the digestate HTC filtrates (2–13%), it was clear that the HTC treatments promoted the formation of phosphate in both sludge HTC filtrates. Phosphate was present in concentrations of 40–99 mg/L in the concentrated digestate, 87–176 mg/L in the diluted digestate and 15.8–65.1 mg/L in all the mixed sludge HTC filtrates, while in any of the cake filtrates phosphate was not present. However, some phosphorous precipitation occurred from the liquid onto hydrochar during the HTC treatment (Fig. 6), as the total phosphorous concentrations fluctuated with treatment temperature and time.

In contrast, nitrogen was more prone to be dissolved during the HTC treatments. The lability of nitrogen reduced the nitrogen contents in all digestate hydrochars by 23–39% and 17–31% relative to the concentrated and diluted digestates, respectively. In contrast, the concentrated mixed sludge hydrochars all had 6–17% higher nitrogen contents, except that produced at 210°C, than the cake. The diluted mixed sludge hydrochar nitrogen contents were all 12–46% lower than the cake, except the one produced at 250°C for 120 min. The sludge TS content seemed to determine more the distribution of nitrogen than the different HTC conditions, particularly with mixed sludge. The lower TS content sludges tended to release more nitrogen to the liquid and gas phases than the higher TS content sludges, which appeared as lower nitrogen yields: diluted sludge hydrochars had nitrogen recoveries of 37–46% (digestate) and 50–61% (mixed sludge), while the concentrated sludge hydrochars had nitrogen recoveries of 46–64% (digestate) and 63–100% (mixed sludge). Regardless of the decreased nitrogen recoveries in hydrochars, the carbonization reactions reportedly increase the stability of nitrogen in hydrochar upon soil application, preventing nitrogen runoff (Chu et al., 2020). For example, in rice paddy field trials, sewage sludge digestate hydrochar had increased ammonium-nitrogen retention, and subsequently increased rice grain nitrogen content by 30% and yield by 24% compared to sewage sludge digestate (Chu et al., 2020).

HTC increased the filtrate nitrogen content, particularly for digestate. The diluted sludges were more prone to have nitrogen dissolved into the HTC filtrate. The cake filtrates of mixed sludge had 2%–4% of the total nitrogen, while the HTC filtrates from diluted sludges had on average  $46\pm 3\%$  (digestate) and  $27\pm 6\%$  (mixed sludge), and the concentrated sludge HTC filtrates had  $33\pm 6\%$  (digestate) and  $7\pm 3\%$  (mixed sludge) of the total nitrogen. The HTC filtrates' nitrogen concentrations were affected by the treatment severity, particularly in HTC filtrates of mixed sludge, which decreased by up to 76% by increasing temperature and time. The HTC filtrates of the digestates, the decreasing effect was not as clearly observed. The treatment severity also affected the ammonium nitrogen concentration in the mixed sludge HTC filtrates, decreasing them from 0.13–0.15 g/L to 0.01–0.02 g/L with increasing severity. The mixed sludge HTC filtrates' decreasing total nitrogen concentrations by treatment severity indicated that organic nitrogen was released to the liquid phase during HTC but was then converted to ammonia and ammonium nitrogen, which are easily evaporated at higher temperatures, leading to decreased total nitrogen and ammonium nitrogen concentrations in the HTC filtrates (Idowu et al., 2017). The

volatilisation of nitrogen compounds was observed in the current study upon increasing the HTC temperature and time. During HTC treatment, a decline in nitrogen content in hydrochars has been reported to occur because of the decomposition of labile and organic nitrogen compounds, while the volatile nitrogen compounds are already devolatilised below temperatures of 220°C to the liquid and gas phases (Zhuang et al., 2018). The increase in ammonium-nitrogen concentration in the filtrate at increased HTC temperatures has been connected to the hydrolysis of proteins through peptides and amino acids to fatty acids and ammonia (Marin-Batista et al., 2020).

### 5.1.3 Hydrochar energy recovery

The energy content and solid fuel properties of the different hydrochars, cakes and sludges were assessed for estimating the energy recovery potential of wastewater sludge hydrochars. The energy content and solid fuel properties of the hydrochars, cakes, and concentrated and diluted sludges are presented in Table 12. The HHVs of the digestate hydrochars were decreased in the mildest HTC treatments by 1.0–1.4% compared to the original digestate but increased by 2–5% at severer conditions. The mixed sludge hydrochars' HHVs were all increased by 7–37% respective to original sludges. The increasing severity of the HTC treatment steadily increased the hydrochar HHVs for both sludges (Fig. 9). As the HHV increase was smaller, also the energy densification was lower for digestate than for mixed sludge, being 0.95–1.05 or 1.07–1.38, respectively (Table 12). Also the energy yields were lower for digestate than mixed sludge (Fig. 4). The increased HHV and energy densification were the cause of increased carbon and decreased oxygen contents in mixed sludge and decreased hydrogen content in digestate (Table 12). This indicated that decarboxylation reactions were dominating in the HTC of mixed sludge (Lin et al., 2015), whereas other reactions, *i.e.*, demethylation and dehydration, seemed more prominent in the HTC of digestate as the hydrogen content was slightly increased in the digestate hydrochars (Lin et al., 2015; Martinez et al., 2021).

**Table 12.** Heating values, energy densifications, and elemental compositions (C, H, N, S, O) of digestates, mixed sludges, and their respective hydrochars (Papers I and II).

Material	HHV (MJ/kg-TS)	Ed (daf)	C (% TS)	H (% TS)	N (% TS)	S (% TS)	O (% TS)
Concentrated digestate	11.49 ± 0.2	n.a.	30.30 ± 0.4	4.40 ± 0.02	3.5 ± 0.1	2.3 ± 0.2	59.40
Concentrated digestate hydrochars							
210°C for 30 min	11.33 ± 0.1	1.11 ± 0.1	31.07 ± 0.02	3.87 ± 0.04	2.54 ± 0.02	1.83 ± 0.04	60.70
210°C for 120 min	11.38 ± 0.1	1.17 ± 0.02	31.00 ± 0.4	3.69 ± 0.03	2.57 ± 0.04	1.80 ± 0.1	60.06
230°C for 30 min	11.63 ± 0.03	1.19 ± 0.02	31.40 ± 0.9	4.00 ± 0.1	2.70 ± 0.1	1.93 ± 0.1	60.00
230°C for 120 min	11.89 ± 0.1	1.27 ± 0.05	30.30 ± 0.1	3.58 ± 0.02	2.40 ± 0.1	1.77 ± 0.02	61.94
250°C for 30 min	11.85 ± 0.02	1.32 ± 0.02	30.03 ± 0.4	3.78 ± 0.04	2.26 ± 0.03	2.16 ± 0.1	61.78
250°C for 120 min	12.12 ± 0.1	1.38 ± 0.02	30.30 ± 0.7	3.48 ± 0.1	2.15 ± 0.05	2.17 ± 0.02	61.90
Diluted digestate	11.93 ± 0.1	n.a.	28.6 ± 0.2	4.21 ± 0.04	3.10 ± 0.04	2.3 ± 0.02	61.92
Diluted digestate hydrochars							
210°C for 30 min	11.35 ± 0.01	1.13 ± 0.03	30.41 ± 0.3	3.98 ± 0.02	2.58 ± 0.04	1.91 ± 0.1	61.23
210°C for 120 min	11.38 ± 0.03	1.14 ± 0.01	30.01 ± 0.6	3.80 ± 0.1	2.38 ± 0.1	2.00 ± 0.05	61.81
230°C for 30 min	11.82 ± 0.1	1.19 ± 0.01	29.72 ± 0.3	3.99 ± 0.04	2.42 ± 0.01	2.10 ± 0.2	61.77
230°C for 120 min	11.48 ± 0.2	1.19 ± 0.02	29.59 ± 0.4	3.66 ± 0.03	2.14 ± 0.04	2.18 ± 0.1	62.44
250°C for 30 min	11.86 ± 0.1	1.23 ± 0.01	30.41 ± 1.3	4.00 ± 0.2	2.31 ± 0.05	2.23 ± 0.1	61.03
250°C for 120 min	12.19 ± 0.4	1.36 ± 0.01	30.38 ± 0.3	3.84 ± 0.1	2.30 ± 0.04	2.19 ± 0.1	61.29
Concentrated mixed sludge	14.9 ± 0.02	n.a.	42.4 ± 0.1	5.78 ± 0.02	1.24 ± 0.04	0.37 ± 0.03	50.21
Concentrated mixed sludge cake	15.0 ± 0.01	1.00 ± 0.00	42.6 ± 0.2	5.78 ± 0.00	1.33 ± 0.06	0.39 ± 0.04	49.90
Concentrated mixed sludge hydrochars							
210°C for 30 min	16.0 ± 0.4	1.08 ± 0.00	46.08 ± 0.7	5.68 ± 0.01	1.14 ± 0.1	0.42 ± 0.0	46.68
210°C for 120 min	16.0 ± 0.1	1.08 ± 0.00	48.74 ± 0.4	5.62 ± 0.01	1.58 ± 0.05	0.44 ± 0.02	43.62
230°C for 30 min	16.7 ± 0.2	1.14 ± 0.00	49.2 ± 0.5	5.66 ± 0.02	1.48 ± 0.05	0.40 ± 0.03	43.26
230°C for 120 min	17.9 ± 0.8	1.24 ± 0.00	52.41 ± 0.3	5.63 ± 0.02	1.62 ± 0.02	0.45 ± 0.01	39.89
250°C for 30 min	20.1 ± 0.1	1.40 ± 0.01	52.39 ± 0.7	5.39 ± 0.02	1.54 ± 0.07	0.45 ± 0.01	40.23
250°C for 120 min	20.4 ± 0.1	1.49 ± 0.04	55.47 ± 1.0	5.12 ± 0.04	1.63 ± 0.06	0.51 ± 0.04	37.27
Diluted mixed sludge	14.9 ± 0.02	n.a.	42.4 ± 0.2	5.78 ± 0.03	1.24 ± 0.05	0.37 ± 0.04	50.21
Diluted mixed sludge cake	15.0 ± 0.1	1.00 ± 0.00	42.6 ± 0.2	5.78 ± 0.01	1.68 ± 0.08	0.46 ± 0.04	49.44
Diluted mixed sludge hydrochars							
210°C for 30 min	16.1 ± 0.02	1.08 ± 0.00	46.05 ± 0.5	5.75 ± 0.06	0.9 ± 0.01	0.30 ± 0.02	47.00
210°C for 120 min	16.6 ± 0.2	1.11 ± 0.00	47.56 ± 0.14	5.70 ± 0.08	1.20 ± 0.05	0.30 ± 0.00	45.24
230°C for 30 min	16.5 ± 0.03	1.11 ± 0.00	47.48 ± 0.4	5.76 ± 0.07	1.08 ± 0.03	0.28 ± 0.01	45.40
230°C for 120 min	18.1 ± 0.01	1.26 ± 0.00	50.59 ± 0.1	5.58 ± 0.01	1.30 ± 0.02	0.30 ± 0.01	42.23
250°C for 30 min	18.8 ± 0.1	1.32 ± 0.00	52.99 ± 0.1	5.58 ± 0.01	1.48 ± 0.04	0.38 ± 0.01	39.57
250°C for 120 min	20.5 ± 0.1	1.49 ± 0.00	56.81 ± 0.3	5.17 ± 0.02	1.84 ± 0.01	0.41 ± 0.01	35.77

HHV, higher heating value; TS, total solids; Ed, energy densification; daf, dry ash free

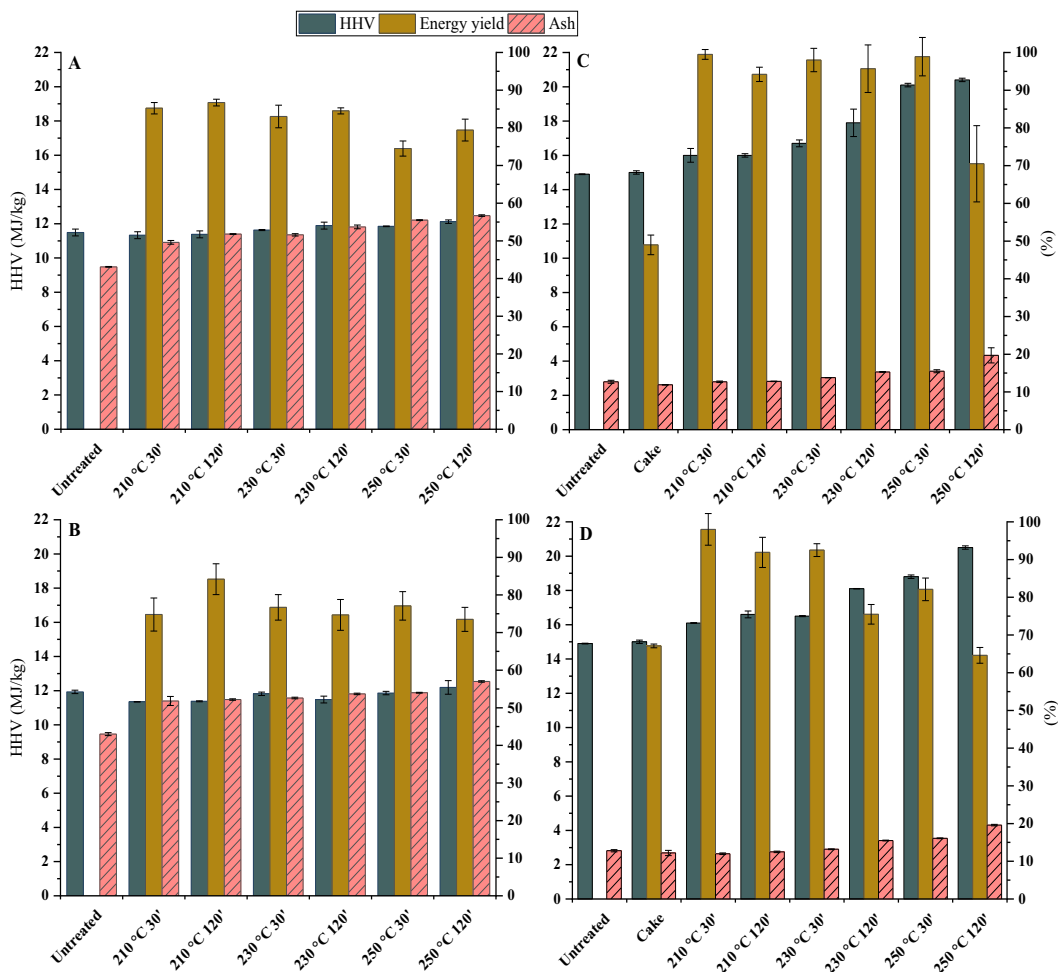


**Figure 9.** Energy yields, ash contents (in % of total solids (TS)), and higher heating values (HHV) of concentrated digestate hydrochar (A), diluted digestate hydrochar (B), concentrated mixed sludge hydrochar (C), and diluted mixed sludge hydrochar (D) (Papers I and II).

The hydrochar behaviour upon combustion was assessed by the ash content. The ash contains inorganic elements that are responsible for fouling, slagging and corrosion of the combustion equipment which include alkali and earth alkali metals (Na, K, Mg and Ca) as well as P, Fe, Si and S (Smith et al., 2016). The studied pulp-mill mixed sludge had initially low potassium content compared to other lignocellulosic biomasses, such as corn stover and switch grass, because of the preceding pulping process that removes hemicellulose and extractives with which potassium in virgin wood associates (Reza et al., 2013). The calcium content in the hydrochars were, in contrast, high compared to other biomasses (Smith et al., 2016), which likely resulted from the use of calcium carbonate as an agent for paper coating in paper making (Nurmesniemi et al., 2007).

The ash content was significantly lower in the mixed sludge (13%) than in the digestate (43%), for which the hydrochars from mixed sludge had lower ash contents (12–20%) than digestate hydrochars (49–57%). All the digestate hydrochars possessed 15–30% higher ash contents than the original digestate, while

only the mixed sludge hydrochars from 230°C and 250°C had higher (3–55%) ash contents than the original mixed sludge. The hydrochar ash contents were independent of the initial sludge TS content. The increasing severity of the HTC treatments increased the hydrochar ash contents from 49% to 57% and from 12% to 20% in digestate and mixed sludge hydrochars, respectively. Although the percentage of ash content increased, the ash yields decreased by the severity, which indicated that part of the ash inorganics were increasingly dissolved when HTC temperature and residence time were increased. For instance, the potassium and calcium contents in the mixed sludge hydrochars were reduced during HTC, diminishing the fouling or slagging in furnaces caused by the alkali metals in hydrochar ash if incinerated (Smith et al., 2016). As observed in the present study, the ash content in hydrochars tends to increase along with treatment severity, which could challenge the argument of HTC improving the solid fuel properties of pulp and paper industry sludges more at higher temperatures. Therefore, although the severest conditions result in highest increases in HHVs and energy densifications and decreases in oxygen content (Martinez et al., 2021; Saha et al., 2019), the increasing ash content should be accounted in the interpretation of the feasibility of the severest treatment conditions, which could result in the recommendation of mild reaction severities (De la Rubia et al., 2018).

The NO<sub>x</sub> and SO<sub>x</sub> emission potential was addressed by determining the sulfur and nitrogen contents of hydrochars (Table 12). The HTC treatments reduced the sulfur contents of the original digestates and diluted mixed sludge, while the sulfur content of the concentrated mixed sludge slightly increased. The fact that the diluted mixed sludge hydrochars had on average 25% lower sulfur content than concentrated mixed sludge hydrochars, indicated that the diluted mixed sludge was more prone to release sulfur in the liquid and gas phases during HTC treatment than concentrated mixed sludge. The increasing HTC treatment severity increased the sulfur contents in all hydrochars. Nitrogen contents that contribute to NO<sub>x</sub> emissions in the hydrochars were more dependent on the sludge origin than the HTC treatment, as the digestate nitrogen content were reduced by 21–39% but those of mixed sludge were increased by up to 48% after the severest HTC treatments. The mixed sludge hydrochar nitrogen content was in the range of that in coal (on average  $1.5 \pm 0.4\%$  daf) (Netherlands Energy Research Centre (ECN)), whereas the digestate hydrochars had nitrogen contents of 4.6–5.6% daf. The comparatively high sulphur content in the present digestate may arise from the addition of phosphorous precipitation chemical, Fe(II)SO<sub>4</sub>, at the WWTP, which is also supported by the high iron concentrations in the hydrochars that are ca. 10-fold higher than that reported for dewatered digestate by Marin-Batista et al. (2020). Both digestate and mixed sludge of lower TS content were more prone to release sulphur and nitrogen to the liquid and gas phases during HTC treatments than higher TS sludges. Mere filtration had no effect on the dissolution of these elements. However, the differences in the contents of nitrogen and sulphur between the resulting hydrochars were small (Table 12).

#### 5.1.4 Hydrochar in carbon sequestration

The fate of carbon in HTC was assessed based on its contents in the hydrochars and the mass balance results (Fig 6, Table 12). The carbon content of the digestate was increased only by a maximum of 2–3 %, resulting in carbon contents of 29–31% TS in the hydrochars, which is a typical range for hydrochars from digested sewage sludge (Aragón-Briceño et al., 2021a; Parmar and Ross, 2019). The mixed sludge carbon content in hydrochar was increased by 8–34% with increasing treatment severity, and the ash-free carbon content increased from 48.6% in the mixed sludges and cakes to 52.8%–69.1% (concentrated) and to 52.3%–70.7% (diluted) in the hydrochars. In addition, the average carbon recoveries were higher for mixed

sludge (on average  $94\pm 11\%$  and  $84\pm 14\%$ ) than digestate (on average  $82\pm 7\%$  and  $80\pm 5\%$ ) in the hydrochars from the concentrated and diluted sludge, respectively, decreasing with treatment severity.

The role of hydrochar in carbon sequestration is encouraged by the carbon balance, showing that most of the sludge carbon is recovered in the hydrochar fraction. Based on the present results, carbon recovery in the hydrochar is favored by the lower HTC temperatures and by using more concentrated sludges. The evaluation of the HTC treatment conditions should also consider the reactions in the sludge matrix induced by the higher temperature, such as protonation of OH-groups, aromatization, and decarboxylation, demethylation and dehydration reactions (Schulze et al., 2016), which stabilize carbon in the hydrochar. It has been reported that hydrochars of straw digestate produced at  $210^{\circ}\text{C}$  has emitted up to 11.9% of the total carbon, while that at  $250^{\circ}\text{C}$  has emitted 3.2% upon a 120-day incubation test (Schulze et al., 2016). The stability of carbon in hydrochar is also influenced by the duration of the soil application of hydrochar, as hydrochar from corn silage has been reported to decompose by up to 50% after 100 d of soil application stimulating  $\text{CH}_4$  and  $\text{CO}_2$  emissions (Malghani et al., 2013), while long-term carbon stability estimates with chemical incubation tests have suggested that 37% of the hydrochar carbon remains in soil after 10 years, but after several decades, the sequestration potential will be slightly negative ( $-0.7\%$ ) (Naisse et al., 2015). However, hydrochar outperforms mere digested biomass samples in crop field studies by increasing  $\text{CH}_4$  uptake and reducing  $\text{CO}_2$  emissions (Adjuik et al., 2020; Schimmelpfennig et al., 2014). The carbon decomposition likely derives from increased microbial activity due to the easily degradable carbon of hydrochar (Kambo and Dutta, 2015) which correlates with hydrophilic functional groups, high O/C and H/C ratios, and with low C/N ratio and lignin content (Eibisch et al., 2013; Schimmelpfennig and Glaser, 2012). Suitable HTC conditions, possibly with catalysts and/or additives, should be targeted to yield hydrochar with high aromatic carbon structures with low O/C and H/C ratios (Eibisch et al., 2013; Schimmelpfennig and Glaser, 2012), or to consider water washing of hydrochar to remove hydrophilic functional groups (Eibisch et al., 2013). However, as the hydrochar structure and properties vary according to its origin, more studies specifically on hydrochar from sewage sludge digestate are needed, as majority of the research about hydrochar as carbon storage concern hydrochars of lignocellulosic and/or starchy origin (Catenacci et al., 2022).

### 5.1.5 HTC filtrates' biogas production

The energy recovery potential of the HTC filtrates for biogas production was evaluated based on their SCOD and VFA concentrations as well as with experimental BMP assays. For both sludges, the SCOD was increased ten-fold by the HTC treatment, resulting in ranges in digestate HTC filtrates of 37–44 g/L and 28–32 g/L and in mixed sludge HTC filtrates of 23–52 g/L and 23–41 g/L from concentrated and diluted sludges, respectively. The diluted sludges resulted in lower SCOD concentrations, but when accounting the dilution of the mixed sludge (32% TS diluted to 15% TS) (Eq. 5), the diluted HTC filtrates had 1.3-fold higher SCODs than those from concentrated mixed sludge.

The SCODs were slightly higher in the HTC filtrates from higher treatment temperatures, but no major effects of the HTC conditions were obvious. However, the SCOD composition concerning the VFAs varied between the HTC treatments and the two sludges. The VFAs accounted for 10–33% and 11–34% (digestate) and 15–36% and 13–20% (mixed sludge) of the HTC filtrates' SCOD from concentrated and diluted sludges, respectively, while the SCOD of the cake filtrates comprised completely of VFAs. The TVFA concentrations increased up to 3.4-folds (digestate) and 4.4-folds (mixed sludge) with a temperature increase from  $210^{\circ}\text{C}$  to  $250^{\circ}\text{C}$ . The higher treatment temperature especially increased the concentration of propionate in digestate HTC filtrates from around 0.4 g/L at  $210^{\circ}\text{C}$  up to 6.9 g/L at  $250^{\circ}\text{C}$ , while the

changes in other VFA concentrations were low. In all mixed sludge HTC filtrates, the dominant VFA was acetic acid, the concentration of which increased with treatment severity by 57% (to 7.2 g/L) and by 79% (to 4.4 g/L) in concentrated and diluted mixed sludge treatments, respectively. Based on the VFA concentrations and their relatively minor increases respective to that of the increases in SCODs, the majority of SCOD was made of non-VFAs. Interestingly, the non-VFA content in digestate HTC filtrates decreased with treatment severity, while in mixed sludge HTC filtrates, the non-VFA content increased.

The BMPs were determined for the HTC and cake filtrates from concentrated sludges (Fig. 10). The specific BMP yields of the digestate HTC filtrates were around two-folds (185–206 L-CH<sub>4</sub>/kg-SCOD) higher compared with the BMP of the cake filtrate (97 L-CH<sub>4</sub>/kg-SCOD), whereas the specific BMPs of the mixed sludge HTC filtrates were lower (190–266 L-CH<sub>4</sub>/kg SCOD) than that of the cake filtrate (318 ± 45 L-CH<sub>4</sub>/kg SCOD). However, as the concentration of SCOD was much higher in the mixed sludge HTC filtrates (23–44 g/L) than in the respective cake filtrate (4 g/L), the volumetric BMPs were 5–6-fold higher in the HTC filtrates (6.2–11.4 L-CH<sub>4</sub>/L) than in the cake filtrate (1.2 L-CH<sub>4</sub>/L). These volumetric BMPs of mixed sludge HTC filtrates increased with increasing temperature and residence time from 6.2 to 11.4 L-CH<sub>4</sub>/L, except for the severest treatment (250°C for 120 min) (7.7 L-CH<sub>4</sub>/L). The digestate BMPs experienced less variation and no clear impact from the different HTC conditions could be observed.

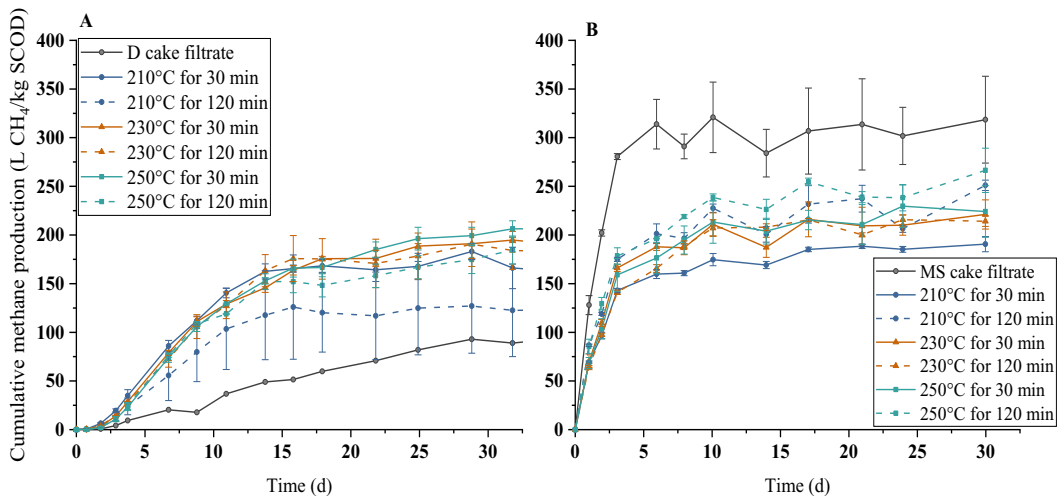


**Figure 10.** The cumulative methane production curves of digestate HTC filtrates (A) and mixed sludge HTC filtrates (B) as well as their cake filtrates. The methane productions of the inocula have been subtracted from the results (Papers I and II).

## 5.2 Effect of pyrolysis liquid addition on methane production from sewage sludge and thermally pretreated sewage sludge

### 5.2.1 Characterization of pyrolysis liquid for AD

The present pyrolysis liquid had a COD of 3.7 g/L, SCOD of 3.6 g/L and the TVFA content was 0.9 g-COD/L. The VFAs were comprised of acetic acid (37% of the TVFA), butyric acid (24%), and valeric acid (39%). The total soluble nitrogen content in the pyrolysis liquid was 3.6 g/L, of which 61 mg/L was ammonium-nitrogen, and the phosphate concentration was 7 mg/L. The pyrolysis liquid was alkaline (pH 9.1) which may be the cause of the low TVFA concentration and presence of buffering compounds (Villamil et al., 2018). In addition, the nitrogen compounds can contribute the alkalinity of the pyrolysis liquid (Azua et al., 2013), which seems typical for pyrolysis liquids of a sewage sludge origin (Seyedi et al., 2019; Yue et al., 2019).

The BMPs of the pyrolysis liquid alone and at 1% or 5% (v/w) shares of pyrolysis liquid on the methane production from sewage sludge and THSS were determined. The pyrolysis liquid alone did not produce any methane, indicating that the COD in the pyrolysis liquid was not readily biodegradable and/or that it contained some inhibitory compounds preventing methane production. THSS with 1% and 5% (v/w) additions of pyrolysis liquid resulted in 14% and 19% lower BMPs,  $295 \pm 15$  L CH<sub>4</sub>/kg-VS and  $277 \pm 25$  L CH<sub>4</sub>/kg-VS, respectively, than THSS without pyrolysis liquid (342 L CH<sub>4</sub>/kg-VS). The methane production from sewage sludge was less affected by the pyrolysis liquid, resulting in 10% lower BMPs ( $305 \pm 8$  L CH<sub>4</sub>/kg-VS for 1% (v/w) of pyrolysis liquid and  $300 \pm 52$  L CH<sub>4</sub>/kg-VS for 5% (v/w)) than the BMP of sewage sludge ( $333 \pm 29$  L CH<sub>4</sub>/kg-VS). In both sewage sludge and THSS assays, the methane production was slower with pyrolysis liquid than without, particularly for THSS at both shares and for sewage sludge at 5% (v/w) share.

The higher inhibitory effect of pyrolysis liquid on THSS than sewage sludge could be due to the differing VFA contents of these substrates. Sewage sludge contained more VFAs than THSS, because of which the starting of methane production could be faster from sewage sludge, possibly diminishing the inhibitory impacts of pyrolysis liquid (Torri and Fabbri, 2014). Besides the different VFA contents, the changes in C/N balance possibly caused by THP, could also increase the susceptibility to inhibition (review by (Feng and Lin, 2017). Also the fact that the different proportions (1% vs. 5% (v/w)) of the present pyrolysis liquid added to THSS resulted in similar BMPs, indicates that the pyrolysis liquid contained some inhibitory compounds, such as nitrogen-containing compounds, phenols, and/or their derivatives (Seyedi et al., 2019), concentrations of which were already sufficient at the lower pyrolysis liquid share to hinder the microorganisms activity.



## 5.2.2 Pyrolysis liquid in semi-continuous AD reactors

The negative effect from pyrolysis liquid on the AD of sewage sludge and THSS observed in the BMP assays was further studied in three parallel thermophilic laboratory semi-CSTRs, to see whether the inhibitory effect could be alleviated with a semi-continuous feeding regime. Because of the decrease of 14–19% in methane production in BMP assays from THSS upon the addition of 5% (v/w) pyrolysis liquid, a lower share in the semi-CSTR studies was used. The reactor experiment lasted for 221 days. The initial OLR was 3 kg-VS/m<sup>3</sup>d and the HRT 19.6 d (Table 7). THSS was used as substrate in all three reactors, in one of which sewage sludge was fed instead after 44 days. Due to the substrate change, the methane yield decreased to 88±12 L/kg-VS, while in the reactors fed with THSS, the methane yields increased to above 200 L/kg-VS. The addition of pyrolysis liquid in the reactor feeds started on day 79, gradually increasing its share from 0.15% (v/w) to 1% (v/w), while one of the reactors (fed with THSS) was kept as control, not being fed with pyrolysis liquid. The addition of pyrolysis liquid at 1% (v/w) did not have a drastic (negative) effect on the process, as confirmed by the similar methane yields and digestate characteristics (pH, SCOD, TVFA) in all three reactors during the stable operational period (days 153–221). Rather, the small differences in the methane yields and in its fluctuations (Fig. 11), in ammonification of organic nitrogen (63% vs. 39%), and in final digestate TVFA contents (0.3 vs. 0.6 g-COD/L) could be attributed to the differences between the main feeds, *i.e.*, THSS and sewage sludge.

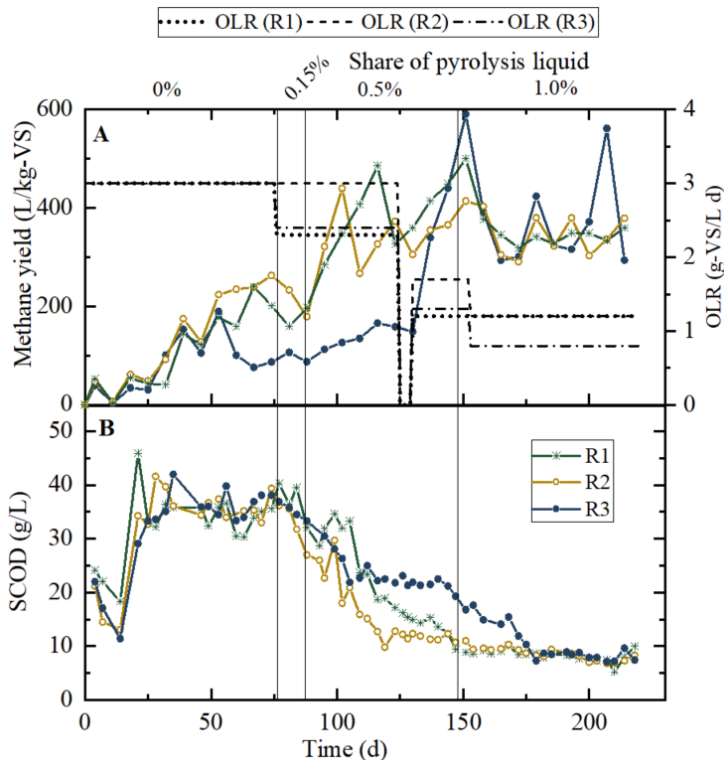


**Figure 11.** Methane yields (A) and SCOD of digestates (B) in semi-CSTR experiment with pyrolysis liquid addition (Paper III).

The THSS resulting in higher methane yields than sewage sludge with higher OLRs (2.3–3 kg-VS/m<sup>3</sup>d), implied that the THP treatment for sewage sludge promoted the hydrolysis step in AD, enabling increased

loading rates and solid contents of the feed (Higgins et al., 2017), as after decreasing the OLR and prolonging the HRT, sewage sludge started to produce more methane than THSS. It has been reported that even up to 1.3-fold higher methane yields from sewage sludge than THSS are possible at an OLR of 3.8 kg COD/m<sup>3</sup> d, but after increasing the OLR, the methane yield from THSS was increased by 6.2% while that from sewage sludge decreased by 5.4% (Choi et al., 2018).

The difference between the inhibitory effect of the pyrolysis liquid addition in the semi-CSTR experiment and BMP assay could be explained by the lower pyrolysis liquid shares. However, THSS experienced inhibition in the batch assays already at 1% (v/w) loading, suggesting that an already working digestion process before starting a gradual pyrolysis liquid feeding could alleviate the inhibitory effect. Semi-continuous feeding allows microorganisms to acclimate to the prevailing substrates and enable higher pyrolysis liquid loadings (Seyedi et al., 2020; Zhou et al., 2019). The inhibitory effect of pyrolysis liquid can also be alleviated by a supplementation of nutrients and/or biochar, which enhance the microorganism growth and detoxify organic compounds, respectively (Wen et al., 2020). Based on the above-mentioned results, pyrolysis liquid could be added to anaerobic digesters, but its origin and characteristics determine its applicable share of the main feed, but also the properties of the main feed should be considered.

### 5.3 Scale-up assessment of HTC integration in biogas plants

#### 5.3.1 Mass, nutrient, and carbon flows and recoveries

The HTC integration to a centralized biogas plant was evaluated regarding the mass and nutrient flows inside the plant and the amounts and concentrations of nutrients and carbon in the end products. Due to the circulating liquid side streams (reject water, condensate from stripping, and HTC filtrate) inside the biogas plant, the mass and nutrient balance flow calculations were repeated until attaining stabilized values, the original layout required a minimum of 41 calculation rounds and the layout with HTC 29 rounds (Paper IV).

The outflow product amount and nutrient contents changes are shown in Table 13. The most important difference between the layouts was the amount of the solid product, *i.e.*, digestate cake or hydrochar, the latter having a 60% decrease in wet mass. The amount of ammonia water (15% NH<sub>3</sub>) increased by 33% and that of concentrate 28% upon HTC integration. The largest difference between the layouts was the amount of condensate discharged to WWTP which increased by 71% to 46,539 t/a. The biogas amount was increased only by 1% in the HTC layout from the original, covering 14% of the amount of the incoming sewage sludge in each layout.

**Table 13.** The changes in the amounts of the outflowing products and in the nutrient amounts of the outflowing products following from the HTC integration to biogas plant (Paper IV).

Outflow product stream	Mass	TS	VS	Total N	NH <sub>4</sub> -N	Total P
Hydrochar vs. digestate cake	- 60 %	- 17 %	- 21 %	- 39 %	- 100 %	- 1 %
Ammonia water	+33 %	0 %	0 %	+ 33 %	+ 33 %	0 %
Concentrate	+28 %	+28 %	+30 %	+ 75 %	0 %	+ 27 %
Condensate	+71 %	0 %	0 %	+ 33 %	+ 33 %	0 %
CH <sub>4</sub>	+1 %	n.a.	n.a.	n.a.	n.a.	n.a.
CO <sub>2</sub>	+1 %	n.a.	n.a.	n.a.	n.a.	n.a.

n.a. not applicable; TS, total solids; VS, volatile solids

The main advantage from HTC integration to biogas plant for treating digestate is the drastically reduced amount of solid end product, which supports its transportation for carbon storage and/or nutrient source. Therefore, HTC could be used as an effective and complementary dewatering process, as the applicability of sewage sludge digestate cake as a nutrient source is negatively affected by its large annual amounts concerning the increasing transportation costs (Medina-Martos et al., 2020; Tampio et al., 2016).

The differences in the product amounts were explained with the inflows into the unit processes and with the circulating liquid streams inside the biogas plant. The main difference between the layouts, which was also the reason for the increased amounts of ammonia water, concentrate and condensate, was the volume of reject water available for nutrient recovery in the evaporator-stripping unit. In the original layout, 148,209 t/a of reject water was produced of which 44% was used for AD feed dilution and the rest 56% (82,962 t/a) was fed to evaporator-stripping unit, while in the layout with HTC, of the total produced volume of reject water (146,739 t/a) up to 72% was available for nutrient recovery. In other words, as the HTC filtrate was completely used for diluting the AD feed, the need of reject water decreased.

The ammonia water represented the most nitrogen containing product in the layout with HTC, containing 47% and 94% of the outflowing total nitrogen and ammonium-nitrogen, respectively. Ammonia water is a valuable ammonia source for industries, *e.g.*, as a sustainable nutrient source in aerobic industrial wastewater treatment process. In the original layout, the digestate cake contained most of the outflowing total nitrogen (56%) and 47% of the ammonium nitrogen, the second most ammonium nitrogen containing stream being the ammonia water (49% of the total ammonium-nitrogen outflow). In addition, HTC integration increased the amount of nitrogen in the concentrate by 75% (Table 13). Interestingly, the total amount of recovered ammonium-nitrogen in the original layout was 724 t/a, whereas with HTC, the total amount of ammonium-nitrogen recovered was 502 t/a. However, nearly half of the recovered ammonium-nitrogen in the original layout was in the digestate cake, while with HTC, 95% of the recovered ammonium nitrogen was in the ammonia water. Another feature of HTC is the generation of HTC gas to which nitrogen assumingly evaporates as  $\text{NH}_3$  (Zhuang et al., 2017). In this study, HTC gas contained up to 4% of the total nitrogen outflow (37 t/a), decreasing the total recovered amount of nitrogen by 3.7% compared to the original layout. This urges to consider nitrogen recovery from the HTC gas, *e.g.*, by directing it to ammonium stripping where it would increase  $\text{NH}_3$  content in the input gas, also supply heat to the process.

The HTC integration had no effect on phosphorous recovery, because of the presence of phosphorous precipitating iron salts used in the wastewater treatment for phosphorous recovery (Huang et al., 2017) and because HTC is incapable of affecting phosphorous release from solids when bound to salts (Breulmann et al., 2017). Inside the plant, phosphorous was only distributed into the end products slightly differently: originally, 5% (23t/a) and 95% (463 t/a) of phosphorous entering the biogas plant was recovered in the concentrate and digestate cake, while with HTC 6% (29 t/a) and 94% (457 t/a) was recovered in the concentrate and hydrochar. The amount of recovered carbon in the digestate cake (3,646 t/a) was 17% higher than that in hydrochar (3,119 t/a), because of carbon dissolution to the HTC filtrate and evaporation to the HTC gas.

### 5.3.2 Energy balance

The calculated produced amount of energy in the biogas plant was increased by 1.4% to 65.0 GWh/a by HTC integration, but which also increased the total energy demand of the unit processes by 4% to 16.2 GWh/a. Nevertheless, the biogas plant layout with HTC integration resulted in a positive net energy

balance of 47.7 GWh/a, increasing from the 47.4 GWh/a of the original layout. The higher temperature of HTC than hygienization had a low impact on the plant's energy demand, rather the integration and thereby the HTC filtrate recycling influenced the net energy balance by increasing evaporator-stripping energy demand, biogas production, and decreasing the AD feed heating demand (Table 14).

**Table 14.** The annual energy demand of the different unit processes and their total energy demand in a biogas plant with HTC integration and without (original layout) (Paper IV).

Unit process	Layout with HTC (MWh/a (% of total))			Original layout (MWh/a (% of total))		
	Heat	Electricity	Energy in total	Heat	Electricity	Energy in total
AD	-1,963 (44%)	-650 (6%)	-2,613 (16.2%)	-2,508 (45%)	-641 (6%)	-3,149 (20.3%)
Dewatering	n.a. (n.a.)	-1,626 (14%)	-1,626 (10.1%)	n.a. (n.a.)	-1,634 (16%)	-1,634 (10.5%)
Evaporator-stripping	-2,431 (55%)	-2,642 (22%)	-5,073 (31.4%)	-1,908 (34%)	-2,074 (21%)	-3,982 (25.6%)
HTC/Hygienization	-28 (1%)	-1,155 (10%)	-1,183 (7.3%)	-1,177 (21%)	n.a. (n.a.)	-1,177 (7.6%)
LGB-upgrading	n.a. (n.a.)	-5,679 (48%)	-5,679 (35.1%)	n.a. (n.a.)	-5,599 (56%)	-5,599 (36.0%)
Total	-4,421 (100%)	-11,753 (100%)	-16,174 (100%)	-5,593 (100%)	-9,948 (100%)	-15,541 (100%)

n.a. not applicable; AD, anaerobic digestion, HTC, hydrothermal carbonization; LGB, liquefied biogas

More detailed energy calculations of the HTC and hygienization units revealed that the digestate heating to the HTC treatment temperature required 8,366 MWh/a while to the hygienization temperature 6,339 MWh/a. This difference stems from the lower amount and higher TS content of the digestate fed to HTC than of the digestate fed to hygienization. The energy demand can be partly compensated by the means of heat recovery in heat exchangers (by 71% in HTC and by 82% in hygienization) and by the heat of digestate carbonization reaction (by 29%) in HTC. As a result, HTC with filtration required 7% of the total energy demand of the biogas plant, while the three hygienization units required 8% (Table 14). Heat recovery from the cooling of the reactor products is essential for achieving energetically and economically efficient process (Erlach 2014), as with heat recovery the energy demand can be reduced by 59% and without heat recovery, the energy needed to heat the HTC reactor with non-preheated digestate feed (25% TS) could represent about 65% of the total energy input to HTC (Danso-Boateng et al., 2015). Additionally, the exothermic carbonization reactions, *i.e.*, the heat of reaction, in HTC can represent around 19–35% of the energy demand (Danso-Boateng et al., 2015).

The possibility to rearrange the liquid flow recycling inside the biogas plant and to utilize HTC filtrate in AD inside the biogas plant increased the energy efficiency of the AD as the HTC filtrate (70°C) could contribute to the heating of AD feed also by replacing cooler reject water (40°C) in the diluting liquids. The liquid flow rearrangement by HTC integration increased the evaporator-stripping unit's energy demand by 27% due to higher volumes of reject water to be treated. However, it did not affect the energy consumed by the evaporator-stripping unit against the nitrogen recovered, being 21.3 kWh/kg-N with HTC and originally 22.2 kWh/kg-N, as the original reject water had lower total and ammonium nitrogen concentrations. Hence, AD represented a viable disposal route for the HTC filtrate, although the methane production increased only by 1.4% from 675 to 684 kWh/t of sewage sludge (Table 4). Similar to the present study, also in one HTC integration assessment, despite the HTC filtrate feeding to AD, the methane yields resulted similar (100 and 103 m<sup>3</sup> CH<sub>4</sub>/t of primary and secondary sludge with and without HTC, respectively) (Medina-Martos et al. 2020). The BMP and COD of the HTC filtrate depend on the HTC conditions (Paper II), therefore HTC temperature optimization and considering the product yields and energy demand, could possibly result in improved methane production. The HTC filtrate recycling to

increase biogas production cannot necessarily be relied on as a productivity increasing factor in large scale, rather regard the HTC filtrate digestion as a feasible waste stream treatment method.

## 6 CONCLUSIONS AND RECOMMENDATIONS FOR FUTURE RESEARCH

The main objective of this thesis was to evaluate the potential of HTC in wastewater sludge management and in wastewater sludge processing into value-added products concerning nutrient, carbon, and energy recovery. The evaluation was conducted through the analysis of the HTC products, *i.e.*, solid hydrochar and the liquid filtrate, concerning their chemical constituents, solids contents, and energy production potentials. The energy production potential of hydrochar was analyzed based on its solid fuel properties for combustion, which was compared with those of the untreated counterpart, while that of the filtrate was based on its intended exploitation in AD. The aim was also to discover the effect of different HTC treatment conditions (temperatures of 210°C, 230°C, and 250°C, and residence times of 30 and 60 min) and sludge solids contents (15% TS, 25% TS, and 32% TS) on the resulting properties of the products. A further objective was to assess the effects of pyrolysis liquid addition on AD of sewage sludge to evaluate whether pyrolysis liquid could be treated on-site in centralized biogas plant, and thus avoid external wastewater treatment. Concerning this treatment possibility, the potential inhibitory effect stemming from the AD of pyrolysis liquid from municipal sewage sludge digestate was studied by carrying out batch and semi-continuous AD experiments.

The results of this thesis showed that HTC can be used to improve the treatment and use of municipal sewage sludge digestate and pulp and paper mixed sludge. Both sludges experienced improvement in dewaterability, solid fuel properties, carbon sequestration, and nutrient concentrations but to a different extent. The dewaterability improvement was experienced in practice for digestates as the non-HTC treated digestates could not be filtrated similarly to the HTC-treated ones. The dewaterability improvement could also be deduced from the hydrochar TS contents, which were in the range of 35–62%, while the digestates had TS contents of 15% or 25%. The significant improvement in dewaterability of sewage sludge digestate supports the management and utilization requirements imposed for wastewater sludges.

HTC treatments concentrated nutrients in hydrochars and over 90% of phosphorous was recovered in the hydrochars of digestate and mixed sludge, resulting in concentrations of up to 56 g/kg-TS and 7 g/kg-TS, respectively. Nitrogen was distributed more evenly between hydrochar, HTC filtrate and gas, the less severe HTC conditions favouring nitrogen recovery, as the amount of evaporated nitrogen increased at temperatures of 250°C. As the nutrient contents of the hydrochars from sewage sludge digestate were higher than those from pulp and paper mixed sludge, digestate hydrochars appeared more applicable in nutrient recovery. However, digestate hydrochar use on fields or soil either as a plain nutrient source or as carbon storage can be hindered by the potential adverse effects from unremoved or destroyed contaminants, such as plasticizer, heavy metals, or even degradation products of medicines. The mixed sludge's initial low nutrient contents led to low nutrient contents in hydrochars, and for this reason, mixed sludge hydrochars could be prioritized for carbon sequestration, as the carbon contents were increased in all hydrochars.

The improved usability of hydrochars in energy recovery concerned particularly the mixed sludge derived hydrochars, which had increased HHVs (from original 15 up to 20.5 MJ/kg), energy densifications of up to 1.49, and decreased oxygen contents compared with the respective mixed sludge cakes. The solid

fuel properties of digestate hydrochars were also improved, but to a lesser extent, and their high ash content could decrease the attractiveness for energy recovery *via* combustion. For both digestate and mixed sludge, the increasing treatment severity improved the solid fuel properties, on which the initial sludge solids contents seemed to have an insignificant effect. The lowered amount and increased TS content, *i.e.*, reduced moisture content, were also factors which supported energy recovery from wastewater sludges in the form of hydrochar.

The HTC filtrate exploitation in AD was supported by their methane production potentials in batch tests, which were 180–206 L-CH<sub>4</sub>/kg-SCOD for digestate HTC filtrates and 190–266 L-CH<sub>4</sub>/kg-SCOD for mixed sludge HTC filtrates. The analyzed characteristics of the HTC filtrates were in line with the methane production potentials, as all HTC filtrates had up to 10-fold increased SCOD concentration and higher TVFA content respective to the untreated sludge cake filtrates. These HTC filtrate characteristics of both sludges behaved similarly with the HTC treatment severity, as severer conditions produced HTC filtrates with increased SCOD concentrations and TVFA contents. An exception was pH which in the digestate HTC filtrates increased with treatment severity from 8.4 to 9.7, while in those of the mixed sludge decreased from 5.2 to 4.3. These pH changes were due to the feedstock composition differences, as sewage sludge digestates contain protein that degrades into ammonium, while pulp and paper industry sludges are lignocellulosic which degrade mostly into acidic compounds.

As all the HTC conditions applied in this study generated hydrochars of little variations in properties, it could be recommended to use the lowest temperature (210°C) and shortest residence time (30 min) for hydrochar production from digestate. The optimum temperature for mixed sludge treatment in HTC for the production of hydrochar depended on the target use, as on the basis of carbon content, lower temperatures were favored, but solid fuel properties were most enhanced at 250°C. However, the temperature of 230°C could be regarded as the optimum temperature for generating filtrates with the highest methane production potential. The different optimum conditions resulting in different outcomes should be evaluated together with the prevailing regulations and economic benefit. Hence, an extrapolation study was conducted to a centralized biogas plant, which indicated that the integration of HTC to a biogas plant could enhance the annual biogas production by 5% and ammonium recovery by 25%. The produced hydrochar could be used to produce 83 GJ or to direct 350 t/a phosphorous to agriculture or in carbon sequestration and receive app. 1.1 M€/a in emission trading. Even though hydrochar was used for energy recovery, HTC integration would increase the recovery of nutrients and renewable energy owing to the utilization of the HTC filtrate in AD. As the scale-up assessment in this thesis showed, the ammonium nitrogen in the dewatered digestate ends up in the liquid streams at the biogas plant by HTC deployment, enabling its more efficient recovery in ammonia water that currently has higher value and utilization potential than mere digestate. In addition, the results from the extrapolation calculations of HTC integration to large scale can be used as an indicative example concerning preparation for a possible re-dimensioning requirement of the unit processes at centralized biogas plants because of the expected mass and nutrient flow changes.

The potential simultaneous exploitation and disposal of pyrolysis liquid of sewage sludge digestate through AD was found to be applicable at a share of 1% (v/w) of the main substrate (sewage sludge or THSS). The tested pyrolysis liquid share was relevant to the scale of centralized biogas plant. Pyrolysis liquid appeared inhibitory towards methane production from THSS only in batch tests, at 1% and 5% (v/w) shares, while sewage sludge seemed less liable to the inhibition. In semi-CSTRs no inhibition was observed for either main substrate, implying the importance to utilize the microorganism gradual acclimation capability when pyrolysis liquid or other liquids from thermal treatments are to be fed to AD.

Further research on the production of hydrochars from wastewater sludges should increasingly focus on other hydrochar applications than fuel when optimizing the treatment conditions, such as fertilizer use, carbon sequestration, and use as contaminant removing absorbent. Particularly, hydrochar use for carbon sequestration should be addressed concerning the long-term stability of carbon in soil, effects of feedstock, treatment conditions, additives, and hydrochar activation, because the degree of contaminant removal or destruction during HTC lacks evidence. Hence, more research is needed, particularly for sewage sludge originating hydrochars, on the fate of pharmaceuticals and their degradation intermediates as well as on microplastics. Hydrochar production from wastewater sludges should enable safe nutrient reuse and ensure phosphorous plant availability when phosphorous precipitating chemicals are used at WWTPs. Another matter that requires further research is the economic and environmental feasibility of the deployment of HTC or pyrolysis in connection to WWTPs and biogas plants. The economic and environmental benefit from increasing sludge value by thermal treatment and from the avoidance of external wastewater treatment for the liquid product from the thermal treatment could advance the implementation of these technologies in connection with AD.



## REFERENCES

- Adjuik, T., Rodjom, A.M., Miller, K.E., Reza, M.T.M., Davis, S.C., 2020. Application of hydrochar, digestate, and synthetic fertilizer to a miscanthus *X* *giganteus* crop: Implications for biomass and greenhouse gas emissions. *Appl. Sci. Switz.* 10, 1–21. <https://doi.org/10.3390/app10248953>
- Ahmed, M., Andreottola, G., Elagroudy, S., Negm, M.S., Fiori, L., 2021. Coupling hydrothermal carbonization and anaerobic digestion for sewage digestate management: Influence of hydrothermal treatment time on dewaterability and bio-methane production. *J. Environ. Manage.* 281. <https://doi.org/10.1016/j.jenvman.2020.111910>
- Alvarenga, P., Mourinha, C., Farto, M., Santos, T., Palma, P., Sengo, J., Morais, M.C., Cunha-Queda, C., 2015. Sewage sludge, compost and other representative organic wastes as agricultural soil amendments: Benefits versus limiting factors. *Waste Manag.* 40, 44–52. <https://doi.org/10.1016/j.wasman.2015.01.027>
- Anjum, M., Al-Makishah, N.H., Barakat, M.A., 2016. Wastewater sludge stabilization using pre-treatment methods. *Process Saf. Environ. Prot.* 102, 615–632. <https://doi.org/10.1016/j.psep.2016.05.022>
- Appels, L., Baeyens, J., Degrève, J., Dewil, R., 2008. Principles and potential of the anaerobic digestion of waste-activated sludge. *Prog. Energy Combust. Sci.* 34, 755–781. <https://doi.org/10.1016/j.peccs.2008.06.002>
- Aragón-Briceño, C., Ross, A.B., Camargo-Valero, M.A., 2017. Evaluation and comparison of product yields and bio-methane potential in sewage digestate following hydrothermal treatment. *Appl. Energy* 208, 1357–1369. <https://doi.org/10.1016/j.apenergy.2017.09.019>
- Aragón-Briceño, C.I., Grasham, O., Ross, A.B., Dupont, V., Camargo-Valero, M.A., 2020. Hydrothermal carbonization of sewage digestate at wastewater treatment works: Influence of solid loading on characteristics of hydrochar, process water and plant energetics. *Renew. Energy* 157, 959–973. <https://doi.org/10.1016/j.renene.2020.05.021>
- Aragón-Briceño, C.I., Pozarlik, A.K., Bramer, E.A., Niedzwiecki, L., Pawlak-Kruczek, H., Brem, G., 2021a. Hydrothermal carbonization of wet biomass from nitrogen and phosphorus approach: A review. *Renew. Energy* 171, 401–415. <https://doi.org/10.1016/j.renene.2021.02.109>
- Aragón-Briceño, C.I., Ross, A.B., Camargo-Valero, M.A., 2021b. Mass and energy integration study of hydrothermal carbonization with anaerobic digestion of sewage sludge. *Renew. Energy* 167, 473–483. <https://doi.org/10.1016/j.renene.2020.11.103>
- Astals, S., Venegas, C., Peces, M., Jofre, J., Lucena, F., Mata-Alvarez, J., 2012. Balancing hygienization and anaerobic digestion of raw sewage sludge. *Water Res.* 46, 6218–6227. <https://doi.org/10.1016/j.watres.2012.07.035>
- Azuara, M., Kersten, S.R.A., Kootstra, A.M.J., 2013. Recycling phosphorus by fast pyrolysis of pig manure: Concentration and extraction of phosphorus combined with formation of value-added pyrolysis products. *Biomass Bioenergy* 49, 171–180. <https://doi.org/10.1016/j.biombioe.2012.12.010>
- Bargmann, I., Rillig, M.C., Kruse, A., Greef, J.M., Kücke, M., 2014. Effects of hydrochar application on the dynamics of soluble nitrogen in soils and on plant availability. *J. Plant Nutr. Soil Sci.* 177, 48–58. <https://doi.org/10.1002/jpln.201300069>
- Bayr, S., Rintala, J., 2012. Thermophilic anaerobic digestion of pulp and paper mill primary sludge and co-digestion of primary and secondary sludge. *Water Res.* 46, 4713–4720. <https://doi.org/10.1016/j.watres.2012.06.033>
- Becker, G.C., Wüst, D., Köhler, H., Lautenbach, A., Kruse, A., 2019. Novel approach of phosphate-reclamation as struvite from sewage sludge by utilising hydrothermal carbonization. *J. Environ. Manage.* 238, 119–125. <https://doi.org/10.1016/j.jenvman.2019.02.121>
- Berge, N.D., Ro, K.S., Mao, J., Flora, J.R.V., Chappell, M.A., Bae, S., 2011. Hydrothermal carbonization of municipal waste streams. *Environ. Sci. Technol.* 45, 5696–5703. <https://doi.org/10.1021/es2004528>

- Bougrier, C., Delgenès, J.P., Carrère, H., 2008. Effects of thermal treatments on five different waste activated sludge samples solubilisation, physical properties and anaerobic digestion. *Chem. Eng. J.* 139, 236–244. <https://doi.org/10.1016/j.cej.2007.07.099>
- Breulmann, M., van Afferden, M., Müller, R.A., Schulz, E., Fühner, C., 2017. Process conditions of pyrolysis and hydrothermal carbonization affect the potential of sewage sludge for soil carbon sequestration and amelioration. *J. Anal. Appl. Pyrolysis* 124, 256–265. <https://doi.org/10.1016/j.jaap.2017.01.026>
- Bridgwater, A.V., 2012. Review of fast pyrolysis of biomass and product upgrading. *Biomass Bioenergy* 38, 68–94. <https://doi.org/10.1016/j.biombioe.2011.01.048>
- Catenacci, A., Boniardi, G., Mainardis, M., Gievers, F., Farru, G., Asunis, F., Malpei, F., Goi, D., Cappai, G., Canziani, R., 2022. Processes, applications and legislative framework for carbonized anaerobic digestate: Opportunities and bottlenecks. A critical review. *Energy Convers. Manag.* 263, 115691. <https://doi.org/10.1016/j.enconman.2022.115691>
- Celletti, S., Bergamo, A., Benedetti, V., Pecchi, M., Patuzzi, F., Basso, D., Barattieri, M., Cesco, S., Mimmo, T., 2021. Phytotoxicity of hydrochars obtained by hydrothermal carbonization of manure-based digestate. *J. Environ. Manage.* 280, 111635. <https://doi.org/10.1016/j.jenvman.2020.111635>
- Chen, Y., Cheng, J.J., Creamer, K.S., 2008. Inhibition of anaerobic digestion process: A review. *Bioresour. Technol.* 99, 4044–4064. <https://doi.org/10.1016/j.biortech.2007.01.057>
- Choi, J.M., Han, S.K., Lee, C.Y., 2018. Enhancement of methane production in anaerobic digestion of sewage sludge by thermal hydrolysis pretreatment. *Bioresour. Technol.* 259, 207–213. <https://doi.org/10.1016/j.biortech.2018.02.123>
- Chorazy, T., Čáslavský, J., Žvaková, V., Raček, J., Hlavínek, P., 2020. Characteristics of Pyrolysis Oil as Renewable Source of Chemical Materials and Alternative Fuel from the Sewage Sludge Treatment. *Waste Biomass Valorization* 11, 4491–4505. <https://doi.org/10.1007/s12649-019-00735-5>
- Chu, Q., Xue, L., Singh, B.P., Yu, S., Müller, K., Wang, H., Feng, Y., Pan, G., Zheng, X., Yang, L., 2020. Sewage sludge-derived hydrochar that inhibits ammonia volatilization, improves soil nitrogen retention and rice nitrogen utilization. *Chemosphere* 245, 125558. <https://doi.org/10.1016/j.chemosphere.2019.125558>
- Corradini, F., Meza, P., Eguiluz, R., Casado, F., Huerta-Lwanga, E., Geissen, V., 2019. Evidence of microplastic accumulation in agricultural soils from sewage sludge disposal. *Sci. Total Environ.* 671, 411–420. <https://doi.org/10.1016/j.scitotenv.2019.03.368>
- Danso-Boateng, E., Shama, G., Wheatley, A.D., Martin, S.J., Holdich, R.G., 2015. Hydrothermal carbonisation of sewage sludge: Effect of process conditions on product characteristics and methane production. *Bioresour. Technol.* 177, 318–327. <https://doi.org/10.1016/j.biortech.2014.11.096>
- de Jager, M., Röhrdanz, M., Giani, L., 2020. The influence of hydrochar from biogas digestate on soil improvement and plant growth aspects. *Biochar* 2, 177–194. <https://doi.org/10.1007/s42773-020-00054-2>
- De la Rubia, M.A., Villamil, J.A., Rodriguez, J.J., Mohedano, A.F., 2018. Effect of inoculum source and initial concentration on the anaerobic digestion of the liquid fraction from hydrothermal carbonisation of sewage sludge. *Renew. Energy* 127, 697–704. <https://doi.org/10.1016/j.renene.2018.05.002>
- Demirbas, A., Edris, G., Alalayah, W.M., 2017. Sludge production from municipal wastewater treatment in sewage treatment plant. *Energy Sources Part Recovery Util. Environ. Eff.* 39, 999–1006. <https://doi.org/10.1080/15567036.2017.1283551>
- Di Costanzo, N., Cesaro, A., Di Capua, F., Esposito, G., 2021. Exploiting the nutrient potential of anaerobically digested sewage sludge: A Review. *Energies* 14, 8149. <https://doi.org/10.3390/en14238149>
- do Carmo Precci Lopes, A., Mudadu Silva, C., Pereira Rosa, A., de Ávila Rodrigues, F., 2018. Biogas production from thermophilic anaerobic digestion of kraft pulp mill sludge. *Renew. Energy* 124, 40–49. <https://doi.org/10.1016/j.renene.2017.08.044>
- Eibisch, N., Helfrich, M., Don, A., Mikutta, R., Kruse, A., Ellerbrock, R., Flessa, H., 2013. Properties and degradability of hydrothermal carbonization products. *Journal Environ. Qual.* 42, 1565–1573. <https://doi.org/10.2134/jeq2013.02.0045>

- Erlach, B., 2014. Biomass upgrading technologies for carbon-neutral and carbon-negative electricity generation: techno-economic analysis of hydrothermal carbonization and comparison with wood pelletizing, torrefaction and anaerobic digestion (PhD thesis). Technical University of Berlin.
- Escala, M., Zumbühl, T., Koller, Ch., Junge, R., Krebs, R., 2013. Hydrothermal carbonization as an energy-efficient alternative to established drying technologies for sewage sludge: A feasibility study on a laboratory scale. *Energy Fuels* 27, 454–460. <https://doi.org/10.1021/ef3015266>
- EU 2019/1009, 2019. Council Regulation (EC) 2019/1009 of 5 June 2019. *Off. J. Eur. Union* 62.
- European Parliament EU/2018/851 30 May 2018 Amending Directive 2008/98/EC on Waste. *Off. J. Eur. Communities* 2018, 150, 109–140.
- Fang, J., Zhan, L., Ok, Y.S., Gao, B., 2018. Minireview of potential applications of hydrochar derived from hydrothermal carbonization of biomass. *J. Ind. Eng. Chem.* 57, 15–21. <https://doi.org/10.1016/j.jiec.2017.08.026>
- Feng, Q., Lin, Y., 2017. Integrated processes of anaerobic digestion and pyrolysis for higher bioenergy recovery from lignocellulosic biomass: A brief review. *Renew. Sustain. Energy Rev.* 77, 1272–1287. <https://doi.org/10.1016/j.rser.2017.03.022>
- Ferrentino, R., Merzari, F., Fiori, L., Andreottola, G., 2020. Coupling hydrothermal carbonization with anaerobic digestion for sewage sludge treatment: Influence of HTC liquor and hydrochar on biomethane production. *Energies* 13, 6262. <https://doi.org/10.3390/en13236262>
- Flaga, A., 2007. The aspects of sludge thermal utilization. *Inst. Heat Eng. Air Prot. Crac. Univ. Technol. Kraków Pol.* 9–18.
- Fonts, I., Azuara, M., Gea, G., Murillo, M.B., 2009. Study of the pyrolysis liquids obtained from different sewage sludge. *J. Anal. Appl. Pyrolysis* 85, 184–191. <https://doi.org/10.1016/j.jaap.2008.11.003>
- Fonts, I., Gea, G., Azuara, M., Ábrego, J., Arauzo, J., 2012. Sewage sludge pyrolysis for liquid production: A review. *Renew. Sustain. Energy Rev.* 16, 2781–2805. <https://doi.org/10.1016/j.rser.2012.02.070>
- Funke, A., Ziegler, F., 2010. Hydrothermal carbonization of biomass: A summary and discussion of chemical mechanisms for process engineering. *Biofuels Bioprod. Biorefining* 4, 160–177. <https://doi.org/10.1002/bbb.198>
- Gao, N., Kamran, K., Quan, C., Williams, P.T., 2020. Thermochemical conversion of sewage sludge: A critical review. *Prog. Energy Combust. Sci.* 79, 100843. <https://doi.org/10.1016/j.peccs.2020.100843>
- Gherghel, A., Teodosiu, C., De Gisi, S., 2019. A review on wastewater sludge valorisation and its challenges in the context of circular economy. *J. Clean. Prod.* 228, 244–263. <https://doi.org/10.1016/j.jclepro.2019.04.240>
- Harirchi, S., Wainaina, S., Sar, T., Nojoudi, S.A., Parchami, Milad, Parchami, Mohsen, Varjani, S., Khanal, S.K., Wong, J., Awasthi, M.K., Taherzadeh, M.J., 2022. Microbiological insights into anaerobic digestion for biogas, hydrogen or volatile fatty acids (VFAs): a review. *Bioengineered* 13, 6521–6557. <https://doi.org/10.1080/21655979.2022.2035986>
- He, C., Giannis, A., Wang, J.Y., 2013. Conversion of sewage sludge to clean solid fuel using hydrothermal carbonization: Hydrochar fuel characteristics and combustion behavior. *Appl. Energy* 111, 257–266. <https://doi.org/10.1016/j.apenergy.2013.04.084>
- He, C., Wang, K., Yang, Y., Amaniampong, P.N., Wang, J.-Y., 2015. Effective nitrogen removal and recovery from dewatered sewage sludge using a novel integrated system of accelerated hydrothermal deamination and air stripping. *Environ. Sci. Technol.* 49, 6872–6880. <https://doi.org/10.1021/acs.est.5b00652>
- Higgins, M.J., Beightol, S., Mandahar, U., Suzuki, R., Xiao, S., Lu, H.W., Le, T., Mah, J., Pathak, B., DeClippeleir, H., Novak, J.T., Al-Omari, A., Murthy, S.N., 2017. Pretreatment of a primary and secondary sludge blend at different thermal hydrolysis temperatures: Impacts on anaerobic digestion, dewatering and filtrate characteristics. *Water Res.* 122, 557–569. <https://doi.org/10.1016/j.watres.2017.06.016>
- Hockman, S.K., Broch, A., Robbins, C., 2011. Hydrothermal carbonization (HTC) of lignocellulosic biomass. *Energy Fuels* 25, 1802–1810. <https://doi.org/10.1021/ef101745n>

- Holliger, C., Alves, M., Andrade, D., Angelidaki, I., Astals, S., Baier, U., Bougrier, C., Buffière, P., Carballa, M., de Wilde, V., Ebertseder, F., Fernández, B., Ficara, E., Fotidis, I., Frigon, J.-C., de Lacroix, H.F., Ghasimi, D.S.M., Hack, G., Hartel, M., Heerenklage, J., Horvath, I.S., Jenicke, P., Koch, K., Krautwald, J., Lizasoain, J., Liu, J., Mosberger, L., Nistor, M., Oechsner, H., Oliveira, J.V., Paterson, M., Pauss, A., Pommier, S., Porqueddu, I., Raposo, F., Ribeiro, T., Rüsche Pfund, F., Strömberg, S., Torrijos, M., van Eekert, M., van Lier, J., Wedwitschka, H., Wierinck, I., 2016. Towards a standardization of biomethane potential tests. *Water Sci. Technol.* 74, 2515–2522. <https://doi.org/10.2166/wst.2016.336>
- Hornung, A., 2012. Biomass pyrolysis, in: Meyers, R.A. (Ed.), *Encyclopedia of Sustainability Science and Technology*. Springer New York, New York, NY, pp. 1517–1531. [https://doi.org/10.1007/978-1-4419-0851-3\\_258](https://doi.org/10.1007/978-1-4419-0851-3_258)
- Huang, R., Tang, Y., 2015. Speciation dynamics of phosphorus during (hydro)thermal treatments of sewage sludge. *Environ. Sci. Technol.* 49, 14466–14474. <https://doi.org/10.1021/acs.est.5b04140>
- Hübner, T., Mumme, J., 2015. Integration of pyrolysis and anaerobic digestion - Use of aqueous liquor from digestate pyrolysis for biogas production. *Bioresour. Technol.* 183, 86–92. <https://doi.org/10.1016/j.biortech.2015.02.037>
- Idowu, I., Li, L., Flora, J.R.V., Pellechia, P.J., Darko, S.A., Ro, K.S., Berge, N.D., 2017. Hydrothermal carbonization of food waste for nutrient recovery and reuse. *Waste Manag.* 69, 480–491. <https://doi.org/10.1016/j.wasman.2017.08.051>
- Ischia, G., Fiori, L., 2021. Hydrothermal carbonization of organic waste and biomass: A review on process, reactor, and plant modeling. *Waste Biomass Valorization* 12, 2797–2824. <https://doi.org/10.1007/s12649-020-01255-3>
- Kabadayi Catalkopru, A., Kantarli, I.C., Yanik, J., 2017. Effects of spent liquor recirculation in hydrothermal carbonization. *Bioresour. Technol.* 226, 89–93. <https://doi.org/10.1016/j.biortech.2016.12.015>
- Kacprzak, M., Neczaj, E., Fijalkowski, K., Grobelak, A., Grosser, A., Worwag, M., Rorat, A., Brattebo, H., Almás, Á., Singh, B.R., 2017. Sewage sludge disposal strategies for sustainable development. *Environ. Res.* 156, 39–46. <https://doi.org/10.1016/j.envres.2017.03.010>
- Kambo, H.S., Dutta, A., 2015. A comparative review of biochar and hydrochar in terms of production, physico-chemical properties and applications. *Renew. Sustain. Energy Rev.* 45, 359–378. <https://doi.org/10.1016/j.rser.2015.01.050>
- Keiller, B.G., Muhlack, R., Burton, R.A., van Eyk, P.J., 2019. Biochemical compositional analysis and kinetic modeling of hydrothermal carbonization of australian saltbush. *Energy Fuels* 33, 12469–12479. <https://doi.org/10.1021/acs.energyfuels.9b02931>
- Kim, D., Lee, K., Park, K.Y., 2014. Hydrothermal carbonization of anaerobically digested sludge for solid fuel production and energy recovery. *Fuel* 130, 120–125. <https://doi.org/10.1016/j.fuel.2014.04.030>
- Li, H.-J., Liu, X.-L., Ding, K., Song, H.-B., Tang, L.-F., 2014. Functionalized bis(1-methylimidazol-2-yl)methane and 1-(1-methylimidazol-2-yl)methyl-3,5-dimethylpyrazole and their reactions. *J. Organomet. Chem.* 757, 8–13. <https://doi.org/10.1016/j.jorganchem.2014.01.021>
- Liang, Y., Xu, D., Feng, P., Hao, B., Guo, Y., Wang, S., 2021. Municipal sewage sludge incineration and its air pollution control. *J. Clean. Prod.* 295, 126456. <https://doi.org/10.1016/j.jclepro.2021.126456>
- Libra, J.A., Ro, K.S., Kammann, C., Funke, A., Berge, N.D., Neubauer, Y., Titirici, M.M., Fühner, C., Bens, O., Kern, J., Emmerich, K.H., 2011. Hydrothermal carbonization of biomass residuals: A comparative review of the chemistry, processes and applications of wet and dry pyrolysis. *Biofuels* 2, 71–106. <https://doi.org/10.4155/bfs.10.81>
- Lin, Y., Ma, X., Peng, X., Hu, S., Yu, Z., Fang, S., 2015. Effect of hydrothermal carbonization temperature on combustion behavior of hydrochar fuel from paper sludge. *Appl. Therm. Eng.* 91, 574–582. <https://doi.org/10.1016/j.applthermaleng.2015.08.064>
- Lucian, M., Fiori, L., 2017. Hydrothermal carbonization of waste biomass: Process design, modeling, energy efficiency and cost analysis. *Energies* 10. <https://doi.org/10.3390/en10020211>

- Luste, S., Luostarinen, S., 2010. Anaerobic co-digestion of meat-processing by-products and sewage sludge - Effect of hygienization and organic loading rate. *Bioresour. Technol.* 101, 2657–2664. <https://doi.org/10.1016/j.biortech.2009.10.071>
- Madigan, M.T., Bender, K.S., Buckley, D.H., Sattley, W.M., Stahl, D.A., Brock, T.D., 2019. Brock biology of microorganisms, Fifteenth edition, global edition. ed. Pearson, NY, NY.
- Mäkelä, M., Benavente, V., Fullana, A., 2016. Hydrothermal carbonization of industrial mixed sludge from a pulp and paper mill. *Bioresour. Technol.* 200, 444–450. <https://doi.org/10.1016/j.biortech.2015.10.062>
- Malghani, S., Gleixner, G., Trumbore, S.E., 2013. Chars produced by slow pyrolysis and hydrothermal carbonization vary in carbon sequestration potential and greenhouse gases emissions. *Soil Biol. Biochem.* 62, 137–146. <https://doi.org/10.1016/j.soilbio.2013.03.013>
- Mao, C., Feng, Y., Wang, X., Ren, G., 2015. Review on research achievements of biogas from anaerobic digestion. *Renew. Sustain. Energy Rev.* 45, 540–555. <https://doi.org/10.1016/j.rser.2015.02.032>
- Marin-Batista, J.D., Mohedano, A.F., Rodríguez, J.J., de la Rubia, M.A., 2020. Energy and phosphorous recovery through hydrothermal carbonization of digested sewage sludge. *Waste Manag.* 105, 566–574. <https://doi.org/10.1016/j.wasman.2020.03.004>
- Martinez, C.L.M., Sermyagina, E., Vakkilainen, E., 2021. Hydrothermal carbonization of chemical and biological pulp mill sludges. *Energies* 14. <https://doi.org/10.3390/en14185693>
- McIntosh, S., Padilla, R.V., Rose, T., Rose, A.L., Boukaka, E., Erler, D., 2022. Crop fertilisation potential of phosphorus in hydrochars produced from sewage sludge. *Sci. Total Environ.* 817. <https://doi.org/10.1016/j.scitotenv.2022.153023>
- Medina-Martos, E., Istrate, I.R., Villamil, J.A., Gálvez-Martos, J.L., Dufour, J., Mohedano, Á.F., 2020. Techno-economic and life cycle assessment of an integrated hydrothermal carbonization system for sewage sludge. *J. Clean. Prod.* 277. <https://doi.org/10.1016/j.jclepro.2020.122930>
- Merzari, F., Langone, M., Andreottola, G., Fiori, L., 2019. Methane production from process water of sewage sludge hydrothermal carbonization. A review. Valorising sludge through hydrothermal carbonization. *Crit. Rev. Environ. Sci. Technol.* 49, 947–988. <https://doi.org/10.1080/10643389.2018.1561104>
- Meyer, T., Amin, P., Allen, D.G., Tran, H., 2018. Dewatering of pulp and paper mill biosludge and primary sludge. *J. Environ. Chem. Eng.* 6, 6317–6321. <https://doi.org/10.1016/j.jece.2018.09.037>
- Meyer, T., Edwards, E.A., 2014. Anaerobic digestion of pulp and paper mill wastewater and sludge. *Water Res.* 65, 321–349. <https://doi.org/10.1016/j.watres.2014.07.022>
- Mulchandani, A., Westerhoff, P., 2016. Recovery opportunities for metals and energy from sewage sludges. *Bioresour. Technol.* 215, 215–226. <https://doi.org/10.1016/j.biortech.2016.03.075>
- Naisse, C., Girardin, C., Lefevre, R., Pozzi, A., Maas, R., Stark, A., Rumpel, C., 2015. Effect of physical weathering on the carbon sequestration potential of biochars and hydrochars in soil. *GCB Bioenergy* 7, 488–496. <https://doi.org/10.1111/gcbb.12158>
- Netherlands Energy Research Centre (ECN), PHYLLIS Database web site [WWW Document]. URL <http://www.ecn.nl/phyllis>.
- Nguyen, L.H., Van, H.T., Chu, T.H.H., Nguyen, T.H.V., Nguyen, T.D., Hoang, L.P., Hoang, V.H., 2021. Paper waste sludge-derived hydrochar modified by iron (III) chloride for enhancement of ammonium adsorption: An adsorption mechanism study. *Environ. Technol. Innov.* 21, 101223. <https://doi.org/10.1016/j.cti.2020.101223>
- Nurmesniemi, H., Pöykiö, R., Keiski, R.L., 2007. A case study of waste management at the Northern Finnish pulp and paper mill complex of Stora Enso Veitsiluoto Mills. *Waste Manag.* 27, 1939–1948. <https://doi.org/10.1016/j.wasman.2006.07.017>
- Nyktari, E., Danso-Boateng, E., Wheatley, A., Holdich, R., 2017. Anaerobic digestion of liquid products following hydrothermal carbonisation of faecal sludge at different reaction conditions. *Desalination Water Treat.* 91, 245–251. <https://doi.org/10.5004/dwt.2017.20782>

- Oliveira, I., Blöhse, D., Ramke, H.-G., 2013. Hydrothermal carbonization of agricultural residues. *Bioresour. Technol.* 142, 138–146. <https://doi.org/10.1016/j.biortech.2013.04.125>
- Park, E.S., Kang, B.S., Kim, J.S., 2008. Recovery of oils with high caloric value and low contaminant content by pyrolysis of digested and dried sewage sludge containing polymer flocculants. *Energy Fuels* 22, 1335–1340. <https://doi.org/10.1021/ef700586d>
- Parmar, K.R., Ross, A.B., 2019. Integration of hydrothermal carbonisation with anaerobic digestion; Opportunities for valorisation of digestate. *Energies* 12. <https://doi.org/10.3390/en12091586>
- Pecchi, M., Baratieri, M., 2019. Coupling anaerobic digestion with gasification, pyrolysis or hydrothermal carbonization: A review. *Renew. Sustain. Energy Rev.* 105, 462–475. <https://doi.org/10.1016/j.rser.2019.02.003>
- Puhakka, J.A., Alavakeri, M., Shieh, W.K., 1992. Anaerobic treatment of kraft pulp-mill waste activated-sludge: Gas production and solids reduction. *Bioresour. Technol.* 39, 61–68. [https://doi.org/10.1016/0960-8524\(92\)90057-5](https://doi.org/10.1016/0960-8524(92)90057-5)
- Rajagopal, R., Massé, D.I., Singh, G., 2013. A critical review on inhibition of anaerobic digestion process by excess ammonia. *Bioresour. Technol.* 143, 632–641. <https://doi.org/10.1016/j.biortech.2013.06.030>
- Reza, M.T., Lynam, J.G., Uddin, M.H., Coronella, C.J., 2013. Hydrothermal carbonization: Fate of inorganics. *Biomass Bioenergy* 49, 86–94. <https://doi.org/10.1016/j.biombioe.2012.12.004>
- Rogalinski, T., Liu, K., Albrecht, T., Brunner, G., 2008. Hydrolysis kinetics of biopolymers in subcritical water. *J. Supercrit. Fluids* 46, 335–341. <https://doi.org/10.1016/j.supflu.2007.09.037>
- Roy, U.K., Radu, T., Wagner, J., 2022. Hydrothermal carbonisation of anaerobic digestate for hydro-char production and nutrient recovery. *J. Environ. Chem. Eng.* 10, 107027. <https://doi.org/10.1016/j.jece.2021.107027>
- Saha, N., Saha, A., Saha, P., McGaughy, K., Franqui-Villanueva, D., Orts, W.J., Hart-Cooper, W.M., Toufiq Reza, M., 2019. Hydrothermal carbonization of various paper mill sludges: An observation of solid fuel properties. *Energies* 12, 1–18. <https://doi.org/10.3390/en12050858>
- Salman, C.A., Schwede, S., Thorin, E., Li, H., Yan, J., 2019. Identification of thermochemical pathways for the energy and nutrient recovery from digested sludge in wastewater treatment plants. *Energy Procedia* 158, 1317–1322. <https://doi.org/10.1016/j.egypro.2019.01.325>
- Salman, C.A., Schwede, S., Thorin, E., Yan, J., 2017. Enhancing biomethane production by integrating pyrolysis and anaerobic digestion processes. *Appl. Energy* 204, 1074–1083. <https://doi.org/10.1016/j.apenergy.2017.05.006>
- Schimmelpfennig, S., Glaser, B., 2012. One step forward toward characterization: Some important material properties to distinguish biochars. *J. Environ. Qual.* 41, 1001–1013. <https://doi.org/10.2134/jeq2011.0146>
- Schimmelpfennig, S., Müller, C., Grünhage, L., Koch, C., Kammann, C., 2014. Biochar, hydrochar and uncarbonized feedstock application to permanent grassland-Effects on greenhouse gas emissions and plant growth. *Agric. Ecosyst. Environ.* 191, 39–52. <https://doi.org/10.1016/j.agee.2014.03.027>
- Schulze, M., Mumme, J., Funke, A., Kern, J., 2016. Effects of selected process conditions on the stability of hydrochar in low-carbon sandy soil. *Geoderma* 267, 137–145. <https://doi.org/10.1016/j.geoderma.2015.12.018>
- Seyedi, S., Venkiteshwaran, K., Benn, N., Zitomer, D., 2020. Inhibition during anaerobic co-digestion of aqueous pyrolysis liquid from wastewater solids and synthetic primary sludge. *Sustain. Switz.* 12, 8–11. <https://doi.org/10.3390/SU12083441>
- Seyedi, S., Venkiteshwaran, K., Zitomer, D., 2019. Toxicity of various pyrolysis liquids from biosolids on methane production yield. *Front. Energy Res.* 7, 1–12. <https://doi.org/10.3389/fenrg.2019.00005>
- Singh, S., Rinta-Kanto, J.M., Kettunen, R., Tolvanen, H., Lens, P., Collins, G., Kokko, M., Rintala, J., 2019. Anaerobic treatment of LCFA-containing synthetic dairy wastewater at 20 °C: Process performance and microbial community dynamics. *Sci. Total Environ.* 691, 960–968. <https://doi.org/10.1016/j.scitotenv.2019.07.136>

- Smith, A.M., Singh, S., Ross, A.B., 2016. Fate of inorganic material during hydrothermal carbonisation of biomass: Influence of feedstock on combustion behaviour of hydrochar. *Fuel* 169, 135–145. <https://doi.org/10.1016/j.fuel.2015.12.006>
- Sousa, A.A.T.C., Figueiredo, C.C., 2016. Sewage sludge biochar: Effects on soil fertility and growth of radish. *Biol. Agric. Hortic.* 32, 127–138. <https://doi.org/10.1080/01448765.2015.1093545>
- Spinosa, L., Ayol, A., Baudez, J.-C., Canziani, R., Jenicek, P., Leonard, A., Rulkens, W., Xu, G., Van Dijk, L., 2011. Sustainable and Innovative Solutions for Sewage Sludge Management. *Water* 3, 702–717. <https://doi.org/10.3390/w3020702>
- Stoica, A., Sandberg, M., Holby, O., 2009. Energy use and recovery strategies within wastewater treatment and sludge handling at pulp and paper mills. *Bioresour. Technol.* 100, 3497–3505. <https://doi.org/10.1016/j.biortech.2009.02.041>
- Tchobanoglous, G., 2014. *Wastewater engineering: treatment and resource recovery*, 5. ed., internat. student ed. ed. McGraw-Hill, New York, NY.
- Torri, C., Fabbri, D., 2014. Biochar enables anaerobic digestion of aqueous phase from intermediate pyrolysis of biomass. *Bioresour. Technol.* 172, 335–341. <https://doi.org/10.1016/j.biortech.2014.09.021>
- Villamil, J.A., Mohedano, A.F., Rodriguez, J.J., de la Rubia, M.A., 2018. Valorisation of the liquid fraction from hydrothermal carbonisation of sewage sludge by anaerobic digestion. *J. Chem. Technol. Biotechnol.* 93, 450–456. <https://doi.org/10.1002/jctb.5375>
- vom Eyser, C., Palmu, K., Schmidt, T.C., Tuerk, J., 2015. Pharmaceutical load in sewage sludge and biochar produced by hydrothermal carbonization. *Sci. Total Environ.* 537, 180–186. <https://doi.org/10.1016/j.scitotenv.2015.08.021>
- Wang, L., Chang, Y., Li, A., 2019. Hydrothermal carbonization for energy-efficient processing of sewage sludge: A review. *Renew. Sustain. Energy Rev.* 108, 423–440. <https://doi.org/10.1016/j.rser.2019.04.011>
- Wang, L., Zhang, L., Li, A., 2014. Hydrothermal treatment coupled with mechanical expression at increased temperature for excess sludge dewatering: Influence of operating conditions and the process energetics. *Water Res.* 65, 85–97. <https://doi.org/10.1016/j.watres.2014.07.020>
- Wang, T., Zhai, Y., Zhu, Y., Li, C., Zeng, G., 2018. A review of the hydrothermal carbonization of biomass waste for hydrochar formation: Process conditions, fundamentals, and physicochemical properties. *Renew. Sustain. Energy Rev.* 90, 223–247. <https://doi.org/10.1016/j.rser.2018.03.071>
- Wen, C., Moreira, C.M., Rehmann, L., Berruti, F., 2020. Feasibility of anaerobic digestion as a treatment for the aqueous pyrolysis condensate (APC) of birch bark. *Bioresour. Technol.* 307, 123199. <https://doi.org/10.1016/j.biortech.2020.123199>
- Wirth, B., Mumme, J., 2014. Anaerobic digestion of waste water from hydrothermal carbonization of corn silage. *Appl. Bioenergy* 1. <https://doi.org/10.2478/apbi-2013-0001>
- Wirth, B., Mumme, J., Erlach, B., 2012. Anaerobic treatment of waste water derived from hydrothermal carbonization. 20th Eur. Biomass Conf. Exhib. 18–22.
- Wirth, B., Reza, T., Mumme, J., 2015. Influence of digestion temperature and organic loading rate on the continuous anaerobic treatment of process liquor from hydrothermal carbonization of sewage sludge. *Bioresour. Technol.* 198, 215–222. <https://doi.org/10.1016/j.biortech.2015.09.022>
- Xu, Z., Bai, X., 2022. Microplastic degradation in sewage sludge by hydrothermal carbonization: efficiency and mechanisms. *Chemosphere* 297, 134203. <https://doi.org/10.1016/j.chemosphere.2022.134203>
- Yang, Y., Heaven, S., Venetsaneas, N., Banks, C.J., Bridgwater, A.V., 2018. Slow pyrolysis of organic fraction of municipal solid waste (OFMSW): Characterisation of products and screening of the aqueous liquid product for anaerobic digestion. *Appl. Energy* 213, 158–168. <https://doi.org/10.1016/j.apenergy.2018.01.018>
- Ylivainio, K., Lehti, A., Jermakka, J., Wikberg, H., Turtola, E., 2021. Predicting relative agronomic efficiency of phosphorus-rich organic residues. *Sci. Total Environ.* 773, 145618. <https://doi.org/10.1016/j.scitotenv.2021.145618>

- Yue, X., Arena, U., Chen, D., Lei, K., Dai, X., 2019. Anaerobic digestion disposal of sewage sludge pyrolysis liquid in cow dung matrix and the enhancing effect of sewage sludge char. *J. Clean. Prod.* 235, 801–811. <https://doi.org/10.1016/j.jclepro.2019.07.033>
- Zhang, W., Wu, S., Guo, J., Zhou, J., Dong, R., 2015. Performance and kinetic evaluation of semi-continuously fed anaerobic digesters treating food waste: Role of trace elements. *Bioresour. Technol.* 178, 297–305. <https://doi.org/10.1016/j.biortech.2014.08.046>
- Zhao, X., Becker, G.C., Faweya, N., Rodriguez Correa, C., Yang, S., Xie, X., Kruse, A., 2018. Fertilizer and activated carbon production by hydrothermal carbonization of digestate. *Biomass Convers. Biorefinery* 8, 423–436. <https://doi.org/10.1007/s13399-017-0291-5>
- Zhen, G., Lu, X., Kato, H., Zhao, Y., Li, Y.-Y., 2017. Overview of pretreatment strategies for enhancing sewage sludge disintegration and subsequent anaerobic digestion: Current advances, full-scale application and future perspectives. *Renew. Sustain. Energy Rev.* 69, 559–577. <https://doi.org/10.1016/j.rser.2016.11.187>
- Zhou, H., Brown, R.C., Wen, Z., 2019. Anaerobic digestion of aqueous phase from pyrolysis of biomass: Reducing toxicity and improving microbial tolerance. *Bioresour. Technol.* 292, 121976. <https://doi.org/10.1016/j.biortech.2019.121976>
- Zhuang, X., Huang, Y., Song, Y., Zhan, H., Yin, X., Wu, C., 2017. The transformation pathways of nitrogen in sewage sludge during hydrothermal treatment. *Bioresour. Technol.* 245, 463–470. <https://doi.org/10.1016/j.biortech.2017.08.195>
- Zhuang, X., Zhan, H., Huang, Y., Song, Y., Yin, X., Wu, C., 2018. Conversion of industrial biowastes to clean solid fuels via hydrothermal carbonization (HTC): Upgrading mechanism in relation to coalification process and combustion behavior. *Bioresour. Technol.* 267, 17–29. <https://doi.org/10.1016/j.biortech.2018.07.002>



## PUBLICATIONS



# PUBLICATION

I

## **Hydrothermal carbonization of mechanically dewatered digested sewage sludge—Energy and nutrient recovery in centralised biogas plant**

Anna Hämäläinen, Marika Kokko, Viljami Kinnunen, Tuomi Hilli & Jukka Rintala

Water Research, 201, 117284  
<https://doi.org/10.1016/j.watres.2021.117284>

**Publication reprinted with the permission of the copyright holders.**





# Hydrothermal carbonisation of mechanically dewatered digested sewage sludge—Energy and nutrient recovery in centralised biogas plant

Anna Hämäläinen<sup>a,\*</sup>, Marika Kokko<sup>a</sup>, Viljami Kinnunen<sup>b</sup>, Tuomo Hilli<sup>c</sup>, Jukka Rintala<sup>a</sup>

<sup>a</sup> Faculty of Engineering and Natural Sciences, Tampere University, P.O.Box 541, 33104 Tampere University, Finland

<sup>b</sup> Gasum Oy, Revontulenpuisto 2C, 02100 Espoo, Finland

<sup>c</sup> Fifth Innovation Oy, Väinöläkatu 26, 33500 Tampere, Finland

## ARTICLE INFO

### Article history:

Received 2 February 2021

Revised 18 May 2021

Accepted 19 May 2021

Available online 25 May 2021

### Keywords:

Sewage sludge digestate  
Hydrothermal carbonisation  
Hydrochar  
Phosphorous  
Nutrient recovery  
Energy recovery

## ABSTRACT

This study aimed to assess the role of hydrothermal carbonisation (HTC) in digestate processing in centralised biogas plants receiving dewatered sludge from regional wastewater treatment plants and producing biomethane and fertilisers. Chemically conditioned and mechanically dewatered sludge was used as such (total solids (TS) 25%) or as diluted (15% TS) with reject water in 30 min or 120 min HTC treatments at 210 °C, 230 °C or 250 °C, and the produced slurry was filtered to produce hydrochars and filtrates. The different hydrochars contributed to 20–55% of the original mass, 72–88% of the TS, 74–87% of the energy content, 71–92% of the carbon, above 86% of phosphorous and 38–64% of the nitrogen present in the original digestates. The hydrochars' energy content (higher heating values were 11.3–12.2 MJ/kg-TS) were similar to that of the digestates, while the ash contents increased (from 43% up to 57%). HTC treatments produced filtrates in volumes of 42–76% of the dewatered digestate, having a soluble chemical oxygen demand (SCOD) of 28–44 g/L, of which volatile fatty acids (VFAs) contributed 10–34%, and methane potentials of 182–206 mL-CH<sub>4</sub>/g-SCOD without any major indication of inhibition. All 32 pharmaceuticals detected in the digestates were below the detection limit in hydrochars and filtrates, save for ibuprofen and benzotriazole in filtrate, while heavy metals were concentrated in the hydrochars but below the national limits for fertiliser use, save for mercury. The integration of HTC to a centralised biogas plant was extrapolated to enhance the annual biogas production by 5% and ammonium recovery by 25%, and the hydrochar was estimated to produce 83 GJ upon combustion or to direct 350 t phosphorous to agriculture annually.

© 2021 The Authors. Published by Elsevier Ltd.

This is an open access article under the CC BY license (<http://creativecommons.org/licenses/by/4.0/>)

## 1. Introduction

Municipal wastewaters are typically treated using an activated sludge process that results in high amounts of sewage sludge, including primary sludge consisting of wastewater solids and biosludge consisting of aerobic microbes. In wastewater treatment plants, sewage sludge is often gravimetrically thickened and then stabilised in anaerobic digestion (AD), which recovers the energy from the process as biogas, which is valued as a renewable energy source. The digested material is typically mechanically dewatered using polymers into solid fraction and liquid fraction, referred to as reject water. The solid fraction (total solids (TS) 15–30%) with high organic and nutrient content may be composted to be used as soil

amendment or combusted (Alvarenga et al., 2015). The reject water is usually circulated to the wastewater treatment plant.

The sewage sludge energy content recovered in AD has recently been increasingly considered for upgrading into biofuel or gas grid injection to promote energy transition; for economic reasons, centralised biogas plants treating dewatered sludge from several sewage plants are used. Furthermore, the recovery of sewage sludge nutrients and residual carbon, especially that of phosphorous, is of major interest because of diminishing phosphorous resources and to reduce the climate impacts of nitrogen fertilizer production (Becker et al., 2019). However, in practice, the use of sewage sludge digestates in agriculture is a concern because of contaminants; thus, the use of sewage sludge-based nutrients is facing major challenges. The concern is about certain contaminants, such as heavy metals, pharmaceuticals and microplastics, which the biological processes alone are incapable of converting

\* Corresponding author.

E-mail address: [anna.hamalainen@tuni.fi](mailto:anna.hamalainen@tuni.fi) (A. Hämäläinen).

into something more harmless and part of which can also end up in the digestate (Alvarenga et al., 2015).

Hence, to harness sewage sludge digestate in a safe manner, an additional post-treatment step needs to be considered. One such recently discussed sludge post-treatment is hydrothermal carbonisation (HTC) (Aragón-Briceño et al., 2017). HTC is a thermal treatment applicable for organic material and is conducted at temperatures of 180–250 °C with residence times from 0.5 to several hours (Libra et al., 2011). Particularly, HTC is considered for moist (TS 10–50%) organic material, which differentiates it from other thermal processes, for example pyrolysis, which typically requires a higher solids content (TS > 90%) (Bridgwater et al., 1999) and utilises comparatively high temperatures (500–800 °C) (Paneque et al., 2017). HTC yields a moist carbonaceous solid fraction that is usually separated into a solid and liquid, i.e. hydrochar and filtrate, respectively. In addition, HTC releases exhaust gas comprising primarily of CO<sub>2</sub> but also of other compounds, such as hydrogen sulphide, nitrogen dioxide, nitric oxide and ammonia, hence requiring further treatment (Berge et al., 2011; Danso-Boateng et al., 2015). The amounts and characteristics of the three fractions are affected by the feedstock (e.g., Berge et al., 2011) and the used HTC conditions, such as temperature and residence time. HTC has been studied for a range of feedstocks to produce hydrochar, which could be used as is or after downstream processing, for example, as a soil amendment (Bargmann et al., 2014), for sequestering atmospheric carbon to soils (Libra et al., 2011), as an adsorbent (Sun et al., 2011), or for combustion (Smith et al., 2016).

HTC treatment has also been studied for sewage sludge, for example, to screen the effects of HTC on the treatment of sludges from different phases of the plant (Merzari et al., 2020), to compare with different feedstocks, including agricultural waste (He et al., 2019), and to determine the effects of HTC treatment conditions on hydrochar (Danso-Boateng et al., 2015). The AD process affects the characteristics of the sludge in many ways; for example, it lowers the carbon content of the sludge, impacts its sulphur and phosphate chemistry, and increases the ammonium concentration. Thus, the characteristics of the hydrochar and filtrate from the HTC treatment of digestate may differ from those of the HTC-treated raw sewage sludge (Aragón-Briceño et al., 2017). There are several laboratory studies on the HTC treatment of digested sewage sludge that have shown, for example, that the filtrate of HTC-treated digested sewage sludge at 240 °C has a clear inhibition towards methane production (Marin-Batista et al., 2020), whereas at lower temperatures, no clear inhibition has been reported (Aragón-Briceño et al., 2017). Regarding the effects of HTC on digestate phosphorous, Marin-Batista et al. (2020) reported an increase in phosphorous content in the filtrate with increasing HTC temperatures, while Merzari et al. (2020) observed no increase, or even a decrease, in the filtrate's phosphorous content after HTC. However, the studies on sewage sludge digestates differ, for example, in the origin of the digestate (before or after dewatering), in the HTC conditions studied and in the processing of the samples in the laboratory before HTC. For example, Merzari et al. (2020) studied dewatered sewage sludge digestate (TS 25%) that they, however, diluted for the HTC treatment (15 g sludge and 10 g water), resulting in ca. 17% TS digestate. Aragón-Briceño et al. (2020), on the other hand, studied sewage sludge digestate with an original TS of 3% but processed the sample in the laboratory to study HTC at eight different TS contents (2.5–30%). Thus, there is a lack of information on the dewatered digestates representing real conditions. Also, the separation techniques employed to obtain hydrochar and filtrate vary, including filtering through a cellulose filter paper (Merzari et al., 2020), vacuum filtration (0.9 mm) followed by an additional supernatant filtration (0.45 µm) (Marin-Batista et al., 2020) and through glass microfibre filters (Aragón-Briceño et al., 2020).

The current work examined the effects of HTC process parameters on the amounts and characteristics of the hydrochar and filtrate produced from dewatered digested sewage sludge. The studied dewatered digestate was obtained directly from the centralised biogas plant, and it was studied as such (TS of 25%) and after dilution with dewatering reject water to TS of 15%, using temperatures of 210 °C, 230 °C and 250 °C and residence times of 30 or 120 min. The separation of hydrochar and filtrate was conducted at a pilot scale. The energy and nutrient characteristics and recovery of both fractions were determined, and the mass balances were evaluated. Results from the laboratory scale study are needed to assess the technological and economic feasibility of scale-up applications for centralised biogas plants.

## 2. Materials and methods

### 2.1. Digestates and reject water

In the HTC experiments, mechanically dewatered digestate from an industrial thermophilic sewage sludge digester was used. Mechanical dewatering of digested sludge was done in the plant with a decanter centrifuge, along with polymer addition. Also, reject water from dewatering was used. The materials were obtained from a centralised biogas plant in Topinoja (Turku, Finland), which treated during the experiments annually 75,000 t (ca. 23% TS, 16,500 t-TS/a) of mechanically dewatered sewage sludge transported from six regional municipal wastewater treatment plants, producing 30,000 t of dewatered digestate (ca. 30% TS, 9000 t-TS/a). For the biomethane potential (BMP) assays, the inoculum was from a mesophilic municipal biowaste digestion facility (Riihimäki, Finland). All samples were anaerobically stored at 4 °C for 1–2 months until used. In the HTC experiments, the digestate was used as such (TS 25%, referred to as digestate) or diluted to 15% TS by adding 400 mL of reject water to 600 g of the digestate (referred to as diluted digestate). The dilutions were performed right before the HTC treatments. The material characteristics are shown in Table 1.

### 2.2. HTC treatments

The HTC treatment used a two-litre Parr® 4500 pressure reactor with an external circulating cooling water system and internal rotary mixer (initially 40 rpm). The final mixing speed increased as a result of the viscosity decrease of the samples during the treatments (Table 2). The sample wet weight for the experiments was 1 kg, and the treatment temperatures were 210 °C, 230 °C or 250 °C with residence times of 30 or 120 min (Table 2).

The heating of the reactor vessel to the target temperatures was achieved within ca. 90 min. The temperature was manually adjusted using Parr® 4848 reactor controllers. The vessel pressure started to increase after the inside temperature reached 100 °C and then increased to 20 to 40 bar depending on the applied temperature. The vessel was held at the target temperature for the pre-set residence time. The realised temperatures fluctuated but remained within ±9 °C from the targeted temperature (Table 2). The 250 °C runs started when the vessel temperature had reached 245 °C because of difficulties in attaining the targeted temperature within 90 min. In all the runs, after the residence time, the heating was switched off, an arbitrary volume of gas was released, and cooling water circulation was initiated in the water jacket. The gas release reduced the inside pressure and temperature by 2–4 bar and 1–4 °C, respectively, of which purpose was to prevent possible condensation. The water cooling lasted until the vessel temperature had decreased to 40–70 °C, which was achieved within 30–40 min. After the HTC treatments, the whole sample volume was weighed,

**Table 1**

Material characteristics. Total volatile fatty acids (TVFA) comprise of acetate, propionate, isobutyrate, butyrate, isovalerate and valerate.

	Digestate	Diluted digestate	Reject water	Inoculum
<b>pH</b>	7.5	7.9	8	8.4
<b>Total solids (%)</b>	25.6 ± 0.6	14.5 ± 0.2	n.a.	5.1 ± 0.1
<b>Volatile solids (%)</b>	14.6 ± 0.3	7.7 ± 0.8	n.a.	3.3 ± 0.1
<b>VS/TS (%)</b>	57	53	n.a.	64
<b>Ash at 550 °C (%)</b>	43.0 ± 0.1	43.0 ± 0.4	n.a.	n.a.
<b>Ash at 815 °C (%)</b>	40.9 ± 0.1	41.1 ± 0.2	n.a.	n.a.
<b>SCOD (g/L)</b>	2.1 ± 0.01	7.03 ± 0.1	10.3 ± 0.01	10.1 ± 0.01
<b>TVFA (g/L COD)</b>	0.0 ± 0.0	n.a.	1.4 ± 0.1	0.6 ± 0.1
<b>Total nitrogen (g/kg-TS)</b>	35.2 ± 0.1	31.0 ± 0.4	3.9	n.a.
<b>Ammonium-nitrogen (g/L)</b>	n.a.	n.a.	2.91	n.a.
<b>Total phosphorous (g/kg-TS)</b>	37.2	31.5	2.30 <sup>a</sup>	14.1
<b>Phosphate-phosphorous (mg/L)</b>	n.a.	n.a.	58.7	n.a.

n.a. not applicable

<sup>a</sup> calculated (g/L)

**Table 2**

The target temperatures and realised HTC treatment conditions for digestate and diluted digestate.

Sample	HTC parameters				
	Min. treatment temperature (°C)	Max. treatment temperature (°C)	Max. pressure (bar)	Average treatment pressure (bar)	Final mixing speed (rpm)
<i>Digestate HTC</i>					
210 °C, 30min	202	215	29.4	22.7	43
210 °C, 120min	206	214	26.8	20.5	44
230 °C, 30min	229	232	38.8	32.2	45
230 °C, 120min	221	235	34.4	31.0	46
250 °C, 30min	242	251	43.7	42.6	46
250 °C, 120min	243	252	44.5	41.1	46
<i>Diluted digestate HTC</i>					
210 °C, 30min	207	217	25.5	20.8	40
210 °C, 120min	203	214	19.4	23.1	40
230 °C, 30min	227	232	33.1	29.6	46
230 °C, 120min	226	232	30.2	28.2	46
250 °C, 30min	244	252	42.5	40.5	46
250 °C, 120min	243	252	42.7	40.1	46

recovered and stored at 4 °C prior to solid–liquid separation by filtration.

Filtration for the HTC-treated sludges (called slurry) was conducted in a small-scale pressurised filtration unit. The temperature during filtration was ca. 60 °C, which was attained by warming up the samples (ca. 1 kg) in a water bath before filtration. The heated sample was placed onto a filter cloth inside a cylinder. The pressure in the closed cylinder gradually increased: 5 min to 1 bar, 10 min to 4 bar and then to the final pressure of 15 bar. The total pressing time for the digestate samples was about 20 min, whereas for the diluted digestate samples, it was about 30 min. The end-products of filtration are from now on called hydrochar (solid fraction) and filtrate (liquid fraction). The hydrochar product is comprised of both moisture that was not removed by filtration and of dry solids that are obtained after evaporation. The weights of the recovered filtrate and hydrochar were recorded.

### 2.3. Biomethane potential assays

The BMPs of the filtrates of the HTC-treated digestates were determined in static 37-day long batch assays in triplicate at 35 °C. In all assays, 120 mL serum bottles and 3.4 g (wet weight) of inoculum were used. The SCOD concentration of the filtrate was set to 2 g-SCOD/L. NaHCO<sub>3</sub> (4 g/L) was used as a buffer, and distilled water was added to the bottles to reach the volumes of 64 mL. The initial pH was adjusted between 7 and 8 with HCl (1 M), after which the bottles were closed with rubber stoppers. Anaerobic conditions were created inside by flushing with nitrogen gas for 3 min. Assays containing only water, buffer and in-

oculum functioned as the control, and their methane production was subtracted from the methane production of the sample assays. The methane concentrations in the BMP determination were measured with a GC-FID (Perkin Elmer Clarus), as described previously (Kinnunen et al., 2015) and the BMPs were calculated as presented in Eq. S1.

### 2.4. Chemical analysis and calculations

The TS and volatile solids (VS) were gravimetrically determined according to standard methods (APHA 2540). The ash content measurements at 550 °C and 815 °C followed the same gravimetric principle. The pH level was measured with a WTW pH 3210 metre using WTW SenTix® 41 electrode. COD and SCOD were analysed according to Finnish standard methods (SFS 5504). Volatile fatty acids (VFA) were determined with GC-FID, as described previously (Kokko et al., 2018). Prior to the analysis of VFA and SCOD, the samples were filtered through a 0.45 µm filter (Chromafil Xtra PET).

The total nitrogen and soluble ammonium-nitrogen in the liquid phase were analysed using Hach Lange kits (LCK 238, LCK 338, LCK 305 and LCK 303) according to the instructions provided by the company. The other cations than ammonium-nitrogen in the liquid samples were analysed according to the ion chromatography standard SFS-EN ISO 10,304–1 using an ion chromatograph (Dionex DX-120, USA) with AS40 autosampler, IonPac CS12A cation exchange column and CSRS 300 suppressor (4 mm). The eluent contained 2 mM methane sulphonic acid, and the flow rate was 1 mL/min.

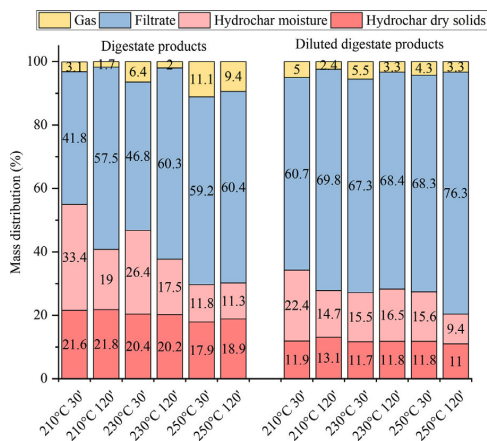


Fig. 1. The mass distribution of digestate and diluted digestate after the HTC treatments at different conditions into hydrochar, filtrate and gas fractions. Hydrochar and filtrate were produced by filtration. The hydrochar mass fraction is expressed as wet weight.

The solid phase total carbon, hydrogen, nitrogen and sulphur were determined by elemental analysis in Thermo Scientific FlashSmart Elemental analyzer (CHNS/O) with TCD (Thermal Conductivity Detector). Before the analysis, samples were properly homogenized; samples were first dried in oven at 100 °C overnight, after which the dry samples were grinded with mortar to obtain fine powder. The samples for CHNS analysis were weighted (2–3 mg) on a microgram balance (Mettler Toledo WXTS Microbalance) in tin cups. Calibration was evaluated analysing BBOT (2,5-Bis(5-tert-butyl-2-benzo-oxazol-2-yl)) as a standard. Gases used were helium as a carrier gas and oxygen as a gas for sample oxidation. The total phosphorous and other elements in the solid and liquid samples were determined with inductively coupled plasma mass spectrometry (ICP-MS). For further details of this analysis, see Supporting Information. The calorific values of the solid samples were determined in duplicate with a Parr® 6725 Semi-micro Oxygen Bomb Calorimeter, according to the ISO 1928 standard. Prior to the analysis, the samples were dried overnight at 100 °C. The sample weight for the analysis was 0.2–0.3 g.

The hydrochar yields (Y), energy densification (E<sub>d</sub>) and energy recovery of hydrochar were calculated as described previously (Danso-Boateng et al., 2015). The energy content and energy recoveries of the filtrates were calculated based on the results of the BMP and the mass distribution after different HTC runs. The mass of digestate converted to gas during HTC treatment was calculated by the difference in the masses of the input digestate and the obtained slurry after HTC (Eq. S7). For further details of the calculations, see Supporting Information.

### 3. Results and discussion

#### 3.1. Mass and TS recoveries

The HTC treatment yielded three fractions, the relative mass yields of which depended on the applied HTC conditions (Fig. 1). The produced hydrochar masses (wet basis) covered 30–55% and 20–34% of the original masses of the digestate and diluted digestate, respectively (Fig. 1). The moisture content of the hydrochars after filtration ranged between 37 and 61% and 46 and 65% for the digestate and diluted digestate, respectively (Table 3). The VS/TS ratio decreased from 57% of the digestates to 43–50% in the hydrochars.

The hydrochar yields (dry basis) were between 72% and 87% and between 72% and 88% for the digestate and diluted digestate (Table 3), respectively, suggesting that the TS content of the digestate does not affect the recovery of TS in hydrochar. With the digestate, an increased treatment temperature decreased the hydrochar mass and TS yields and increased the yields of the filtrate and gas (Fig. 1), while the effects were not so clear for the diluted digestate. The mass of the filtrate varied between 42% and 60% and between 60% and 76% for the digestate and diluted digested (Fig. 1), respectively. The calculated gas formation ranged from 1 to 11% of the original digestate mass and was larger in the HTC of the digestate than in the HTC of diluted digestate. The highest hydrochar TS yields of 87.6% and 88.3% were obtained at 210 °C for 120 min for the digestate and diluted digestate, respectively, while the residence time had no clear effect on hydrochar TS yield.

The present study and other research (Aragón-Briceño et al., 2017) have shown that in processing mechanically dewatered digestate, HTC treatment with subsequent solids separation can produce hydrochar with recoveries even above 70–85% of the original TS while contributing to around 40–50% of the original mass. The present hydrochar yields on a TS basis (72–88%) are at the upper range of the hydrochar yields of 66–75% (at 220–250 °C) and 67–74% (at 180–210 °C) reported in other HTC studies with digested sewage sludge with a TS content of 17% (Merzari et al., 2020) or 16.5% (Marin-Batista et al., 2020), respectively, with decreased hydrochar yields at increased temperatures, which is also observed in the current study. However, a hydrochar yield of 51% was obtained at 240 °C (Marin-Batista et al., 2020), indicating that the original characteristics of the sewage sludge digestate have a major effect on the product characteristics. In HTC studies conducted with digested sewage sludge at a lower TS content of below 5%, the hydrochar yields on a TS basis have varied from 47% (Berge et al., 2011) to 56–78% (Aragón-Briceño et al., 2017; Merzari et al., 2020) without a clear effect of temperature on hydrochar yield, as what is found at higher digestate TS contents. Thus, the hydrochar TS yield may not be fully deduced from the TS content or the HTC conditions, but also from the chemical characteristics of the sludge (Merzari et al., 2020; Parmar and Ross, 2019). The hydrochar mass yield in the present study (30–55% for digestate and 20–34% for diluted digestate) was considerably lower than the 66–88% obtained for digested sewage sludge with TS content of 17% (Merzari et al., 2020). However, it should be noted that the reported mass and TS yields of hydrochar and filtrate are affected along with the digestate characteristics by the separation technique used to separate the hydrochar and filtrate, which vary by research.

#### 3.2. Energy characteristics

##### 3.2.1. Hydrochar

The energy content and solid fuel properties of the different hydrochars and digestates were assessed using moisture content, heating values, and the ash content, which is responsible for the combustion furnace fouling (Jenkins et al., 1998). The energy content and solid fuel properties of the 12 hydrochars, and the digestate and diluted digestate are presented in Table 3. The HHV of all the hydrochars were of a similar range (11.3–12.2 MJ/kg-TS) as the digestates' HHVs (11.5–11.9 MJ/kg-TS), with energy densification values of 0.95–1.05. The HHV of the digestate hydrochars was 1.2–5.5% higher than the HHV of the digestate after all the treatments, except for the mildest ones conducted at 210 °C. Conversely, the HHV of diluted digestate hydrochar increased by 2.2% from the digestate HHV only in the severest treatment (250 °C, 120 min), while the other treatment conditions decreased the HHV by 0.6–4.9%. The ash content (determined at 550 °C) of the hydrochars increased from 50% to 57% with increasing treatment temperature



**Table 3**

The characteristics of the digestates and their respective hydrochars.

Sample	Proximate analyses					Heating values				Ultimate analyses				Yield (%)	Energy densification
	Moisture (%)	VS <sup>a</sup> (%)	VS/TS	Ash <sup>a</sup> 550 °C (%)	Ash <sup>a</sup> 815 °C (%)	LHV <sup>a</sup> (MJ/kg)	HHV <sup>a</sup> (MJ/kg)	C (%) <sup>b</sup>	H (%) <sup>b</sup>	N (%) <sup>b</sup>	S (%) <sup>b</sup>	O (%) <sup>b</sup>	P (%) <sup>b</sup>		
Digestate	75.00	14.00	57.00	43.10	40.90	10.60	11.49	30.30	4.40	3.50	2.30	59.50	3.72	n.a.	n.a.
Diluted digestate	85.00	8.0	57.0	42.90	41.00	11.10	11.90	28.60	4.20	3.10	2.30	61.80	3.15	n.a.	n.a.
<i>Hydrochars of HTC treated digestate</i>															
210 °C for 30min	60.70	19.80	50.40	49.60	47.70	10.56	11.33	31.07	3.87	2.54	1.83	60.69	5.33	86.46	0.99
210 °C for 120min	46.60	25.90	48.50	51.80	49.60	10.60	11.38	31.00	3.69	2.57	1.80	60.94	5.11	87.58	0.99
230 °C for 30min	56.40	21.10	48.40	51.60	49.60	10.83	11.63	31.40	4.00	2.70	1.93	59.97	4.65	81.97	1.01
230 °C for 120min	46.30	24.90	46.40	53.70	51.50	11.17	11.89	30.30	3.58	2.40	1.77	61.95	4.73	81.62	1.03
250 °C for 30min	39.80	26.80	44.50	55.50	52.50	11.10	11.85	30.03	3.78	2.26	2.16	61.77	4.94	72.24	1.03
250 °C for 120min	37.30	27.10	43.20	56.70	54.30	11.43	12.12	30.30	3.48	2.15	2.17	61.90	5.67	75.24	1.05
<i>Hydrochars of HTC treated diluted digestate</i>															
210 °C for 30min	65.30	16.70	48.10	51.80	49.50	10.57	11.35	30.41	3.98	2.58	1.91	61.12	4.95	78.65	0.95
210 °C for 120min	52.70	22.60	47.80	52.20	50.20	10.61	11.38	30.01	3.80	2.38	2.00	61.81	3.74	88.29	0.95
230 °C for 30min	57.00	20.40	47.40	52.60	50.30	11.01	11.82	29.72	3.99	2.42	2.10	61.77	5.07	77.40	0.99
230 °C for 120min	58.40	19.20	46.20	53.70	50.90	10.75	11.48	29.59	3.66	2.14	2.18	62.43	4.94	77.65	0.96
250 °C for 30min	56.90	20.00	46.40	54.00	51.60	11.05	11.86	30.41	4.00	2.31	2.23	61.05	4.65	77.58	0.99
250 °C for 120min	46.00	23.20	43.00	57.00	54.20	11.42	12.19	30.38	3.84	2.30	2.19	61.29	5.02	72.00	1.02

VS: volatile solids, TS: total solids, LHV: lower heating value, HHV: higher heating value, C: carbon, H: hydrogen, N: nitrogen, S: sulphur, P: phosphorous.

<sup>a</sup> reported against total solids.<sup>b</sup> calculated as difference between 100 and total sum of C, H, N and S on dry basis.

and residence time, while the ash contents of both the digestate and diluted digestate were 43%.

Based on the current study and what is reported in the literature, it appears that the effects of HTC treatment on the HHV of the digestate are quite minimal (less than 4.5%). The HHV of the digestates used in the present study (11.5–11.9 MJ/kg-TS) was much lower than reported in other studies with digestate TS content of 16.5% (14.9 MJ/kg-TS; [Marin-Batista et al., 2020](#)) or 17% (16.0 MJ/kg-TS; [Merzari et al., 2020](#)). A lower HHV of the digestate (10.7 MJ/kg-TS) has been reported with 2.9% TS in the digestate ([Merzari et al., 2020](#)). The HHVs of the hydrochars differed less than 2% ([Martin-Batista et al., 2020](#)) and less than 5% ([Merzari et al., 2020](#)) from the HHVs of the digestates with a TS content above 15%, which is in accordance with the findings of the present study. Higher differences in the HHVs of the digestate and hydrochar of 7.2–26% have been reported for digestates with a lower TS content of 2.9–4.5% ([Table 5](#)). While a high ash content of the feedstock is related to decreased HHVs ([Zhuang et al., 2018](#)), it does not explain the difference in the observed HHV for the different digestate hydrochars between the present and previous studies ([Marin-Batista et al., 2020](#); [Merzari et al., 2020](#)). Thus, it seems that the HHV of the digested sewage sludge hydrochar depends on the HHV of the digestate used as feedstock.

Although the effects of HTC treatment on the HHV are often negligible, HTC treatment results in higher ash content of the hydrochar compared with the original digestate. In the present study, the ash content of the digested sewage sludge increased from 43% to as high as 50–57% on HTC treatment, while with other digested sewage sludge, the ash content increased from 40% to 42–48% ([Marin-Batista et al., 2020](#)) and from 28% to 35–43% ([Merzari et al., 2020](#)) on HTC treatment of digestates with TS content of 16.5% and 17%, respectively. HTC treatment of digested sewage sludge with a lower TS content of 2.9–3.0% has resulted in an even higher increase in the ash content, from 35% to 55% ([Berge et al., 2011](#)) and from 45% to 57–77% ([Merzari et al., 2020](#)). [Merzari et al. \(2020\)](#) linked the lower ash content of the dewatered digestate (28.4%) compared with the original digestate (45%) to the removal of inorganic compounds, such as NH<sub>4</sub>-N, CaCO<sub>3</sub>, Mg and Na, that end up in the reject water during conditioning and dewatering.

In terms of fouling, slagging and corrosion, the inorganics contained in the ash influence the fuel behaviour upon combustion,

thus affecting the choice of an appropriate combustion technology ([Smith et al., 2016](#)). These ash-forming inorganic elements include alkali and earth alkali metals (Na, K, Mg and Ca) as well as P, Fe, Si and S ([Smith et al., 2016](#)). In the present study, the increase in the concentrations of calcium with temperature of HTC treatment in the hydrochars were similar for the digestate and diluted digestate (from 22 to 24 to 23.2–35.1 g-Ca/kg-TS), whereas those of sodium and potassium were decreased for diluted digestate (from 6.2 to 3.0–4.2 g-Na/kg-TS and from 2.4 to 1.5–2.0 g-K/kg-TS) and were increased or unaffected for digestate (from 4.25 to 2.8–4.1 g-Na/kg-TS and from 1.7 to 1.6–2.0 g-K/kg-TS) ([Table S1](#)). In the case of iron, a larger decrease in concentration from 229 to 165–201 g-Fe/kg-TS was observed with the digestate than with the diluted digestate (from 184 to 133–182 g-Fe/kg-TS), which could be due to the degradation of digestate particles and their extraction into the liquid fraction ([Wang et al., 2019](#)). In addition, in the present study, the HTC treatment slightly decreased the sulphur concentrations from 23 g-S/kg-TS of digestates to 18–22 g-S/kg-TS of hydrochars. These concentrations of sulphur were higher than in the digested sewage sludge hydrochars reported elsewhere (maximum sulphur concentration of 12 g-S/kg-TS; [Aragón-Briceño et al., 2017](#); [Parmar and Ross, 2019](#)), which was because of their lower initial digestate sulphur concentration when compared with the present digestate. The comparatively high sulphur content in the present digestate may arise from the addition of phosphorous precipitation chemical, Fe(II)SO<sub>4</sub>, at the WWTP, which is also supported by the high iron concentrations in the hydrochars that are ca. 10-fold higher than that reported for dewatered digestate by [Marin-Batista et al. \(2020\)](#).

### 3.2.2. Filtrate

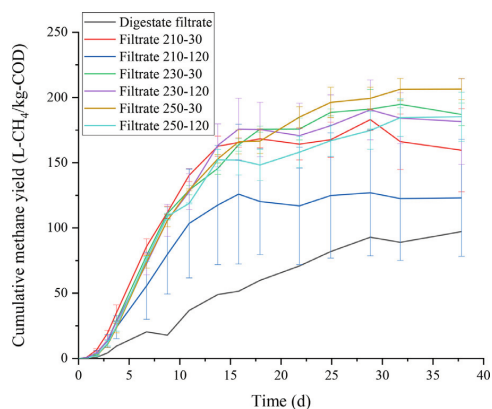
The HTC treatment produced filtrates with pH of 8.4–9.0 from the digestate (initial pH 7.5) and with a pH of 9.3–9.7 for the diluted digestate (initial pH 7.9). HTC treatment of digested sewage sludge results in alkaline filtrates ([Aragón-Briceño et al., 2017](#); [Marin-Batista et al., 2020](#)), even though the degradation products of hydrolysis generated during HTC often promote acidity rather than alkalinity ([Qiao et al., 2011](#)). However, the final pH is also impacted by volatilisation, for example, of ammonia, during HTC treatment ([Liu et al., 2019](#)). Even though the pH values of the filtrate are higher than those considered optimum for anaerobic treatment, the treatment of the filtrates in AD may be managed

**Table 4**

The characteristics of the reject water, filtrate of digestate and filtrates after HTC treatment.

Sample	Energy content				Nutrients			
	SCOD (g/L)	TVFA (g/L COD)	BMP (L CH <sub>4</sub> /kg SCOD)	pH	N (g/L)	NH <sub>4</sub> -N (g/L)	P (mg/L)	PO <sub>4</sub> <sup>2-</sup> (mg/L)
Reject water	10.3	1.4	n.a.	8.0	3.7	2.9	n.a.	58.6
Filtrate of digestate	2.1	n.d.	97 ± n.a.	8.0	0.3	n.d.	1080	n.d.
<i>Filtrates of HTC treated digestate</i>								
210 °C for 30min	38.9	3.9	183 ± 8.3	8.4	5.4	2.6	700	40
210 °C for 120min	44.4	5.1	126 ± 48.4	8.7	6.1	3.2	810	49
230 °C for 30min	36.8	7.2	195 ± 2.5	8.9	5.3	2.8	590	48
230 °C for 120min	40.3	12.4	191 ± 23	8.9	5.6	3.3	800	99
250 °C for 30min	38.5	11.4	206 ± 8.1	8.9	4.9	2.7	890	67
250 °C for 120min	38.8	12.8	185 ± 18.8	8.9	5.0	2.9	510	68
<i>Filtrates of HTC treated diluted digestate</i>								
210 °C for 30min	30	3.3	n.a.	9.3	4.6	2.3	730	129
210 °C for 120min	31.9	3.5	n.a.	9.4	4.8	2.6	770	97
230 °C for 30min	28	6.7	n.a.	9.6	4.3	2.5	330	87
230 °C for 120min	28.6	7.6	n.a.	9.7	4.6	2.8	1130	88
250 °C for 30min	28.8	6.0	n.a.	9.7	4.3	2.8	550	119
250 °C for 120min	28	9.5	n.a.	9.5	4.3	2.8	680	176

n.a. not analysed, n.d. not detected, SCOD: soluble chemical oxygen demand, TVFA: total volatile fatty acids, BMP: biochemical methane potential.

**Fig. 2.** The cumulative methane production of the filtrates from digestate before (digestate filtrate) and after the HTC treatment (filtrate obtained at HTC temperature between 210 and 250 °C and residence times of 30 or 120 min).

without pH adjustment because the process' operation and co-digestion can be adjusted.

The SCODs of the HTC filtrates ranged from 37 to 44 g/L and from 28 to 32 g/L for the digestate and diluted digestate, respectively, being 10–20 times higher than in the feedstocks. The SCODs were slightly higher at higher HTC treatment temperatures, but no major effects of the HTC conditions were obvious. However, even though the SCOD changed only a little, its composition varied because total VFA contributed ca. 30% of the SCOD at higher temperatures, while at 210 °C TVFAs were ca. 10% of SCOD. The higher treatment temperature especially increased the propionate concentration from around 0.4 g/L at 210 °C to 6.9 g/L at 250 °C, while the changes in other VFA concentrations were low. Increased residence time increased acetate concentration slightly ( $\leq 1.8$  g/L) at all temperatures. Even though the SCOD composition varied in different filtrates, the cumulative methane production profiles of all the filtrates were almost similar with an initial two-day lag phase (Fig. 2). The resulting BMPs varied from 185 to 206 mL-CH<sub>4</sub>/g-SCOD with little difference and without a clear impact resulting from the HTC conditions (Table 4). The BMP yields of the HTC filtrates were around two-fold higher compared with the BMP yield of the filtrate of the original digestate.

The present and previous studies have shown that HTC treatment increases the SCOD of the filtrate several fold compared with the SCOD of the sewage sludge digestate, resulting in reported SCOD values ranging from 5.7 g/L up to 72 g/L for HTC filtrates (Table 6). This increase in SCOD is a result from the hydrolysis of fats, carbohydrates and proteins into smaller units, that is, fatty acids, VFAs, sugars and amino acids (Qiao et al., 2011). With a specific feedstock, the feedstock solids content used in the HTC treatment affects the SCOD concentration. For example, HTC treatment (250 °C, 30 min) of sewage sludge digestate increased filtrate SCODs from 9.7 g/L up to 72 g/L when the TS content of the digestate used in HTC treatment was increased from 2.5% to 30% (Aragón-Briceño et al., 2020). Contrary to our study, Aragón-Briceño et al. (2020) reported that HTC treatment decreased the share of VFAs of the SCOD because it was around 15% for the digestate and, at the highest, 10% for HTC filtrate. Furthermore, the share of the VFAs of the SCOD decreased with increasing loading from 10% to ca. 5% of the highest solids loading of 72 g/L (Aragón-Briceño et al., 2020). It should be noted that in HTC treatments, some produced compounds may also volatilise and be discharged in the gas phase.

Based on the current study and the literature, the HTC treatment of digested sewage sludge has resulted in two- to three-fold higher methane production per g-SCOD (Aragón-Briceño et al., 2017) compared with reject water from sewage sludge digestate, even though the effects on SCOD composition vary. The batch assays used to determine methane production have not suggested major inhibition in most of the studies (Aragón-Briceño et al., 2020; Parmar and Ross, 2019). On the other hand, severe inhibition was observed in BMP assays with a 240 °C filtrate (Marin-Batista et al., 2020). However, it should be noted that the methane potential is assayed in specific conditions (e.g., batch, with different substrate dilutions) and care should be taken in practice if an anaerobic process is used for the treatment of filtrates. It should also be noted that the volume of the filtrate may be up to 76% of the digestate and close to the feedstock volume. Furthermore, the introduction of the filtrate into the digester affects the composition of the reject water, the digestate to be treated in HTC and, subsequently, the filtrate characteristics.

### 3.2.3. Overall energy balance

The combined energy contents (kWh/kg feed) and recoveries (% of the original feed) of the hydrochars (as HHV) and filtrates (as BMP) were assessed for the digestate and of the hydrochars for

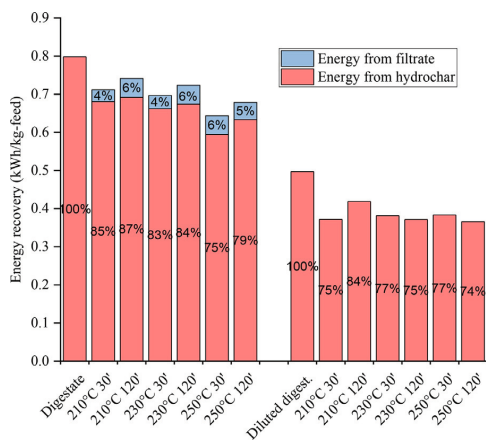


**Fig. 3.** The energy recovered (as kWh/kg feed) in the hydrochar and filtrate after the HTC treatment of digestate and diluted digestate compared to the energy content of the digestate and diluted digestate, respectively. The energy yields (% of the HTC feed) of the hydrochars are marked on the columns. The energy contents of the filtrates originating from the diluted digestates were not determined.

the diluted digestate (Fig. 3). The values presented do not consider the energy consumed in the HTC. The hydrochars covered 74–87% of the total energy content of the digestate and diluted digestate, while the filtrates covered 4–6% of the total energy content of the digestate. The highest energy contents were obtained in the digestate hydrochars from the treatments at 210 °C and 230 °C (0.66–0.69 kWh/kg feed). Overall, the hydrochar energy content was more influenced by the digestate TS content than the different HTC conditions. It has been observed that the energy recovery in hydrochar decreases with increasing temperature and time (Aragón-Briceño et al., 2017; Danso-Boateng et al., 2015) but, according to the present results, also with the TS content of the original digestate. The energy balance suggests that HTC downgrades the energetic potential of digested sewage sludge by 7–20%. However, the benefit of the HTC treatment may not come from the absolute energy recovery alone but from the improved suitability for combustion, here considering that the moisture content and a favourable ash composition may diminish fouling (Smith et al., 2016).

### 3.3. Nutrients

To assess the fate of the nutrients present in the dewatered sewage sludge digestate and diluted digestate, the hydrochars' and filtrates' phosphorous and nitrogen contents were analysed for the different HTC conditions studied (Tables 3 and 4).

For the total phosphorous concentrations, HTC showed an increase by 25–52% and 19–61% compared with the original digestate (37.2 g/kg-TS) and diluted digestate (31.5 g/kg-TS), respectively. The filtrates from the digestate and diluted digestate had total phosphorous concentrations of 510–890 mg/L and 330–1130 mg/L and phosphate concentrations of 40–99 mg/L and 87–176 mg/L, respectively. Although phosphate was increasingly formed during the HTC treatments (not detected in the original digestate filtrate), the total phosphorous concentration of the filtrates decreased (1080 mg/L in the original digestate filtrate), indicating that part of the total phosphorous was transferred to the hydrochar fraction.

In the present study, the recovery of phosphorous in the hydrochar was higher or similar, as previously reported, even though the initial phosphorous concentrations were at a lower range.

Much like in our study, an increase in phosphorous concentrations from 45.8 g/kg-TS to 52.8–63.0 g/kg-TS (with an increase of 15–38%) and from 9.2 g/kg-TS to 9.2–10.9 g/kg-TS (with an increase of 0–18%) have been shown to occur with digested TS contents of 16.5% and 17%, respectively (Marin-Batista et al., 2020; Merzari et al., 2020). The phosphorous content (g/kg-TS) of the hydrochar has been increased with increasing HTC treatment temperature and residence time (Marin-Batista et al., 2020; Merzari et al., 2020), as also reported in the current study. The difference in the phosphorous concentrations in the hydrochars in different studies (Table 5) is dictated by the digested phosphorous concentration and may also be affected by the phosphorous removal method at WWTP. Phosphorous is often precipitated at WWTPs with aluminium or iron salts. In the present study, sewage sludge originated from WWTP using iron salts for phosphorous precipitation, resulting in iron concentrations of 180–230 mg/g-TS in the digested sewage sludge. The Al and Fe concentrations in the digested sewage sludge were 41.9 mg/g-TS and 15.8 mg/g-TS in (Marin-Batista et al., 2020), whereas in (Merzari et al., 2020) the Al concentration in the digested sewage sludge, it was around 2–5 mg/g-TS. However, in these two studies, the unit processes of wastewater treatment, for example, phosphorous removal technologies were not defined, making it difficult to interpret some nutrient results.

Phosphorous only exists either in a solid or liquid state; hence, the phosphorous balance was created by summing the elemental phosphorous analysed in the filtrate and hydrochar. The total phosphorous mass balance in Fig. 4B exceeded the input mass of phosphorous in nearly all treatments, which was due to heterogeneity of the analysed material and a small sample amount in the ICP-MS analysis. However, it can be concluded that the majority (>90%) of the phosphorous was recovered in the hydrochar (Fig. 4A and 4B), to which the different HTC conditions gave little variety. The dissolved phosphorous in the filtrates were slightly higher for the HTC-treated diluted digestate (4–13%) than for digestate (2–5%). It has been reported that lower solids loading (studied TS ranged from 2.5 to 30%) of sewage sludge digestate promotes phosphorous solubility which can be attributed to the decreased precipitation of phosphorous with metal ions that are present in lesser amounts with lower solids input (Aragón-Briceño et al., 2020). The dissolution of phosphorous from the digestate was enhanced with the longer treatment times, except for HTC-treated digestate at 250 °C. Thus, to enable the utilisation of phosphorous, it should be either leached from the hydrochar (Becker et al., 2019), or the hydrochar should be amenable as a fertiliser (Bargmann et al., 2014).

The total nitrogen concentration in the hydrochars were 21.4–25.8 g-TN/kg-TS and reduced by 23–39% and 17–31% relative to the digestate and diluted digestate, respectively (Table 3). The total nitrogen concentrations in the filtrates varied in the range of 4.9–6.1 g/L for the digestate and 4.3–4.8 g/L for the diluted digestate, while the ammonium-nitrogen concentrations presented only slight variations between treatments (2.5–3.3 g/L). There was a significant increase in the total nitrogen and ammonium-nitrogen concentrations when compared with their concentrations in the liquid fraction of the digestate (0.32 g-TN/L, <2 mg-NH<sub>4</sub>-N/L). However, in the reject water used to dilute the digestate, the total nitrogen and ammonium-nitrogen concentrations were 3.7 g/L and 2.9 g/L, respectively.

The present study has shown that HTC converts nitrogen from the solid phase of the dewatered digestate into the liquid phase. Similarly, a decrease in hydrochar nitrogen content compared with the dewatered digestate has been reported in other studies from 51 to 41–42 g-TN/kg-TS at HTC temperatures of 180–240 °C (Marin-Batista et al., 2020), from 40 to 19–28 g-TN/kg-TS at 250 °C (Aragón-Briceño et al., 2020), and from 58.1 to 31.2–42.7 g-TN/kg-TS at HTC temperature of 190–250 °C (Merzari et al., 2020). With a digestate without dewatering, a decrease in hydrochar nitrogen

**Table 5**

Comparison of different hydrochars from various HTC treatments obtained from literature with the hydrochars of the present study. The values are expressed against total solids.

Hydrochar origin	HTC conditions	HHV (MJ/kg)		Ash (%)		C (%)		N (%)		S (%)		P (g/kg)		Reference
		30 min	60 min	30 min	60 min	30 min	60 min	30 min	60 min	30 min	60 min	30 min	60 min	
Digested sewage sludge 1 <sup>a</sup>	210 °C, 15% TS	11.35	11.38	51.80	52.20	30.41	30.01	2.58	2.38	1.91	2.00	49.53	37.38	present study
	230 °C, 15% TS	11.82	11.48	52.60	53.70	29.72	29.59	2.42	2.14	2.10	2.18	50.71	49.40	
	250 °C, 15% TS	11.86	12.19	54.00	57.00	30.41	30.38	2.31	2.30	2.23	2.19	46.50	50.18	
Digested sewage sludge 1 <sup>a</sup>	210 °C, 25% TS	11.33	11.38	49.60	51.80	31.07	31.00	2.54	2.57	1.83	1.80	53.27	51.15	present study
	230 °C, 25% TS	11.63	11.89	51.60	53.70	31.40	30.30	2.70	2.40	1.93	1.77	46.54	47.29	
Digested sewage sludge 2	250 °C, 25% TS	11.85	12.12	55.50	56.70	30.03	30.30	2.26	2.15	2.16	2.17	49.39	56.65	Marin-Batista et al., 2020
	180 °C, 16.5% TS	n.a.	14.70	n.a.	42.90	n.a.	30.80	n.a.	4.20	n.a.	1.00	n.a.	52.80	
	210 °C, 16.5% TS	n.a.	14.90	n.a.	43.90	n.a.	31.80	n.a.	4.10	n.a.	1.00	n.a.	53.20	
Digested sewage sludge 3	240 °C, 16.5% TS	n.a.	15.10	n.a.	48.10	n.a.	32.60	n.a.	4.10	n.a.	1.10	n.a.	63.00	Aragón-Briceño et al., 2017
	160 °C, 4.5% TS	16.97	n.a.	38.63	n.a.	35.53	n.a.	5.11	n.a.	1.07	n.a.	n.a.	n.a.	
	220 °C, 4.5% TS	14.33	n.a.	45.11	n.a.	33.21	n.a.	2.01	n.a.	1.09	n.a.	n.a.	n.a.	
Digested sewage sludge 4	250 °C, 4.5% TS	17.80	n.a.	36.88	n.a.	38.03	n.a.	4.23	n.a.	1.19	n.a.	n.a.	n.a.	Merzari et al., 2019
	190 °C, 3% TS	9.27	7.97	57.21	67.1	19.22	14.16	1.58	1.07	n.a.	n.a.	7.2	7.4	
	220 °C, 3% TS	8.96	7.86	72.57	67.88	11.7	10.21	0.8	0.66	n.a.	n.a.	7.5	7.5	
Digested sewage sludge 4	250 °C, 3% TS	8.59	9.37	73.42	76.97	12.51	12.02	0.7	0.69	n.a.	n.a.	7.4	6.7	Merzari et al., 2019
	190 °C, 17% TS	16.3	15.96	35.66	37.05	36.61	35.07	4.27	3.95	n.a.	n.a.	9.20	9.40	
	220 °C, 17% TS	15.7	15.47	40.48	41.1	35.19	35.75	3.48	3.45	n.a.	n.a.	10.50	10.60	
Raw sewage sludge 1	250 °C, 17% TS	15.98	15.33	43.36	43.14	35.3	35.57	3.16	3.12	n.a.	n.a.	10.80	10.90	Merzari et al., 2020
	190 °C, 3% TS	19.45	20.71	24.91	24.40	44.56	46.11	2.23	2.10	n.a.	n.a.	6.20	6.80	
	220 °C, 3% TS	20.06	18.72	28.58	31.20	44.86	43.15	1.87	1.86	n.a.	n.a.	7.80	9.40	
Digested sewage sludge 5	250 °C, 3% TS	18.06	19.17	34.63	37.18	41.68	41.21	1.89	1.99	n.a.	n.a.	9.90	10.2	Parmar K. and Ross A. 2019
	150 °C, 20% TS	n.a.	15.00 <sup>b</sup>	n.a.	43.80	n.a.	33.40	n.a.	3.20	n.a.	0.30	n.a.	n.a.	
	200 °C, 20% TS	n.a.	15.10 <sup>b</sup>	n.a.	44.40	n.a.	34.00	n.a.	2.40	n.a.	0.90	n.a.	n.a.	
	250 °C, 20% TS	n.a.	15.30 <sup>b</sup>	n.a.	47.50	n.a.	34.70	n.a.	2.40	n.a.	0.70	n.a.	n.a.	

n.a. not applicable.

<sup>a</sup> 120 min instead of 60 min.

<sup>b</sup> theoretical.

**Table 6**

Comparison of different filtrates from various HTC treatments obtained from literature with the filtrates of the present study.

Filtrate origin	HTC conditions	BMP (ml CH <sub>4</sub> /g Soluble COD) (g/l)				pH				Total Nitrogen (g/l)				Total Phosphorous (mg/l)				Reference
		30 min		60 min		30 min		60 min		30 min		60 min		30 min		60 min		
Digested sewage sludge 1 <sup>a</sup>	210 °C, 15% TS	n.a.	n.a.	30.00	31.90	9.34	9.37	4.6	4.8	2.33	2.59	725.20	772.28	128.80	96.92	present study		
	230 °C, 15% TS	n.a.	n.a.	28.00	28.60	9.58	9.70	4.3	4.6	2.50	2.83	330.57	n.a.	86.51	87.92			
	250 °C, 15% TS	n.a.	n.a.	28.80	28.00	9.70	9.50	4.3	4.3	2.83	2.76	545.71	688.12	119.34	176.16			
Digested sewage sludge 1 <sup>a</sup>	210 °C, 25% TS	183.1	182.6	38.90	44.40	8.42	8.69	5.4	6.1	2.62	3.23	701.30	810.95	39.94	48.50	present study		
	230 °C, 25% TS	190.5	194.8	36.80	40.30	8.95	8.95	5.3	5.6	2.85	3.35	592.42	803.00	48.39	99.11			
	250 °C, 25% TS	206.5	185.3	38.50	38.80	8.90	8.91	4.9	5.0	2.71	2.93	892.50	509.53	67.45	67.54			
Digested sewage sludge 2	180 °C, 16.5% TS	n.a.	325 <sup>b</sup>	n.a.	56.20	n.a.	7.40	n.a.	8.10 <sup>c</sup>	n.a.	4.90	n.a.	11.1 <sup>d</sup>	n.a.	n.a.	Marin-Batista et al., 2020		
	210 °C, 16.5% TS	n.a.	279 <sup>b</sup>	n.a.	61.50	n.a.	7.90	n.a.	9.00 <sup>c</sup>	n.a.	5.20	n.a.	19.2 <sup>d</sup>	n.a.	n.a.			
	240 °C, 16.5% TS	n.a.	<20 <sup>b</sup>	n.a.	53.90	n.a.	8.90	n.a.	9.70 <sup>c</sup>	n.a.	6.30	n.a.	25.3 <sup>d</sup>	n.a.	n.a.			
Digested sewage sludge 3	160 °C, 4.5% TS	260	n.a.	12.60	n.a.	9.15	n.a.	11.11	n.a.	1.26 <sup>e</sup>	n.a.	n.a.	n.a.	94.03 <sup>f</sup>	n.a.	Aragón-Briceño et al., 2017		
	220 °C, 4.5% TS	277	n.a.	13.00	n.a.	7.14	n.a.	12.31	n.a.	1.70 <sup>e</sup>	n.a.	n.a.	n.a.	72.60 <sup>f</sup>	n.a.			
	250 °C, 4.5% TS	226	n.a.	12.20	n.a.	8.08	n.a.	6.56	n.a.	1.70 <sup>e</sup>	n.a.	n.a.	n.a.	103.83 <sup>f</sup>	n.a.			
Digested sewage sludge 4	190 °C, 3% TS	n.a.	n.a.	6.40	6.70	7.10	6.80	1.30 <sup>e</sup>	1.20 <sup>e</sup>	0.70	0.70	19.60	22.70	n.a.	n.a.	Merzari et al., 2019		
	220 °C, 3% TS	n.a.	n.a.	6.70	6.70	6.80	6.20	1.40 <sup>e</sup>	0.90 <sup>e</sup>	0.80	1.00	19.80	17.80	n.a.	n.a.			
	250 °C, 3% TS	n.a.	n.a.	8.30	5.70	7.30	6.90	1.30 <sup>e</sup>	1.50 <sup>e</sup>	1.00	0.80	19.30	12.20	n.a.	n.a.			
Digested sewage sludge 4	190 °C, 17% TS	n.a.	n.a.	49.80	55.10	6.00	6.00	4.50 <sup>e</sup>	4.10 <sup>e</sup>	2.70	3.80	0.30	0.40	n.a.	n.a.	Merzari et al., 2019		
	220 °C, 17% TS	n.a.	n.a.	44.80	45.70	6.00	5.90	2.40 <sup>e</sup>	1.50 <sup>e</sup>	4.40	4.60	0.20	0.20	n.a.	n.a.			
	250 °C, 17% TS	n.a.	n.a.	57.50	46.80	6.00	5.50	1.70 <sup>e</sup>	1.40 <sup>e</sup>	6.90	6.50	0.20	0.20	n.a.	n.a.			
Raw sewage sludge 1	190 °C, 3% TS	n.a.	n.a.	10.50	13.40	6.00	5.30	0.10 <sup>e</sup>	0.10 <sup>e</sup>	0.40	0.60	32.50	38.40	n.a.	n.a.	Merzari et al., 2020		
	220 °C, 3% TS	n.a.	n.a.	11.90	13.50	6.00	6.10	0.10 <sup>e</sup>	0.10 <sup>e</sup>	0.40	0.50	20.20	16.40	n.a.	n.a.			
	250 °C, 3% TS	n.a.	n.a.	15.30	13.70	5.80	6.00	0.10 <sup>e</sup>	0.10 <sup>e</sup>	0.60	0.60	16.10	11.10	n.a.	n.a.			
Digested sewage sludge 5	150 °C, 20% TS	n.a.	100.2	n.a.	31.00 <sup>g</sup>	n.a.	5.60	n.a.	2.40	n.a.	n.a.	n.a.	n.a.	n.a.	n.a.	Parmar K. and Ross A. 2019		
	200 °C, 20% TS	n.a.	181.7	n.a.	38.90 <sup>g</sup>	n.a.	6.20	n.a.	4.50	n.a.	n.a.	n.a.	n.a.	n.a.	n.a.			
	250 °C, 20% TS	n.a.	151.9	n.a.	43.60 <sup>g</sup>	n.a.	7.60	n.a.	4.70	n.a.	n.a.	n.a.	n.a.	n.a.	n.a.			

n.a. not applicable, COD: chemical oxygen demand.

<sup>a</sup> 120 min instead of 60 min.

<sup>b</sup> ml CH<sub>4</sub>/g-VS.

<sup>c</sup> Total Kjeldahl nitrogen.

<sup>d</sup> % of total phosphorous in digestate.

<sup>e</sup> mg-N/L

<sup>f</sup> mg-P/L

<sup>g</sup> total COD.

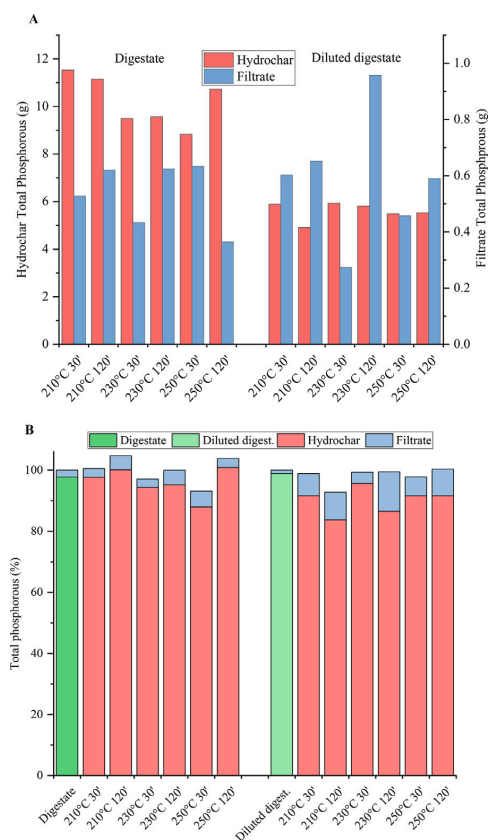


**Fig. 4.** The phosphorous mass distribution in grams (A) and in percentages of the input total phosphorous (B) into hydrochar and filtrate after the HTC treatment of digestate and diluted digestate at different temperatures (210–250 °C) and residence times (30 or 120 min). Digestates and hydrochars are presented as their total mass after filtration including their moisture. The input phosphorous mass seemed to be exceeded in a few treatments, which due to the heterogeneity of the analysed material and a small sample amount in the ICP-MS analysis, causing some error.

content from 50.4 to 20.1–42.3 g-TN/kg-TS was observed at HTC temperatures of 220 °C and 250 °C, while at an HTC temperature of 160 °C, the nitrogen content increased from 50.4 to 51.1 g-TN/kg-TS (Aragón-Briceño et al., 2017). An increase in the HTC temperature decreased the nitrogen content in the solid fraction (Aragón-Briceño et al., 2017; Merzari et al., 2020), which was also found to be the case in the current study. The observed increase of nitrogen percentage in the hydrochar fraction at a higher TS content of the hydrochar, was also reported by Aragón-Briceño et al. (2020), who tested HTC treatment with digested sewage sludge TS contents from 2.5 to 30%.

During HTC treatment, a decline in nitrogen content in hydrochars has been reported to occur because of the decomposition of labile and organic nitrogen compounds, while the volatile nitrogen compounds are already devolatilised below temperatures of 220 °C to the liquid and gas phases (Zhuang et al., 2018). The increase in ammonium-nitrogen concentration in the filtrate at increased HTC temperatures has been connected to the hydrolysis of proteins through peptides and amino acids to fatty acids and ammonia (Marin-Batista et al., 2020). The volatilisation of nitrogen compounds was observed in the current study (Fig. 5), both in the

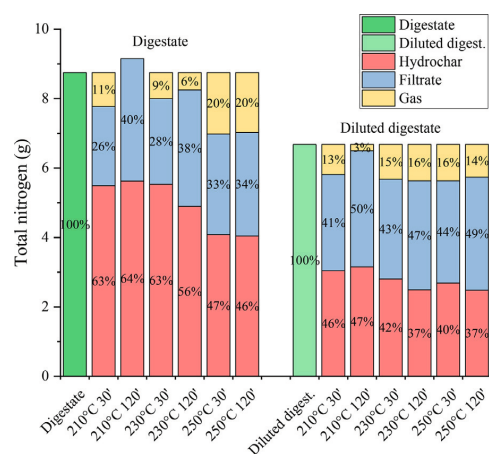


**Fig. 5.** The mass distribution of total nitrogen of unfiltered digestate and diluted digestate into hydrochar, filtrate and gas phases after the HTC treatments at temperatures of 210–250 °C and residence times of 30 or 120 min. Hydrochar and digestates are presented in total mass including their moisture content. The recovered total nitrogen in the product fractions compared to the total nitrogen in the input digestate is marked in percentages on the columns.

filtrates and hydrochars upon increasing the HTC temperature and time.

The original nitrogen content and its distribution to the HTC products are presented in Fig. 5. The total nitrogen lost in the gas phase varied between 3% and 20%, which, however, was calculated by difference, therefore giving some room for error. The nitrogen recovery into the product fractions depended on the digestate TS because the digestate hydrochars retained 46–64% and the diluted digestate hydrochars 36–46% of the total nitrogen. The filtrates from the digestate and diluted digestate contained 26–40% and 41–48% of the total nitrogen, respectively. High volumes of filtrate and high concentrations of nitrogen in the filtrate present an interesting option for nitrogen recovery. If the filtrate was fed back to the biogas digester, the ammonium-nitrogen could be recovered from the filtrate, in addition to that in the reject water from the mechanical dewatering of digestate, for example, with ammonium stripping. But then again, the unionised form of ammonium, ammonia (NH<sub>3</sub>), at too high concentrations can inhibit methanogens in AD (Jiang et al., 2019), which could be avoided by treating the filtrate directly in ammonium stripping. However, the hydrochar also contained a large portion (21.4–27.0 g/kg-TS) of the total nitrogen.

The carbon contents of the hydrochars ranged from 29 to 31% (Table 3), which is typical for hydrochars from digested sewage sludge (Table 5). The carbon recoveries were on average 82±7% and 83±5% in the hydrochars from the digestate and diluted digestate, respectively, decreasing with treatment severity.

### 3.4. Trace elements, heavy metals and pharmaceuticals

The trace elements (Cu, Zn, Al and Ni) and heavy metals (Au, As, Cd, Cr, Hg and Pb) of the hydrochars and filtrates were analysed (Tables S1 and S2). All the concentrations were below the permitted limit values dictated by the EU (86/278/EEC) and Finnish authorities (Ylivainio and Turtola, 2016), except the limit concentration of mercury for fertilisers used in Finland (0.001 mg-Hg/g TS) was already exceeded in the digestates (0.02 mg-Hg/g-TS) and its concentration increased in HTC to 0.02–0.03 mg-Hg/g-TS in the hydrochars. Overall, the heavy metal and trace element concentra-

tions (per TS) were slightly increased in all hydrochars from those of the digestates, which could be attributed to the mass decrease of the solid phase during HTC and/or to the precipitation of these metal ions as salts in the hydrochar (Zhang et al., 2014).

Pharmaceuticals are known to be present in sewage sludge and digestates (Radjenović et al., 2009). The present results showed two hormones and 23 pharmaceuticals in the digestate, for example, 0.15 mg/kg-TS estrone, 2.4 mg/kg-TS tetracycline, 0.24 mg/kg-TS diclofenac and 0.93 mg/kg-TS doxycycline in the solid fraction and 8 µg/L tetracycline and 5.4 µg/L diclofenac in the liquid fraction of the digestate (Table S3). After HTC treatment, no hormones or pharmaceuticals analyzed were detected in the hydrochar fraction (below the detection limit). In the filtrate, only two pharmaceuticals were detected: 330 µg/L benzotriazole and 230 µg/L ibuprofen, while the concentrations of the other pharmaceuticals were below the detection limit. The detection limits for most of the hormones and pharmaceuticals in the hydrochar and filtrate were under 0.5 mg/kg-TS and 1.0 µg/L, respectively, while the detection limits after HTC were higher for ciprofloxacin (<50 µg/L), tetracycline (<10 µg/L), and mirtazapine, sertraline, norsertaline and cetirizine (<5 µg/L) in the filtrate. Thus, the presence of ciprofloxacin and tetracycline in the filtrate cannot be excluded. Benzotriazole is widely used in cosmetics and in corrosion prevention, thus ending up in municipal wastewater (Zhang et al., 2011). Although in the current study HTC treatment removed most of the pharmaceuticals, not all possible hormones and pharmaceuticals, nor their degradation products, were analysed. Other studies have also concluded that HTC has potential to degrade organic pollutants while emphasising its limitedness in complete removal or detoxification of chlorinated aromatics and, for example, phenazone (vom Eyser et al., 2015; Weiner et al., 2013).

#### 4. Practical implications

The present results and previous information on HTC treatment of digestate can be used to assess the potential of HTC for individual cases and, for example, to calculate a techno-economic analysis. In each case, the utilisation of biogas, hydrochars and filtrates, as well as the energy and nutrient contents in these streams, depend on many local factors, which further affect the technological system, its economics and sustainability. An example extrapolation calculation for integrating HTC into a biogas process was done for a centralised Topinoja biogas plant, from where the dewatered sewage sludge digestate for the current study was obtained and compared with the process at the time of the experiments (Fig. 6). The biogas plant annually treats 75,000 t of sewage sludge (22% TS) and produces 30,000 t of dewatered digestate (30% TS). The HTC assessment was done by averaging the results from three HTC runs with the digestate (210 °C for 120 min and 230 °C for 30 min or 120 min) considered relevant for practical application. It was assumed that ca. 40% of the digestate volume (36,000 t; 25% TS) ends up in hydrochar and the rest to filtrate (minimal losses of mass to the gas phase). In such a case, ca. 14,400 t of hydrochar would be produced, which has a TS content of 50% and an energy content of ca. 11.5 MJ/kg-TS. The hydrochar could currently be considered for different end use applications, for example, used in agriculture, where it would promote carbon and nutrient utilisation, thus benefitting circular economy, or for co-combustion, with an annual energy production from the hydrochar of ca. 82,800 GJ (Fig. 6). The economic benefit from the hydrochar production for energy recovery has been reported to even exceed the profits from biogas production per tonne of sewage sludge (Aragón-Briceño et al., 2021).

If the filtrate, ca. 18,000 t/a, was fed to the biogas process, it would enhance the annual methane production with ca. 140,000 m<sup>3</sup> (1.4 GWh), that is, 4.5%, from the current annual methane production of ca. 3 million m<sup>3</sup> (30 GWh). Furthermore, the feeding

of the filtrate to the biogas process would enable the recovery of the ammonium-nitrogen present in the filtrate (ca. 3.1 g-NH<sub>4</sub>-N/L) from the reject water of the digestate after dewatering. In the Topinoja plant, ammonium is recovered from the dewatering reject water via ammonia stripping (ca. 4000 t of ammonium water; 12% NH<sub>4</sub>-N) and directing filtrate to the biogas process could increase the volume of ammonium water up to 5000 t (Fig. 6).

It has been reported that the integration of HTC with AD has potential to increase the profits for WWTP (Aragón-Briceño et al., 2021), which however is case-dependant as the required capital costs for the investment to an existing WWTP vary and may not be covered by the revenues from hydrochar utilisation (Medina-Martos et al., 2020). Nevertheless, the utilisation of hydrochar may have more potential in respect to digestate due to its higher phosphorous and lower pharmaceutical contents as well as decreased end product volume, which decreases the transportation needs and costs. Furthermore, directing the hydrochar to agriculture could also promote carbon storage and carbon neutral agriculture, which should be further evaluated. Returning the filtrate with readily biodegradable organic and high ammonium-nitrogen contents to the biogas process requires optimisation of its downstream processes, e.g., the energy balance considerations and use of polymers in digestate dewatering.

#### 5. Conclusions

The current study evaluated HTC treatment (at 210–250 °C, for 30 or 60 min) and subsequent filtration of mechanically dewatered digestate (TS 25%) from a full-scale centralised biogas plant treating mechanically dewatered sewage sludge. The volume of different hydrochars was 30–55% of the dewatered digestate's volume, and the TS content of the hydrochars was 53–64%. The hydrochars contained over 90% of the phosphorous in the digestate (up to 56 g/kg-TS), ca. 30% carbon per TS, pharmaceuticals were below detection limits, and heavy metals were under legislative limits (apart from mercury). The high phosphorous content of hydrochars could favour its use in agriculture as fertiliser. The hydrochars could also be, for example, co-combusted, since the hydrochars' HHV (11.3–12.2 MJ/kg-TS) was similar to that of the digestate, although the high ash content (50–57%) may reduce its attractiveness. As all the HTC conditions applied in this study generated hydrochars of little variations in properties, it could be recommended to use the lowest temperature (210 °C) and shortest residence time (30 min) for hydrochar production from digestate. Another HTC end product is filtrate, which had a high SCOD content of 39–44 g/L, of which 10–33% was VFAs, methane potential of ca. 190 L-CH<sub>4</sub>/kg-SCOD and high nitrogen content of 4.9–6.1 g/L. Feeding the filtrate to the biogas digester would enable increased methane production and enhanced nitrogen recovery from the reject water of the anaerobic digester. The temperature of 230 °C could be regarded as the optimum temperature for generating filtrates with the highest methane production potential and ammonium content enabling ammonium recovery. Extrapolating the results to a centralised biogas plant, indicated that the integration of HTC to a biogas plant could enhance the annual biogas production by 5% and ammonium recovery by 25%, while the produced hydrochar could be used to produce 83 GJ or to direct 350 t phosphorous to agriculture annually.

#### Declaration of Competing Interest

The authors declare that they have no known competing financial interests or personal relationships that could have appeared to influence the work reported in this paper.

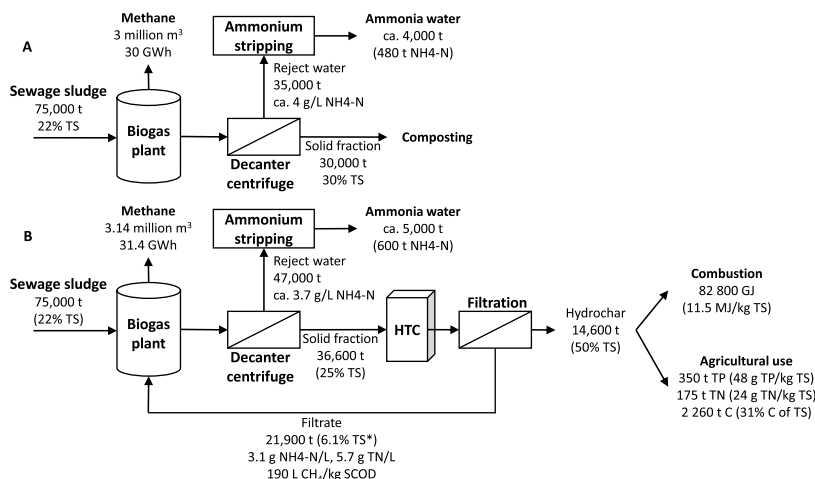


**Fig. 6.** The process layout of the biogas plant at the time of the present experiments (A) and extrapolation on how the integration of hydrothermal carbonisation (HTC) to the biogas plant would affect the overall scheme. For the hydrochar and filtrate characteristics, average values are taken from the following runs with digestate: 210 °C for 120 min and 230 °C for 30 min or 120 min. TS: total solids, TP: total phosphorous, TN: total nitrogen, NH<sub>4</sub>-N: ammonium-nitrogen.

## Acknowledgments

The financial support by Maj and Tor Nessling Foundation (Anna Hämäläinen), Gasum and Fifth Innovation are gratefully acknowledged. The authors acknowledge Kirsi Järvi, Antti Nuottajärvi, Essi Sariola-Leikas and Harri Ali-Löytty for their support in the laboratory.

## Supplementary materials

Supplementary material associated with this article can be found, in the online version, at doi:10.1016/j.watres.2021.117284.

## References

- Alvarenga, P., Mourinha, C., Farto, M., Santos, T., Palma, P., Sengo, J., Morais, M.C., Cunha-Queda, C., 2015. Sewage sludge, compost and other representative organic wastes as agricultural soil amendments: benefits versus limiting factors. *Waste Manag.* 40, 44–52. doi:10.1016/j.wasman.2015.01.027.
- Aragón-Briceño, C., Ross, A.B., Camargo-Valero, M.A., 2017. Evaluation and comparison of product yields and bio-methane potential in sewage digestate following hydrothermal treatment. *Appl. Energy* 208, 1357–1369. doi:10.1016/j.apenergy.2017.09.019.
- Aragón-Briceño, C.I., Grasham, O., Ross, A.B., Dupont, V., Camargo-Valero, M.A., 2020. Hydrothermal carbonization of sewage digestate at wastewater treatment works: influence of solid loading on characteristics of hydrochar, process water and plant energetics. *Renew. Energy* 157, 959–973. doi:10.1016/j.renene.2020.05.021.
- Aragón-Briceño, C.I., Ross, A.B., Camargo-Valero, M.A., 2021. Mass and energy integration study of hydrothermal carbonization with anaerobic digestion of sewage sludge. *Renew. Energy* 167, 473–483. doi:10.1016/j.renene.2020.11.103.
- Bargmann, I., Rillig, M.C., Kruse, A., Greef, J.M., Kücke, M., 2014. Effects of hydrochar application on the dynamics of soluble nitrogen in soils and on plant availability. *J. Plant Nutr. Soil Sci.* 177, 48–58. doi:10.1002/jpln.201300069.
- Becker, G.C., Wüst, D., Köhler, H., Lautenbach, A., Kruse, A., 2019. Novel approach of phosphate-reclamation as struvite from sewage sludge by utilising hydrothermal carbonization. *J. Environ. Manage.* 238, 119–125. doi:10.1016/j.jenvman.2019.02.121.
- Berge, N.D., Ro, K.S., Mao, J., Flora, J.R.V., Chappell, M.A., Bae, S., 2011. Hydrothermal carbonization of municipal waste streams. *Environ. Sci. Technol.* 45, 5696–5703. doi:10.1021/es2004528.
- Bridgwater, A.V., Meier, D., Radlein, D., 1999. An overview of fast pyrolysis of biomass. *Org. Geochem.* 30, 1479–1493. doi:10.1016/S0146-6380(99)00120-5.
- Danso-Boateng, E., Shama, G., Wheatley, A.D., Martin, S.J., Holdich, R.G., 2015. Hydrothermal carbonisation of sewage sludge: effect of process conditions on product characteristics and methane production. *Bioresour. Technol.* 177, 318–327. doi:10.1016/j.biortech.2014.11.096.
- He, C., Zhang, Z., Ge, C., Liu, W., Tang, Y., Zhuang, X., Qiu, R., 2019. Synergistic effect of hydrothermal co-carbonization of sewage sludge with fruit and agricultural wastes on hydrochar fuel quality and combustion behavior. *Waste Manag.* 100, 171–181. doi:10.1016/j.wasman.2019.09.018.
- Jenkins, B.M., Baxter, L.L., Miles, T.R., Miles, T.R., 1998. Combustion properties of biomass. *Fuel Process. Technol.* 54, 17–46. doi:10.1016/S0378-3820(97)00059-3.
- Jiang, Y., McAdam, E., Zhang, Y., Heaven, S., Banks, C., Longhurst, P., 2019. Ammonia inhibition and toxicity in anaerobic digestion: a critical review. *J. Water Process Eng.* 32. doi:10.1016/j.jwpe.2019.100899.
- Kinnunen, V., Ylä-Outinen, A., Rintala, J., 2015. Mesophilic anaerobic digestion of pulp and paper industry biosludge-long-term reactor performance and effects of thermal pretreatment. *Water Res.* 87, 105–111. doi:10.1016/j.watres.2015.08.053.
- Kokko, M., Koskue, V., Rintala, J., 2018. Anaerobic digestion of 30–100-year-old boreal lake sedimented fibre from the pulp industry: extrapolating methane production potential to a practical scale. *Water Res.* 133, 218–226. doi:10.1016/j.watres.2018.01.041.
- Libra, J.A., Ro, K.S., Kammann, C., Funke, A., Berge, N.D., Neubauer, Y., Titirici, M.M., Fühner, C., Bens, O., Kern, J., Emmerich, K.H., 2011. Hydrothermal carbonization of biomass residuals: a comparative review of the chemistry, processes and applications of wet and dry pyrolysis. *Biofuels* 2, 71–106. doi:10.4155/bfs.10.81.
- Liu, J., de Neergaard, A., Jensen, L.S., 2019. Increased retention of available nitrogen during thermal drying of solids of digested sewage sludge and manure by acid and zeolite addition. *Waste Manag.* 100, 306–317. doi:10.1016/j.wasman.2019.09.019.
- Marin-Batista, J.D., Mohedano, A.F., Rodríguez, J.J., de la Rubia, M.A., 2020. Energy and phosphorous recovery through hydrothermal carbonization of digested sewage sludge. *Waste Manag.* 105, 566–574. doi:10.1016/j.wasman.2020.03.004.
- Medina-Martos, E., Istrate, I.R., Villamil, J.A., Gálvez-Martos, J.L., Dufour, J., Mohedano, Á.F., 2020. Techno-economic and life cycle assessment of an integrated hydrothermal carbonization system for sewage sludge. *J. Clean. Prod.* 277. doi:10.1016/j.jclepro.2020.122930.
- Merzari, F., Goldfarb, J., Andreottola, G., Mimmo, T., Volpe, M., Fiori, L., 2020. Hydrothermal carbonization as a strategy for sewage sludge management: influence of process withdrawal point on hydrochar properties. *Energies* 13. doi:10.3390/en13112890.
- Paneque, M., De la Rosa, J.M., Kern, J., Reza, M.T., Knicker, H., 2017. Hydrothermal carbonization and pyrolysis of sewage sludges: what happen to carbon and nitrogen? *J. Anal. Appl. Pyrolysis* 128, 314–323. doi:10.1016/j.jaap.2017.09.019.
- Parmar, K.R., Ross, A.B., 2019. Integration of hydrothermal carbonisation with anaerobic digestion; opportunities for valorisation of digestate. *Energies* 12. doi:10.3390/en12091586.
- Qiao, W., Yan, X., Ye, J., Sun, Y., Wang, W., Zhang, Z., 2011. Evaluation of biogas production from different biomass wastes with/without hydrothermal pretreatment. *Renew. Energy* 36, 3313–3318. doi:10.1016/j.renene.2011.05.002.
- Radjenović, J., Petrović, M., Barceló, D., 2009. Fate and distribution of pharmaceuticals in wastewater and sewage sludge of the conventional activated sludge (CAS) and advanced membrane bioreactor (MBR) treatment. *Water Res.* 43, 831–841. doi:10.1016/j.watres.2008.11.043.
- Smith, A.M., Singh, S., Ross, A.B., 2016. Fate of inorganic material during hydrothermal carbonisation of biomass: influence of feedstock on combustion behaviour of hydrochar. *Fuel* 169, 135–145. doi:10.1016/j.fuel.2015.12.006.
- Sun, K., Ro, K., Guo, M., Novak, J., Mashayekhi, H., Xing, B., 2011. Sorption of bisphenol A, 17 $\alpha$ -ethynyl estradiol and phenanthrene on thermally and hydrothermally produced biochars. *Bioresour. Technol.* 102, 5757–5763. doi:10.1016/j.biortech.2011.03.038.

- vom Eyser, C., Palmu, K., Schmidt, T.C., Tuerk, J., 2015. Pharmaceutical load in sewage sludge and biochar produced by hydrothermal carbonization. *Sci. Total Environ.* 537, 180–186. doi:10.1016/j.scitotenv.2015.08.021.
- Wang, L., Chang, Y., Liu, Q., 2019. Fate and distribution of nutrients and heavy metals during hydrothermal carbonization of sewage sludge with implication to land application. *J. Clean. Prod.* 225, 972–983. doi:10.1016/j.jclepro.2019.03.347.
- Weiner, B., Baskyr, I., Poerschmann, J., Kopinke, F.D., 2013. Potential of the hydrothermal carbonization process for the degradation of organic pollutants. *Chemosphere* 92, 674–680. doi:10.1016/j.chemosphere.2013.03.047.
- Ylivainio, K., Turtola, E., 2016. Report on specifications of waste materials to be suitable for recycling. *Bonus Promise Deliv.* 3.2.
- Zhang, J.H., Lin, Q.M., Zhao, X.R., 2014. The hydrochar characters of municipal sewage sludge under different hydrothermal temperatures and durations. *J. Integr. Agric.* 13, 471–482. doi:10.1016/S2095-3119(13)60702-9.
- Zhang, Z., Ren, N., Li, Y.F., Kunisue, T., Gao, D., Kannan, K., 2011. Determination of benzotriazole and benzophenone UV filters in sediment and sewage sludge. *Environ. Sci. Technol.* 45, 3909–3916. doi:10.1021/es2004057.
- Zhuang, X., Zhan, H., Huang, Y., Song, Y., Yin, X., Wu, C., 2018. Conversion of industrial biowastes to clean solid fuels via hydrothermal carbonization (HTC): upgrading mechanism in relation to coalification process and combustion behavior. *Bioresour. Technol.* 267, 17–29. doi:10.1016/j.biortech.2018.07.002.



**Hydrothermal carbonisation of mechanically dewatered digested sewage sludge – Energy and nutrient recovery in centralized biogas plant – Supporting Information**

Anna Hämäläinen<sup>a</sup>, Marika Kokko<sup>a</sup>, Viljami Kinnunen<sup>b</sup>, Tuomo Hilli<sup>c</sup>, Jukka Rintala<sup>a</sup>

<sup>a</sup> Faculty of Engineering and Natural Sciences, Tampere University, P.O. Box 541, 33104 Tampere University, Finland

<sup>b</sup> Gasum Oy, Revontulenpuisto 2 C, 02100 Espoo, Finland

<sup>c</sup> Fifth Innovation Oy, Väinölänkatu 26, 33500 Tampere, Finland

## Materials and methods

The total phosphorous and other elements (Na, Al, Si, K, Ca, Cr, Fe, Ni, Cu, Zn, As, Cd, Pb, Hg) in both solid and liquid samples were determined with inductively coupled plasma mass spectrometry (ICP-MS) (Thermo Scientific iCAP™ RQ). The sample preparation for the ICP-MS analysis used microwave digestion (CEM Corporation MARS 6, Teflon vessels): solid sludge samples ( $m = 0.25$  g) or liquid filtrate samples ( $V = 0.5$  mL) underwent microwave digestion in a mixture of ultra-pure concentrated acids (5 mL of  $\text{HNO}_3$  and 5 mL of  $\text{H}_2\text{O}_2$ ) at 200 °C for 15 min. For the ICP-MS analysis, the sample solutions were diluted to 30 mL with Milli-Q water, and 50  $\mu\text{L}$  of each resulting solution was diluted in 4.95 mL of 2%  $\text{HNO}_3$ . The ICP-MS instrument was calibrated with the use of multielement standard solutions prepared from single element standard solutions. The multielement standard solutions for quantitative analysis were prepared in 2%  $\text{HNO}_3$  and contained (with the strongest standard solution): Si, Fe (10,000  $\mu\text{g/L}$ ), Al, P (5,000  $\mu\text{g/L}$ ), Pb (1,000  $\mu\text{g/L}$ ), K (500  $\mu\text{g/L}$ ), Ca, Cr, Ni, Cu, Zn, As, Cd, Au, and Bi (100  $\mu\text{g/L}$ ). The standard solutions were prepared using serial dilution. The single element standard stock solutions had a concentration of 1,000 ppm, except Na had a concentration of 50,000 ppm. Super pure chemicals (Romil-SpA™) and Milli-Q water (Merck Millipore) were used in the solution preparation. 103Rh was used as an internal standard in the ICP-MS analysis. Argon and helium functioned as the carrier and cell gas, respectively. The ICP-MS analyses were performed in kinetic energy discrimination mode.

The pharmaceutical analysis was ordered from Eurofins Environment Testing Finland Oy. For this analysis, hydrochar and filtrate samples from digestate treated at 230°C for 30 min were delivered. The digestate sample that represented the reference prior to the HTC treatment was centrifuged (1500 rpm for 20 minutes) to obtain two phases (liquid and solid) for the analysis.

## Calculations

The biomethane potentials were calculated as follows:

$$BMP \left( \frac{\text{mL CH}_4}{\text{g SCOD}} \right) = \frac{\text{Cumulative production (mL CH}_4\text{)}}{\text{substrate volume (g)} \cdot \text{SCOD} \left( \frac{\text{g}}{\text{L}} \right)} \quad (\text{S1})$$

The hydrochar yields (Y), energy densification ( $E_d$ ) and energy recovery of hydrochar were calculated as described previously (Danso-Boateng et al., 2015), where HHV is the higher heating value.

$$Yield (\%) = \frac{\text{mass of dry hydrochar}}{\text{mass of dry digestate}} \cdot 100 \quad (S2)$$

$$E_d = \frac{HHV_{\text{hydrochar}}}{HHV_{\text{digestate}}} c \quad (S3)$$

$$Energy\ recovery (\%) = Yield (\%) \cdot E_d \quad (S4)$$

The energy content and energy recoveries of the filtrates were calculated as follows:

$$Energy\ content (MJ\ l_{\text{filtrate}}^{-1}) = \varepsilon (MJ\ l^{-1}) \cdot BMP \cdot SCOD \quad (S5)$$

$$Energy\ recovery\ in\ filtrate (\%) = \frac{Energy\ content (MJ\ l_{\text{filtrate}}^{-1}) \cdot mass\ of\ filtrate}{HHV \cdot dry\ mass\ of\ digestate} \quad (S6)$$

where  $\varepsilon$  represents the energy density of methane (0.0378 MJ/L), BMP is given as L-CH<sub>4</sub>/kg-SCOD and SCOD as g/L.

The amount of digestate converted to gas during HTC treatment was calculated by the following difference:

$$Gas (g) = wet\ mass\ of\ digestate - (wet\ mass\ hydrochar + mass\ of\ filtrate) \quad (S7)$$

**Table S1.** Elemental concentrations in digestate and diluted digestate as well as in their respective hydrochars and filtrates from different HTC treatments compared to the statutory concentrations in sewage sludge originating soil amenders in EU and in Finland.

Sample	Na		K		Ca		Fe		Al		Cr		Ni	
	Hydrochar <sup>a</sup> (mg/g)	Filtrate (mg/L)	Hydrochar <sup>a</sup> (mg/g)	Filtrate (mg/L)	Hydrochar <sup>a</sup> (mg/g)	Filtrate (mg/L)	Hydrochar <sup>a</sup> (mg/g)	Filtrate (mg/L)	Hydrochar <sup>a</sup> (mg/g)	Filtrate (mg/L)	Hydrochar <sup>a</sup> (mg/g)	Filtrate (mg/L)	Hydrochar <sup>a</sup> (mg/g)	Filtrate (mg/L)
Max. permitted in EU <sup>b</sup> /Finland <sup>c</sup>	n.a.	n.a.	n.a.	n.a.	n.a.	n.a.	n.a.	n.a.	n.a.	n.a.	n.a./0.30	n.a.	0.3/0.10	n.a.
Digestate	4.25	n.d.	1.66	n.d.	24.380	n.d.	228.73	n.d.	9.490	n.d.	0.04	n.d.	0.03	n.d.
210°C for 30min	4.12	1.85	1.97	0.17	30.23	24.79	173.28	0.25	12.62	0.21	0.05	0.00	0.04	0.00
210°C for 120min	3.22	0.86	1.67	0.19	30.05	0.07	170.08	0.36	12.06	0.07	0.05	0.00	0.04	0.00
230°C for 30min	3.07	0.73	1.73	0.16	29.11	0.12	167.09	0.12	12.64	0.02	0.05	0.00	0.04	0.00
230°C for 120min	3.60	0.72	1.80	0.13	28.32	0.10	164.85	0.15	11.98	0.01	0.05	0.00	0.04	0.00
250°C for 30min	2.84	0.79	1.62	0.17	30.48	0.10	175.23	0.10	12.64	0.02	0.06	0.00	0.04	0.00
250°C for 120min	3.34	0.86	2.01	0.18	35.08	0.11	201.32	0.08	15.50	0.02	0.07	0.00	0.05	0.00
Diluted digestate	6.18	n.d.	2.37	n.d.	22.04	n.d.	184.00	n.d.	9.69	n.d.	0.04	n.d.	0.03	n.d.
210°C for 30min	4.20	0.59	2.03	0.11	29.68	0.08	171.29	0.18	12.67	0.03	0.05	0.00	0.04	0.00
210°C for 120min	3.00	0.61	1.46	0.14	23.29	0.36	132.58	2.57	9.62	0.16	0.04	0.00	0.03	0.00
230°C for 30min	4.08	0.69	1.93	0.13	31.93	0.09	181.56	0.12	13.13	0.02	0.06	0.00	0.04	0.00
230°C for 120min	3.62	0.73	1.99	0.15	30.79	0.06	176.68	0.12	13.43	0.03	0.06	0.00	0.04	0.00
250°C for 30min	3.93	0.72	1.78	0.13	29.02	0.08	168.29	0.08	12.15	0.01	0.06	0.00	0.04	0.00
250°C for 120min	3.26	8.70	1.85	0.19	31.54	0.08	182.30	0.08	13.50	0.02	0.06	0.00	0.04	0.00

<sup>a</sup> reported towards total solids, <sup>b</sup> 86/278/EEC, <sup>c</sup> Ylivainio and Turtola, 2016, n.d. not determined, n.a. not applicable

**Table S2.** Elemental concentrations in digestate and diluted digestate as well as in their respective hydrochars and filtrates from different HTC treatments compared to the statutory concentrations in sewage sludge originating soil amenders in EU and in Finland.

Sample	Cu		Zn		As		Cd		Au		Pb		Hg	
	Hydrochar <sup>a</sup> (mg/g)	Filtrate (mg/L)	Hydrochar <sup>a</sup> (mg/g)	Filtrate (mg/L)	Hydrochar <sup>a</sup> (mg/g)	Filtrate (mg/L)	Hydrochar <sup>a</sup> (mg/g)	Filtrate (mg/L)	Hydrochar <sup>a</sup> (mg/g)	Filtrate (mg/L)	Hydrochar <sup>a</sup> (mg/g)	Filtrate (mg/L)	Hydrochar <sup>a</sup> (mg/g)	Filtrate (mg/L)
Max. permitted in EU <sup>b</sup> /Finland <sup>c</sup>	1.0-1.75/0.60	n.a.	2.5-4.0/1.50	n.a.	n.a./0.025	n.a.	0.02-0.04/0.0015	n.a.	n.a.	n.a.	0.75/0.10	n.a.	0.016-0.025/0.001	n.a.
Digestate	0.41	n.d.	0.41	n.d.	0.008	n.d.	0.001	n.d.	0.000	n.d.	0.027	n.d.	0.022	n.d.
210°C for 30min	0.47	0.01	0.93	0.01	0.011	0.001	0.001	0.000	0.001	0.000	0.027	0.002	0.024	0.000
210°C for 120min	0.52	0.00	0.95	0.01	0.010	0.000	0.001	0.000	0.001	0.000	0.029	0.000	0.025	0.000
230°C for 30min	0.49	0.00	0.96	0.01	0.011	0.000	0.001	0.000	0.000	0.000	0.029	0.000	0.026	0.000
230°C for 120min	0.48	0.00	0.95	0.00	0.011	0.000	0.001	0.000	0.000	0.000	0.030	0.000	0.025	0.000
250°C for 30min	0.52	0.00	1.01	0.00	0.011	0.000	0.002	0.000	0.000	0.000	0.032	0.000	0.028	0.000
250°C for 120min	0.61	0.00	1.17	0.00	0.013	0.000	0.001	0.000	0.000	0.000	0.037	0.000	0.032	0.000
Diluted digestate	0.38	n.d.	0.38	n.d.	0.009	n.d.	0.001	n.d.	0.000	n.d.	0.028	n.d.	0.021	n.d.
210°C for 30min	0.55	0.00	1.01	0.00	0.011	0.000	0.001	0.000	0.001	0.000	0.033	0.000	0.026	0.000
210°C for 120min	0.37	0.01	0.77	0.01	0.008	0.000	0.001	0.000	0.001	0.000	0.024	0.000	0.020	0.000
230°C for 30min	0.55	0.00	1.06	0.01	0.012	0.000	0.001	0.000	0.000	0.000	0.035	0.000	0.028	0.000
230°C for 120min	0.59	0.00	1.07	0.00	0.012	0.000	0.001	0.000	0.000	0.000	0.032	0.000	0.028	0.000
250°C for 30min	0.50	0.00	0.97	0.00	0.011	0.000	0.001	0.000	0.000	0.000	0.031	0.000	0.027	0.000
250°C for 120min	0.54	0.00	1.05	0.01	0.012	0.000	0.001	0.000	0.000	0.000	0.034	0.000	0.028	0.000

<sup>a</sup> reported towards total solids, <sup>b</sup> 86/278/EEC, <sup>c</sup> Ylivainio and Turtola, 2016, n.d. not determined, n.a. not applicable

**Table S3.** Pharmaceuticals analysed from digested sewage sludge and digestate filtrate before and hydrochar and filtrate after the HTC treatment at 230°C for 30 minutes.

Analysed compound	Solid phase		Liquid phase	
	Before HTC	After HTC	Before HTC	After HTC
	mg/kg-TS		µg/L	
<i>Hormones</i>				
Estrone	0.15	<0.050	0	0
Progesterone	0.1	<0.050	0	0
<i>Pharmaceuticals</i>				
Benzotriazole	0	0	<20	330
Bisoprolol (β-Adrenergics)	0.11	<0.050	2.2	<1.0
Diclofenac	0.24	<0.050	5.4	<0.50
Doxycycline	0.93	<0.050	0	0
Fenbendazole	0.11	<0.050	1.2	<0.50
Fluoxetine	0.045	<0.050	0	0
Hydrocortisone	0.3	<0.50	0	0
Ibuprofen	0	0	<50	230
Carbamazepine	0.086	<0.50	0	0
Quetiapine	0	0	2	<0.50
Ketoconazole	0	0	4	<1.0
Clozapine	0	0	6.1	<0.50
Caffeine	0.15	<0.050	0	0
Lamotrigine	0	0	5	<0.50
Losartan	0	0	11	<0.50
Metoprolol	0.23	<0.050	2.5	<0.50
Mirtazapine	0	0	1	<5.0
Ofloxacin	1.2	<0.50	0	0
Propranolol	0.098	<0.050	1	<1.0
Sertraline and nortsertraline	0	0	8.1	<5.0
Cetirizine	0	0	3.2	<5.0
Ciprofloxacin	3.8	<0.50	20	<50
Citalopram	0.39	<0.050	0	0
Tetracycline	2.4	<0.050	8	<10

## References

Danso-Boateng, E., Shama, G., Wheatley, A.D., Martin, S.J., Holdich, R.G., 2015. Hydrothermal carbonisation of sewage sludge: Effect of process conditions on product characteristics and methane production. *Bioresour. Technol.* 177, 318–327.

Ylivainio, K., Turtola, E., 2016. Report on specifications of waste materials to be suitable for recycling. Bonus Promise Deliv. 3.2.





**PUBLICATION**  
**II**

**Hydrothermal carbonization of pulp and paper industry wastewater  
treatment sludges—characterization and potential use of hydrochars and  
filtrates**

Anna Hämäläinen, Marika Kokko, Viljami Kinnunen, Tuomi Hilli & Jukka Rintala

Bioresource Technology, 355, 127158  
<https://doi.org/10.1016/j.biortech.2022.127258>

**Publication reprinted with the permission of the copyright holders.**





## Hydrothermal carbonization of pulp and paper industry wastewater treatment sludges - characterization and potential use of hydrochars and filtrates

Anna Hämäläinen<sup>a,\*</sup>, Marika Kokko<sup>a</sup>, Viljami Kinnunen<sup>b</sup>, Tuomo Hilli<sup>c</sup>, Jukka Rintala<sup>a</sup>

<sup>a</sup> Faculty of Engineering and Natural Sciences, Tampere University, P.O.Box 541, 33104 Tampere University, Finland

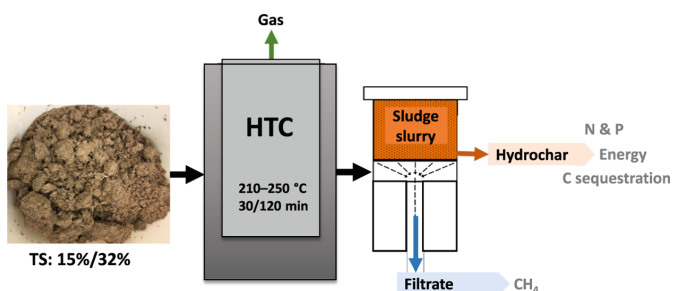
<sup>b</sup> Gasum Oy, Revontulenpuisto 2C, 02100, Espoo, Finland

<sup>c</sup> Fifth Innovation Oy, Väinöläkatu 26, 33500, Tampere, Finland

### HIGHLIGHTS

- Mixed sludge from pulp and paper mill wastewater treatment was treated with HTC.
- HTC enhanced energy recovery in hydrochars having 37% increased heating value.
- No significant sludge dewaterability improvement was observed after HTC.
- HTC increased filtrate organics content and volumetric methane production potential.
- Mixed sludge hydrochars are potential for carbon sequestration.

### GRAPHICAL ABSTRACT



### ARTICLE INFO

#### Keywords:

Pulp and paper mixed sludge  
Hydrothermal carbonization  
Energy recovery  
Anaerobic digestion  
Carbon sequestration

### ABSTRACT

The pulp and paper industry's mixed sludge represents waste streams with few other means of disposal than incineration. Hydrothermal carbonization (HTC) could be advantageous for the sludge refinement into value-added products, thus complementing the concept of pulp and paper mills as biorefineries. Laboratory HTC was performed on mixed sludge (at 32% and 15% total solids) at temperatures of 210–250 °C for 30 or 120 min, and the characteristics of the HTC products were evaluated for their potential for energy, carbon, and nutrient recovery. The energy content increased from 14.9 MJ/kg in the mixed sludge up to 20.5 MJ/kg in the hydrochars. The produced filtrates had 12–15-fold higher COD and 3–5-fold higher volumetric methane production than untreated sludge filtrates, even though the methane yield against g-COD was lower. The increased value of the hydrochars in terms of energy content and carbon sequestration potential promote HTC deployment in sludge treatment and upgrading.

\* Corresponding author.

E-mail address: [anna.hamalainen@tuni.fi](mailto:anna.hamalainen@tuni.fi) (A. Hämäläinen).

<https://doi.org/10.1016/j.biortech.2022.127258>

Received 25 March 2022; Received in revised form 28 April 2022; Accepted 30 April 2022

Available online 5 May 2022

0960-8524/© 2022 The Authors. Published by Elsevier Ltd. This is an open access article under the CC BY license (<http://creativecommons.org/licenses/by/4.0/>).

## 1. Introduction

Global pulp and paper manufacturing uses, in addition to various wood and other plant materials, plenty of water and chemicals in different production processes. Thus, the industry generates large volumes of wastewaters with different compositions and with relatively high biological and chemical oxygen demand (BOD and COD) concentrations (several g/L), wood debris, and soluble wood material, as well as chemical residues (Faubert et al., 2016). This wastewater is commonly treated through primary sedimentation and biological treatments in an activated sludge process at the mill, producing mixed sludge that consists of primary and secondary sludge. Primary sludge contains wood fibers, papermaking fillers, pitch, and by-products of lignin, whereas secondary sludge is mostly composed of microbial mass and non-biodegradable lignin (Faubert et al., 2016). Due to the high organic carbon content of the sludge (approximately 50 %TS), its presence in landfill may cause leaching and greenhouse gas production, and thus is not permitted by the European Union Waste Framework Directive (2008/98/EC), which has prompted sludge incineration for energy recovery. However, incineration of high-water-content sludges necessitates efficient mechanical and thermal dewatering, which can account for more than half of the wastewater treatment costs at pulp and paper mills because of the difficulty of dewatering the secondary sludge, which contains extra-cellular polymeric substances (Meyer et al., 2018). Thus, direct incineration is not considered economically feasible. The development of mixed sludge utilization is recommended for the current aim of introducing the concept of biorefinery into pulp and paper industry mills, including, for example, bioprocesses, such as anaerobic digestion (AD) and fermentation, and thermal processes, such as pyrolysis and hydrothermal carbonization (HTC), which represent solutions to produce energy from waste sludge (Gottumukkala et al., 2016).

HTC has attracted interest in several fields for its potential role in the refining of various raw biomasses (Pecchi and Baratieri, 2019) as well as in the management of the sludge (Ahmed et al., 2021; Lin et al., 2015) as it allows the use of moist biomass as feedstock, reducing the need for dewatering. HTC is conducted at moderate temperatures (200–300 °C), and pressure is autogenously generated (Fang et al., 2018), which enables the water contained in the sludge to function as a solvent, reactant, or even a catalyst during the treatment (Mäkelä et al., 2015). HTC generates three product components: (i) a solid hydrochar that can be further deployed in energy generation, in soil for nutrient recovery and carbon sequestration, in removal of heavy metals and pesticides from water, and in improving the outcome of composting and fermentation (Sun et al., 2020); (ii) a liquid product (referred to here as a filtrate) from which nutrients can be extracted for recovery; and (iii) a gas comprising mainly of CO<sub>2</sub> (Aragón-Briceño et al., 2021). Hence, by refining sludge into value-added products, HTC could potentially be incorporated into the concept of biorefinery in the pulp and paper industry. In practice, the deployment of HTC should be considered on a case-by-case basis, depending on the existing local infrastructures, such as power plants and their feedstocks, as well as on the logistics for hydrochar transportation. Also, any existing wastewater treatment facility at the mill or locally could be engaged in the filtrate treatment. The utilization alternatives for hydrochar and filtrate should be considered based on the local targets for renewable energy and carbon sequestration, taking into account also other political and environmental objectives.

Studies on the use of HTC for lignocellulosic biomass have mostly focused on virgin materials and agricultural or food waste (Fang et al., 2018; Pecchi and Baratieri, 2019), and little attention has been paid to lignocellulosic pulp and paper waste sludges. The few published studies on the HTC of pulp and paper industry sludges have only considered the energy content and fuel properties of hydrochar (Martinez et al., 2021; Saha et al., 2019; Wang et al., 2021). However, because of the increasing need of nutrient recycling, carbon sequestration and of the large volumes of mixed sludge generated, mixed sludge hydrochar's role as a nutrient and carbon source should also be examined simultaneously

with energy recovery. Furthermore, the value of the extracted filtrate should be further delineated, such as in AD for increasing methane recovery and subsequent nitrogen recovery by stripping, as previous studies have only considered the use of filtrate as diluent for HTC feed. (Areeprasert et al., 2014; Kabadayi Catalkopru et al., 2017; Mäkelä et al., 2018).

After HTC treatment, the treated sludge is separated into hydrochar and filtrate, usually by filtration, an essential part of the HTC process. However, the existing studies have not compared the effects of HTC to mere filtration of the sludge. The studies on HTC have been promising improving sludge dewaterability and the utilization of moist waste for energy recovery (Areeprasert et al., 2014; Mäkelä and Yoshikawa, 2016). However, as there are only few studies on HTC treatment of pulp and paper industry sludges, it would be necessary to study the matter more comprehensively to determine, whether the whole HTC process can bring additional value to sludge utilization. HTC deployment in pulp and paper could reduce sludge volume and improve its applicability as a hydrochar in carbon sequestration, energy recovery, or nutrient recovery, and as a filtrate in the generation of renewable energy.

The objective of this study was to evaluate the potential role of HTC in pulp and paper industry sludge management and the process of upgrading to value-added products. To test the capability of HTC in decreasing the volume of mixed sludge and simultaneously increasing its energy content and land applicability, HTC was performed at laboratory scale using a mechanically dewatered mixed sludge at two dilutions of 32% and 15% total solids (TS) at temperatures of 210–250 °C and residence times of 30 and 120 min. A pilot filtration process was applied to induce the HTC-treated sludge to produce hydrochar and filtrate, and as a reference, filtration alone was used to produce sludge cake and cake filtrate. The generated hydrochar and filtrate products were characterized, and their potential uses were assessed.

## 2. Materials and methods

### 2.1. Sludge and inoculum

The pulp and paper industry sludge for the HTC treatment experiments was a mixture of primary and secondary sludge (referred to as a mixed sludge) from the activated sludge process used in treating wastewater from pulp-and-paper mill integration (Finland), which uses wood as a raw material and both kraft and mechanical pulping processes. The sludge had been mechanically dewatered at the mill. For the biochemical methane potential (BMP) assays, granular sludge (7.4% TS, 6.8% VS) from a mesophilic upflow anaerobic sludge blanket (UASB) reactor treating industrial wastewater was used as an inoculum (Jokioinen, Finland; Singh et al., 2019). All sludges were stored at 4 °C for 1–2 months until used.

For the HTC treatments, the mixed sludge was used as received, with 32% TS and as diluted with tap water to 15% TS (referred to as diluted mixed sludge). Sludge dilution to 15% TS was conducted right before the HTC treatment by adding 530 ml of tap water to 470 g of mixed sludge (32% TS). Mixed sludge characteristics are shown in Tables 1 and 2.

### 2.2. HTC treatments

The HTC treatments were conducted in a two-liter Parr® 4500 pressure reactor with an external circulating water cooling system (see supplementary material), as previously described in detail (Hämäläinen et al., 2021). The wet weight of the input sludge for the experiments was 700 g for mixed sludge (32% TS) and 1 kg for diluted mixed sludge (15% TS); the weight difference between them was due to the difference in their density, as only 700 g of mixed sludge was enough to fill the working volume (1 L) of the reactor. The treatment temperatures were 210 °C, 230 °C, and 250 °C with residence times of 30 or 120 min. Each treatment had one replicate and the sludges were not mixed during the HTC treatments due to their fibrous texture.

**Table 1**

The CHNS-analysis results, computational oxygen contents and phosphorous concentrations in the mixed sludge cakes and in their respective hydrochars. The results are averages of 2 replicates.

Sample	C (% TS)	H (% TS)	N (% TS)	S (% TS)	O <sup>c</sup> (% TS)	P (% TS)
Mixed sludge	42.4 ± 0.1	5.8 ± 0.02	1.2 ± 0.04	0.4 ± 0.03	50.2 ± 0.2	0.4
Mixed sludge cake	42.6 ± 0.2	5.8 ± 0.00	1.3 ± 0.06	0.4 ± 0.04	49.9 ± 0.3	0.2
<i>Mixed sludge hydrochars</i>						
210 °C for 30 min	46.1 ± 0.7	5.7 ± 0.01	1.1 ± 0.1	0.4 ± 0.0	46.7 ± 0.8	0.5
210 °C for 120 min	48.7 ± 0.4	5.6 ± 0.01	1.6 ± 0.05	0.4 ± 0.02	43.6 ± 0.4	0.4
230 °C for 30 min	49.2 ± 0.5	5.7 ± 0.02	1.5 ± 0.05	0.4 ± 0.03	43.3 ± 0.6	0.3
230 °C for 120 min	52.4 ± 0.3	5.6 ± 0.02	1.6 ± 0.02	0.5 ± 0.01	39.9 ± 0.3	0.3
250 °C for 30 min	52.4 ± 0.7	5.4 ± 0.02	1.5 ± 0.07	0.5 ± 0.01	40.2 ± 0.8	0.5
250 °C for 120 min <sup>a</sup>	55.5 ± 1.0	5.1 ± 0.04	1.6 ± 0.06	0.5 ± 0.04	37.3 ± 1.0	0.6
Diluted mixed sludge <sup>b</sup>	42.4 ± 0.2	5.8 ± 0.03	1.2 ± 0.05	0.4 ± 0.04	50.2 ± 0.2	0.3
Diluted mixed sludge cake	42.6 ± 0.2	5.8 ± 0.01	1.7 ± 0.08	0.5 ± 0.04	49.4 ± 0.3	0.3
<i>Diluted mixed sludge hydrochars</i>						
210 °C for 30 min	46.1 ± 0.5	5.8 ± 0.06	0.9 ± 0.01	0.3 ± 0.02	47.0 ± 0.6	0.3
210 °C for 120 min	47.6 ± 0.1	5.7 ± 0.08	1.2 ± 0.05	0.3 ± 0.00	45.2 ± 0.8	0.4
230 °C for 30 min	47.5 ± 0.4	5.8 ± 0.07	1.1 ± 0.03	0.3 ± 0.01	45.4 ± 0.5	0.3
230 °C for 120 min	50.6 ± 0.1	5.6 ± 0.01	1.3 ± 0.02	0.3 ± 0.01	42.2 ± 0.1	0.4
250 °C for 30 min	53.0 ± 0.1	5.6 ± 0.01	1.5 ± 0.04	0.4 ± 0.01	39.6 ± 0.1	0.7
250 °C for 120 min	56.8 ± 0.3	5.2 ± 0.02	1.8 ± 0.01	0.4 ± 0.01	35.8 ± 0.3	0.7

TS: total solids

<sup>a</sup> failed HTC-treatment and sample recovery

<sup>b</sup> computational CHNS-analysis

<sup>c</sup> calculated as difference between 100 and total sum of C, H, N and S on TS basis

The reactor vessel achieved the target temperatures within approximately 70–95 min. The temperature was manually adjusted using Parr® 4848 reactor controllers and held at the target temperature for the pre-set residence time. Above 100 °C, the vessel pressure increased from atmospheric pressure up to 20–40 bar, depending on the applied temperature. The realized temperatures fluctuated but remained within ± 8 °C from the target temperature. The 250 °C runs were started when the vessel temperature had reached 245 °C because of difficulties in attaining the targeted temperature within 90 min. Part of the generated gases was released at the end of the treatment to speed up cooling. Cooling the sludge to 50 ± 6 °C by water circulation took around 30–40 min, after which the HTC-treated sludges were recovered from the vessel, weighed, and stored at 4 °C prior to their filtration.

Filtrations of the HTC-treated sludges and of the original mixed and diluted mixed sludges as a reference were performed using a small-scale pressurized filtration unit at 60 °C (see supplementary material). The solid and liquid products are referred to as hydrochar and HTC filtrate, respectively, while the reference products of the original sludges are referred to as the cake and cake filtrate. The filtration procedure is described in detail in Hämäläinen et al. (2021). In mass balance calculations, both the weight of the hydrochar as well as the TS content of the

hydrochar are considered.

### 2.3. Biochemical methane potential assays

The BMPs of the HTC and cake filtrates were determined in mesophilic (35 °C), static, 30-day long batch assays in triplicate. The assays were assembled in 120 ml serum bottles with a liquid volume of 64 ml, containing 1.7 g of inoculum (1.75 g-VS/L), the filtrate sample in final concentration of 1.75 g of soluble chemical oxygen demand (SCOD) per liter, NaHCO<sub>3</sub> (4 g/L) as a buffer, and distilled water to reach the liquid volume. The initial pH was adjusted to between 7 and 8 with HCl (1 M), after which the bottles were closed with rubber stoppers and flushed with nitrogen gas for around 3 min. As control assays, bottles containing only inoculum, water, and buffer were prepared to subtract inoculum's methane production from the methane production of the sample assays. The methane concentrations in the BMP assays were measured with a GC-FID (Perkin Elmer Clarus) and calculated as described previously (Hämäläinen et al., 2021; Kinnunen et al., 2015).

### 2.4. Chemical analysis and calculations

The TS (referred to also as dry solids) and VS were gravimetrically determined according to the standard APHA 2540 method. The ash content measurements at 550 °C followed the same gravimetric principle. The pH was measured with a WTW pH 3210 m using a WTW SenTix® 41 electrode. Then, COD and SCOD were analyzed according to Finnish standard methods (SFS 5504). Volatile fatty acids (VFA) were determined with GC-FID, as described previously (Kokko et al., 2018). For the VFA and SCOD analyses, samples were filtered through a 0.45 µm filter (Chromafil Xtra PET). The total nitrogen and soluble ammonium-nitrogen in the filtrates were analyzed using Hach Lange kits (LCK 238, LCK 338, LCK 305, and LCK 303) according to the company instructions. The other cations in the filtrates were analyzed according to the ion chromatography standard SFS-EN ISO 10304-1 using an ion chromatograph (Dionex DX-120, USA) with an AS40 autosampler, Ion-Pac CS12A cation exchange column, and CSRS 300 suppressor (4 mm). The eluent contained 2 mM methane sulphonic acid, and the flow rate was 1 ml/min.

The total carbon, hydrogen, nitrogen, and sulphur concentrations of the mixed sludges, hydrochars, and cakes (Table 1) were determined by elemental analysis in a Thermo Scientific FlashSmart Elemental Analyzer (CHNS/O) with thermal conductivity detector (TCD), before which dried samples (dried overnight at 105 °C) were homogenized by grinding them with mortar into a fine powder. The sample size for CHNS analysis was 2–3 mg, weighed on a microgram balance (Mettler Toledo WXTS Microbalance) in tin cups. BBOT-standard (2,5-Bis[5-*tert*-butyl-2-benzo-oxazol-2-yl]) provided by Thermo Fisher Scientific was used for calibration. Helium was used as a carrier gas and oxygen to oxidize the sample. The other elements in the hydrochars, cakes, and filtrates were determined with inductively coupled plasma mass spectrometry (Hämäläinen et al., 2021). The higher heating values (HHV) of the hydrochars and cakes were determined in duplicate according to the ISO 1928 standard with a Parr® 6725 Semi-Micro Oxygen Bomb Calorimeter. For this analysis, the sample size (dried at 105 °C overnight) was 0.2–0.3 g. All the chemicals used in the analyses were of analytical grade.

The sludge mass converted to gas in the HTC treatment was computationally obtained from the difference in the masses of the input sludge and the obtained hydrochar and filtrate after HTC.

The parameters used for assessing the energy properties of mixed sludges, cakes, and hydrochars in Table 2 were calculated as presented in Equations (1)–(4). Solid yield (Eq. (1)) on a dry ash-free basis describes the recovered amount of solid fraction (cake or hydrochar) without ash from the mixed sludge without ash (Mäkelä et al., 2015). Similarly, energy yield (Eq. (2)) represents the amount of recovered energy from the original sludge. The energy densification (Eq. (3))

**Table 2**  
Solid fuel properties of the mixed sludge (32% TS) and diluted mixed sludge (15% TS) and of their respective cakes and hydrochars.

Sample	TS (%)	VS (%)	VS/TS (%)	Ash 550 °C (%)	HHV (MJ/kg TS)	Solid yield (% daf)	Energy yield (%)	Energy densification (daf)	Carbon content (% daf)
Mixed sludge	32.1 ± 0.8	28.0 ± 0.6	87	12.7 ± 0.4	14.9 ± 0.02	n.a.	n.a.	n.a.	48.6 ± 0.1
Mixed sludge cake	49.7 ± 1.0	43.8 ± 0.8	88	11.9 ± 0.04	15.0 ± 0.01	95.2 ± 4.8	48.99 ± 2.6	1.00 ± 0.00	48.4 ± 0.2
<i>Mixed sludge hydrochars</i>									
210 °C for 30 min	46.64 ± 1.1	40.7 ± 1.0	87	12.7 ± 0.2	16.0 ± 0.4	93.0 ± 1.1	99.50 ± 1.3	1.08 ± 0.00	52.8 ± 0.7
210 °C for 120 min	50.24 ± 1.4	43.8 ± 1.2	87	12.8 ± 0.05	16.0 ± 0.1	88.1 ± 1.5	94.24 ± 1.9	1.08 ± 0.00	55.9 ± 0.5
230 °C for 30 min	47.39 ± 0.2	40.9 ± 0.2	86	13.8 ± 0.02	16.7 ± 0.2	87.4 ± 2.5	97.96 ± 3.1	1.14 ± 0.00	57.1 ± 0.6
230 °C for 120 min	52.16 ± 5.0	46.6 ± 0.7	89	15.3 ± 0.1	17.9 ± 0.8	79.7 ± 5.0	95.68 ± 6.3	1.24 ± 0.00	61.9 ± 0.4
250 °C for 30 min	54.34 ± 5.7	45.9 ± 5.0	84	15.5 ± 0.4	20.1 ± 0.1	73.5 ± 3.6	98.85 ± 5.1	1.40 ± 0.01	62.0 ± 0.6
250 °C for 120 min <sup>a</sup>	49.07 ± 7.5	36.1 ± 4.3	74	19.7 ± 2.0	20.4 ± 0.1	51.6 ± 3.4	70.52 ± 10.1	1.49 ± 0.04	69.1 ± 1.3
Diluted mixed sludge	15.5 ± 1.2	13.5 ± 1.0	87	12.8 ± 0.3	14.9 ± 0.02	n.a.	n.a.	n.a.	48.6 ± 0.2
Diluted mixed sludge cake	49.0 ± 1.5	43.0 ± 1.7	88	12.2 ± 0.7	15.0 ± 0.1	95.4 ± 0.8	67.05 ± 0.5	1.00 ± 0.00	48.6 ± 0.6
<i>Diluted mixed sludge hydrochars</i>									
210 °C for 30 min	48.21 ± 1.3	42.4 ± 1.1	88	12.0 ± 0.2	16.1 ± 0.02	93.2 ± 3.7	98.01 ± 4.2	1.08 ± 0.00	52.3 ± 0.6
210 °C for 120 min	47.63 ± 0.6	41.7 ± 0.6	88	12.5 ± 0.2	16.6 ± 0.2	85.0 ± 3.3	91.88 ± 4.0	1.11 ± 0.00	54.4 ± 0.2
230 °C for 30 min	48.08 ± 0.7	41.7 ± 0.6	87	13.2 ± 0.1	16.5 ± 0.03	86.3 ± 1.4	92.52 ± 1.7	1.11 ± 0.00	54.7 ± 0.4
230 °C for 120 min	46.81 ± 0.8	39.6 ± 0.7	85	15.5 ± 0.1	18.1 ± 0.01	64.0 ± 2.3	75.48 ± 2.6	1.26 ± 0.00	59.9 ± 0.2
250 °C for 30 min	47.84 ± 0.3	40.1 ± 0.3	84	16.1 ± 0.1	18.8 ± 0.1	66.9 ± 2.5	82.07 ± 3.0	1.32 ± 0.00	63.2 ± 0.2
250 °C for 120 min	45.38 ± 0.2	36.5 ± 0.1	80	19.6 ± 0.2	20.5 ± 0.1	48.4 ± 1.6	64.57 ± 2.1	1.49 ± 0.00	70.7 ± 0.2

TS: total solids, VS: volatile solids, HHV: higher heating value, daf: dry ash free  
<sup>a</sup> failed HTC-treatment and sample recovery, n.a.: not applicable

describes how energy is concentrated in the hydrochar and cake relative to the mixed sludge and is calculated by relating their HHVs.

$$\text{Solid yield}(\%, \text{daf}) = \frac{m_{\text{product}}}{m_{\text{sludge}}} \cdot \frac{\left(1 - \frac{\text{ash}_{\text{product}}}{100}\right)}{\left(1 - \frac{\text{ash}_{\text{sludge}}}{100}\right)} \cdot 100\% \quad (1)$$

$$\text{Energy yield}(\%) = \frac{m_{\text{product}}}{m_{\text{sludge}}} \cdot \frac{\text{HHV}_{\text{product}}}{\text{HHV}_{\text{sludge}}} \cdot 100\% \quad (2)$$

$$\text{Energy densification (daf)} = \frac{\text{HHV}_{\text{product}}}{\text{HHV}_{\text{sludge}}} \cdot \frac{\left(1 - \frac{\text{ash}_{\text{product}}}{100}\right)}{\left(1 - \frac{\text{ash}_{\text{sludge}}}{100}\right)} \quad (3)$$

where *daf* signifies dry ash-free, *m* dry (overnight at 105 °C, equals TS) sample mass (kg), and *product* stands for either hydrochar or cake. The ash-free carbon content, and O/C and H/C -ratios were calculated as follows in Equations (4), 5 and 6:

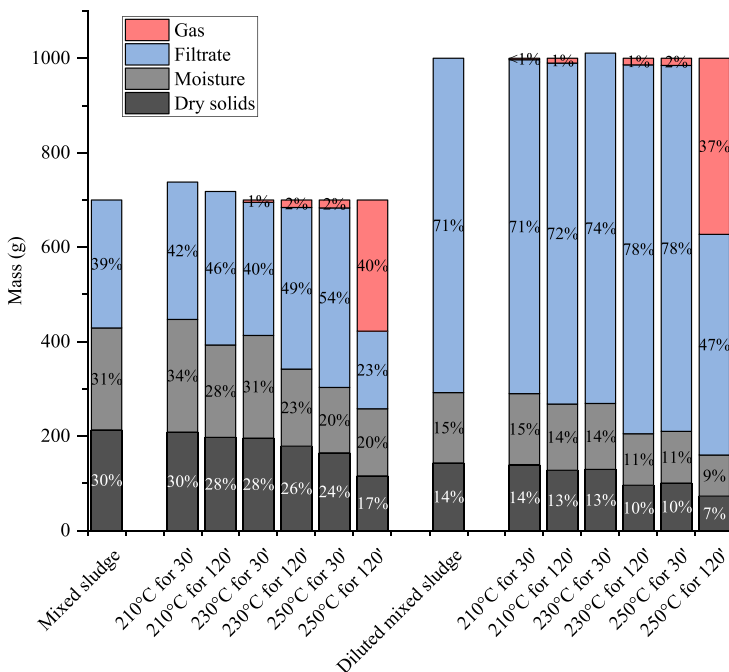


**Fig. 1.** The mass distribution of the mixed sludge and diluted mixed sludge after filtration (=cakes) as well as after the HTC treatment followed by filtration (hydrochars). The masses of the cakes and hydrochars are divided into dry solids (TS) and the remaining moisture content. The amount of mixed sludge fed to the HTC was 700 g and that of diluted mixed sludge 1000 g.

$$\text{Carbon content (\%, daf)} = \frac{C_{\text{sample}}}{1 - \frac{\text{ash}}{100}} \quad (4)$$

where  $C$  denotes sample total carbon content (%), respectively and  $\text{sample}$  denotes either mixed sludge, diluted mixed sludge, cake, or hydrochar.

When comparing the SCOD and TVFA concentrations of the mixed sludge and diluted mixed sludge filtrates, a computational factor was used to consider the addition of water used for dilution in diluted mixed sludge samples. Thus, the diluted mixed sludge filtrate SCOD and VFA concentrations were obtained with Eq. (5).

$$\text{Concentration as undiluted} = \frac{c \cdot V_{\text{HTC filtrate}}}{V_{\text{HTC filtrate}} + V_{\text{cake filtrate}} - V_{\text{water added}}} \quad (5)$$

where  $c$  denotes concentration (SCOD or VFA) and  $V$  volume.

### 3. Results and discussion

#### 3.1. Mass distribution

The mass distribution of the mixed sludges after filtration or after HTC and filtration is shown in Fig. 1. HTC treatments had an effect on the mass distribution by altering hydrochar composition (dry solids and moisture) and HTC filtrate shares relative to filtration alone, except at the mildest HTC conditions (Fig. 1). The mass of the hydrochars decreased (from 61% to 37% and from 29% to 16%) and those of the filtrates increased (from 39% to 54% and from 71% to 78%) from the masses of cake and filtrate, and mixed and diluted mixed sludge, respectively, due to the HTC treatment (Fig. 1). Based on the mass distribution after the HTC treatments (Fig. 1), the amount of gas generated was small (less than 2%) in all HTC treatments for both sludges, except in

the most severe HTC conditions (37%–40% of the initial mass), indicating the dissolved solids were mainly recovered in the filtrate. Overall, the effects of HTC treatment on the relative mass distribution into the hydrochar and gas fractions seemed independent of the initial mixed sludge TS content (Fig. 1).

The cakes had ash-free solid yields of 95%, implying that filtration alone extracted only a small part of the dry ash-free (DAF) solids into the cake filtrate (Table 2). The hydrochars' ash-free solid yields were 51.6%–93.0% for mixed sludge and 48.4%–93.2% for diluted mixed sludge and decreased with increasing treatment severity (Table 2), which indicates that after both the HTC treatments and filtration, the amount of dissolved (and at 250 °C, evaporated) dry ash-free solids were up to 51.6% of the input solids. The TS content of the cakes was 49–50% and the VS content 43–44%, which was similar to or higher than in the mixed sludge and diluted mixed sludge hydrochar, in which the TS content was 46%–54% and 45%–48% and the VS content 36%–47% and 36%–42%, respectively (Table 2). The VS/TS ratios of the hydrochars and cakes (0.80–0.88) were similar to or slightly lower than in the mixed and diluted mixed sludges (0.88).

The hydrochar total masses (including both dry solids and moisture) were reduced only 1–1.8-fold after filtration relative to the cake total masses (Fig. 1), implying the dewaterability of the mixed and diluted mixed sludge with the applied filtration unit was only slightly improved after HTC. Only after the severest treatments (250 °C, 120 min), could major improvements in dewaterability be estimated (1.65–1.8-fold reductions). HTC has been reported to improve the dewaterability of sewage sludge by attaining a 5-fold decrease in the masses of sewage sludge hydrochars relative to the untreated filter-cakes of sewage sludge at HTC temperatures of 195 °C and 240 °C (Saveyn et al., 2009). The dewaterability improvement in sewage sludge was also observed as higher TS (50%) and lower VS/TS (30%–40%) content in the hydrochars after filtration (piston filter press, 400 kPa, 1000 s with cationic polymer

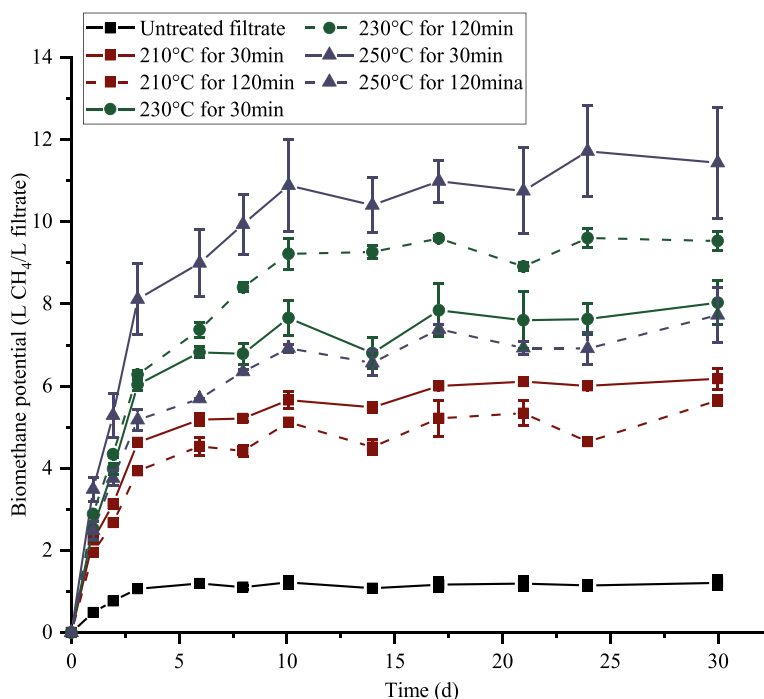


Fig. 2. Biomethane potentials of the mixed sludge cake filtrate (untreated filtrate) and HTC cake filtrates of mixed sludge (TS 32%) from different HTC conditions. The methane production of the inoculum has been subtracted from the results.

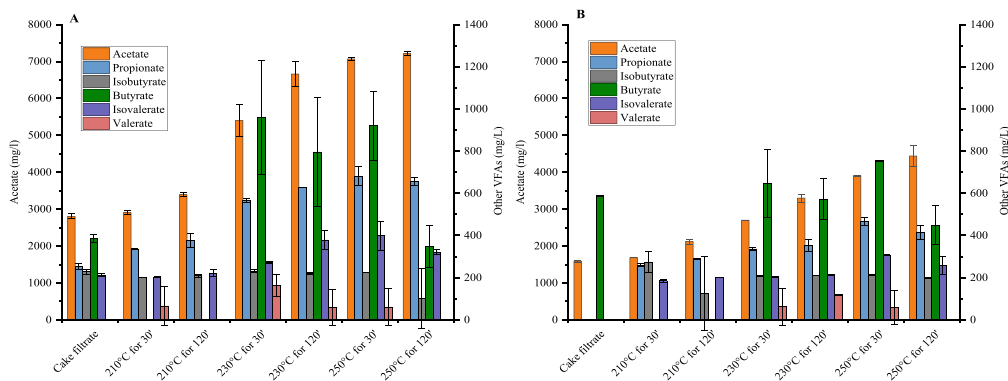


Fig. 3. The volatile fatty acid (VFA) profiles in the cake filtrates and HTC filtrates obtained from mixed sludge (A) or diluted mixed sludge (B).

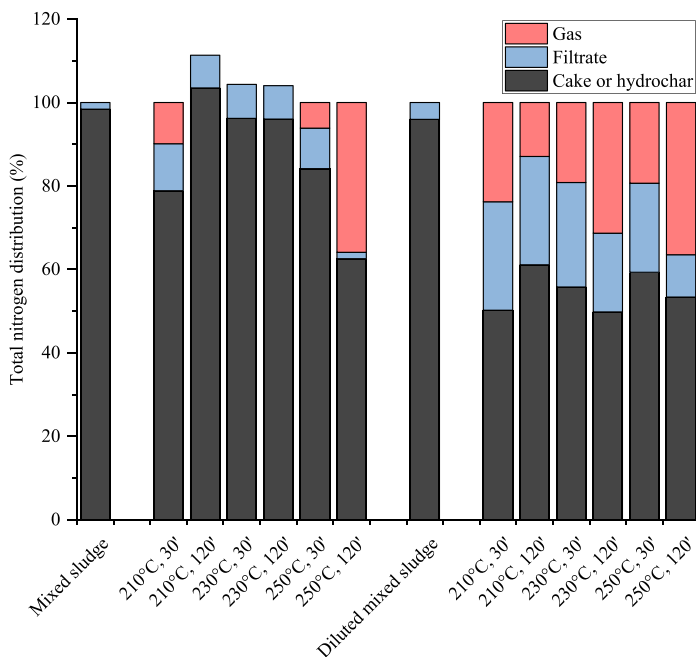


Fig. 4. Distribution of total nitrogen in mixed sludge and diluted mixed sludge (Diluted MS) after filtration (cake and filtrate) and HTC-treated mixed sludge and diluted mixed sludge after filtration (hydrochar, filtrate and gas).

added prior to filtering) compared to the untreated filter-cakes of sewage sludge (10%–20% TS, 60%–70% VS/TS) (Savayn et al., 2009). In the present study, no such increases in TS or VS content were obtained in the hydrochar and sludge cakes, as the TS of the hydrochars were 93%–109% of the cake TS (Table 2). However, our earlier study on HTC of digested sewage sludge with the same operation parameters, HTC, and filtration equipment as used in the present study showed improvement in the dewaterability by increasing the TS content in hydrochar by 200% (from 30% of the sludge-cake up to 60% of the hydrochar) (Hämäläinen et al., 2021). It is likely that the type of pulp-and-paper mill sludge, specifically one containing plenty of fiber-like material rather than colloidal matter, which possesses a high water-holding capacity, affects the filtration performance positively (Meyer et al., 2018) even without HTC, and thus the impact of HTC is lower. Furthermore, the used

filtration equipment deserves further consideration as it increased the cake TS up to even 50% from the 32% TS achieved with the mill site’s full-scale equipment.

### 3.2. Energy recovery from hydrochar

The effects of HTC treatment on energy recovery from pulp and paper mill mixed sludge were assessed based on the HHVs and energy yields, while the NO<sub>x</sub> and SO<sub>x</sub> emission potential and the possibility for slugging and fouling during incineration of hydrochar were addressed by determining the sulfur and nitrogen contents and by the ash content and the changes in alkali metal compositions, respectively.

The HHVs of the hydrochars steadily increased with increasing treatment temperature and residence time for both mixed sludges



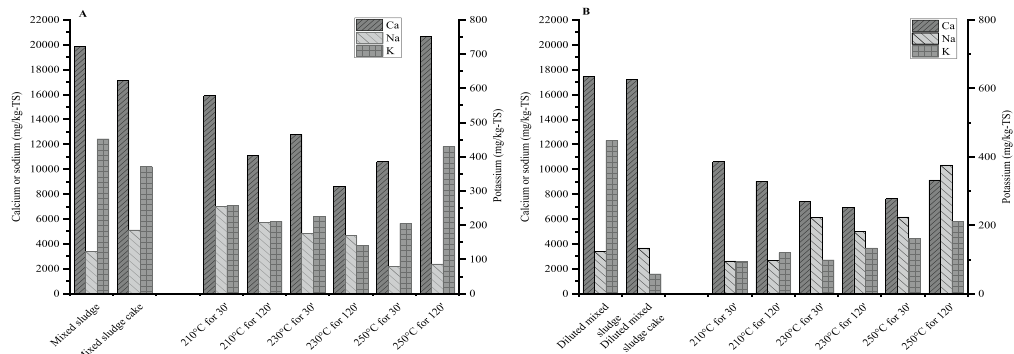


Fig. 5. Calcium, sodium, and potassium concentrations in the mixed sludge and in its cake and hydrochars (A), and in the diluted mixed sludge and in its cake and hydrochars (B).

(Table 2). The HHVs of the mixed sludges were 14.9 MJ/kg-TS, 15 MJ/kg-TS in the cake, and in the hydrochars the HHVs increased to 16.0–20.4 MJ/kg-TS and 16.1–20.5 MJ/kg-TS from the mixed and diluted mixed sludge, respectively. The increasing HHVs resulted in energy densifications of 1.08–1.49 for both mixed and diluted mixed-sludge hydrochars (Table 4). The energy yields of the mixed and diluted mixed-sludge hydrochars were between 70.5% and 99.5% and between 64.6% and 98.0%, respectively (Table 2). In the mixed-sludge hydrochars, a clear decrease in the energy yields was observed only after the severest treatment (at 250 °C for 120 min), whereas in the diluted mixed-sludge hydrochars, there was a decreasing trend with the

increasing treatment temperature and residence time.

The ash content (Table 2) increased from that of the mixed sludges and their cakes (12%) up to 19.7% in the hydrochars, upon which the prolonging of the residence time (from 30 to 120 min) had an increasing effect at 230 °C and 250 °C treatment temperatures, which is undesirable because ash only adds to the hydrochar volume and causes fouling and slagging during incineration (Jenkins et al., 1998). The hydrochar ash content was independent in the initial TS content of the mixed sludge (Table 2). Although the percentage of ash content increased, the ash yields decreased according to the treatment severity from 93% to 80% in mixed sludge hydrochars and from 85% to 72% in diluted mixed-

Table 3

The characteristics and nutrient contents of the mixed sludge and diluted mixed sludge cake filtrates and of their respective HTC filtrates.

Sample	pH	COD	SCOD	TVFA	NON-VFA-COD	BMP	Total phosphorous	PO <sub>4</sub> <sup>3-</sup>	Total nitrogen	NH <sub>4</sub> -N	NH <sub>4</sub> -N/N <sub>tot</sub>
	(-)	(g/L)	(g/L)	(g-COD/L)	(g/L)	(L CH <sub>4</sub> /kg-SCOD)	(mg/L)	(mg/L)	(g/L)	(g/L)	(%)
Mixed sludge cake filtrate	6.15	4.3 ± 0.02	3.8 ± 0.02	4.9 ± 0.02	-1.1	318.5 ± 45	1.02	0.00	0.18	0.10	56
<i>Mixed sludge HTC filtrates</i>											
210 °C for 30 min	5.17	33.5 ± 0.2	30.5 ± 0.05	4.5 ± 0.2	26.0	190.6 ± 8	0.49	15.81	1.17	0.13	11
210 °C for 120 min	5.16	23.6 ± 0.03	23.3 ± 0.01	5.0 ± 0.1	18.3	251.0 ± 5	0.46	20.46	0.73	0.10	13
230 °C for 30 min	4.90	35.5 ± 0.03	36.3 ± 0.01	9.7 ± 0.8	26.6	221.1 ± 15	0.53	28.71	0.87	0.05	6
230 °C for 120 min	4.65	44.4 ± 0.02	44.5 ± 0.03	10.8 ± 0.7	33.7	215.8 ± 5	0.96	43.82	0.71	0.01	2
250 °C for 30 min	4.51	50.6 ± 0.04	51.8 ± 0.02	11.6 ± 0.2	40.2	229.7 ± 22	0.56	60.78	0.77	0.01	1
250 °C for 120 min <sup>a</sup>	4.54	28.2 ± 0.03	28.2 ± 0.01	10.2 ± 0.5	18.0	266.5 ± 23	0.99	33.09	0.28	0.02	6
Diluted mixed sludge cake filtrate	6.30	2.7 ± 0.02	2.6 ± 0.01	2.8 ± 0.04	-0.2	n.d.	1.36	0.00	0.14	0.07	48
<i>Diluted mixed sludge HTC filtrates</i>											
210 °C for 30 min	5.10	23.1 ± 0.01	23.3 ± 0.01	3.1 ± 0.07	20.2	n.d.	0.66	28.24	0.92	0.15	17
210 °C for 120 min	5.15	25 ± 0.03	24.4 ± 0.02	3.3 ± 0.4	21.1	n.d.	0.74	31.34	0.90	0.13	14
230 °C for 30 min	4.89	28.7 ± 0.01	28.9 ± 0.03	5.5 ± 0.1	23.4	n.d.	0.95	34.79	0.85	0.09	10
230 °C for 120 min	4.62	31.6 ± 0.04	31.7 ± 0.02	6.2 ± 0.2	25.5	n.d.	1.22	35.49	0.61	0.02	3
250 °C for 30 min	4.35	41.4 ± 0.03	41.0 ± 0.00	7.4 ± 0.2	33.6	n.d.	0.69	51.69	0.69	0.01	2
250 °C for 120 min	4.33	40.6 ± 0.02	39.3 ± 0.01	7.1 ± 0.00	32.2	n.d.	1.13	65.11	0.55	0.01	2

COD: chemical oxygen demand, SCOD: soluble COD, TVFA: total volatile fatty acids, BMP: biomethane potential

<sup>a</sup> failed HTC-treatment and sample recovery, n.d. not determined

Table 4

Metal contents of the mixed sludge (32% TS) and diluted mixed sludge (15% TS) and of their respective cakes and hydrochars. Note that Al and Fe are given in a different unit (g/kg-TS) than the other metals (mg/kg-TS).

Sample	Al (g/kg-TS)	Fe (g/kg-TS)	Cr (mg/kg-TS)	Ni (mg/kg-TS)	Cu (mg/kg-TS)	Zn (mg/kg-TS)	As (mg/kg-TS)	Cd (mg/kg-TS)	Au (mg/kg-TS)	Pb (mg/kg-TS)	Hg (mg/kg-TS)
Mixed sludge	56.0	1.83	27.95	8.46	21.0	115.77	1.41	1.29	0.07	10.59	0.17
Mixed sludge cake	40.4	3.47	18.76	5.14	17.2	85.13	1.10	0.95	0.07	8.06	0.21
<i>Hydrochars from mixed sludge</i>											
210 °C for 30 min	45.0	1.59	21.77	5.22	50.9	90.52	1.54	1.02	0.31	10.44	0.10
210 °C for 120 min	38.0	1.44	18.12	4.43	15.4	77.56	0.76	0.80	0.21	6.69	0.09
230 °C for 30 min	42.7	1.56	20.98	5.70	18.5	88.55	0.90	1.04	0.09	8.71	0.09
230 °C for 120 min	43.4	1.29	20.32	6.43	16.2	68.42	0.80	0.89	0.08	7.25	0.09
250 °C for 30 min	48.4	1.54	28.04	7.90	18.2	77.46	1.13	0.97	0.08	8.84	0.10
250 °C for 120 min <sup>a</sup>	66.0	2.69	33.77	8.52	26.9	123.85	1.30	1.60	0.10	13.14	0.14
Diluted mixed sludge	38.6	1.37	19.46	4.36	14.4	80.22	0.87	0.83	0.08	6.98	0.07
Diluted mixed sludge cake	40.3	1.41	19.72	4.74	15.1	77.06	0.72	0.89	0.06	8.00	0.08
<i>Hydrochars from diluted mixed sludge</i>											
210 °C for 30 min	41.3	1.37	19.47	5.13	15.6	88.97	0.75	0.93	0.18	7.42	0.09
210 °C for 120 min	46.7	1.48	22.05	6.01	19.9	91.05	0.97	1.01	0.19	8.43	0.14
230 °C for 30 min	44.9	1.44	22.90	6.77	17.5	89.61	0.65	1.04	0.17	8.47	0.09
230 °C for 120 min	51.6	1.58	24.43	8.40	98.4	126.41	0.89	1.22	0.11	15.26	0.10
250 °C for 30 min	63.8	1.89	33.97	10.50	25.3	108.66	1.16	1.37	0.10	11.91	0.18
250 °C for 120 min	75.0	2.77	36.94	12.92	28.9	113.92	1.18	1.40	0.11	13.37	0.16

TS: total solids

<sup>a</sup> failed HTC-treatment and sample recovery

sludge hydrochars, indicating that part of the ash inorganics were increasingly dissolved when HTC temperature and residence time were increased.

The fates of the elements in HTC were evaluated based on their contents in the hydrochars and cakes (Table 1, Fig. 5) and the mass balance results (Fig. 1). The ash-free carbon content increased from 48.6% in the mixed sludges and cakes to 52.8%–69.1% and to 52.3%–70.7% in the hydrochars (Table 2), and the oxygen content decreased to about 35.8%–47.0% in all hydrochars from an oxygen content of 50.2% in the mixed sludges (Table 1). In contrast, the hydrogen content was nearly unaffected by the HTC-treatment (Table 1) as the hydrogen content decreased only during the severest treatments at 250 °C.

Biomass generally has lower sulfur content than coal (on average  $1.4 \pm 1.7\%$  DAF) and thus has the capability to reduce SO<sub>x</sub> emissions if replacing coal (Netherlands Energy Research Centre [ECN]; Williams et al., 2012). In the present study, sulfur content was higher in mixed sludge hydrochars than in the original mixed sludge or in its cake, but the hydrochars from diluted mixed sludge possessed a lower sulfur content than the original diluted mixed sludge or its cake (Table 1). Diluted mixed-sludge hydrochars had on average 25% lower sulfur content than mixed sludge hydrochars, indicating that the diluted mixed sludge was more prone to release sulfur in the liquid and gas phases during HTC treatment than mixed sludge. The sulfur yields were 78%–100% and 52%–73% in hydrochars from mixed and diluted mixed sludge, respectively, showing that sulfur was reduced in both mixed sludges by HTC. Nitrogen content that contributes to NO<sub>x</sub> emissions in the present mixed sludges and in their hydrochars was in the range of that in coal (on average  $1.5 \pm 0.4\%$  DAF) (Netherlands Energy Research Centre [ECN]) (Table 1). Like sulfur, nitrogen dissolved and/or evaporated more from diluted mixed sludge than mixed sludge during HTC (Fig. 4), as the nitrogen yields in diluted mixed sludge hydrochars were of 53%–61% and those of mixed sludge hydrochars ranged from 63% (at 250 °C, 120 min) to above 100%.

The presence of low melting temperature alkali metals in biomass derived solid fuels differentiates them from coal, which leads to concerns about their deposition on furnace walls (Chen et al., 2021). Therefore, their reduction from biomasses intended for energy recovery would be favorable to diminishing the formation of slag. The greatest

dissolution of potassium and calcium occurred at 230 °C for both mixed sludges, and overall, the diluted mixed-sludge hydrochars resulted in lower yields of potassium and calcium (18%–23% and 25%–55%, respectively) than mixed-sludge hydrochars (33%–53% and 34%–74%, respectively). Sodium dissolved to a lesser extent than potassium or calcium, as its yields increased with treatment severity from 65% to 100% in the diluted mixed-sludge hydrochars but decreased with treatment severity from 100% to 36% in mixed-sludge hydrochars. Based on the mass balance, mere filtration of the mixed sludges only affected the dissolution of potassium and calcium, resulting in yields of 56% and 91% in diluted mixed-sludge cakes, and of 78% and 82% in mixed-sludge cakes, respectively, whereas sodium was not dissolved by filtration alone (with yields of 100% in both cakes).

The results show that HTC improved the fuel properties of the mixed sludges by generating hydrochars with higher HHV and ash-free carbon content and lower oxygen content compared to the respective cakes, and the improvement was independent of the initial TS content of the mixed sludge. The hydrochars' HHV, energy densification, and carbon and ash content all increased with treatment severity, whereas the energy yields decreased because of the decrease in hydrochar masses. The increases in HHV and energy densification via increases in treatment severity derived mainly from the increased carbon and decreased oxygen content, likely resulting from the decarboxylation reactions that took place during HTC (Lin et al., 2015). The other reactions causing changes in the elemental composition of sludge, i.e., demethylation and dehydration, seemed less prominent as the hydrogen content was nearly unaltered (Lin et al., 2015; Martinez et al., 2021). In earlier studies, HTC was argued to improve the solid fuel properties of pulp-and-paper industry sludges more the higher the temperatures used, which could be observed as increased HHVs and energy densifications and decreased oxygen content (Martinez et al., 2021; Saha et al., 2019). However, as also observed in the present study, the ash content in hydrochars tends to increase along with treatment severity (Martinez et al., 2021), but ash yields decrease with increasing HTC temperature (Mäkelä et al., 2016).

The fact that the dissolution of sulfur and nitrogen was more favorable in the HTC treatments of diluted mixed sludge than mixed sludge indicate energy recovery from mixed-sludge hydrochar by incineration could possibly result in higher NO<sub>x</sub> and SO<sub>x</sub> formations (Lin et al., 2015)

relative to the incineration of diluted mixed-sludge hydrochars or even the cakes or mixed sludge. On the contrary, potassium and calcium concentrations in both mixed sludge hydrochars were reduced by dissolution during HTC, which would diminish the fouling or slugging in furnaces caused by the alkali metals in hydrochar ash if incinerated (Smith et al., 2016). As the lowest yields of potassium and calcium were obtained in hydrochars at 230 °C and 120 min, some absorption in hydrochar after their dissolution could have occurred after the temperature was further increased to 250 °C (Reza et al., 2013). However, the studied pulp-mill sludge had initially low potassium content compared to other lignocellulosic biomasses, such as corn stover and switch grass, as potassium in virgin wood is associated with hemicellulose and extractives that have already been removed in the preceding pulping process (Reza et al., 2013). The calcium content in the hydrochars were, in contrast, high compared to other biomasses (Smith et al., 2016), which likely resulted from the use of calcium carbonate as an agent for paper coating in paper making (Nurmesniemi et al., 2007).

Overall, the HTC treatment of the present mixed sludges of different TS contents (32% and 15%) resulted in quite similar solid fuel properties in their hydrochars, whereas differences in their ash yields and dissolutions of sulfur, nitrogen, and ash components were observed, supporting the conclusion that HTC of mixed sludge for energy recovery could be more feasible for lower TS content mixed sludge. Mäkelä and Yoshikawa (2016) found that increasing sludge TS content in the HTC feed increases the obtained energy yield and carbon recovery in hydrochars, suggesting that sludge with high TS content could react more favorably to HTC treatment than low TS sludge. However, they also found that feed TS content inversely correlates with the hydrochar ash content (Mäkelä and Yoshikawa, 2016). The differences in the fuel properties of hydrochars between different studies probably originates, aside from the operation conditions, from the feedstock composition differences, which can be highly case specific (Saha et al., 2019; Wang et al., 2021). It is also noteworthy that the methods for separating the obtained HTC-treated sludge into hydrochar and filtrate differ (Martinez et al., 2021; Saha et al., 2019), probably impeding their comparison; for example, the large range in reported solid yields (41%–87% DAF) can be partly explained by the separation method used, whether it be laboratory scale vacuum filtration through 1.6 or 20 µm filter paper, or pressure filtration. The filtration technique may also affect the amount of organic material (COD) in the resulting filtrates, which then directly influences the filtrate properties.

### 3.3. Filtrate

The HTC filtrates were more acidic (4.3–5.2) than the cake filtrates (6.2–6.3), and the pH of the HTC filtrates decreased from 5.1 to 4.3–4.5 with an increase in treatment temperature from 210 °C to 250 °C (Table 3). The COD concentrations in the HTC filtrates were several folds higher compared to the cake filtrates, at 8-fold (4.3 vs. 23.6–50.6 g/L) and 12-fold (2.7 vs. 23.1–41.4 g/L) higher for mixed and diluted mixed sludge, respectively (Table 3). The SCODs in the HTC filtrates covered 91%–100% of the respective CODs, while the SCOD in the cake filtrates covered 88% (mixed sludge) and 96% (diluted mixed sludge) of the COD (Table 3). The diluted mixed sludge HTC filtrates had a lower SCOD (23–41 g/L) than that of mixed sludge (23–52 g/L), but when taking into account the dilution of the mixed sludge (32% TS diluted to 15% TS) (Eq. (5)), the SCOD in the diluted mixed-sludge HTC filtrates were on average 1.3-fold higher than in those of mixed sludge. The VFAs accounted for 15%–36% and 13%–20% of the HTC filtrates' SCOD from mixed and diluted mixed sludge, respectively, while the SCOD of the original mixed sludges and cake filtrates was completely made of VFAs. Most of the HTC filtrates (except after the treatment at 210 °C for 30 min) had higher TVFA concentration than the cake filtrates (Fig. 3; Table 3), increasing 2.3-fold with a temperature increase from 210 °C to 250 °C. The VFA concentrations in the diluted mixed-sludge HTC filtrates were 3.1–7.1 g-COD/L, which was on average 64% of those

concentrations in the mixed-sludge HTC filtrates (4.5–10.2 g-COD/L), but when taking into account the dilution of the mixed sludge (Eq. (5)), they were on average 94% of the mixed-sludge HTC filtrates' VFA concentrations. The non-VFA content of the SCOD in the HTC filtrates also increased with the treatment temperature, as at 210 °C the non-VFA accounted for 18.3 g-COD/L and at 250 °C the non-VFA content was up to 40 g-COD/L. The dominant VFA was acetic acid, the concentration of which increased with treatment severity from 2900 to 7210 mg/L (mixed-sludge HTC filtrates) and from 1680 to 4440 mg/L (diluted mixed-sludge HTC filtrates). Butyric acid was generated at 230 °C and 250 °C, reaching concentrations of 350–960 mg/L and 450–750 mg/L, respectively.

The BMPs were determined for the HTC and cake filtrates from mixed sludge. The specific BMPs of the HTC filtrates were lower (190–266 L-CH<sub>4</sub>/kg SCOD) than that of the cake filtrate, which was 318 ± 45 L-CH<sub>4</sub>/kg SCOD (Table 3). However, as the concentration of SCOD was much higher in the HTC filtrates (23–44 g/L) than in the cake filtrate (4 g/L), the volumetric BMPs were 5–6-fold higher in the HTC filtrates than in the cake filtrate (1.2 L-CH<sub>4</sub>/L) (Fig. 2). The volumetric BMPs in the HTC filtrates increased along with increases in temperature and residence time from 6.2 to 11.4 L-CH<sub>4</sub>/L (Fig. 2), except for the severest treatment at 250 °C for 120 min (7.7 L-CH<sub>4</sub>/L).

In the present study, the HTC treatment clearly increased the COD, SCOD, and TVFA concentrations relative to the cake filtrates, and the increasing effect was notable at higher treatment temperatures and residence times. Most of the increased COD comprised of non-VFAs (Table 3), and was apparently not readily degradable as indicated by the lower specific BMP compared to the cake filtrate. The non-VFA COD could possibly encompass other acids and lignocellulose degradation products, such as glycolic acid, levulinic acid, phenols, furfural, and hydroxymethyl furfural, of which at least furfurals are inhibitory for microorganisms in AD (Aragón-Briceno et al., 2021; Kim and Karthikeyan, 2021). The fact that the diluted mixed sludge yielded on average 35% and 3% higher COD and non-VFA COD concentrations than mixed sludge, when the dilution factor was considered (Eq. (5)), respectively, could result from enhanced carbon dissolution obtained by lowering the sludge TS content (Mäkelä et al., 2018). The COD increase with temperature increase can be assumed to derive from the increased dissolution of VS from the sludge during HTC, as the amount of dissolved VS increased from 9% at 210 °C to 50%–53% at 250 °C in hydrochars from both mixed sludges. However, the COD concentration increases were also derived from the hydrolysis of organic matter during the HTC treatments (Merzari et al., 2019) as indicated by the fact that although the amount of VS dissolved by filtration alone was nearly the same as after HTC at 210 °C and filtration (6%–7%), the COD in cake filtrates was 11%–12% of the COD in the HTC filtrates at 210 °C. Thus, the COD concentrations in the HTC filtrates are affected by the filtration method and the feedstock sludge type; for example, much lower CODs (using vacuum filtration with a 1.6 µm pore size filter) have been reported for both primary and biosludge HTC filtrates from a pulp and paper mill (126–331 mg/L and 24–81 mg/L, respectively, at temperatures of 180 °C–240 °C) than in the present study (Martinez et al., 2021).

As the HTC filtrate characteristics indicate, the filtrates contain plenty of soluble organic matter and nutrients (see Section 3.4) and cannot be disposed of without further treatment. The alternatives to the use or treatment of the HTC filtrates include recycling the filtrates back into the HTC reactor when additional water is needed for the feedstock dilution (Kabadayi Catalkopru et al., 2017), feeding it to a wastewater treatment plant (Mäkelä et al., 2018) or producing methane through AD (Hämäläinen et al., 2021). The effect of filtrate recirculation on the HTC products, with the aim of adjusting the feed moisture content prior to HTC treatment, has been evaluated by several authors (Mäkelä et al., 2018; Tasca et al., 2019; Wang et al., 2019) and filtrate recirculation has been demonstrated to enhance dewaterability and the mass and energy yields of hydrochar compared to hydrochar where no filtrate circulation was used. There is an improvement because the circulated filtrate

contains organic acids generated in HTC that promote polymer deposition and dehydration reactions in HTC (Tasca et al., 2019). The circulation of the filtrate to HTC has also been reported to result in hydrochars with increased carbon stability in soil compared to hydrochars where no filtrate circulation was used, which is due to a decrease in hydrochar volatile matter with lower amount of decomposed carbon (Schulze et al. 2016). The filtrate could be fed to the wastewater treatment plant in a mill, where it could supply part of the nutrient additions needed in the pulp and paper mill wastewater treatment (Hynninen, 1998). On the other hand, filtrate treatment may require an increase in wastewater treatment capacity. As shown in the present study, HTC filtrates are rich with COD and VFAs. Thus, methane production, for example, in an existing high-rate anaerobic reactor, together with other concentrated wastewater streams at the mill site could be considered if the filtrate volumes, potential inhibitory compounds, and low pH could be managed.

### 3.4. Nutrients, carbon, and heavy metals

Hydrochar utilization was evaluated from the perspective of using the nutrients and carbon recovered in the hydrochar for application in soil, in which the nutrient concentrations are regarded as more useful than their yields that were discussed above (see Section 3.2). The filtrates' potential for nutrient recovery was also addressed based on the nutrient concentrations.

The hydrochars and cakes contained nearly all the phosphorous (>99%) present in the mixed and diluted mixed sludges, while up to one third of total nitrogen was in the HTC filtrates and 2%–4% was in the cake filtrates (Fig. 4). According to the mass distribution, all the HTC filtrates contained less than 0.18% of the total phosphorous (Table 3). However, phosphate was found in the HTC filtrates in concentrations of 15.8–65.1 mg/L, while phosphate was not present at all in the cake filtrates. The nitrogen content in the hydrochars was in the range of 9–18.4 g/kg-TS, increasing with treatment temperature, whereas the cake nitrogen content was 13–17 g/kg-TS, which was slightly higher than the initial mixed-sludge concentration (12.4 g/kg-TS) (Table 1). Nitrogen in the diluted mixed sludge was more prone to dissolve into the HTC filtrate ( $27 \pm 6\%$  of the total nitrogen) than nitrogen in the mixed sludge ( $7 \pm 3\%$  of the total nitrogen), as shown by the nitrogen mass balance (Fig. 2). The HTC filtrate nitrogen concentrations (0.28–1.17 g/L) decreased with increasing treatment severity with both mixed sludges and were higher than in the cake filtrates (0.14–0.18 g/L) (Table 4). The ammonium nitrogen concentration in the HTC filtrates also decreased from 0.13 to 0.15 g/L to 0.01–0.02 g/L with increasing severity (Table 4). The amount of nitrogen in the gas phase appeared to be greater in the treatments of diluted mixed sludge, increasing by the treatment severity (13%–36% of total nitrogen), than in those of the mixed sludge (0–10%), except at 250 °C for 120 min (36%) (Fig. 4).

The contents of other nutrients (potassium, calcium, and sodium) in hydrochars, cakes, and in mixed sludges are presented in Fig. 5. Of these nutrients, the calcium and potassium content was lower in hydrochars than in the mixed sludges and cakes, while the sodium content was in some cases higher than in the mixed sludges. The calcium content was 11–21 g/kg-TS and 7–11 g/kg-TS in mixed and diluted mixed sludge hydrochars, respectively, while the initial sludge concentrations were 20 g/kg-TS and 17 g/kg-TS, respectively. Sodium concentrations increased from 3.6 g/kg-TS in the mixed sludge up to 7.0 g/kg-TS (at 210 °C) but decreased with treatment severity to 2.4 g/kg-TS, whereas in the diluted mixed-sludge hydrochars the concentrations increased up to 10 g/kg-TS with an increase in temperature to 250 °C. The mixed sludge hydrochar potassium content (141–430 mg/kg-TS) was on average 1.8-fold higher than that of the diluted mixed sludge (93–211 mg/kg-TS). The contents of heavy metals (Cr, Fe, Ni, Cu, Zn, As, Cd and Pb) present in the mixed sludges remained nearly the same in the hydrochars and cakes, and their yields were 100%. However, Fe and Zn were also found in the HTC filtrates in concentrations of 0.01–0.51 mg/L

and 0.01 mg/L, respectively, as was aluminum in concentrations of 0.05–0.2 mg/L (Table 4). Of the metals in the hydrochars, aluminum was found in the highest content (38–75 g/kg-TS), as it was in the original mixed sludges (39–56 g/kg-TS) (Table 4).

It appears that HTC only slightly promoted the dissolution of the phosphorus and partially that of nitrogen in the filtrates (as compared to filtration alone) from the studied pulp and paper mill sludges. Additionally, the sludge TS content seemed to determine whether nitrogen was dissolved in the filtrate and to what extent, rather than the different HTC conditions (Fig. 4), the lower TS content sludge releasing more nitrogen to the liquid and gas phases than higher TS content sludge. The HTC filtrates' decreasing total nitrogen concentrations by treatment severity indicated that organic nitrogen was released to the liquid phase during HTC but was then converted to ammonia and ammonium nitrogen, which are easily evaporated at higher temperatures, leading to decreased total nitrogen and ammonium nitrogen concentrations in the HTC filtrates (Idowu et al., 2017).

Phosphate was present only in the HTC filtrates, and its concentration increased with treatment severity. Alkali phosphates have high solubility, but phosphate remains in the hydrochar when the original feed contains aluminum and iron, which interact with it (Alhniidi et al., 2020). The present mixed sludge contained aluminum at a content of 56 mg/kg-TS, which was a more probable reason for the decreasing phosphorus solubility than the iron with concentrations of 1.8 mg/kg-TS in the original mixed sludge. Adding metals, e.g., in sludge pretreatment prior to HTC, to adjust the initial metal content in the sludge, could enable the recovery of phosphorus in the hydrochar (Alhniidi et al., 2020). The bioavailability of phosphorous in the hydrochar should be determined, if fertilizer use is being considered, as it could be bound to the added metals and mineral compounds (Huang and Tang, 2015). Hence, the origin and type of the sludge treated in HTC evidently affects the resulting nutrient contents of the hydrochar and filtrate. For example, the nitrogen content of hydrochars (at 260 °C) produced from two mixed pulp and paper mill sludges from different mills either decreased from the original 2.3% to 2.1% or increased from the original 0.7% to 1.6% (Saha et al., 2019).

Similar to nitrogen, the contents and yields of phosphorous, potassium, calcium, and sodium were all higher in the mixed sludge hydrochars than in the diluted mixed-sludge hydrochars, but the changes in these concentrations were small between the hydrochars and filtrates from the different HTC conditions. Hence, the use of HTC in the optimization for nutrient recovery from pulp and paper mixed sludge could focus instead on the pretreatment of the sludge to increase or decrease its metal and TS contents, and on the minimization of nutrient evaporation to the gas phase. For example, the filtrates could be treated in a stripping process if the nitrogen concentrations would be at feasible levels. The hydrochar nutrients and carbon could be recovered by its application in soils where it would increase the soil nitrogen and carbon supply (Bargmann et al., 2014) and reduce soil acidity (Dai et al., 2017), which could increase tree growth, and thus, forest productivity and returns from forests to the pulp and paper industry (Mohammadi et al., 2019). However, as the nutrient contents were comparatively low in the original mixed sludges relative to other waste biomasses (Aragón-Briceño et al., 2021), the hydrochars in this study would not fulfill, for example, the criteria for forest fertilizers set by the Finnish authorities because the P + K content was on average  $0.47 \pm 0.16\%$ -TS and the calcium contents were between 0.9 and 1.3%-TS, covering only a fourth and sixth of the minimum required content, respectively (Decree of Ministry of Agriculture and Forestry of Finland, 2011).

The fact that the HTC-treatments increased the ash-free carbon content of the mixed sludges (from 48.5% to above 52%) (See Section 3.2) (Table 2), encourages the examination of the role of HTC treatment of pulp and paper industry sludges in carbon sequestration. HTC temperature has been found to influence the stability of carbon in straw digestate hydrochars; hydrochar at 250 °C emitted 28% less carbon (3.2% of total carbon) when applied in soil than at 230 °C (4.4% of total

carbon), and hydrochar at 230 °C emitted 60% less carbon than hydrochar at 210 °C (11.9% of total carbon), which could be explained by the protonation of OH-groups, aromatization and decreasing O/C and H/C ratios (Schulze et al., 2016). The carbon stability of hydrochar can be evaluated via the dissolved organic carbon content, which directly correlates with the carbon release induced by hydrochar in soil (Bargmann et al., 2014) and by the hydrochar volatile matter that inversely affects it (Schulze et al., 2016). According to a life-cycle assessment (LCA), the HTC-treatment of pulp and paper sludge and with its subsequent soil application could possibly obtain net reductions of 1.13 tons of CO<sub>2</sub>-equivalent to one ton of dried sludge (Mohammadi et al., 2019). In addition to the HTC temperature, the duration of hydrochar soil application influences the amount of emitted carbon, as a short-term soil application (3 months) appears to increase the soil's carbon emission through decomposition and leaching, but during a long-term application (1 year), two thirds of the carbon in hydrochar is still in the soil, independent of whether the soil is sandy or coarse (Malghani et al., 2013).

#### 4. Conclusions

HTC treatment of pulp and paper mill sludges produced hydrochars with increased HHVs (from original 15 up to 20.5 MJ/kg) and energy densification (up to 1.49) improving energy recovery, while sludge dewaterability was little affected. HTC produced filtrates with high COD, increasing with treatment severity up to 51 g/L, which could supplement methane production though 65–79% was non-VFA-COD. Hydrochar characteristics were unaffected by the sludge solids content, while lower sludge solids content generated filtrates with less COD and nutrients. Hydrochars' carbon and nutrient contents increased with treatment severity, but for their low nutrient content, carbon sequestration could be prioritized.

#### CRedit authorship contribution statement

**Anna Hämäläinen:** Investigation, Visualization, Writing – original draft. **Marika Kokko:** Supervision, Writing – review & editing. **Viljami Kinnunen:** Resources, Methodology. **Tuomo Hilli:** Supervision, Methodology. **Jukka Rintala:** Project administration, Writing – review & editing.

#### Declaration of Competing Interest

The authors declare that they have no known competing financial interests or personal relationships that could have appeared to influence the work reported in this paper.

#### Acknowledgements

The financial support of the Maj and Tor Nessling Foundation (Anna Hämäläinen), the Industrial Research Fund at Tampere University of Technology (Anna Hämäläinen), Gasum Ltd. and Fifth Innovation is gratefully acknowledged. The authors thank Kirsi Järvi, Antti Nuotajarvi, Essi Sariola-Leikas and Harri Ali-Löytty for their support in the laboratory.

#### References

- Ahmed, M., Andreottola, G., Elagroudy, S., Negm, M.S., Fiori, L., 2021. Coupling hydrothermal carbonization and anaerobic digestion for sewage digestate management: Influence of hydrothermal treatment time on dewaterability and bio-methane production. *J. Environ. Manage.* 281, 111910.
- Alhindi, M.J., Wüst, D., Funke, A., Hang, L., Kruse, A., 2020. Fate of nitrogen, phosphate, and potassium during hydrothermal carbonization and the potential for nutrient recovery. *ACS Sustain. Chem. Eng.* 8, 15507–15516. <https://doi.org/10.1021/acscuschemeng.0c04229>.
- Aragón-Briceño, C.I., Pozarlik, A.K., Bramer, E.A., Niedzwiecki, L., Pawlak-Kruczek, H., Brem, G., 2021. Hydrothermal carbonization of wet biomass from nitrogen and phosphorus approach: A review. *Renew. Energy* 171, 401–415. <https://doi.org/10.1016/j.renene.2021.02.109>.
- Areeprasert, C., Zhao, P., Ma, D., Shen, Y., Yoshikawa, K., 2014. Alternative solid fuel production from paper sludge employing hydrothermal treatment. *Energy and Fuels* 28, 1198–1206. <https://doi.org/10.1021/ef402371h>.
- Bargmann, I., Rillig, M.C., Kruse, A., Greef, J.M., Kücke, M., 2014. Effects of hydrochar application on the dynamics of soluble nitrogen in soils and on plant availability. *J. Plant Nutr. Soil Sci.* 177, 48–58. <https://doi.org/10.1002/jpln.201300069>.
- Dai, Z., Zhang, X., Tang, C., Muhammad, N., Wu, J., Brookes, P.C., Xu, J., 2017. Potential role of biochars in decreasing soil acidification - A critical review. *Sci. Total Environ.* 581–582, 601–611. <https://doi.org/10.1016/j.scitotenv.2016.12.169>.
- Decree of Ministry of Agriculture and Forestry of Finland (24/2011, amendments up to 7/2013) [https://mmm.fi/documents/1410837/2061117/MMMa\\_24\\_2011\\_lannoitevalmistasetus.EN.pdf](https://mmm.fi/documents/1410837/2061117/MMMa_24_2011_lannoitevalmistasetus.EN.pdf), 2011. MMM (24/2011).
- Fang, J., Zhan, L., Ok, Y.S., Gao, B., 2018. Minireview of potential applications of hydrochar derived from hydrothermal carbonization of biomass. *J. Ind. Eng. Chem.* 57, 15–21. <https://doi.org/10.1016/j.jiec.2017.08.026>.
- Faubert, P., Barnabé, S., Bouchard, S., Côté, R., Villeneuve, C., 2016. Pulp and paper mill sludge management practices: What are the challenges to assess the impacts on greenhouse gas emissions? *Resour. Conserv. Recycl.* 108, 107–133. <https://doi.org/10.1016/j.resconrec.2016.01.007>.
- Gottumukkala, L.D., Haigh, K., Collard, F.X., van Rensburg, E., Görgens, J., 2016. Opportunities and prospects of bio refinery-based valorisation of pulp and paper sludge. *Bioresour. Technol.* 215, 37–49. <https://doi.org/10.1016/j.biortech.2016.04.015>.
- Hämäläinen, A., Kokko, M., Kinnunen, V., Hilli, T., Rintala, J., 2021. Hydrothermal carbonisation of mechanically dewatered digested sewage sludge—Energy and nutrient recovery in centralised biogas plant. *Water Res.* 201, 117284 <https://doi.org/10.1016/j.watres.2021.117284>.
- Huang, R., Tang, Y., 2015. Speciation dynamics of phosphorus during (hydro)thermal treatments of sewage sludge. *Environ. Sci. Technol.* 49, 14466–14474. <https://doi.org/10.1021/acs.est.5b04140>.
- Hynninen, P., 1998. Papermaking science and technology. Book 19, Environmental control. Papet Oy, Jyväskylä.
- Idowu, I., Li, L., Flora, J.R.V., Pellechia, P.J., Darko, S.A., Ro, K.S., Berge, N.D., 2017. Hydrothermal carbonization of food waste for nutrient recovery and reuse. *Waste Manag.* 69, 480–491. <https://doi.org/10.1016/j.wasman.2017.08.051>.
- Kabadayi Catakoprur, A., Kantarli, I.C., Yanik, J., 2017. Effects of spent liquor recirculation in hydrothermal carbonization. *Bioresour. Technol.* 226, 89–93. <https://doi.org/10.1016/j.biortech.2016.12.015>.
- Kim, J.R., Karthikeyan, K.G., 2021. Effects of severe pretreatment conditions and lignocellulose-derived furan byproducts on anaerobic digestion of dairy manure. *Bioresour. Technol.* 340, 125632 <https://doi.org/10.1016/j.biortech.2021.125632>.
- Kinnunen, V., Ylä-Outinen, A., Rintala, J., 2015. Mesophilic anaerobic digestion of pulp and paper industry biosludge-long-term reactor performance and effects of thermal pretreatment. *Water Res.* 87, 105–111. <https://doi.org/10.1016/j.watres.2015.08.053>.
- Kokko, M., Koskue, V., Rintala, J., 2018. Anaerobic digestion of 30–100-year-old boreal lake sedimented fibre from the pulp industry: Extrapolating methane production potential to a practical scale. *Water Res.* 133, 218–226. <https://doi.org/10.1016/j.watres.2018.01.041>.
- Lin, Y., Ma, X., Peng, X., Hu, S., Yu, Z., Fang, S., 2015. Effect of hydrothermal carbonization temperature on combustion behavior of hydrochar fuel from paper sludge. *Appl. Therm. Eng.* 91, 574–582. <https://doi.org/10.1016/j.applthermaleng.2015.08.064>.
- Mäkelä, M., Benavente, V., Fullana, A., 2016. Hydrothermal carbonization of industrial mixed sludge from a pulp and paper mill. *Bioresour. Technol.* 200, 444–450. <https://doi.org/10.1016/j.biortech.2015.10.062>.
- Mäkelä, M., Benavente, V., Fullana, A., 2015. Hydrothermal carbonization of lignocellulosic biomass: Effect of process conditions on hydrochar properties. *Appl. Energy* 155, 576–584. <https://doi.org/10.1016/j.apenergy.2015.06.022>.
- Mäkelä, M., Forsberg, J., Söderberg, C., Larsson, S.H., Dahl, O., 2018. Process water properties from hydrothermal carbonization of chemical sludge from a pulp and board mill. *Bioresour. Technol.* 263, 654–659. <https://doi.org/10.1016/j.biortech.2018.05.044>.
- Mäkelä, M., Yoshikawa, K., 2016. Ash behavior during hydrothermal treatment for solid fuel applications. Part 2: Effects of treatment conditions on industrial waste biomass. *Energy Convers. Manag.* 121, 409–414. <https://doi.org/10.1016/j.enconman.2016.05.015>.
- Malghani, S., Gleixner, G., Trumbore, S.E., 2013. Chars produced by slow pyrolysis and hydrothermal carbonization vary in carbon sequestration potential and greenhouse gases emissions. *Soil Biol. Biochem.* 62, 137–146. <https://doi.org/10.1016/j.soilbio.2013.03.013>.
- Martinez, C.L.M., Sermayagina, E., Vakkilainen, E., 2021. hydrothermal carbonization of chemical and biological pulp mill sludges. *Energies* 14. <https://doi.org/10.3390/en14185693>.
- Merzari, F., Langone, M., Andreottola, G., Fiori, L., 2019. Methane production from process water of sewage sludge hydrothermal carbonization. A review. Valorising sludge through hydrothermal carbonization. *Crit. Rev. Environ. Sci. Technol.* 49, 947–988. <https://doi.org/10.1080/10643389.2018.1561104>.
- Meyer, T., Amin, P., Allen, D.G., Tran, H., 2018. Dewatering of pulp and paper mill biosludge and primary sludge. *J. Environ. Chem. Eng.* 6, 6317–6321. <https://doi.org/10.1016/j.jece.2018.09.037>.
- Mohammadi, A., Sandberg, M., Venkatesh, G., Eskandari, S., Dalgaard, T., Joseph, S., Granström, K., 2019. Environmental analysis of producing biochar and energy

- recovery from pulp and paper mill biosludge. *J. Ind. Ecol.* 23, 1039–1051. <https://doi.org/10.1111/jiec.12838>.
- Netherlands Energy Research Centre (ECN), n.d. PHYLLIS Database web site [WWW Document]. URL <http://www.ecn.nl/phyllis>.
- Nurmesniemi, H., Pöykkiö, R., Keiski, R.L., 2007. A case study of waste management at the Northern Finnish pulp and paper mill complex of Stora Enso Veitsiluoto Mills. *Waste Manag.* 27, 1939–1948. <https://doi.org/10.1016/j.wasman.2006.07.017>.
- Pecchi, M., Baratieri, M., 2019. Coupling anaerobic digestion with gasification, pyrolysis or hydrothermal carbonization: A review. *Renew. Sustain. Energy Rev.* 105, 462–475. <https://doi.org/10.1016/j.rser.2019.02.003>.
- Reza, M.T., Lynam, J.G., Uddin, M.H., Coronella, C.J., 2013. Hydrothermal carbonization: Fate of inorganics. *Biomass and Bioenergy* 49, 86–94. <https://doi.org/10.1016/j.biombioe.2012.12.004>.
- Saha, N., Saba, A., Saha, P., McGaughy, K., Franqui-Villanueva, D., Orts, W.J., Hart-Cooper, W.M., Toufiq Reza, M., 2019. Hydrothermal carbonization of various paper mill sludges: An observation of solid fuel properties. *Energies* 12, 1–18. <https://doi.org/10.3390/en12050858>.
- Saveyn, H., Curvers, D., Schoutteten, M., Krott, E., Van der Meeren, P., 2009. Improved Dewatering by Hydrothermal Conversion of Sludge. *J. Residuals Sci. Technol.* 6, 51–56. [https://doi.org/1544-8053/09/01\\_051-06](https://doi.org/1544-8053/09/01_051-06).
- Schulze, M., Mumme, J., Funke, A., Kern, J., 2016. Effects of selected process conditions on the stability of hydrochar in low-carbon sandy soil. *Geoderma* 267, 137–145. <https://doi.org/10.1016/j.geoderma.2015.12.018>.
- Singh, S., Rinta-Kanto, J.M., Kettunen, R., Tolvanen, H., Lens, P., Collins, G., Kokko, M., Rintala, J., 2019. Anaerobic treatment of LCFA-containing synthetic dairy wastewater at 20 °C: Process performance and microbial community dynamics. *Sci. Total Environ.* 691, 960–968. <https://doi.org/10.1016/j.scitotenv.2019.07.136>.
- Smith, A.M., Singh, S., Ross, A.B., 2016. Fate of inorganic material during hydrothermal carbonisation of biomass: Influence of feedstock on combustion behaviour of hydrochar. *Fuel* 169, 135–145. <https://doi.org/10.1016/j.fuel.2015.12.006>.
- Sun, X., Atiyeh, H.K., Li, M., Chen, Y., 2020. Biochar facilitated bioprocessing and biorefinery for productions of biofuel and chemicals: A review. *Bioresour. Technol.* 295, 122252 <https://doi.org/10.1016/j.biortech.2019.122252>.
- Tasca, A.L., Puccini, M., Gori, R., Corsi, I., Galletti, A.M.R., Vito, S., 2019. Hydrothermal carbonization of sewage sludge: A critical analysis of process severity, hydrochar properties and environmental implications. *Waste Manag.* 93, 1–13. <https://doi.org/10.1016/j.wasman.2019.05.027>.
- Wang, F., Wang, J., Gu, C., Han, Y., Zan, S., Wu, S., 2019. Effects of process water recirculation on solid and liquid products from hydrothermal carbonization of Laminaria. *Bioresour. Technol.* 292, 121996 <https://doi.org/10.1016/j.biortech.2019.121996>.
- Wang, S., Wen, Y., Hammarström, H., Jönsson, P.G., Yang, W., 2021. Pyrolysis behaviour, kinetics and thermodynamic data of hydrothermal carbonization-Treated pulp and paper mill sludge. *Renew. Energy* 177, 1282–1292. <https://doi.org/10.1016/j.renene.2021.06.027>.
- Williams, A., Jones, J.M., Ma, L., Pourkashanian, M., 2012. Pollutants from the combustion of solid biomass fuels. *Prog. Energy Combust. Sci.* 38, 113–137. <https://doi.org/10.1016/j.peccs.2011.10.001>.

## SUPPLEMENTARY MATERIAL

### **Hydrothermal carbonization of pulp and paper industry wastewater treatment sludges — characterization and potential use of hydrochars and filtrates**

**Anna Hämäläinen,<sup>a\*</sup> Marika Kokko,<sup>a</sup> Viljami Kinnunen,<sup>b</sup> Tuomo Hilli,<sup>c</sup> Jukka Rintala<sup>a</sup>**

<sup>a</sup> Faculty of Engineering and Natural Sciences, Tampere University, P.O.Box 541, 33104 Tampere University, Finland

<sup>b</sup> Gasum Oy, Revontulenpuisto 2C, 02100 Espoo, Finland

<sup>c</sup> Fifth Innovation Oy, Väinöläkatu 26, 33500 Tampere, Finland

\* Corresponding author (e-mail: [anna.hamalainen@tuni.fi](mailto:anna.hamalainen@tuni.fi))



**Figure S1.** The HTC reactor used in the experiments was a two-liter Parr® 4500 pressure reactor with an external circulating cooling water jacket surrounding the vessel.



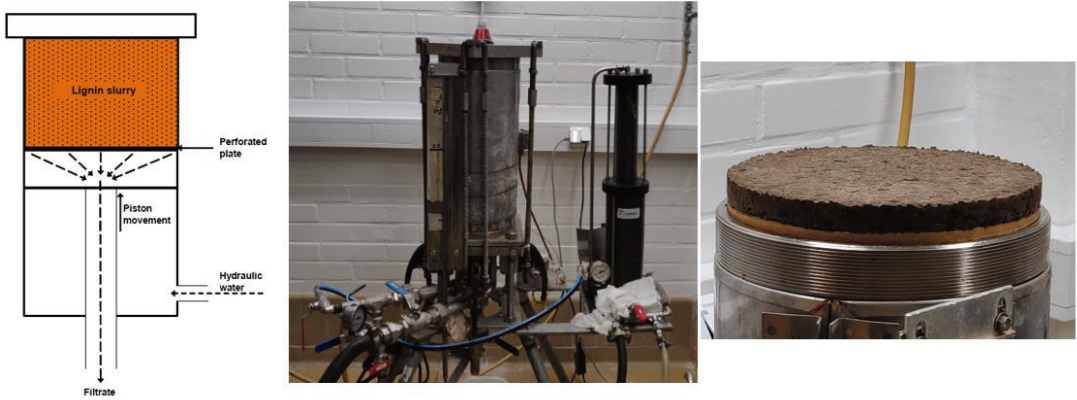


**Figure S2.** The filtration equipment used in the present study. The leftmost figure presents the filtration unit graphically, indicating the direction of movement for the piston and the recovery point for the filtrate. The figure in the middle represents the entire cylindrical filtration unit. The HTC treated sludge was placed onto a filter cloth inside the cylinder. The rightmost figure presents the obtained cake or hydrochar after the separation by filtration.



PUBLICATION  
III

**The effects of digestate pyrolysis liquid on the thermophilic anaerobic digestion of sewage sludge—Perspective for a centralized biogas plant using thermal hydrolysis pretreatment**

Anna Hämäläinen, Marika Kokko, Pritha Chatterjee, Viljami Kinnunen & Jukka Rintala

Waste Management, 147, 73–82  
<https://doi.org/10.1016/j.wasman.2022.05.013>

**Publication reprinted with the permission of the copyright holders.**





## Country report

# The effects of digestate pyrolysis liquid on the thermophilic anaerobic digestion of sewage sludge — Perspective for a centralized biogas plant using thermal hydrolysis pretreatment

Anna Hämäläinen<sup>a,\*</sup>, Marika Kokko<sup>a</sup>, Pritha Chatterjee<sup>a,c</sup>, Viljami Kinnunen<sup>b</sup>, Jukka Rintala<sup>a</sup>

<sup>a</sup> Faculty of Engineering and Natural Sciences, Tampere University, P.O.Box 541, 33104 Tampere University, Finland

<sup>b</sup> Gasum Ltd., Revontulenpuisto 2C, 02100 Espoo, Finland

<sup>c</sup> Department of Civil Engineering, Indian Institute of Technology Hyderabad, Hyderabad, India



## ARTICLE INFO

## Keywords:

Anaerobic digestion  
 Digested sewage sludge  
 Pyrolysis liquid  
 Thermal prehydrolysis

## ABSTRACT

The use of pyrolysis process to valorize digestate from anaerobic digestion (AD) of municipal sewage sludge for biochar production was piloted in a central biogas plant. The pyrolysis also generates pyrolysis liquid with high organics and nutrient contents that currently has no value and requires treatment, which could potentially be done in AD. As the pyrolysis liquid may contain inhibitory compounds, we investigated the effects of adding the pyrolysis liquid on AD of sewage sludge and thermal hydrolysis pretreated sewage sludge (THSS) simulating the full-scale centralized biogas plant conditions. In batch assays, the pyrolysis liquid as such did not produce any methane, and the 1% and 5% (v/w) shares suppressed the methane production from THSS by 14–19%, while a smaller decrease in methane production was observed with sewage sludge. However, in the semi-continuous reactor experiments, pyrolysis liquid at a 1% (v/w) share was added in sewage sludge or THSS feed without affecting the methane yields or digestate characteristics. The laboratory results indicated that pyrolysis liquid can be treated in AD, while extrapolating the results to the centralized biogas plant indicated minor increase in the overall methane production and an increased potential for ammonium recovery.

## 1. Introduction

For decades, anaerobic digestion (AD) has been a common technique used for sanitizing sewage sludge, and the importance of the produced biogas has also increased, along with targets to produce renewable energy. Recently, large-scale centralized biogas plants have been implemented to improve the economics of sludge management and, for example, to promote the economics of upgrading biogas so that it can be used in vehicles. At the same time, promoting sustainability for example through using of the sludge nutrients, has created the need for upgrading the digestate into a more economically transferable and safe product. The need for digestate upgrading is urgent because the use of digested sewage sludge as such in agriculture is limited, which stems from the concern regarding the potential presence of organic contaminants, pathogens, microplastics, and heavy metals (Alvarenga et al., 2015; Corradini et al., 2019). Thus, AD process of sewage sludge requires complementing technologies to ensure the efficient use of nutrients while enhancing the utilization of the energy potential of sewage sludge.

Different technologies have been integrated or studied in sewage

sludge management systems that utilize AD, such as thermal hydrolysis pretreatment (THP) of the feed, which aims at destroying pathogens and improving biogas production through the solubilization of organics (Barber, 2016; Bougrier et al., 2008). THP is conducted at temperatures of 120–180 °C and is more effective than standard hygienization (1 h at 70°C) in the destabilization of flocs and cell lysis, which leads to increased biodegradability and decreased viscosity of the sludge (Bougrier et al., 2008; Carrere et al., 2016). Applied or studied downstream treatment technologies for digestates from sewage sludge AD plants include the pyrolysis, combustion, and hydrothermal carbonization of the dewatered digestate, as well as evaporation and stripping of the liquid digestate (Hämäläinen et al., 2021; Salman et al., 2017). Coupling of these processing technologies with AD targets both the reduction of digestate volume and contaminants, as well as the increase in the concentration of nutrients and carbon, aiming to generate valuable and safe nutrient products or carbon sinks and/or additional energy recovery.

Pyrolysis has been studied for various biomasses such as lignocellulosic biomasses (Yogalakshmi, 2022) and waste materials, such as the organic fraction of municipal solid waste (Yang et al., 2018) and sewage

\* Corresponding author.

<https://doi.org/10.1016/j.wasman.2022.05.013>

Received 30 January 2022; Received in revised form 2 May 2022; Accepted 14 May 2022

Available online 25 May 2022

0956-053X/© 2022 The Author(s). Published by Elsevier Ltd. This is an open access article under the CC BY license (<http://creativecommons.org/licenses/by/4.0/>).

sludge (Naqvi et al., 2021) as well as for digestates from AD plants treating these type of waste materials (Pecchi and Baratieri, 2019). The pyrolysis of organic matter is conducted in the absence of oxygen, and it yields three product fractions: solid biochar, liquid pyrolysis oil and pyrolysis gas (Torri and Fabbri, 2014), the amounts and compositions of which are affected by the biomass feed composition and moisture content as well as the pyrolysis conditions, including temperature, applied heat transfer rates, and residence times (Bridgwater, 2012).

Pyrolysis is normally considered for biomasses with a low moisture content (below 10%) (Fonts et al., 2009), which is justified with energy balances because the water content of the feed is directly proportional to pyrolysis energy consumption (Kim and Parker, 2008) and to the water content of the resulting pyrolysis oil (Shen and Zhang, 2005). For waste materials with high initial moisture content, for example sewage sludge, a low moisture content has been achieved in laboratory studies using drying at < 110 °C (Naqvi et al., 2021), while in full-scale sewage plant scale-up evaluations drying is assumed to be accomplished by using heat from burning of pyrolysis gas (Li and Feng, 2018). However, because the potential integration of pyrolysis with AD and other units in the biogas plant has many alternatives, the integrated system should consider—besides the energy balance of the pyrolysis—the overall energy balance of the plant and the different uses of the plant products, including the fate of nutrients, carbon, and contaminants (Barry et al., 2019; Li and Feng, 2018; Naqvi et al., 2021). These different targets and options of sewage management plants also motivate the study of pyrolysis with less-dried feeds. For example, the effect of the feed moisture content (12.7–45.8%) and pyrolysis temperature (450–850 °C) on the three pyrolysis products generated from organic fraction of municipal solid waste has recently been studied, and this research has reported that the effect of the feed moisture content on the energy distribution in pyrolysis products was relatively small (Yang et al., 2018). However, the feed moisture content affected the composition as well as the anaerobic toxicity of the pyrolysis liquid which decreased with the increasing feed moisture content (Yang et al., 2018). Furthermore, demonstration-scale trials concerning the implementation of pyrolysis in the centralized sewage biogas plant concept have shown that the preceding drying to > 90% total solids (TS) of digested sewage sludge may be costly, prompting to research on the pyrolysis for moist feed.

As a rule, lower pyrolysis temperatures (~290 °C) principally produce biochar, and higher temperatures (~750–900 °C) create pyrolysis gas, while moderate temperatures (~500 °C) mainly yield pyrolysis oil (Azuara et al., 2013; Bridgwater, 2012). Pyrolysis of slow heat transfer rates and long residence times (slow pyrolysis) generate mainly biochar, compared with fast heat transfer rates and short residence times that target for pyrolysis oil production, while intermediate conditions (intermediate pyrolysis) generate lower viscosity and tar content pyrolysis oils compared with fast pyrolysis (Hornung, 2012). The pyrolysis oil (yield 45–50 w%) from intermediate pyrolysis tends to be divided into two phases: a tarry organic phase (bio oil) (52–57% of the pyrolysis oil) and an aqueous phase (pyrolysis liquid 43–48%) (Bridgwater, 2012; Park et al., 2008; Torri and Fabbri, 2014). The pyrolysis oil from sewage sludge contains a variety of compounds including acids, alcohols, amines, and aldehydes originating from the sludge and the reactions taking place in the pyrolysis itself, but only 2–10 w% of water (Park et al., 2008), hence enabling its potential utilization in fuel applications or in the manufacture of chemicals (Bridgwater, 2012). The pyrolysis liquid is mostly comprised of water, the content of which depends on the pyrolysis temperature (Fonts et al., 2012), the biomass ash content and the number of OH-groups in the sewage sludge digestate (Fonts et al., 2009). The pyrolysis liquid originating from digested sewage sludge contains polar ketones and amines (Park et al., 2008) as well as volatile fatty acids (VFAs), ammonium-nitrogen and phenolics (Seyedi et al., 2019).

Although the bio oil fraction from pyrolysis is considered a useful product, the pyrolysis liquid from sewage sludge digestate often represents a waste management issue because of its low heating value and

disposal regulations and thus, requires careful management (Torri and Fabbri, 2014). One option for managing the liquid from sewage sludge digestate pyrolysis is feeding it to the AD process. This approach could yield some additional methane (Hübner and Mumme, 2015) and could avoid supplementary wastewater treatment units or the need for increased capacity in the biogas plant. Furthermore, it could replace some dilution water used in centralized biogas plants to adjust the feed moisture prior to AD. However, feeding the pyrolysis liquid to AD may pose some risks to operating the AD process because those liquids from the pyrolysis of several biomasses have been found inhibitory in anaerobic batch tests (Hübner and Mumme, 2015; Yang et al., 2018), while only a couple of continuous flow anaerobic reactor studies enabling microbial adaptation are available (Seyedi et al., 2020; Torri and Fabbri, 2014). Thus, the effects of pyrolysis liquid on AD should be determined case by case.

The current study deals with a centralized biogas plant producing vehicle fuel from dewatered sewage sludge of several sewage plants. The biogas plant has several years of experience on the THP of the sewage sludge (referred here as THSS) and, for example, on ammonium recovery from the liquid fraction of the digestate. The plant has interest to screen different methods to develop digestate utilization, and thus, also pyrolysis for biochar production was piloted. As there was concern about the treatment of the produced pyrolysis liquid, its utilization and treatment in the existing AD of the biogas plant was studied in laboratory-scale simulating conditions of the full-scale plant.

The objective of the current study was to evaluate the effect of the pyrolysis liquid of digested sewage sludge on the performance of AD treating sewage sludge or THSS. The studied pyrolysis liquid originated from a pilot-scale pyrolysis, operated with relatively high moisture content digested sewage sludge (70–80% TS) from a full-scale centralized biogas plant applying THP and AD. The influence of the pyrolysis liquid on methane production was first studied in batch assays, after which the long-term operation was studied in continuously stirred tank reactors (CSTR). Subsequently, the feasibility of treating the pyrolysis liquid in AD was determined by using the laboratory results and the mass balances of the centralized biogas plant.

## 2. Materials and methods

### 2.1. Feeds, pyrolysis liquid, and anaerobic inoculum

In the current study, sewage sludge or THSS (thermal hydrolysis with Cambi®, 130–140 °C, 4 bar for 20 min) were used as the feeds for AD. The sewage sludge and THSS were collected every three to four months over the course of study from the reception and feed tank of thermophilic AD digester at the Topinoja centralized biogas plant (Turku, Finland), which annually treats 75,000 t (ca. 22% TS, 16,500 t-TS/a) of dewatered sewage sludge from six municipal wastewater treatment plants.

In the reception tank of the biogas plant from where the sewage sludge sample was taken, dewatered sludge obtained from various wastewater treatment plants is mixed as such and diluted with clean water to around 16% TS before being fed to the THP process semi-continuously, where the temperature is raised with steam injection (leading to a dilution to 12% TS content). The THP-treated sludge and condensate from the THP process led to the AD process. For the current study, a THSS sample was taken from the AD feeding line. Non-condensable gases from THP are directed to the AD process through a different route and, thus, are not present in the THSS sample used in the present study.

Pyrolysis liquid was obtained from an intermediate pyrolysis pilot treating mechanically dewatered digestate (TS 30%) at the Topinoja biogas plant. The pilot pyrolysis process comprised of a screw pre-dryer and vacuum dryer that in addition to removing water (TS content increased to 70–80%) also pre-heated the sludge for the following pyrolysis unit that had two screw-type reactors operating in parallel and at

normal pressure. The pilot had a capacity of 600–800 kg/h. The pyrolysis temperature was around 400 °C, and the residence time was around one hour. The approximate product mass rates from the pyrolysis were 150–200 kg/h sludge biochar, 50–70 kg/h pyrolysis gas, and 50–70 kg/h pyrolysis liquid, which contained both oil and aqueous liquid that were not further fractionated and used.

The inoculum used for the anaerobic batch and CSTR experiments (conducted at 55 °C) was digestate from the thermophilic digester at the Topinoja biogas plant. The sewage sludge, THSS, digestate, and pyrolysis liquid were stored at 4 °C for less than three months before being used in the experiments. Table 1 presents the characteristics of the feeds and inoculums used. The pyrolysis liquid sample used in this study was not analyzed for other parameters, but analyses of other samples from the same pilot has shown that in the pyrolysis liquid all halogens were below detection limit, except Cl (0.028 wt-%), all mineral oils (C10–C40) were below detection limit (<30–150 mg/kg), all metals were below 170 mg/kg, except S (2800 mg/kg), and all heavy metals (Cd, Co, Cr, Cu, Pb, Ni, Mo, V, Hg) were below 10 mg/kg. Table 1 also shows the computational THSS characteristics (as a reference to sewage sludge), illustrating the effects of THP on the sludge characteristics when the effect of dilution in the THP process with steam (from 16 to 10% TS) is extracted (calculations are shown in Section 2.4).

## 2.2. Biochemical methane potential assays

The biochemical methane potentials (BMP) of the sludge substrates alone and those amended with pyrolysis liquid—as well as pyrolysis liquid alone—were determined at thermophilic (55 °C) conditions. The BMP assays were conducted in triplicate in 120 mL serum bottles with a liquid volume of 60 mL. The inoculum volatile solids (VS) content in the batches was set to 7.7 g/L. A  $V_{\text{substrate}}/V_{\text{inoculum}}$  ratio of 0.5 was used in all batches other than the one containing only pyrolysis liquid, in which the substrate concentration was set to 1.4 g of the soluble chemical oxygen demand (SCOD) per liter. The pyrolysis liquid was added in volumes of 1% or 5% of the wet weight of the substrate (v/w) in question (sewage sludge or THSS). Each batch also contained 5 g/L of buffer (NaHCO<sub>3</sub>), and distilled water was added to reach volumes of 60 mL. The initial pH (>8) was adjusted to between 7 and 8 with 1 M HCl, after which the bottles were closed with gas-tight rubber stoppers. Anaerobic conditions were created inside each bottle by flushing it with nitrogen gas for three minutes. Assays containing only inoculum, buffer, and water functioned as a blank, and their methane production was subtracted from the methane production of the sample assays. The methane concentrations were measured one to three times a week, and prior to every measurement, the bottles were manually shaken to mix the contents. The methane concentration was analyzed with a Perkin Elmer Clarus 500 gas chromatograph flame ionization detector (GC-FID)

using He as the carrier gas, as described in Kokko et al. (2018), and the methane volume was calculated from the methane percentage in the serum bottle headspace as described in Angelidaki et al. (2009). The methane concentrations and volumes were reported as the averages of the triplicate assays.

## 2.3. Reactor experiments

Three parallel 6 L semi-continuously fed CSTRs (Kinnunen et al., 2015) (referred to as R1, R2, and R3) were operated for 221 d at 55 °C. The working liquid volume was 4 L, except for R3, in which it was decreased to 3.5 L on day 143 to manage sludge floating. Heating coils in an insulated frame with water recirculation provided a constant temperature for the reactors. The reactor contents were mixed with a mechanical mixer (11 rpm) operated for 30 min at 30-minute intervals until day 140, after which mixing was changed to a continuous mode. The reactors were fed 5 d per week, and prior to every feeding, a measured mass of digestate (reactor content) was removed to keep the reactor liquid surface level constant. The mixing was stopped while feeding. The biogas produced was collected in 10 L aluminum gas bags (Supelco) via gas-tight tubes (Masterflex Tygon).

The reactors were inoculated with 4 L of thermophilic inoculum, before which the inoculum was warmed in a closed container to the reactor temperature in a 55 °C water bath for 2 d. The feeding began the following day after inoculation, which is referred to as day 0. The reactors were manually fed every weekday according to the desired organic loading rate (OLR) by taking the mass of sewage sludge or THSS feed that had the precise amount of daily VS.

The operational parameters of the reactor setup are shown in Table 2. The initial OLR was 3 kg-VS/m<sup>3</sup>d and hydraulic retention time (HRT) 19.6 d, which were used to simulate the operation parameters used in the full-scale plant that the materials originated from.

For the first 44 d, all three reactors received THSS, after which the feed was changed in one reactor (R3) to sewage sludge diluted to the same VS content as THSS (from 11.8% to 7.8% TS) with tap water. From day 77 onwards, the feeds of all three reactors were adjusted by dilution (1.5 times (R1 and R2) or 2.25 times (R3)) with tap water to achieve the desired OLR and HRT. The reactors fed with THSS (R1) and sewage sludge (R3) were adjusted similarly to have OLR and HRT of 2.3 kg-VS/m<sup>3</sup>d and 13 d, respectively, whereas the other THSS-fed reactor (R2) was operated with higher OLR of 3 kg-VS/m<sup>3</sup>d and HRT of 12 d. At this point, the addition of pyrolysis liquid began (0.15% of the wet mass of the feed (v/w)) in the THSS (R2) and sewage sludge (R3) feeds, while the reactor fed with THSS only (R1) served as the control. Later, the share of pyrolysis liquid (in R2 and R3) was increased to 0.5% (v/w) on day 86 and further to 1% (v/w) on day 149. The pyrolysis liquid shares of 0.15%, 0.5% and 1% (v/w) of the feed corresponded to 1.8–2.5%, 6.2–8.1%,

**Table 1**

Characteristics of sewage sludge, THSS, and pyrolysis liquid used in the batch and reactor experiments. THSS computational is calculated by considering the impact of dilution with steam during THP, while the measured THSS also includes the dilution factor from using steam. The thermophilic digestate was used as the inoculum.

	Sewage sludge	THSS computational	THSS measured	Pyrolysis liquid	Thermophilic digestate
pH	6.3	n.a.	6.1	9.1	7.9
TS (%)	15.6 ± 0.5	15.6	10.1 ± 1.0	0.12	8.6 ± 0.3
VS (%)	11.8 ± 0.5	11.8	7.7 ± 0.8	0.08	5.4 ± 0.4
VS/TS (%)	76 ± 0.3	76	76 ± 0.7	67 ± 2.6	62 ± 0.1
COD (g/L)	n.d.	143.5	93.4 ± 11.5	3.7 ± 0.1	69.9 ± 5.9
SCOD (g/L)	35.9 ± 0.5	49.5	32.2 ± 1.4	3.6	21.8 ± 1.5
TVFA (g-COD/L)	21.9 ± 1.7	10.0	6.5 ± 1.4	0.9 ± 0.1	2.0 ± 0.1
Total nitrogen (g/kg-TS)	n.d.	104	68 ± 0.3	n.d.	101
Total soluble nitrogen (mg/L)	7775	6989	4550	3600	6875
NH <sub>4</sub> <sup>+</sup> -N (mg/L)	932.8	1061	691	61.5	4885
PO <sub>4</sub> <sup>3-</sup> (mg/L)	2950	2309	1503	7.1	2302
BMP (L-CH <sub>4</sub> /kg-VS)	332.8 ± 28.6	n.a.	342.1 ± 3.2	0	59.3 ± 4.0

THSS: thermally pretreated sewage sludge, TS: total solids, VS: volatile solids, COD: chemical oxygen demand, SCOD: soluble COD, TVFA: total volatile fatty acids, TKN: total Kjeldahl nitrogen, n.a. not applicable, n.d. not determined.

**Table 2**  
Operational parameters and results from the reactor experiments. The results are the averages from the last HRT or the week of the period in question.

Feed	Reactor												
	R1			R2			R3			SS			
Days	THSS	THSS	THSS	THSS	THSS	THSS	THSS	THSS	THSS	THSS	THSS	THSS	THSS
OLR (kg-VS/m <sup>3</sup> ·d)	0–76	77–125	130–221	0–76	77–85	86–125	130–152	153–221	0–44	45–76	77–85	86–125	130–152
HRT (d)	3	2.3 <sup>a</sup>	1.2 <sup>a</sup>	3	3 <sup>a</sup>	3	1.7 <sup>a</sup>	1.2 <sup>a</sup>	3	3	2.4 <sup>a</sup>	2.4 <sup>a</sup>	1.3 <sup>a</sup>
Pyrolysis liquid (v/w)	0	0	0	0	0	0	0	0	0	0	0	0	0
Feed TS (%)	10.1	5.9	5.9	10.1	8.1	8.1	8.1	5.9	10.1	10.0	6.0	6.2	5.8
Feed VS (%)	7.7	4.4	4.4	7.7	6.1	5.9	5.9	4.4	7.7	7.8	4.3	4.5	4.1
Methane yield (L-CH <sub>4</sub> / kg-VS)	200 ± 41	406 ± 112	362 ± 32	245 ± 15	233 <sup>b</sup>	349 ± 32	378 ± 32 <sup>c</sup>	361 ± 54	121 ± 96	88 ± 12	106 <sup>b</sup>	162 ± 5	456 ± 126 <sup>c</sup>
Methane concentration (%)	57 ± 5	62 ± 4	64 ± 6	59 ± 5	58 ± 4 <sup>b</sup>	63 ± 5	63 ± 4	65 ± 7	57 ± 9	53 ± 4	56 ± 4 <sup>b</sup>	60 ± 3	62 ± 4
VS-removal (%)	23 ± 8	48 ± 7	67 ± 3	28 ± 2	n.d.	55 ± 4	60 ± 0.3	71 ± 1	28 ± 2	22 ± 6	n.d.	46 ± 3	67 ± 2
Digestate characteristics													
VFA (g-COD/L)	13 ± 2	7 ± 2	0.3 ± 0.3	14 ± 2	11 ± 1	4 ± 3	2 ± 0.5	0.3 ± 0.3	9 ± 2	16 ± 3	14 ± 4	7 ± 1	6 ± 1
SCOD (g/L)	34 ± 2	20 ± 3	8 ± 2	36 ± 2	34 ± 3	13 ± 3	11 ± 1	7 ± 1	36 ± 4	36 ± 2	35 ± 1	23 ± 1	21 ± 1
pH	7.6 ± 0.2	7.7 ± 0.2	7.8 ± 0.1	7.6 ± 0.2	7.7 ± 0.1	7.7 ± 0.2	7.9 ± 0.1	7.8 ± 0.1	7.6 ± 0.2	7.6 ± 0.2	7.4	7.6 ± 0.1	7.7 ± 0.1

OLR: organic loading rate, HRT: hydraulic retention time, VS: volatile solids, TVFA: total volatile fatty acids, SCOD: soluble chemical oxygen demand, <sup>a</sup> diluted feed, <sup>b</sup> one week measurement only, <sup>c</sup> average of 0.77 HRT, n.d.: not determined.

and 17–17.4% of the fed amount of TS in feed, respectively, which simulated the potential share (15.5% of the AD feed TS content) at the full-scale biogas plant. On day 130, OLRs were reduced, and HRT was increased to 26 d in all reactors because of the high VFA and SCOD concentrations in the reactors (Table 2). On day 153, the OLR in R2 was further reduced to the same level as in R1 and R3. The feeding of the reactors paused between days 125 and 129 because of technical issues leading to a decrease in the temperature to room temperature.

2.4. Analyses and calculations

TS and VS were gravimetrically determined according to standard methods (APHA 2540). The pH of the samples was measured with a WTW pH 3210 m using a WTW SenTix® 41 electrode.

Total Kjeldahl nitrogen (TKN) was analyzed, as described in Kokko et al. (2018), and total soluble nitrogen, ammonium-nitrogen (NH<sub>4</sub><sup>+</sup>-N), and phosphate phosphorous (PO<sub>4</sub><sup>3-</sup>-P) were analyzed using Hach Lange kits (LCK303, LCK305, LCK338, LCK238, LCK349) according to the instructions provided by the supplier.

VFAs were determined with GC-FID, as described in Kokko et al. (2018). Total chemical oxygen demand (COD) and SCOD were analyzed according to Finnish standard methods (SFS 5504). The samples for SCOD and VFA analyses were centrifuged twice at 4000 rpm (15 min) before being filtered through 0.45 μm (Chromafil Xtra PET) and stored at 4 °C after conservation with 4 M H<sub>2</sub>SO<sub>4</sub> and at –20 °C, respectively. For VFA analysis, a second equivalent filtration also preceded analysis. All analyses were conducted within a week of sample collection.

The volume of biogas produced in the CSTRs was measured three times a week (Monday, Wednesday, and Friday) using the water displacement method, and its content (CH<sub>4</sub> and CO<sub>2</sub>) was analyzed, as described in Mönkäre et al. (2015). The specific methane yield was calculated for each week by summing the methane produced during a week (Monday to Monday) and the VS added during the week (Monday to Friday). The reactors were fed for 5 d a week, but the OLR in kg-VS/m<sup>3</sup> d is expressed as the average daily amount of VS fed to the reactors over a one-week period. The reactor results (Table 2) cover the average of the results from the time of the latest HRT because it was assumed that the digestive conditions were stable enough after a reasonable adaptation period to reliably describe the applied conditions, rather than the adaptation to the conditions.

To differentiate the effects of THP treatment from dilution by steam in the THP process on sewage sludge characteristics, a computational THSS was calculated (Eq (1)) that eliminates the effects from dilution with steam, as follows:

$$THSS_{computational} = THSS_{measured} \cdot \frac{TS_{THSS_{measured}}(\%)}{TS_{sewagesludge}(\%)} \tag{1}$$

3. Results and discussion

3.1. Feeds, pyrolysis liquid, and inoculum characterization

The TS content of sewage sludge and THSS were 10.1% and 15.6%, respectively, here with a VS/TS ratio of 76. The difference in the TS of sewage sludge and THSS is because of the addition of water in the THP process in the form of steam providing heat energy and solid solubilization caused by the treatment temperature (Bouquier et al., 2008). The aim of thermal pretreatment is to inactivate pathogens and/or increase the solubility of the substrate by degrading and subsequently solubilizing polymers, such as fats and proteins. The increased solubility of organics can be measured, for example, by SCOD and VFA concentrations (Astals et al., 2012; Xue et al., 2015). Hence, in the current study, by comparing sewage sludge with the computational THSS, the SCOD concentration increased after THP compared with sewage sludge (49.5 vs. 35.9 g/L), confirming enhanced solubility. However, as the total volatile fatty acid (TVFA) content simultaneously decreased from 21.9 g-



COD/L of sewage sludge to 10 g-COD/L in computational THSS, it is likely that VFAs evaporated during THP and ended up mostly in the non-condensable gases fed directly to the AD reactor. The total soluble nitrogen concentration in sewage sludge (7775 mg/L) was slightly higher than in computational THSS (6989 mg/L), but the ammonium-nitrogen to total soluble nitrogen ratio was higher (0.15) in computational THSS than in sewage sludge (0.12). The decrease in total soluble nitrogen can be a result of protein hydrolysis leading to ammonia formation and subsequent evaporation during THP.

The pilot-scale pyrolysis (400 °C, 1 h, 70% TS) of 1,000 kg of mechanically dewatered thermophilic digestate (30% TS) generated 200 L of pyrolysis liquid with a COD of 3.7 g/L, of which VFAs contributed 0.9 g-COD/L. In addition to VFAs, the COD in the pyrolysis liquid also comprise many other organics, found from other pyrolysis liquid samples generated at the same pilot-scale pyrolysis, including phenols (0.4 wt-%), nitrogen-containing compounds (0.7 wt-%), alcohols (0.2 wt-%), and aldehydes (0.1 wt-%). In addition to these substances, oxygenated hydrocarbons and methoxy-substituted aromatics originating from the digestate are formed by the pyrolysis reactions and which are possibly inhibitory to anaerobic microorganisms (Hübner and Mumme, 2015; Seyedi et al., 2020). The COD and the TVFA concentrations of the present pyrolysis liquid were much lower than those reported for the pyrolysis liquid (COD of ca. 200 g/L and TVFA of 26 g-COD/L) obtained from a pyrolysis at 800 °C of a commercially dried biosolid consisting of a mixture of digested primary sludge and raw waste activated sludge (Seyedi et al., 2019); this is likely because of the different origin, composition, and higher moisture content (20–30%) of the pyrolysis feed and much lower pyrolysis temperature (400 °C) used in the current study, as also reported by Yang et al. (2018). The VFAs in the present pyrolysis liquid comprised acetic acid (37% of the TVFA), butyric acid (24%), and valeric acid (39%), while in the pyrolysis liquid (800 °C) originating from the above-mentioned biosolids the dominant VFA (90%) was acetic acid (Seyedi et al., 2019).

The total soluble nitrogen content in the pyrolysis liquid was 3.6 g/L, of which 61 mg/L was ammonium-nitrogen, and the phosphate concentration was 7 mg/L. Nitrogen is more soluble in thermal treatments than phosphorus which tends to end up in the biochar fraction (Barry et al., 2019). The total nitrogen and ammonium-nitrogen concentrations in the present pyrolysis liquid were 7–10-fold lower than what has been reported for a pyrolysis liquid (25.6 g/L of total nitrogen) from dried sewage sludge (91% TS) produced at 350 °C (Yue et al., 2019) and for a pyrolysis liquid from commercial biosolids produced at 800 °C (63 g/L in ammonia-nitrogen) (Seyedi et al., 2019). The nitrogen compounds can be attributed to the alkalinity of the pyrolysis liquid (Azuara et al., 2013), which seems typical for pyrolysis liquids of a sewage sludge origin (Seyedi et al., 2019; Yue et al., 2019). In the studied pyrolysis liquid, the main cause for the alkaline pH of 9.1 may be the low TVFA concentration and presence of buffering compounds (Villamil et al., 2018).

### 3.2. BMP assays

The effect of pyrolysis liquid (1% or 5% (v/w) shares) on methane production both from sewage sludge and THSS was assessed in BMP assays, and as a reference, methane production from sewage sludge or THSS was assessed as such, as well as methane production from pyrolysis liquid alone (Fig. 1).

Methane production started in all batches with sludges with small deviations and most (>95%) of the methane was produced in around 30 d. The methane production from parallel runs of sewage sludge batches was more scattered than that of THSS, which could be because of the higher heterogeneity of sewage sludge compared with THSS. The BMPs of the sewage sludge and THSS were  $333 \pm 29$  and  $342 \pm 3$  L CH<sub>4</sub>/kg-VS, respectively. The pyrolysis liquid alone did not produce any methane, indicating that the COD in the pyrolysis liquid was not readily biodegradable and/or that it contained some inhibitory compounds

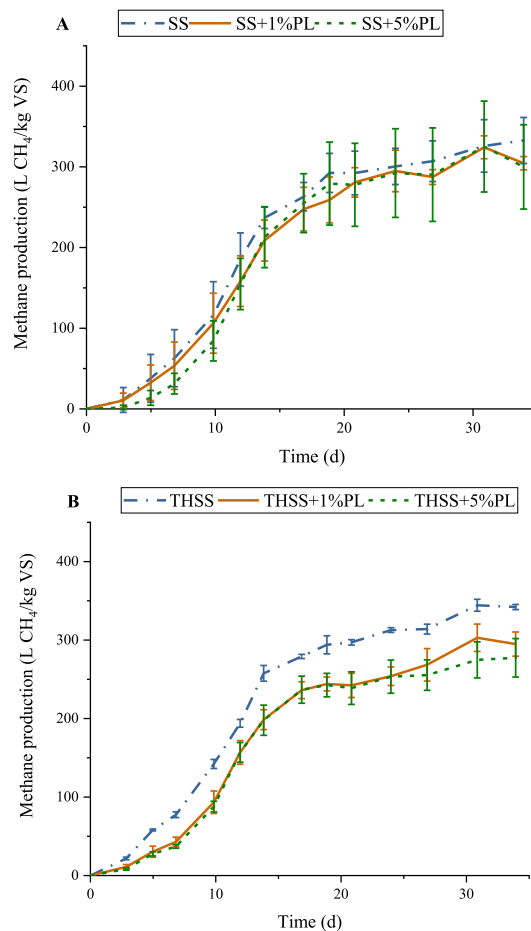


**Fig. 1.** Cumulative methane production in thermophilic (55 °C) BMP assays of sewage sludge (A) and THSS (B) with 0%, 1%, and 5% shares (v/w) of pyrolysis liquid. The inoculum methane production has been subtracted from the results. The intersecting vertical lines represent standard deviations for the averages of the methane productions from the triplicate batches. SS: sewage sludge, THSS: thermally hydrolyzed sewage sludge, PL: pyrolysis liquid.

preventing methane production (see Section 3.1). The addition of pyrolysis liquid decreased methane production from THSS: after 10 d of batch digestion, the methane production with 1% or 5% (v/w) shares of pyrolysis liquid was 66% and 62% of the methane production from THSS alone, respectively. After 20 d, 82% and 80% of the methane were produced, respectively. THSS with 1% and 5% (v/w) additions of pyrolysis liquid eventually resulted in 14% and 19% lower BMPs, that is,  $295 \pm 15$  L CH<sub>4</sub>/kg-VS and  $277 \pm 25$  L CH<sub>4</sub>/kg-VS, respectively, than THSS ( $342$  L CH<sub>4</sub>/kg-VS). In contrast, methane production from sewage sludge seemed nearly unaffected by the addition of pyrolysis liquid. Only the batches with 5% (v/w) of pyrolysis liquid started to produce methane with a 3-d delay, and after 12 d, the difference in methane production was around 12%, and the final BMP value difference was 10% ( $305 \pm 8$  L CH<sub>4</sub>/kg-VS for 1% (v/w) of pyrolysis liquid and  $300 \pm 52$  L CH<sub>4</sub>/kg-VS for 5% (v/w)). The fact that THSS was more inhibited than sewage sludge could be because of the different VFA contents of these substrates because this sewage sludge contained more VFAs than THSS. Because of the higher VFA content, the starting of methane

production could be faster from sewage sludge, which could diminish the inhibitory impacts of pyrolysis liquid (Torri and Fabbri, 2014).

Pyrolysis liquid seemed to have inhibitory effects on methane production, with THSS already at a 1% (v/w) share. Previously, pyrolysis liquid from sewage sludge at a 6% (v/w) share has been reported to delay and decrease the methane production in batch assays from cow dung by doubling the time before the peak production of methane was reached relative to the production without pyrolysis liquid addition (Yue et al., 2019). Thus, the treatment or disposal of pyrolysis liquid alone through AD was considered unattractive (Yue et al., 2019). It is also noteworthy that the different proportions (1% vs. 5% (v/w)) of the present pyrolysis liquid added to THSS resulted in similar BMPs. This would indicate that the present pyrolysis liquid contained at least some of the above-mentioned inhibitory compounds, i.e., nitrogen-containing compounds, phenols, and/or their derivatives, concentrations of which were already sufficient at the lower pyrolysis liquid share to hinder the microorganism activity.

The BMP results suggested that the pyrolysis liquid had a negative effect on methane production and slowed down the start of methane production from sewage sludge and THSS, which was further studied in the CSTR studies. Because of the decrease of 14–19% in methane production in BMP assays from THSS upon the addition of 5% (v/w) pyrolysis liquid, a lower share in the CSTR studies was used (Section 3.3.).

### 3.3. Reactor experiments

The AD of sewage sludge and THSS with and without pyrolysis liquid were studied in three laboratory CSTRs at 55 °C (Fig. 2, Table 2). For the first 44 d of operation, all three reactors received THSS at an OLR of 3 kg-VS/m<sup>3</sup>d and HRT of 19.6 d, which were the operation parameters of the full-scale plant the materials originated from. On day 45, one of the reactor feeds (R3) was changed to sewage sludge while keeping the OLR and HRT the same.

In the beginning of the runs (days 1–44), the methane yields in all three reactors increased up to 143–174 L/kg-VS and SCOD concentrations to 34–37 g/L (Fig. 2). As a result of the change of the feed to sewage sludge (R3), the methane yield decreased to 88 ± 12 L/kg-VS, while in the reactors fed with THSS, the methane yields increased to above 200 L/kg-VS. The SCOD concentrations in all three reactors remained at 34–36 g/L, and the TVFA concentrations steadily increased from 4 to 8 g-COD/L to 11–14 g-COD/L, here with propionate and isovalerate as the main VFAs. The instabilities and incomplete feed degradation during days 0–76 were likely because of the high OLRs (3 kg-VS/m<sup>3</sup>d) that resulted in overloading the reactors and accumulation of TVFAs, though similar or even higher (up to 6 kg-VS/m<sup>3</sup>d) OLRs were used at the full-scale plant. The reason for the accumulation of VFAs in the laboratory runs could not be traced, but it could also be because of the different feeding regimes because in the laboratory, the feeding was once a day for 5 d a week, while the full-scale plant applied a more continuous feeding regime.

Starting from day 79, 0.15% (v/w) pyrolysis liquid was mixed to the feeds of one THSS (R2) and sewage sludge-fed reactors (R3), and after 6 d, the share was raised to 0.5% (v/w). The OLRs were also decreased to 2.3–2.4 kg-VS/m<sup>3</sup>d (R1, R3) on day 77 by diluting the feeds, while in R2, the OLR was held at 3 kg-VS/m<sup>3</sup>d. These results indicate that the addition of pyrolysis liquid did not have a drastic (negative) effect on the process; rather, the dilutions and changes in OLRs resulted in an increase in the methane production of each reactor and decrease in VFA concentrations (Table 2). At the end of the period (days 77–125), the methane yield from THSS (R1) increased up to 406 ± 112 L/kg-VS, while those from THSS (R2) and sewage sludge (R3) amended with pyrolysis liquid had smaller increases up to 349 ± 32 L/kg-VS and 162 ± 5 L/kg-VS, respectively (Table 2). The significant increase in methane production had likely derived from the methanation of the VFAs that had accumulated before day 77 because the TVFA concentrations decreased from 13 to 14 g-COD/L to 7 ± 2 g-COD/L (R1), 4 ± 2 g-COD/L

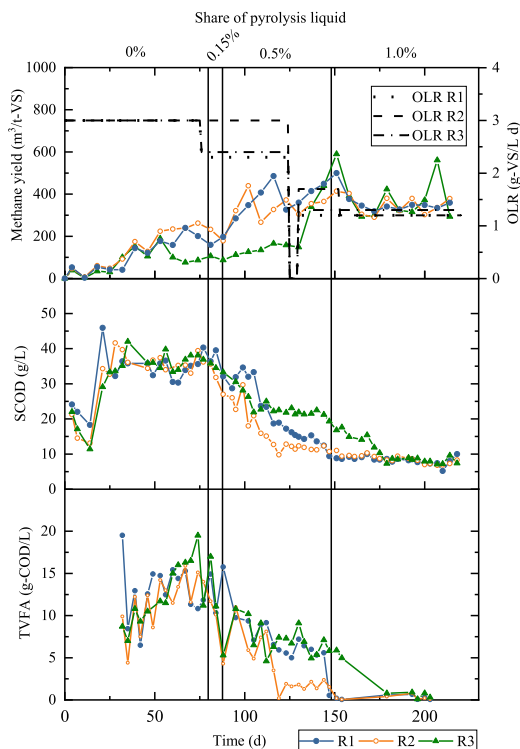


Fig. 2. The methane yields and OLRs used (A) in the reactor experiments with THSS (R1, R2, and R3) and sewage sludge (R3 from day 44 onwards), as well as the SCOD concentrations (B) and TVFA contents (C) of the reactor digestates. The pyrolysis liquid shares in the feeds of R2 and R3 as % (v/w) are marked above the graph. OLR: organic loading rate; SCOD: soluble chemical oxygen demand; TVFA: total volatile fatty acids. The feeding ended, and reactors were at room temperature during days 125–129; hence, the OLRs were reduced to zero.

(R2) and 7 ± 1 g-COD/L (R3). On day 77, the predominant VFAs were propionate (47–50%) and butyrate (26–27%) in the THSS-operated reactors (R1 and R2), but at the end of this period (day 125), the predominant VFA was propionate, accounting for 74–86% of the TVFAs. In contrast, the main VFAs on day 77 in the sewage sludge-operated reactor (R3) were propionate and acetate, comprising each about 35% of the TVFAs, and at the end of the period (day 125), the share of propionate increased to 54% while that of acetate declined to 14%. The SCOD concentrations also decreased from around 34–35 g/L to 20–23 g/L (R1, R3) and 13 g/L (R2).

Because of technical issues, the reactor temperatures declined to room temperature, so the reactor feeding ceased during days 125–129. On day 130, the TVFA concentrations were still rather high (4–7 g-COD/L) in R1 and R3; thus, OLRs were further decreased to 1.2 kg-VS/m<sup>3</sup>d (R1, R3) and 1.7 kg-VS/m<sup>3</sup>d (R2) to ensuring more complete organic degradation. The share of pyrolysis liquid was maintained at 0.5% (v/w). On days 130–152, the methane yields were around 380–450 L/kg-VS (R1 and R2) with THSS, while with sewage sludge, the methane yield increased from 162 L/kg-VS up to 456 L/kg-VS (R3). These methane yields were above the determined BMP values for THSS (342 L/kg-VS) and sewage sludge (333 L/kg-VS), indicating that accumulated SCOD and VFAs were still converted to methane. By day 152, the TVFA concentrations in R1 and R2 dropped to 0.2 g-COD/L, while in R3, TVFAs still comprised 5.9 g-COD/L.

On day 149, the pyrolysis liquid shares were raised to 1% (v/w) (R2, R3), and OLR in R2 decreased to 1.2 kg-VS/m<sup>3</sup>d (R2), while that in R3 was maintained at 1.3 kg-VS/m<sup>3</sup>d. The final period (from day 153 onwards) resulted in a similar methane yield in all three reactors, being 362 ± 32 L CH<sub>4</sub>/kg-VS (R1), 361 ± 54 L CH<sub>4</sub>/kg-VS (R2), and 376 ± 107 L CH<sub>4</sub>/kg-VS (R3). Sewage sludge amended with pyrolysis liquid (R3) had, however, more fluctuation in the methane yields, implying that the operation with sewage sludge was more unstable than with THSS. However, R3 had a smaller working volume, which may also have accounted for the differences in the results. The final running period also enabled efficient organic degradation, hence resulting in final TVFA contents of 0.3 ± 0.3 g-COD/L (R1), 0.3 ± 0.3 g-COD/L (R2), and 0.6 ± 0.4 g-COD/L (R3), as well as SCOD concentrations below 10 g/L. The VS removals were also the highest (67–71%) in all the reactors during the final period (Table 2).

The results show that mixing of pyrolysis liquid at 1% (v/w) in THSS (R2) and sewage sludge (R3) did not inhibit methane production, as confirmed by the similar methane yields and digestate characteristics in all three reactors during the stable operational period (days 153–221) when the digestates' TVFA and SCOD contents were at their lowest. All reactor digestates had a pH in the range of 7.4 to 8.0 for the entire operation (Table 2). The nutrient composition of the digestate did not show any difference from adding pyrolysis liquid; this was analyzed only during the last 22 d of operation (Table 3); rather, differences between the main feeds (THSS and sewage sludge) were observed. The ammonium-nitrogen concentrations increased 5-fold in the THSS digestates (up to 2,300 mg/L) and 3-fold in the digestates of sewage sludge (up to 1,370 mg/L) compared with the feeds. In addition, the relative amount of NH<sub>4</sub><sup>+</sup>-N from total soluble nitrogen in the THSS digestates was higher (63% (R1), 64% (R2)) than in the sewage sludge digestates (39% in R3). These results suggest that the ammonification of organic nitrogen was more exhaustive in the THSS reactors.

The higher methane yields toward VS with THSS than with sewage sludge (obtained when the higher OLRs (2.3–3 kg-VS/m<sup>3</sup> d) were used during days 0–125) may have been because of the THP promoting the hydrolysis step in AD. Thermal pretreatment usually enables increased loading rates and solid concentrations of the feed, thus increasing the methane yield (Higgins et al., 2017). Hence, it is likely that THSS had higher tolerance toward the higher OLRs and shorter HTRs than sewage sludge, which were used at the beginning of the reactor experiment (Table 2). However, when the OLRs and HRTs were decreased and prolonged, respectively, the sewage sludge-operated reactor (R3) started to produce methane superior to THSS reactors. A similar observation was obtained in one previous continuous reactor study: the reactor fed with THSS had higher OLRs than sewage sludge by having a 1.3-fold higher methane yield at an OLR of 3.8 kg COD/m<sup>3</sup> d, while increasing the OLR to 4.4 kg COD/m<sup>3</sup> d decreased the methane yield from sewage sludge by 5.4% but increased the methane yield from THSS by 6.2% (Choi et al., 2018). This may be because of the increased possibility of inhibition by ammonia and increased alkalinity and viscosity because the HRT is prolonged in THSS reactors, giving more time for protein degradation (generating ammonia) and for extracellular microbial by-

product formation, the reactions of which have been accelerated by THP (Barber, 2016).

The batch tests indicated that THSS was prone to inhibition by the pyrolysis liquid, whereas sewage sludge had less of a negative effect from the addition of pyrolysis liquid. One of the reasons for the difference in the susceptibility to inhibition of the two substrates, besides the differing VFA contents (see Section 3.2.), could be changes in C/N balance (review by Feng and Lin, 2017) which is possibly affected during THP. On the other hand, the semi-continuous reactor experiments showed no effect from the addition of pyrolysis liquid for either THSS or sewage sludge. The difference in the inhibitory effect by the pyrolysis liquid between the reactor experiment and the BMP assay could be accounted for the lower pyrolysis liquid shares and for the fact that the digestion process was already working when the pyrolysis liquid addition was started. It is possible that semi-continuous feeding is better suited for the addition of pyrolysis liquid than batch assays because it seems to allow the microorganisms to acclimate to the prevailing substrates and enable higher pyrolysis liquid loadings (Seyedi et al., 2020; Zhou et al., 2019). It has also been shown in anaerobic batch studies that the inhibitory effect stemming from pyrolysis liquid can be alleviated by the addition of either nutrients or biochar (or both together) that enhance the growth of the microbes or detoxify the inhibitory compounds, respectively (Wen et al., 2020). Seyedi et al. (2020) studied the co-digestion of synthetic primary sewage sludge with aqueous pyrolysis liquid from commercial biosolids in a long-term (523 d) semicontinuous reactor trial with stepwise increases in pyrolysis liquid load (from 0.05 (3% of fed sewage sludge COD) to 0.5 (25%) g-COD/L-d), demonstrating that the microorganisms were capable of acclimating to the addition of the pyrolysis liquid with no statistical difference in the methane productions between the control and pyrolysis liquid-supplied digesters at the end of the operation. Zhou et al. (2019) observed that pyrolysis liquid from corn stover, here as the only substrate in wastewater digester inoculum, yielded methane at up to 3% (v/v) share of the inoculum, but at higher shares (5–10%), the methane yields decreased and ceased, whereas in continuous mode (HRT of 20 d), even a loading of 18% (v/v) of pyrolysis liquid generated biogas (yield 90 mL/mL-pyrolysis liquid, of which 50–65% is CH<sub>4</sub>), though with a decreasing trend from a 6% pyrolysis liquid share (160 mL/mL-pyrolysis liquid). These aforementioned studies were conducted at a constant OLR and HRT of the feed (primary sludge or inoculum) (Seyedi et al., 2020; Zhou et al., 2019), while in the present study, OLR, and HRT were altered, along with the pyrolysis liquid share in the reactor experiment. Based on the above-mentioned results, pyrolysis liquid could be added to anaerobic digesters, but its origin and characteristics determine its applicable share of the main feed. In addition, it should be further examined whether greater OLR (>1.2 kg-VS/m<sup>3</sup>d) and shorter HRT (<26–30 d) than what has been used in the present study (during days 153–221) would be more sensitive to the presence of pyrolysis liquid because the studied conditions at 1% (v/w) pyrolysis liquid loading resulted in relatively robust reactor performance. Screening of optimum conditions, such as OLR, using laboratory reactor experiments is useful, as for example, even up to 50% higher methane yield per ton food waste with optimum OLR was achieved in a laboratory study (Megido et al., 2021).

**Table 3**

Nitrogen and phosphorous concentrations in the digestates of the reactor experiment. The values are the averages of three samplings of two parallel samples of the last 22 days of the operation of reactors (days 200–221) fed with THSS (R1), THSS amended with 1% (v/w) pyrolysis liquid (R2), or sewage sludge amended with 1% (v/w) pyrolysis liquid (R3).

Nutrient	Reactor		
	R1	R2	R3
Total nitrogen (g/kg-VS)	153 ± 5	165 ± 3	155 ± 9
Total soluble nitrogen (mg/L)	3530 ± 100	3590 ± 60	3490 ± 210
NH <sub>4</sub> <sup>+</sup> -N (mg/L)	2240 ± 57	2300 ± 142	1370 ± 107
PO <sub>4</sub> <sup>3-</sup> (mg/L)	1130 ± 100	1210 ± 130	1220 ± 90

#### 4. Practical implication

The present results and information from the Topinoja biogas plant have enabled the assessment of the effects of adding the pyrolysis liquid to the AD feed (Fig. 3) in case pyrolysis will be implemented in digester upgrading. An example of this assessment was conducted for the centralized Topinoja biogas plant using the amounts of sludge treated in the plant at the time of the experiments. Because the pyrolysis unit was operated at a pilot scale, its mass flows and product distributions were extrapolated to the Topinoja full-scale plant by mass-balance calculations.

The biogas plant treats approximately 75,000 t/a of sewage sludge

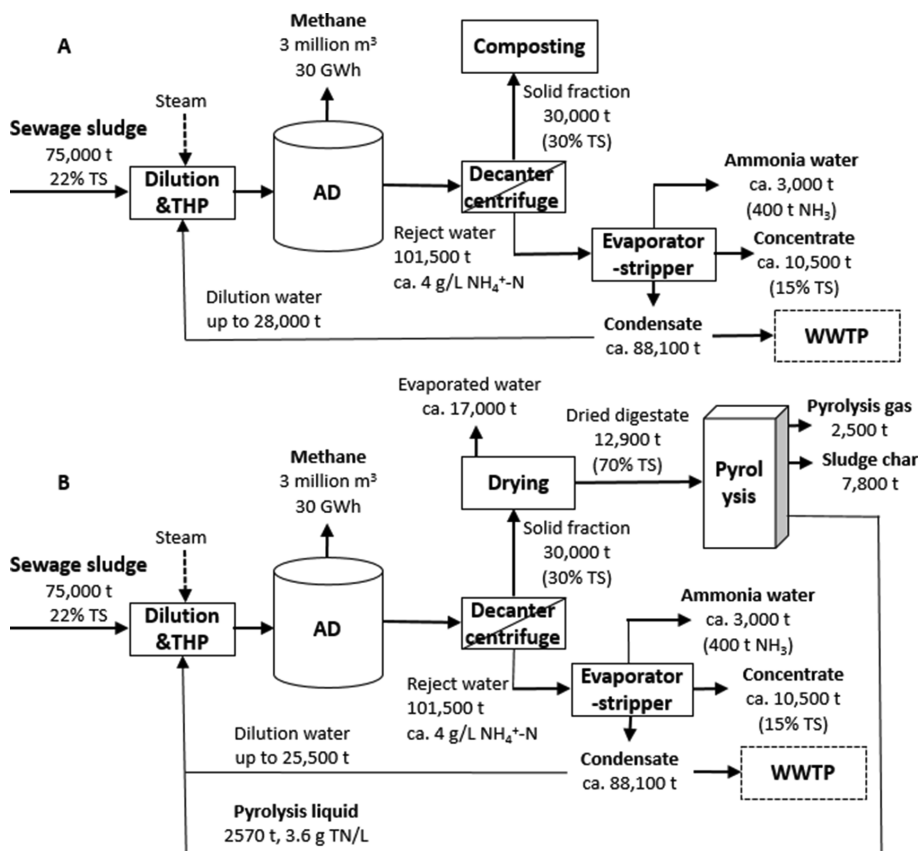


Fig. 3. The process layout of the biogas plant at the time of the experiments (A) and the extrapolation on the integration of a pyrolysis process unit into the same plant (B). The pyrolysis liquid would replace 9% of the dilution water. TS: total solids, TN: total nitrogen, NH<sub>4</sub>-N: ammonium-nitrogen. The structure for the layout has been adapted from Hämäläinen et al. (2021)

(dewatered to solid contents of ~ 22% TS before transporting to Topinoja). The sewage sludge is a mix of primary and secondary sludge from several wastewater treatment plants using an activated sludge process (simultaneous chemical phosphorus removal). In the Topinoja plant, sewage sludge is diluted to ca. 16% TS and then thermally hydrolyzed in a THP unit that uses steam to raise the temperature (TS decreases to ca. 12%), after which the feed (ca. 137,500 t/a) is fed to the AD process. The biogas plant generates ca. 30,000 t of dewatered digestate (TS 30%) annually, which is further composted and used for landscaping purposes. The reject water from the dewatering (ca. 101,500 t/a) is treated in an integrated evaporator-stripper process. The evaporator-stripper process produces around 3,000 t/a of ammonium water at 12–15 NH<sub>3</sub>-% concentration, which is around 10,500 t/a of concentrate at 15% TS, while the rest is relatively pure condensate water that is used as process water to replace clean water in sludge dilution; the rest of the condensate water is discharged to the municipal wastewater treatment plant. Because the dewatered digestate currently has a low-value use, pyrolysis of dewatered digestate could produce a new product—sludge biochar—allowing carbon sequestration and phosphorus recovery, potentially with economic value. The gas fraction from pyrolysis could be combusted for energy that would supply the energy required for the thermal drying of the digestate before pyrolysis, while the pyrolysis liquid is considered a waste stream, with its use remaining open.

If the pyrolysis was to be applied in full scale as in the pilot, the dewatered digestate (30,000 t/a) would enter the thermal and vacuum drying unit prior to pyrolysis. The drying unit dries the digestate to ca. 70% TS content, removing ca. 17,000 t of moisture released as exhaust gas, after which the dried digestate is pyrolyzed at 400 °C for 1 h. The pyrolysis liquid produced annually (ca. 2,600 t) would be considered to be fed to the AD process and replace 9% of the process water used for dilution prior to THP. Based on the current study, the volume of pyrolysis liquid would not suppress methane production because its share of the total input volume and total input TS to the AD process would remain at 1.9% (v/w) and below 17%, respectively. Because of the apparently low biodegradability of the COD of the pyrolysis liquid (ca. 9.5 t COD/a), the pyrolysis liquid would not increase methane production. The total nitrogen content in the pyrolysis liquid (ca. 9.3 t/a) could potentially be ammonified in the AD process, thus enhancing the nitrogen recovery in the evaporator-stripping unit.

Pyrolysis integration into biogas plants primarily aims to produce sludge digestate biochar that is potentially more valuable in further use than digested and composted sewage sludge as such (Sousa and Figueiredo, 2016) and to increase the overall energy efficiency of the plant (Salman et al., 2017). The feeding of pyrolysis liquid to AD would provide a means for its treatment. To show the economic and environmental feasibility of the process, pyrolysis integration into a centralized biogas

plant still requires energy, life cycle assessment (LCA), and economic evaluation for the investment costs of a full-scale pyrolysis process and pre-pyrolysis drying unit.

## 5. Conclusions

The effects of pyrolysis liquid addition on AD of sewage sludge and THSS were studied to evaluate whether pyrolysis liquid could be treated in centralized biogas plant thus avoiding external wastewater treatment. Pyrolysis liquid appears inhibitory towards methane production in batch from THSS, even at a 1% (v/w) share, while sewage sludge seems less liable. However, in semi-continuous CSTRs no inhibition is observed with the pyrolysis liquid addition at shares likely relevant to centralized biogas plant (1% (v/w)). The extrapolated results show that pyrolysis liquid addition to AD feed causes minor increase to the biogas yield but could positively impact the recovery of ammonium-nitrogen.

## Declaration of Competing Interest

The authors declare that they have no known competing financial interests or personal relationships that could have appeared to influence the work reported in this paper.

## Acknowledgments

The financial support from the Maj and Tor Nessling Foundation (Anna Hämäläinen), the Industrial Research Fund at Tampere University of Technology (Anna Hämäläinen), and Gasum Ltd. are gratefully acknowledged. The authors are grateful to Gasum Ltd. Topinoja biogas plant for providing the materials and to the laboratory staff member Antti Nuottajarvi for providing and servicing the equipment used.

## References

- Alvarenga, P., Mourinha, C., Farto, M., Santos, T., Palma, P., Sengo, J., Morais, M.C., Cunha-Queda, C., 2015. Sewage sludge, compost and other representative organic wastes as agricultural soil amendments: Benefits versus limiting factors. *Waste Manag.* 40, 44–52. <https://doi.org/10.1016/j.wasman.2015.01.027>.
- Angelidaki, I., Alves, M., Bolzonella, D., Borzacconi, L., Campos, J.L., Guwy, A.J., Kaluzhnyi, S., Jenikec, P., Lier, J.B. van, 2009. Defining the biomethane potential (BMP) of solid organic wastes and energy crops: a proposed protocol for batch assays. *Water Sci. Technol.* 50, 927–934. <https://doi.org/10.2166/wst.2009.040>.
- Astals, S., Venegas, C., Peces, M., Jofre, J., Lucena, F., Mata-Alvarez, J., 2012. Balancing hygienization and anaerobic digestion of raw sewage sludge. *Water Res.* 46 (19), 6218–6227. <https://doi.org/10.1016/j.watres.2012.07.035>.
- Azuara, M., Kersten, S.R.A., Kostrita, A.M.J., 2013. Recycling phosphorus by fast pyrolysis of pig manure: Concentration and extraction of phosphorus combined with formation of value-added pyrolysis products. *Biomass and Bioenergy* 49, 171–180. <https://doi.org/10.1016/j.biombioe.2012.12.010>.
- Barber, W.P.F., 2016. Thermal hydrolysis for sewage treatment: A critical review. *Water Res.* 104, 53–71. <https://doi.org/10.1016/j.watres.2016.07.069>.
- Barry, D., Barbiero, C., Briens, C., Berruti, F., 2019. Pyrolysis as an economical and ecological treatment option for municipal sewage sludge. *Biomass and Bioenergy* 122, 472–480. <https://doi.org/10.1016/j.biombioe.2019.01.041>.
- Bougrier, C., Delgenès, J.P., Carrère, H., 2008. Effects of thermal treatments on five different waste activated sludge samples solubilisation, physical properties and anaerobic digestion. *Chem. Eng. J.* 139 (2), 236–244. <https://doi.org/10.1016/j.cej.2007.07.099>.
- Bridgwater, A.V., 2012. Review of fast pyrolysis of biomass and product upgrading. *Biomass and Bioenergy* 38, 68–94. <https://doi.org/10.1016/j.biombioe.2011.01.048>.
- Carrere, H., Antonopoulou, G., Affes, R., Passos, F., Battimelli, A., Lyberatos, G., Ferrer, I., 2016. Review of feedstock pretreatment strategies for improved anaerobic digestion: From lab-scale research to full-scale application. *Biore Sour. Technol.* 199, 386–397. <https://doi.org/10.1016/j.biortech.2015.09.007>.
- Choi, J.M., Han, S.K., Lee, C.Y., 2018. Enhancement of methane production in anaerobic digestion of sewage sludge by thermal hydrolysis pretreatment. *Biore Sour. Technol.* 259, 207–213. <https://doi.org/10.1016/j.biortech.2018.02.123>.
- Corradini, F., Meza, P., Eguiluz, R., Casado, F., Huerta-Lwanga, E., Geissen, V., 2019. Evidence of microplastic accumulation in agricultural soils from sewage sludge disposal. *Sci. Total Environ.* 671, 411–420. <https://doi.org/10.1016/j.scitotenv.2019.03.368>.
- Feng, Q., Lin, Y., 2017. Integrated processes of anaerobic digestion and pyrolysis for higher bioenergy recovery from lignocellulosic biomass: A brief review. *Renew. Sustain. Energy Rev.* 77, 1272–1287. <https://doi.org/10.1016/j.rser.2017.03.022>.
- Fonts, I., Azuara, M., Gea, G., Murillo, M.B., 2009. Study of the pyrolysis liquids obtained from different sewage sludge. *J. Anal. Appl. Pyrolysis* 85 (1–2), 184–191. <https://doi.org/10.1016/j.jaap.2008.11.003>.
- Fonts, I., Gea, G., Azuara, M., Abrego, J., Arauzo, J., 2012. Sewage sludge pyrolysis for liquid production: A review. *Renew. Sustain. Energy Rev.* 16 (5), 2781–2805. <https://doi.org/10.1016/j.rser.2012.02.070>.
- Hämäläinen, A., Kokko, M., Kinnunen, V., Hilli, T., Rintala, J., 2021. Hydrothermal carbonisation of mechanically dewatered digested sewage sludge—Energy and nutrient recovery in centralised biogas plant. *Water Res.* 201, 117284. <https://doi.org/10.1016/j.watres.2021.117284>.
- Hornung, A., 2012. In: *Encyclopedia of Sustainability Science and Technology*. Springer, New York, New York, NY, pp. 1517–1531. [https://doi.org/10.1007/978-1-4419-0851-3\\_258](https://doi.org/10.1007/978-1-4419-0851-3_258).
- Hübner, T., Mumme, J., 2015. Integration of pyrolysis and anaerobic digestion - Use of aqueous liquor from digestate pyrolysis for biogas production. *Biore Sour. Technol.* 183, 86–92. <https://doi.org/10.1016/j.biortech.2015.02.037>.
- Kim, Y., Parker, W., 2008. A technical and economic evaluation of the pyrolysis of sewage sludge for the production of bio-oil. *Biore Sour. Technol.* 99 (5), 1409–1416. <https://doi.org/10.1016/j.biortech.2007.01.056>.
- Kinnunen, V., Ylä-Outinen, A., Rintala, J., 2015. Mesophilic anaerobic digestion of pulp and paper industry biosludge-long-term reactor performance and effects of thermal pretreatment. *Water Res.* 87, 105–111. <https://doi.org/10.1016/j.watres.2015.08.053>.
- Kokko, M., Koskue, V., Rintala, J., 2018. Anaerobic digestion of 30–100-year-old boreal lake sedimented fibre from the pulp industry: Extrapolating methane production potential to a practical scale. *Water Res.* 133, 218–226. <https://doi.org/10.1016/j.watres.2018.01.041>.
- Li, H., Feng, K., 2018. Life cycle assessment of the environmental impacts and energy efficiency of an integration of sludge anaerobic digestion and pyrolysis. *J. Clean. Prod.* 195, 476–485. <https://doi.org/10.1016/j.jclepro.2018.05.259>.
- Megido, L., Negral, L., Fernández-Nava, Y., Suárez-Peña, B., Ormaechea, P., Díaz-Caneja, P., Castrillón, L., Marañón, E., 2021. Impact of organic loading rate and reactor design on thermophilic anaerobic digestion of mixed supermarket waste. *Waste Manag.* 123, 52–59. <https://doi.org/10.1016/j.wasman.2021.01.012>.
- Mönkäre, T.J., Palmroth, M.R.T., Rintala, J.A., 2015. Stabilization of fine fraction from landfill mining in anaerobic and aerobic laboratory leach bed reactors. *Waste Manag.* 45, 468–475. <https://doi.org/10.1016/j.wasman.2015.06.040>.
- Naqvi, S.R., Tariq, R., Shahbaz, M., Naqvi, M., Aslam, M., Khan, Z., Mackey, H., Mckay, G., Al-Ansari, T., 2021. Recent developments on sewage sludge pyrolysis and its kinetics: Resources recovery, thermogravimetric platforms, and innovative prospects. *Comput. Chem. Eng.* 150, 107325. <https://doi.org/10.1016/j.compchemeng.2021.107325>.
- Park, E.-S., Kang, B.-S., Kim, J.-S., 2008. Recovery of oils with high calorific value and low contaminant content by pyrolysis of digested and dried sewage sludge containing polymer flocculants. *Energy and Fuels* 22 (2), 1335–1340. <https://doi.org/10.1021/ef700586d>.
- Pecchi, M., Baratieri, M., 2019. Coupling anaerobic digestion with gasification, pyrolysis or hydrothermal carbonization: A review. *Renew. Sustain. Energy Rev.* 105, 462–475. <https://doi.org/10.1016/j.rser.2019.02.003>.
- Salman, C.A., Schwede, S., Thörin, E., Yan, J., 2017. Enhancing biomethane production by integrating pyrolysis and anaerobic digestion processes. *Appl. Energy* 204, 1074–1083. <https://doi.org/10.1016/j.apenergy.2017.05.006>.
- Seyedi, S., Venkiteshwaran, K., Benn, N., Zitomer, D., 2020. Inhibition during anaerobic co-digestion of aqueous pyrolysis liquid from wastewater solids and synthetic primary sludge. *Sustain.* 12, 8–11. <https://doi.org/10.3390/SU12083441>.
- Seyedi, S., Venkiteshwaran, K., Zitomer, D., 2019. Toxicity of various pyrolysis liquids from biosolids on methane production yield. *Front. Energy Res.* 7, 1–12. <https://doi.org/10.3389/fenrg.2019.00005>.
- Shen, L., Zhang, D., 2005. Low-temperature pyrolysis of sewage sludge and putrescible garbage for fuel oil production. *Fuel* 84 (7–8), 809–815. <https://doi.org/10.1016/j.fuel.2004.11.024>.
- Sousa, A.A.T.C., Figueiredo, C.C., 2016. Sewage sludge biochar: Effects on soil fertility and growth of radish. *Biol. Agric. Hortic.* 32 (2), 127–138. <https://doi.org/10.1080/01448765.2015.1093545>.
- Torri, C., Fabbri, D., 2014. Biochar enables anaerobic digestion of aqueous phase from intermediate pyrolysis of biomass. *Biore Sour. Technol.* 172, 335–341. <https://doi.org/10.1016/j.biortech.2014.09.021>.
- Villamil, J.A., Mohamedano, A.F., Rodriguez, J.J., de la Rubia, M.A., 2018. Valorisation of the liquid fraction from hydrothermal carbonisation of sewage sludge by anaerobic digestion. *J. Chem. Technol. Biotechnol.* 93 (2), 450–456. <https://doi.org/10.1002/jctb.5375>.
- Wen, C., Moreira, C.M., Rehmann, L., Berruti, F., 2020. Feasibility of anaerobic digestion as a treatment for the aqueous pyrolysis condensate (APC) of birch bark. *Biore Sour. Technol.* 307, 123199. <https://doi.org/10.1016/j.biortech.2020.123199>.
- Xue, Y., Liu, H., Chen, S., Dichtl, N., Dai, X., Li, N., 2015. Effects of thermal hydrolysis on organic matter solubilization and anaerobic digestion of high solid sludge. *Chem. Eng. J.* 264, 174–180. <https://doi.org/10.1016/j.cej.2014.11.005>.
- Yang, Y., Heaven, S., Venetsaneas, N., Banks, C.J., Bridgwater, A.V., 2018. Slow pyrolysis of organic fraction of municipal solid waste (OFMSW): Characterisation of products and screening of the aqueous liquid product for anaerobic digestion. *Appl. Energy* 213, 158–168. <https://doi.org/10.1016/j.apenergy.2018.01.018>.

Yogalakshmi, K.N., T, P.D., Sivashanmugam, P., Kavitha, S., R, Y.K., Varjani, S., Adishkumar, S., Kumar, G., J, R.B., 2022. Chemosphere Lignocellulosic biomass-based pyrolysis: A comprehensive review 286.

Yue, X., Arena, U., Chen, D., Lei, K., Dai, X., 2019. Anaerobic digestion disposal of sewage sludge pyrolysis liquid in cow dung matrix and the enhancing effect of

sewage sludge char. *J. Clean. Prod.* 235, 801–811. <https://doi.org/10.1016/j.jclepro.2019.07.033>.

Zhou, H., Brown, R.C., Wen, Z., 2019. Anaerobic digestion of aqueous phase from pyrolysis of biomass: Reducing toxicity and improving microbial tolerance. *Bioresour. Technol.* 292, 121976. <https://doi.org/10.1016/j.biortech.2019.121976>.

# PUBLICATION IV

**Towards the implementation of hydrothermal carbonization for nutrients,  
carbon, and energy recovery in centralized biogas plant treating sewage  
sludge**

Anna Hämäläinen, Marika Kokko, Henrik Tolvanen, Viljami Kinnunen & Jukka  
Rintala

Journal of Cleaner Production (submitted)





